



저작자표시-비영리-변경금지 2.0 대한민국

이용자는 아래의 조건을 따르는 경우에 한하여 자유롭게

- 이 저작물을 복제, 배포, 전송, 전시, 공연 및 방송할 수 있습니다.

다음과 같은 조건을 따라야 합니다:



저작자표시. 귀하는 원저작자를 표시하여야 합니다.



비영리. 귀하는 이 저작물을 영리 목적으로 이용할 수 없습니다.



변경금지. 귀하는 이 저작물을 개작, 변형 또는 가공할 수 없습니다.

- 귀하는, 이 저작물의 재이용이나 배포의 경우, 이 저작물에 적용된 이용허락조건을 명확하게 나타내어야 합니다.
- 저작권자로부터 별도의 허가를 받으면 이러한 조건들은 적용되지 않습니다.

저작권법에 따른 이용자의 권리는 위의 내용에 의하여 영향을 받지 않습니다.

이것은 [이용허락규약\(Legal Code\)](#)을 이해하기 쉽게 요약한 것입니다.

[Disclaimer](#)

이학박사 학위논문

**Changes in the structure and function  
of the nearshore benthic fauna communities  
in a rapidly deglaciating Antarctic fjord  
Marian Cove, King George Island,  
the West Antarctic Peninsula**

빙하후퇴에 따른 서남극반도 킹조지섬  
마리안소만의 저서동물 군집 구조와 기능 변화

2022년 8월

서울대학교 대학원

지구환경과학부

김 동 우

**Changes in the structure and function  
of the nearshore benthic fauna communities  
in a rapidly deglaciating Antarctic fjord  
Marian Cove, King George Island,  
the West Antarctic Peninsula**

지도 교수 김 종 성

이 논문을 이학박사 학위논문으로 제출함

2022년 8월

서울대학교 대학원

지구환경과학부

김 동 우

김동우의 이학박사 학위논문을 인준함

2022년 8월

위 원 장 \_\_\_\_\_ (인)

부위원장 \_\_\_\_\_ (인)

위 원 \_\_\_\_\_ (인)

위 원 \_\_\_\_\_ (인)

위 원 \_\_\_\_\_ (인)

# ABSTRACT

On polar coasts, glacial retreat strongly affects benthic invertebrates by oceanographic settings, including physical disturbance, habitat alteration, and food availability. Benthic organisms widely distributed from shallow to deep seabeds of the Antarctic represent an important polar benthic ecosystem, but ecological processes and the impacts of recent glacial retreat remain unanswered. The community structure and function of benthic megafauna were investigated in a glacial retreated fjord in Antarctica to answer the following questions: 1) how do the benthic megafauna communities shift after glacial retreat? 2) what are the sentinel taxa and environmental factors for benthic megafauna distribution in the deglaciated Antarctic nearshore? 3) do the diets of ascidians differ under the influence of the glaciers? To confirm the distributions of the benthic megafauna community in a deglaciated fjord of Antarctica, underwater imagery survey using a ROV was conducted for the first time in Marian Cove (MC). The diets of ascidians were determined from C and N stable isotope analyses

In the glacial retreated fjord, the structural and functional diversities of benthic megafauna communities varied greatly in space. Species diversity increased towards the outer sites where the glacial influence decreased, but the density peaked near the glaciers by the rapid increase of pioneer species (*Molgula pedunculata* and *Cnemidocarpa verrucosa*). Benthic communities matured rapidly at higher taxonomic levels after the glacial retreat (~10 years after seabed exposure). Functional diversity, on the other hand, increased toward the outside of the cove and peaked at 30 m as a result of a lesser disturbance and more food-availability. This study showed that three stages (colonization, transition, and maturing) represent the shift process of the benthic megafauna community after the glacial retreat in the Antarctic nearshore.

The spatial distribution of ascidians explaining 64% of the benthic megafaunal variations indicates that ascidians are suitable indicator taxa for monitoring the responses of the benthic ecosystem to the glacial retreat in Antarctica. The spatial distribution of ascidians was significantly changed with the distance from the glacier and water depth. The density peaked near the glacier by a rapid increase of pioneer



species (*M. pedunculata* and *C. verrucosa*), but diversity increased toward the outer site where the glacial influence decreased. The spatial pattern was not distinct at shallow depths (10 to 30 m) which had relatively severe disturbances. Sediment properties and distance from the glacier indicating the physical disturbance level by the deglaciation were key factors determining the ascidian distributions.

$\delta^{13}\text{C}$  and  $\delta^{15}\text{N}$  analysis showed changes in the diets of the three dominant ascidians according to the effects of the glaciers in the Antarctic nearshore. Benthic diatoms were the primary food (30–70%) for the ascidians in MC, and their contribution to the diets of the ascidians was significant up to 100 m. The diets of the ascidians differed depending on the species. The contribution of pelagic production to *M. pedunculata* with non-selective feeding and cylindrical body form increased toward the outer site abundant in phytoplanktons, but benthic diatoms were still one of the major food sources. On the other hand, benthic diatoms were the major food for *C. verrucosa*, which had a squirting behavior, and *Ascidia challengeri*, which had a laterally flat body, regardless of the influence of the glaciers. These results indicate that benthic diatoms were the primary food for filter feeders in the Antarctic nearshore, and their contribution was particularly high in areas with low pelagic production due to high turbidity by the glacial retreats.

Overall, the present study provides information on benthic ecosystem responses to glacial retreats in Antarctica. Given that the distance from the glacier was proportional to the seabed exposure time in MC, the spatial variation in the benthic megafauna community across the cove indicates the successional processes that occurred in the past after the glacial retreats. Therefore, this study provides a basis for predicting and preparing for changes in the Antarctic marine ecosystem caused by climate change.

**Keywords:** Glacial retreat, Antarctic benthic megafauna, Ascidian, Structural and functional diversities, Succession, Primary food source

**Student Number:** 2015-22652

# TABLE OF CONTENTS

<b>ABSTRACT</b> .....	<b>I–II</b>
<b>TABLE OF CONTENTS</b> .....	<b>III–V</b>
<b>LIST OF ABBREVIATIONS</b> .....	<b>VI</b>
<b>LIST OF TABLES</b> .....	<b>VII–XI</b>
<b>LIST OF FIGURES</b> .....	<b>XII–XVII</b>
<b>CHAPTER. 1. Introduction</b> .....	<b>1–12</b>
1.1. Backgrounds .....	2
1.2. Objectives .....	10
<b>CHAPTER. 2. Shifts in benthic megafauna communities after glacial retreat     in an Antarctic fjord</b> .....	<b>13–63</b>
2.1. Introduction .....	14
2.2. Materials and methods .....	16
2.2.1. Study area .....	16
2.2.2. ROV data acquisition .....	22
2.2.3. Megafaunal community analysis .....	24
2.2.4. Taxonomic and functional diversities .....	25
2.2.5. Statistical analysis .....	38
2.3. Results .....	39
2.3.1. Assemblages of benthic megafauna .....	39
2.3.2. Distribution characteristics of benthic megafauna .....	42
2.3.3. Relationship between the benthic megafauna community and environmental parameters .....	46
2.4. Discussion .....	48
2.4.1. Spatial variation in the structure of the benthic megafauna community	

.....	48
2.4.2. Changes to the functional diversity of the benthic megafauna community in the deglaciating fjord .....	55
2.4.3. Impact of glacial retreat on the benthic community .....	58
2.5. Conclusions .....	63

**CHAPTER. 3. Patterns, drivers and implications of ascidian distributions in  
a rapidly deglaciating fjord, King George Island, West  
Antarctic Peninsula ..... 64–129**

3.1. Introduction .....	65
3.2. Materials and methods .....	68
3.2.1. Study area .....	68
3.2.2. ROV survey and sampling .....	70
3.2.3. ROV images and sample analysis .....	87
3.2.4. Statistical analyses .....	90
3.2.5. Supporting datasets .....	91
3.3. Results .....	92
3.3.1. Environmental characteristics of the study area .....	92
3.3.2. Ascidian contribution to the spatial variations of total epibenthic megafauna .....	99
3.3.3. Spatial patterns of ascidian distribution .....	104
3.3.3.1 Abundance, species composition and diversity .....	104
3.3.3.2 Differences in body size among stations .....	112
3.3.4. Relationship between ascidian assemblages and environmental parameters .....	114
3.4. Discussion .....	116
3.4.1. Ascidiaceans as a key megabenthic community in an Antarctic fjord ..	116
3.4.2. Ascidian assemblages in the ice-proximal zone .....	118
3.4.3. Physical disturbance structuring ascidian communities in shallow habitats .....	120
3.4.4. Successional shifts of ascidian communities in deep habitats .....	125

3.5. Conclusions .....	129
<b>CHAPTER. 4. Changes in ascidian diets under the influence of glacial retreat in a fjord, Antarctic nearshore .....</b>	<b>130–152</b>
4.1. Introduction .....	131
4.2. Materials and methods .....	133
4.2.1. Study area .....	133
4.2.2. Potential food sources selection .....	136
4.2.3. Sample collection .....	138
4.2.4. Stable isotope analysis .....	139
4.2.5. Data analysis and statistics .....	140
4.3. Results .....	141
4.3.1. Stable isotope signatures of ascidians and potential food sources ...	141
4.3.2. Variations of relative contributions of the potential food sources to the diets of the ascidians among the stations and the species .....	144
4.4. Discussion .....	146
4.4.1. Diet change of ascidians .....	146
4.4.2. Effects of glacial retreat on food sources and distribution of ascidians .....	149
4.5. Conclusions .....	152
<b>CHAPTER. 5. Conclusions .....</b>	<b>153–161</b>
5.1. Summary .....	154
5.2. Environmental implications and limitations .....	158
5.3. Future research directions .....	160
<b>BIBLIOGRAPHY .....</b>	<b>162–174</b>
<b>ABSTRACT (IN KOREAN) .....</b>	<b>175–176</b>
<b>APPENDIX .....</b>	<b>177–203</b>

## LIST OF ABBREVIATIONS

ANOSIM	Analysis of similarities
B-POM	Bottom particulate organic matter
BDB	Benthic diatom bush
BDM	Benthic diatom mat
BIOENV	Biota-environment
FD	Functional diversity
IndVal	Indicator value
KGI	King George Island
MC	Marian Cove
MDS	Multidimensional scaling
PCA	Principle component analysis
POM	Particulate organic matter
ROV	Remotely operated vehicle
S-POM	Surface particulate organic matter
SIAR	Stable Isotope Analysis software in R
SOM	Sediment organic matter
SPM	Suspended particulate matter
TC	Total carbon
TD	Taxonomic distinctness
TIC	Total inorganic carbon
TN	Total nitrogen
TOC	Total organic carbon
WAP	West Antarctic Peninsula

# LIST OF TABLES

<b>Table 1.1.</b> .....	<b>12</b>
Summary of the key questions that have not been resolved or clarified in current research of Antarctic benthic ecosystem. Targets for each Chapter are suggested.	
<b>Table 2.1.</b> .....	<b>18</b>
Overview of the sampling, environmental conditions, and benthic megafauna community. Acronyms for phylum are given in parenthesis: (A) ascidian, (P) polychaeta, (B) bryozoa, (M) mollusca.	
<b>Table 2.2.</b> .....	<b>19</b>
Environmental characteristics among ROV survey stations (MC2–MC6) in Marian Cove, Antarctica. *Data were obtained from long-term monitoring project for King Sejong Station (KOPRI 2018). Water temperature and salinity data represent annual mean values. For sediment properties, mean±standard deviation values are presented.	
<b>Table 2.3.</b> .....	<b>23</b>
Sampling information on water depth in each station.	
<b>Table 2.4.</b> .....	<b>26</b>
Summary of statistical analyses with purpose, data, and software.	
<b>Table 2.5.</b> .....	<b>27</b>
Density (ind. m <sup>-2</sup> ) of epibenthic megafauna recorded from 10–90 m depth at MC2 in Marian Cove, Antarctica. Abundance data were obtained using a quadrat frame (50×50 cm) attached to the ROV and then transformed to values per square meter. Values are mean±standard error. (n): number of replicates.	
<b>Table 2.6.</b> .....	<b>29</b>
Density (ind. m <sup>-2</sup> ) of epibenthic megafauna recorded from 10–90 m depth at MC3 in Marian Cove, Antarctica. Abundance data were obtained using a quadrat frame (50×50 cm) attached to the ROV and then transformed to values per square meter. Values are mean±standard error. (n): number of replicates.	

<b>Table 2.7.</b> .....	<b>31</b>
Density (ind. m <sup>-2</sup> ) of epibenthic megafauna recorded from 10–90 m depth at MC4 in Marian Cove, Antarctica. Abundance data were obtained using a quadrat frame (50×50 cm) attached to the ROV and then transformed to values per square meter. Values are mean±standard error. (n): number of replicates.	
<b>Table 2.8.</b> .....	<b>33</b>
Density (ind. m <sup>-2</sup> ) of epibenthic megafauna recorded from 10–90 m depth at MC5 in Marian Cove, Antarctica. Abundance data were obtained using a quadrat frame (50×50 cm) attached to the ROV and then transformed to values per square meter. Values are mean±standard error. (n): number of replicates.	
<b>Table 2.9.</b> .....	<b>35</b>
Density (ind. m <sup>-2</sup> ) of epibenthic megafauna recorded from 50–70 m depth at MC6 in Marian Cove, Antarctica. Abundance data were obtained using a quadrat frame (50×50 cm) attached to the ROV and then transformed to values per square meter. Values are mean±standard error. (n): number of replicates.	
<b>Table 2.10.</b> .....	<b>37</b>
List of biological traits for a number of categories used for assessing the functional diversity of benthic megafauna community.	
<b>Table 2.11.</b> .....	<b>44</b>
Indicator megafauna species for clustered groups in Marian Cove. Given groups representing depths and distance from the glacier, such as A: ice-scouring depths of every stations (10–20 m); B: rarely scoured depths of innermost area (50–70 m); C: rarely scoured depths of inner to outer area (20–90 m); D: deep depths of outermost area (50–90 m).	
<b>Table 2.12.</b> .....	<b>47</b>
Biota-environment (BIOENV) analysis of the relationships between environmental factors and spatial variations in benthic megafauna in Marian Cove, Antarctica. <i>R</i> : Spearman correlation coefficient. * indicates the best results. <i>p</i> <0.05.	
<b>Table 2.13.</b> .....	<b>49</b>
Factors affecting benthic communities and their effects in Antarctica.	
<b>Table 2.14.</b> .....	<b>56</b>
Relative abundance of functional traits (%) in each station.	

<b>Table 3.1.</b> .....	<b>72</b>
Taxonomic composition and abundance (ind. m <sup>-2</sup> ) of epibenthic megafauna recorded from 10-90 m depth at MC2 in Marian Cove. Data were obtained from underwater photographic images collected using a remotely operated vehicle (ROV) during the period of December 31st, 2017, to February 12th, 2018. Abundance data were obtained using a quadrat frame (50×50 cm) attached to the ROV and then transforming the data to values per square meter. Values are mean±standard error. (n): number of replicates.	
<b>Table 3.2.</b> .....	<b>75</b>
Taxonomic composition and abundance (ind. m <sup>-2</sup> ) of epibenthic megafauna recorded from 10-90 m depth at MC3 in Marian Cove. Data were obtained from underwater photographic images collected using a remotely operated vehicle (ROV) during the period of December 31st, 2017, to February 12th, 2018. Abundance data were obtained using a quadrat frame (50×50 cm) attached to the ROV and then transforming the data to values per square meter. Values are mean±standard error. (n): number of replicates.	
<b>Table 3.3.</b> .....	<b>78</b>
Taxonomic composition and abundance (ind. m <sup>-2</sup> ) of epibenthic megafauna recorded from 10-90 m depth at MC4 in Marian Cove. Data were obtained from underwater photographic images collected using a remotely operated vehicle (ROV) during the period of December 31st, 2017, to February 12th, 2018. Abundance data were obtained using a quadrat frame (50×50 cm) attached to the ROV and then transforming the data to values per square meter. Values are mean±standard error. (n): number of replicates.	
<b>Table 3.4.</b> .....	<b>81</b>
Taxonomic composition and abundance (ind. m <sup>-2</sup> ) of epibenthic megafauna recorded from 10-90 m depth at MC5 in Marian Cove. Data were obtained from underwater photographic images collected using a remotely operated vehicle (ROV) during the period of December 31st, 2017, to February 12th, 2018. Abundance data were obtained using a quadrat frame (50×50 cm) attached to the ROV and then transforming the data to values per square meter. Values are mean±standard error. (n): number of replicates.	



<b>Table 3.5.</b> .....	<b>84</b>
Taxonomic composition and average abundance of epibenthic megafauna recorded from 10-90 m depth in Marian Cove. Data were obtained from underwater photographic images collected using a remotely operated vehicle (ROV) during the period of December 31st, 2017, to February 12th, 2018. Abundance data were obtained using a quadrat frame (50×50 cm) attached to the ROV and then transforming the data to values per square meter. Values are mean±standard error. (n): number of replicates.	
<b>Table 3.6.</b> .....	<b>93</b>
Comparison of environmental characteristics among ROV survey stations (MC2, MC3, MC4, and MC5) in Marian Cove. Distances of the stations from the glacier front were determined using the glacier front in the year of 2017 as a baseline (Figure 3.1). *The periods of seabed exposure at the stations were estimated based on glacial retreat lines in Figure 3.1. **Data were obtained from the long-term monitoring dataset collected at the station (see section 3.2.5). ***Sediment composition was determined from quadrat images obtained using an ROV in combination with the results from analysis of sediments collected by divers and grab sampling (refer to section 3.2.3 for more details). Mean±standard deviation values are presented.	
<b>Table 3.7.</b> .....	<b>100</b>
List of ascidian taxa occurring at depths of 10–90 m in Marian Cove constructed from the images taken by ROV survey in December 2017 to February 2018.	
<b>Table 3.8.</b> .....	<b>105</b>
Ascidian biomass (g wet wt m <sup>-2</sup> ) at various water depths across all stations (MC2, MC3, MC4 and MC5). Biomass was estimated using the density data obtained from ROV-acquired images (Table 3.1–3.5) and the allometric relationships shown in Figure 3.3. Values are mean±standard error. n: number of replicates.	

**Table 3.9.** ..... 115  
Summary of biota-environment (BIOENV) analysis of the relationships between environmental factors and ascidian assemblages in Marian Cove. *R*: Spearman correlation coefficient. \* indicates the best results.  $p < 0.01$

**Table 4.1.** ..... 142  
The  $\delta^{13}\text{C}$  and  $\delta^{15}\text{N}$  values of three ascidians and potential food sources in Marian Cove. Food sources and consumers were collected at 30 m depths from December 2017 to February 2018 except P-POM and *P. bouvetensis*. P-POM was collected at surface water from January to February 2019. *P. bouvetensis* was collected at 95 m at MC2' and Collins Harbor (CH) and 260 m of Maxwell Bay (MB) to use as a reference to compare the three shallow-water species on late April 2018. BDB; benthic diatom bush. BDM; benthic diatom mat. P-POM; pelagic particulate organic matter. B-POM; benthic particulate organic matter. SOM; sedimentary organic matter.

# LIST OF FIGURES

<b>Figure 1.1.</b> .....	<b>4</b>
Schematic diagram of Antarctic marine ecosystem and study topics.	
<b>Figure 1.2.</b> .....	<b>5</b>
Illustration showing the effects of glacial retreat induced by climate change on Antarctic marine ecosystems.	
<b>Figure 1.3.</b> .....	<b>8</b>
Importance of benthic megafauna in Antarctic Ocean.	
<b>Figure 1.4.</b> .....	<b>9</b>
Overview of study efforts on Antarctica, glacier, and benthic megafauna.	
<b>Figure 1.5.</b> .....	<b>11</b>
Research questions of the study in terms of benthic megafauna community responses to glacial retreats.	
<b>Figure 2.1.</b> .....	<b>17</b>
(a) Location of Marian Cove (MC). (b) Map showing the bathymetry of MC and survey stations. MC has three basins and is separated from Maxwell Bay by a sill (~40 m) at its mouth. Glacial retreat lines were plotted based on satellite and aerial images (Kim et al., 2021). Image survey and sampling stations (black dashed boxes) were selected based on the period of exposure after glacial retreat, disturbance level, and topography. (c) Topography of MC transect. Black dashed boxes are survey stations and red lines are survey depths. (d) Survey design. Benthic images and samples were collected at six depths (10, 20, 30, 50, 70, and 90 m) at each station, except MC6 (see Table 2.3 for details). At MC6, image surveys were only conducted at 50 m and 70 m. (e) Sediment properties at six depths at each station. SOM is sediment organic matter.	
<b>Figure 2.2.</b> .....	<b>41</b>
Spatial variation in the benthic megafauna community. (a) Change to the number of taxa and density in relation to distance from the glacier. (b) Variation in the number of taxa and density among stations at each depth. (c) Dominant taxa in MC (>2%). Acronyms for phylum are given in parenthesis: (A) ascidian, (P) polychaeta, (B) bryozoa, (M) mollusca. (d) Taxonomic distinctness changes with distance and depth. (e) Spatial variations in functional diversity. Vertical bars of average data indicate standard deviation. Data denoted by the same letter are not significantly different ( $p>0.05$ ) based on the Mann-Whitney test.	

<b>Figure 2.3.</b> .....	<b>43</b>
Distribution characteristics of benthic megafauna in Marian Cove. (a) Cluster analysis results showing the four groups of benthic megafauna assemblages. (b) MDS plot based on Bray Curtis similarity. Dominant taxa of each group were overlapped on the MDS plot. <i>L.e.</i> : <i>Laternula elliptica</i> , <i>M.a.</i> : <i>Margarella antarctica</i> , <i>M.p.</i> : <i>Molgula pedunculata</i> , <i>C.v.</i> : <i>Cnemidocarpa verrucosa</i> , <i>A.c.</i> : <i>Ascidia challengerii</i> , <i>R.p.</i> : <i>Rossella</i> cf. <i>podagrosa</i> , <i>Sp.</i> : Serpulidae spp. * is early successional stage taxa. ** is late successional stage taxa. (c) Quadrat images showing the dominant taxa of each group.	
<b>Figure 2.4.</b> .....	<b>54</b>
Correlation between distance from the glacier and elapsed time after deglaciation.	
<b>Figure 2.5.</b> .....	<b>59</b>
Schematic summarizing the benthic megafauna community in a glacial retreated fjord in Antarctic nearshore. The illustration shows the distribution of benthic megafauna including abundance of key taxa and functional changes to communities. The shifts in number of taxa, density, and functional diversity of the communities according to distance from the glacier at shallow and deep depths were respectively plotted in the two graphs. The words under the dotted lines indicate the characteristics of the benthic megafauna communities.	
<b>Figure 3.1.</b> .....	<b>67</b>
(a) Map showing the locations of King George Island, Maxwell Bay, and its tributary embayments including Marian Cove (MC). (b) Bathymetry of MC. The bathymetric contours were constructed from data obtained through a seismic survey (KOPRI 2011). The area in white represents glacier or snow cover. (c) ROV survey and sampling stations (MC2, MC3, MC4, and MC5) in orange squares and glacial retreat lines over six decades. Glacial retreat lines were drawn based on information obtained from satellite images and aerial photographs (updated from Moon et al. 2015).	
<b>Figure 3.2.</b> .....	<b>71</b>
(a), (b) ROV (VideoRay Pro4) operated from a rubber boat; (c) ROV equipped with an external video camera (GoPro Hero5), a pair of downward lights and a stainless-steel quadrat (50×50 cm).	

**Figure 3.3. .... 89**

Allometric relationships of the three most abundant ascidian species (*C. verrucosa*, *M. pedunculata* and *A. challengerii*). The ascidian samples used for analysis were collected randomly by divers from about 30 m depth. ROV images were taken from above in the water, and body length (L, the longest dimension) of many individuals, particularly those in an upright or standing position could not be determined directly from the images. Therefore, the width (Wd) of each individual was determined from the images and the measured Wd values were converted to body weight (total wet weight, tww) and L, using the allometric relationships. For other species, the relationship obtained from one of the three dominant species was used based on similarity of body form and position. For stalked species (*Distalpia* sp., *Pyura* sp.1, *Pyura* cf. *bouvetensis*, *S. sigillinoides* and *T. speciosum*), the equations for *M. pedunculata* were used, while those of *C. verrucosa* for non-stalked and elongated species (*Pyura* cf. *discoveri*, and Ascidian sp. 17) and those of *A. challengerii* for ovoid or flattened species (e.g. *Aplidium* cf. *radiatum*, *Corella antarctica*, *P. setosa* and Ascidian sp. 16).

**Figure 3.4. .... 95**

Spatial variations in sediment properties across stations (MC5, MC4, MC3, and MC2) and water depths (10, 20, 30, 50, 70 and 90 m). All replicate data from each station were plotted in terms of distance from the glacier, showing stations MC5, MC4, MC3, and MC2 from left to right. Regression lines that are statistically significant are plotted. Data from lines representing statistically insignificant differences (analysis of covariance, ANCOVA,  $p>0.05$ ) were pooled for construction of a single regression equation.

**Figure 3.5. .... 98**

Principal component analysis (PCA) plot showing spatial variations in environmental parameters among stations (MC2, MC3, MC4, and MC5) and depths (10–90 m). Constructed based on the data presented in Table 3.6.

**Figure 3.6. .... 101**

Ascidian abundance and number of taxa present across various depths (10, 20, 30, 50, 70, and 90 m) at four stations (MC2, MC3, MC4, and MC5) in comparison with those of the total megafauna. Total number of taxa represents total sum of taxa occurred at a specific depth of each station. Only mean values represent for abundance (refer to Table 3.1–3.5 for the details of data).

**Figure 3.7. .... 103**

Non-metric multidimensional scaling (MDS) plots for total epibenthic megafauna and the two dominant taxa based on Bray-Curtis similarity matrix data (Table 3.1–3.5). Numbers near the symbols represent water depth (m) of each habitat. Data from 10 m depth were excluded for MDS analysis, as only a few taxa were present at this depth (in the case of ascidians present only at MC5).

**Figure 3.8. .... 108**

Ascidian abundance and composition among various depths (10, 20, 30, 50, 70, and 90 m) at four stations (MC2, MC3, MC4, and MC5) in Marian Cove (MC). Most density peaks occurred at 30 or 50 m, while biomass peaks at 30 m were observed at all stations except MC3. Others include ascidian taxa that account for <3% of the total number of ascidian individuals at all stations. The horizontal bars indicate mean values. Refer to Tables 3.1–3.5 and 3.8 for the data and standard errors.

**Figure 3.9. .... 110**

Images of ascidians within a quadrat (50x50 cm) taken by a ROV, showing distinct shifts in key taxa and the diversity of ascidian communities among stations and water depths in Marian Cove. (a, b) bottom substrates dominated by gravel at 10 m; sea urchins occurring at the highest numbers at this depth at MC3; (c) seabed covered by sand and silty sediment indicating heavy sedimentation near glacier (d) Ascidian communities, mostly comprised of *Molgula pedunculata* and *Cnemidocarpa verrucosa*, covered by dense blooms of the benthic diatom *Paralia* sp. (refer to Ha et al. 2019); (e) Relatively low ascidian abundance on boulder-sized substrate in shallow waters at MC3; (f) *C. verrucosa* population entangled with massive growth of benthic diatom and the surrounding bare seabed covered with a thick layer of muddy sediment at 20 m depth, indicating heavy sedimentation at this site; (g) *A. challengerii*, *Aplidium* cf. *radiatum* and Ascidiacea sp.16 population dominating at 50 m at the distant site; (k, i) *M. pedunculata* and *C. verrucosa* predominating at 30 m depth in the inner cove (MC4, MC5); (h, l, o) *M. pedunculata* and *C. verrucosa*, less abundant but still dominating at 50–90 m in the inner cove; (j, m, n) Diverse taxa occurring at 70–90 m at MC2. Large hexactinellid sponges commonly occurred together. *Mp*: *M. pedunculata*; *Cv*: *C. verrucosa*; *Ac*: *A. challengerii*; *Pd*: *P. cf. discoverii*; *Ps*: *P. setosa*; *Pb*: *P. cf. bouvetensis*; *Ar*: *Aplidium* cf. *radiatum*; A16: Ascidiacea sp.16; A17: Ascidiacea sp.17; *Sn*: *Sterechinus* cf. *neumayeri*. Scale bars: 5 cm

<b>Figure 3.10.</b> .....	<b>113</b>
Comparison of size frequency distributions of three ascidian species among stations (MC2, MC3, MC4, and MC5) at their depth of peak abundance ( <i>M. pedunculata</i> and <i>C. verrucosa</i> at 30 m, <i>A. challengerii</i> at 50 m). Size classes were determined based on total wet weight (tww), which was determined from body width or body length measurements obtained from ROV-acquired images using allometric relationships (refer to the Fig. 3.3 for the details). Figures inside the plots are mean±standard error. <i>n</i> : number of replicates	
<b>Figure 3.11.</b> .....	<b>122</b>
Conceptual drawing of successional shifts in dominant ascidian taxa in Marian Cove, a fjord in the northern WAP that has been rapidly warming and deglaciating over the last six decades. This drawing illustrates how the intensity of physical disturbance, due to ice scouring and sedimentation associated with glacial retreat, acts as a key driver structuring ascidian communities.	
<b>Figure 4.1.</b> .....	<b>134</b>
(a) Map showing the locations of King George Island, Maxwell Bay, and its tributary embayments including Marian Cove (MC). (b) Bathymetry and sampling stations of Maxwell Bay. Bathymetric contours are drawn based on information from the Atlas Hidrografico Chileno Antartica from the Instituto Hidrografico de la Armada, Chile (1982). The area in white represents glacier or snow cover. (c) Sampling stations and glacial retreat lines over six decades. Glacial retreat lines were drawn based on information obtained from satellite images and aerial photographs (updated from D. Kim et al., 2021). Orange squares are stations for sediment and ascidian samples at 30 m. Seawater properties and ascidians at deep depths were collected at orange circles.	
<b>Figure 4.2.</b> .....	<b>137</b>
(a) <i>Molgula pedunculata</i> assemblages densely covered by benthic diatom bush at the outermost site (MC2, the photo from Ahn et al. 2016). in the Marian Cove. (b) A close-up picture showing the thread-like diatom bush attached to the <i>M. pedunculata</i> . (c) Diatom bushes covered ascidians and diatom mats on the surface sediments in the innermost site (MC5).	
<b>Figure 4.3.</b> .....	<b>143</b>
Dual plots of $\delta^{13}\text{C}$ and $\delta^{15}\text{N}$ for three dominant ascidians of shallow depths (~30 m) and one ascidian of deep depths (95 m and 260 m) with potential food sources. P-POM; pelagic particulate organic matter. B-POM; benthic particulate organic matter. BDB; benthic diatom bush. BDM; benthic diatom mat. SOM; sediment organic matter.	

**Figure 4.4.** ..... 145  
SIAR model showing the relative contributions of potential food sources to the diet of three ascidians dominated at shallow depths (~30 m) and one ascidian of deep depths (95 and 260 m) at each station. The gray bars of different widths indicate the 95, 75, and 50% confidence intervals (from lightest to darkest) and the black dots are mean values. Figures on the bars are mean values. P-POM; pelagic particulate organic matter. B-POM; benthic particulate organic matter. SOM; sediment organic matter. Benthic diatom bush and mat was pooled to benthic diatom based on their C and N stable isotope values.

**Figure 4.5.** ..... 151  
Changes in carbon and nitrogen content in sediments with distance from the glacier.

**Figure 5.1.** ..... 157  
Research questions and key findings in the present study.



# **CHAPTER 1.**

## **INTRODUCTION**

## 1.1. Backgrounds

An ecosystem is a geographic space containing abiotic and/or biotic factors. The function of an ecosystem consists of processes that control the fluxes of energy and matter. The topic of this study is the effect of the energy flux called climate change, one of the most urgent agendas in the world, on the Antarctic marine ecosystem (Figure 1.1). To confirm the effect, the influence of glacial retreat induced by global warming on benthic megafauna and their diets and environmental factors were investigated in the Antarctic nearshore, one of the regions most affected by climate change.

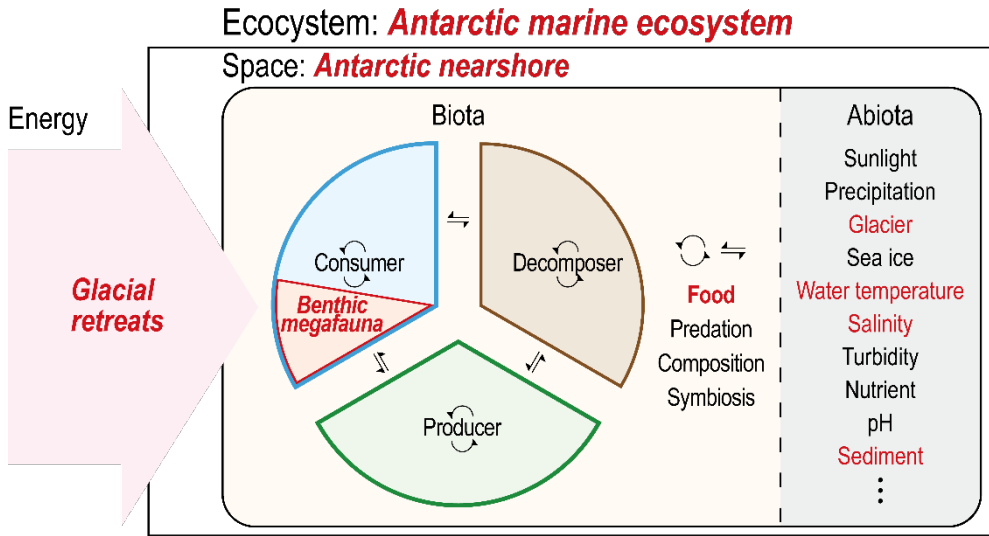
Climate change, which has continuously been observed since the 1850s, has various effects from sea level rise to pandemics (IPCC, 2014; IPCC, 2021). Especially in the Antarctic nearshore, from 1992 to 2017, glaciers decreased by 109 Gt per year due to global warming (Shepherd et al., 2018). As a result, a total of 2720 Gt of glaciers was lost. This is an amount that could raise sea levels by 7.6 mm. Because climate change is expected to continue, the retreat of glaciers in Antarctica is also expected to continue (IPCC, 2021).

Glacial retreat not only has raised the sea level but also is accompanied by various processes that cause environmental changes (Figure 1.2). The loss of the ice-sheet directly reduces the cryosphere. In the regions where glaciers have retreated, benthic and pelagic spaces are newly exposed from the ice. Glacial meltwater flows into the ocean, changes the water temperature and salinity, and increases the turbidity by transporting terrestrial sediments (Yoon et al., 1998; Yoo et al., 2015). Icebergs carved from glaciers drift and cause scouring on the sea floor (Gutt et al., 2001; Smale et al., 2007a). Icebergs also provide nutrients to surrounding water masses, forming mini-ecosystems (Smith Jr et al., 2013).

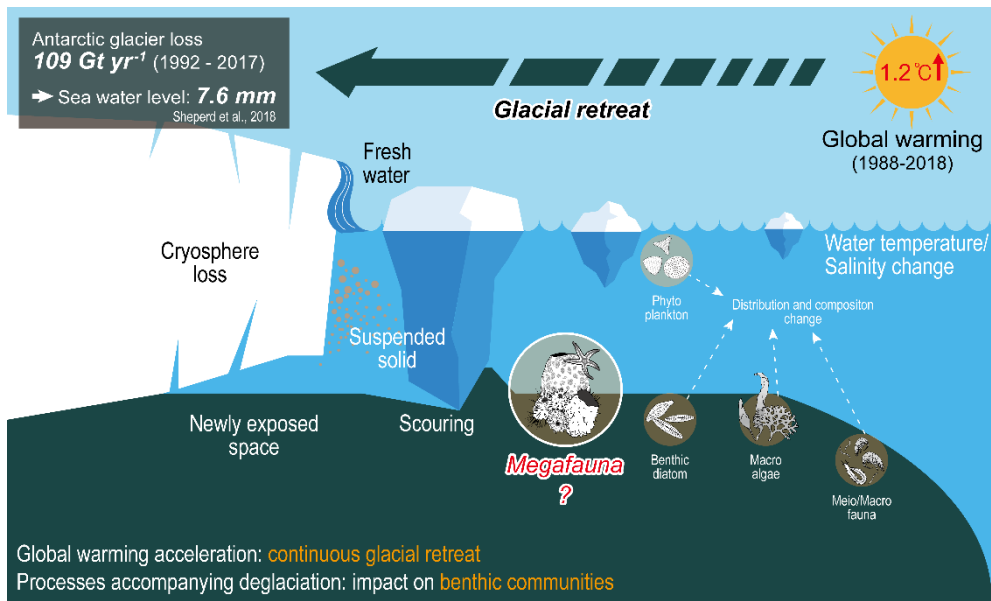
Glacial retreat and accompanying processes affect Antarctic marine ecosystems by environmental changes in habitats (Figure 1.2). The loss of the cryosphere reduces the habitat of organisms living in glaciers such as snow algae (Boetius et al., 2015). The turbidity increase caused by the suspended particulate matters (SPM) introduced into the ocean by glacial retreat reduced the primary production and affected the species composition of phytoplanktons (Kim et al., 2021). In addition, the concentration of SPM changes the distribution of benthic communities, and it affects

the metabolism and feeding activities of the filter feeders dominant in the Antarctic (Torre et al., 2012; Sahade et al., 2015; Braeckman et al., 2021; Torre et al., 2021). Ice-scouring by iceberg increased the mortality of benthic fauna and reduced the biomass and diversity of benthic communities (Smale et al., 2007b; Barnes, 2017).

Glacial retreat also has had a positive impact on the Antarctic marine ecosystem. Newly ice-free areas after glacial retreat provide new habitats for various organisms including micro- to mega-fauna (Lagger et al., 2017; Bae et al., 2021; Gyeong et al., 2021). Glaciers promote primary production by supplying nutrients including Fe (Smith Jr et al., 2013; Wadham et al., 2013). Increased primary production in newly ice-free areas leads to abundant food inflows into benthic ecosystems. Improving the quality and quantity of foods increased the density of benthic invertebrates (Murray & Pudsey, 2004; Raes et al., 2010). Ice-scouring, which increased the mortality of benthic organisms, also contributed to the increase of diversity in the benthic communities by changing the succession stage of the communities (Gutt and Piepenburg, 2003; Robinson et al., 2021).



**Figure 1.1.**  
 Schematic diagram of Antarctic marine ecosystem and study topics.



**Figure 1.2.**

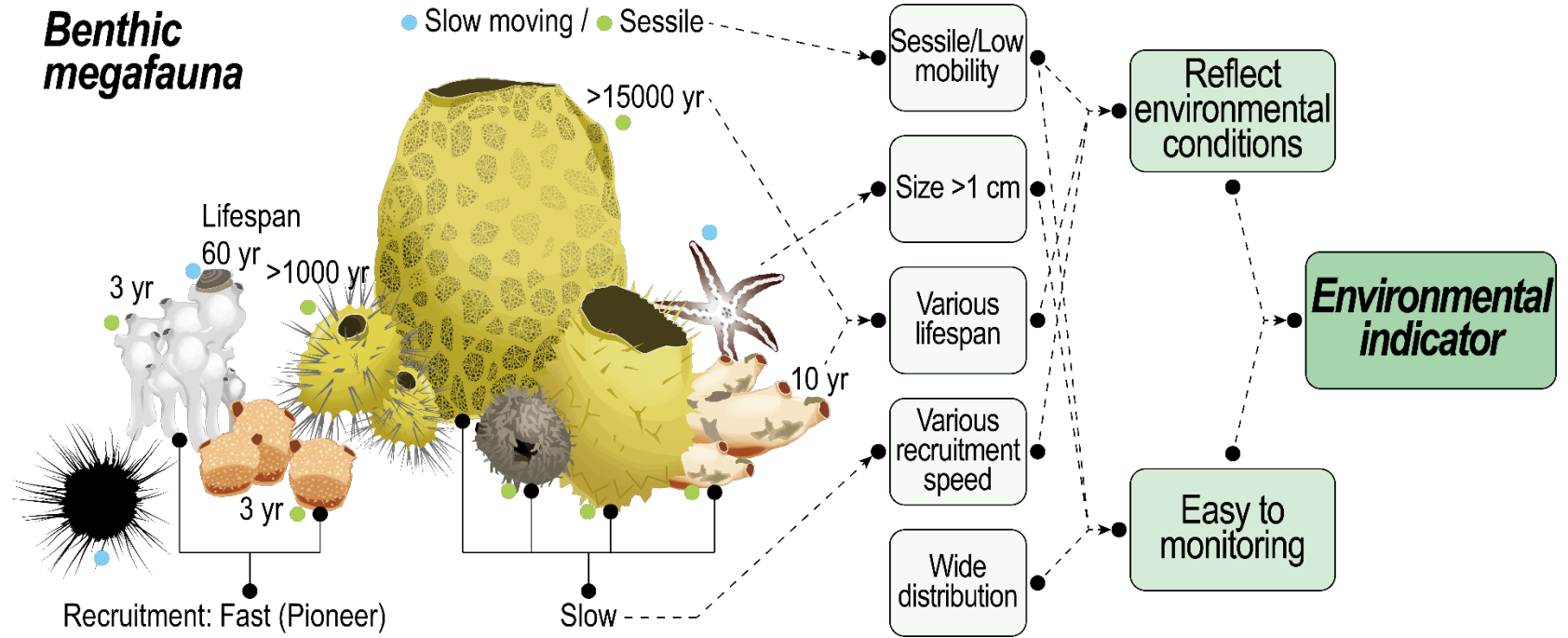
Illustration showing the effects of glacial retreat induced by climate change on Antarctic marine ecosystems.

Over 95% of the Antarctic continent covered by glaciers is too severe for organisms to inhabit. However, the seabed has abundant flora and fauna from shallow to deep depths. Consequently, benthic megafauna are possibly one of the dominant ecotypes of the Antarctic biosphere. Antarctic benthic megafauna, mostly sedentary or slow-moving, are very sensitive to environmental changes (Sicinski et al., 2012; Moon et al., 2015; Sahade et al., 2015; Figure 1.3). Benthic megafauna are suitable as indicators for monitoring changes in marine ecosystems because their biological responses to environmental changes are highly species-specific (Gerdes et al., 2008; Torre et al., 2012; Moon et al., 2015). In addition, benthic megafauna are an important component of the marine ecosystem functioning as a benthic-pelagic energy path in Antarctica (Gili et al., 2001).

Efforts to investigate Antarctica and glaciers sharply increased after it was reported by C. D. Keeling that the atmospheric concentration of carbon dioxide, a greenhouse gas, was increasing (Bacastow et al., 1985) (Figure 1.4). Furthermore, the effects of climate change were significant in Antarctica, and glacial retreat had been confirmed to cause various effects such as sea level rise. Interest in the benthic megafauna had also continuously increased. However, only few studies focused on the effects of glacial retreat on benthic megafauna communities, one of the major components of Antarctic marine ecosystems (Figure 1.4). In particular, little is known about benthic community succession, related environmental factors, and diet change of benthic megafauna in the deglaciaded Antarctic nearshore (Figure 1.4).

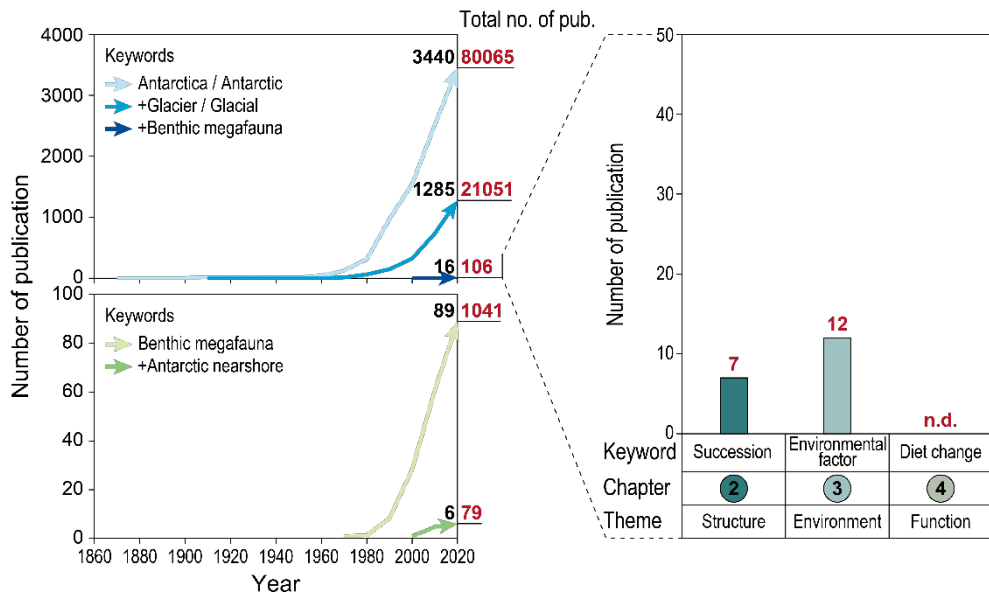
Studies on benthic megafauna had been conducted in Marian Cove (MC) on the West Antarctic Peninsula (WAP) since 1988. In the 1990s and early 2000s, autecological studies were mainly conducted. Through this, the feeding, respiratory metabolism, reproduction, and overwintering strategy of the Antarctic soft-shelled clam (*Laternula elliptica*) were confirmed, and it was revealed that the clam was a key factor of the carbon cycle in the Antarctic nearshore (Ahn et al., 1993; Ahn et al., 1997b; Ahn et al., 1998; Ahn et al., 2000; Ahn et al., 2003). Since the 2000s, studies had been conducted on the effects of glacial retreat on Antarctic benthic ecosystems. MC, where glaciers retreated about 1.9 km over the past 60 years, reflects the characteristic of the WAP where glacier retreat was prominent because the atmospheric temperature had increased by nearly 3°C since the 1950s. MC

provides opportunities to confirm the responses of the benthic community to deglaciation because the effects of glaciers vary significantly with distance. Based on this, it was confirmed that the food sources of *Nacella concinna* depended on the habitat and the size of the individual and that the concentration of heavy metals was affected by the meltwater (Ahn et al., 2004; Choy et al., 2011). As the research subject expanded from a single species to communities, it was confirmed that the community structures of the benthic diatom and megafauna changed according to the distance from the glacier (Moon et al., 2015; Bae et al., 2021). However, previous studies mainly focused on the ecology of a specific species, and studies on communities provided information on limited water depths or restricted areas, making it difficult to understand the overall change pattern of the benthic community by glacial retreats. Therefore, to confirm the effect of glacial retreat on the benthic ecosystems of the Antarctic nearshore, this study investigated the structure and function of the benthic megafauna community by water depth in areas with different glacier influences in a deglaciated fjord in MC.



**Figure 1.3.**  
Importance of benthic megafauna in Antarctic Ocean.





**Figure 1.4.**  
Overview of study efforts on Antarctica, glacier, and benthic megafauna.

## **1.2. Objectives**

The benthic megafauna community is very directly impacted by environmental changes, and it reflects the surrounding environments. In this dissertation, the responses of the benthic megafauna community inhabiting the Antarctic nearshore to glacial retreat were examined from chapters 2 to 4. The structure and function of the benthic megafauna community and environmental factors were investigated in a glacial retreated fjord in Antarctica. Key questions that required clarification in the current research for the benthic megafauna community, along with specific objectives and workflow, are stated as follows (Figure 1.5, and Table 1.1):

- 1. Chapter 2**

Confirmed shifts in the benthic megafauna community after glacial retreats in an Antarctic fjord

- 2. Chapter 3**

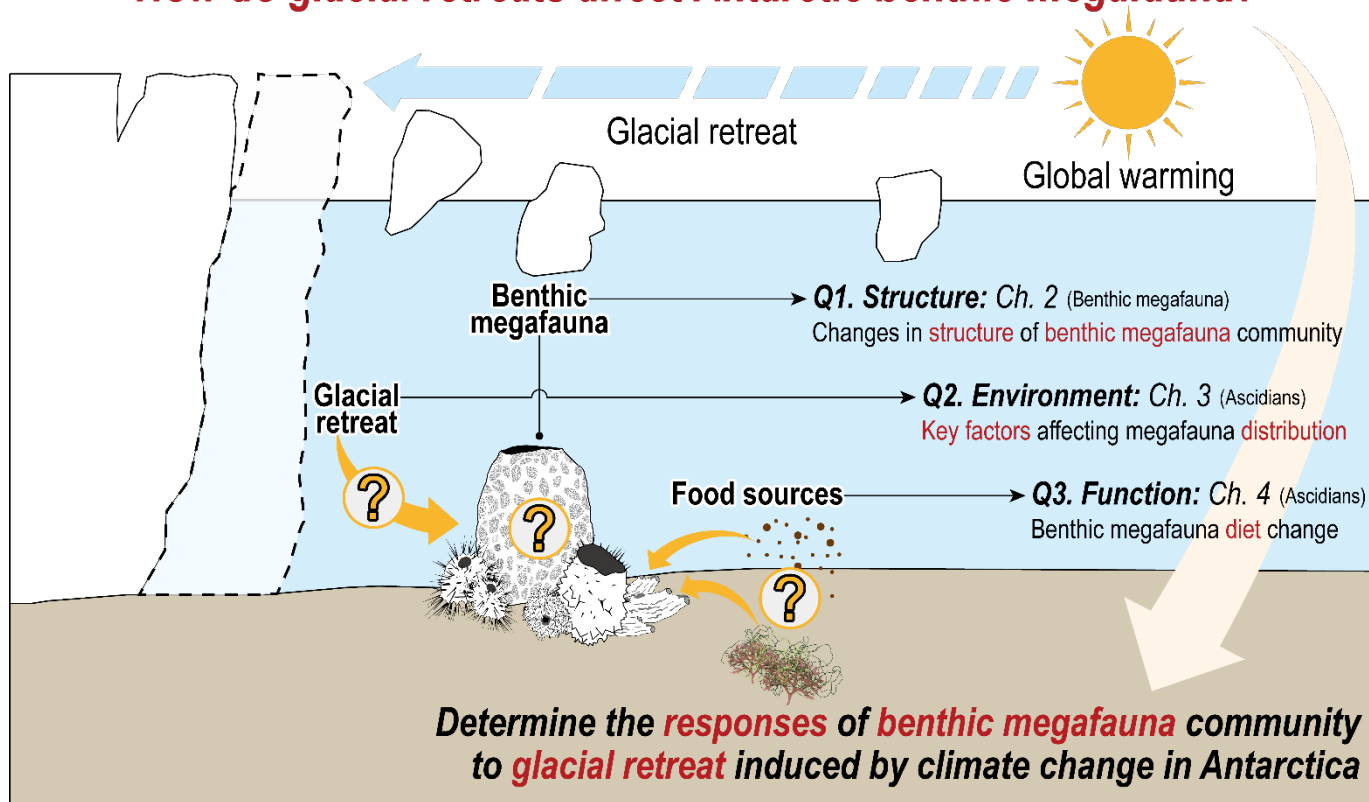
Identified sentinel taxa reflecting the changes in the benthic megafauna community and determined drivers structuring the communities in the deglaciated fjord

- 3. Chapter 4**

Verified changes in contributions of potential food sources and ascidian diets after glacial retreats

Finally, the conclusions including a summary, environmental implications and limitations and future research directions are provided in Chapter 5.

## How do glacial retreats affect Antarctic benthic megafauna?



**Figure 1.5.**

Research questions of the study in terms of benthic megafauna community responses to glacial retreats.

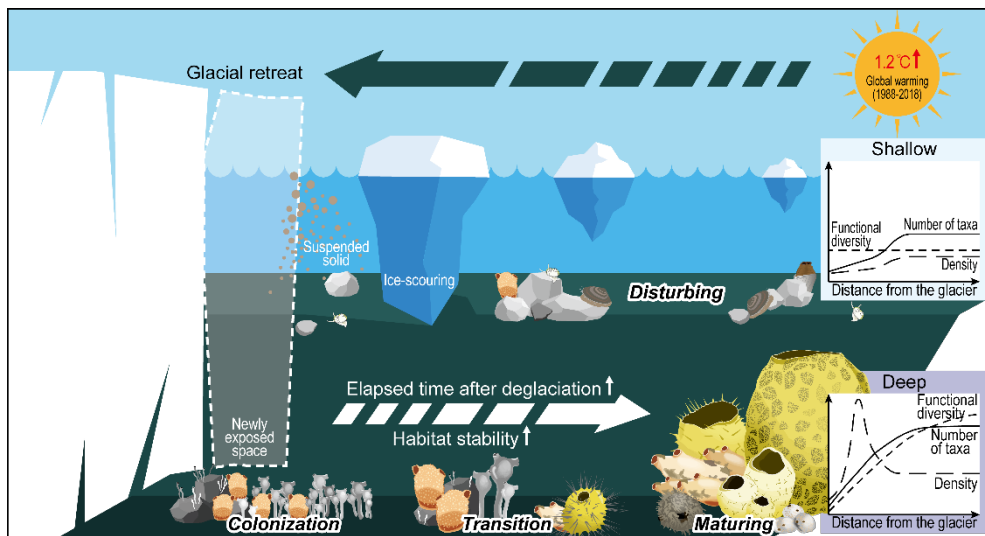
**Table 1.1.**

Summary of the key questions that have not been resolved or clarified in current research of Antarctic benthic ecosystem. Targets for each Chapter are suggested.

Subject		Key question	Ch.	Target
I (Structure)	Shifts in benthic megafauna community after glacial retreat	Any changes in distributions, taxonomic and functional diversities of benthic megafauna communities after glacial retreat?	2	Benthic megafauna
II (Environment)	Drivers structuring benthic community and sentinel taxa in Antarctic nearshore	What environmental factors determine the structure of benthic megafauna communities, and which taxa are suitable as indicator for monitoring of Antarctic nearshore ecosystem?	3	Ascidians
III (Function)	Changes in ascidian diets and food sources after glacial retreat	Any changes in potential food sources and diet compositions of ascidians after glacial retreat?	4	Ascidians & food sources

## CHAPTER 2.

# SHIFTS IN BENTHIC MEGAFAUNA COMMUNITIES AFTER GLACIAL RETREAT IN AN ANTARCTIC FJORD



This chapter has been submitted in Global change biology.

Kim, D. U., Ahn, I. Y., Noh, J., Lee, C., & Khim, J. S. (2021). Shifts in benthic megafauna communities after glacial retreat in an Antarctic fjord. *Global change biology*.

## 2.1. Introduction

Over 95% of the Antarctic continent that is covered by glaciers is too severe for habitation by organisms; however, the seabed supports a wealth of flora and fauna from shallow to deep zones. Consequently, benthic megafauna communities tend to be the largest ecotype and are possibly one of the dominant components of biota in the Antarctic. Benthic megafauna also contributes significantly to the functioning of marine ecosystems, providing benthic-pelagic energy paths through food webs (Tatián et al., 2008; Ha et al., 2019). Different sensitivity to environmental stresses of different benthic megafauna makes them ideal indicators for monitoring changes to marine ecosystems (Gerdes et al., 2008; Torre et al., 2012; Kim et al., 2021). Yet, knowledge remains limited on how glacial retreat, one of the most dramatic environmental changes in Antarctica, affects the structure and function of benthic megafauna communities. It is necessary to understand how benthic megafauna respond to environmental changes, because glacial retreats caused by continued global warming (Clem et al., 2020), have an immediate and significant impact on this group in Antarctica (Sahade et al., 2015).

The glaciers of MC, situated on the WAP, retreated approximately 1.9 km from 1956 to 2017. Benthic megafauna assemblages in MC closely represent those of other Antarctic nearshore areas dominated by suspension feeders (Moon et al., 2015; Kim et al., 2021). Additionally, habitat and benthic community has changed in relation to glaciers (Moon et al., 2015). These characteristics indicate that MC is a suitable region for monitoring the effects of glacial retreat on benthic megafauna communities. Kim et al. (2021) showed that deglaciation significantly impacted benthic megafauna communities, as the ascidian community changed in relation to habitat stability induced by glacial retreat. The major factors related to ascidian distributions were reported to be sedimentation and ice-scouring, with these effects differ according to the distance from the glacier and water depth (Kim et al., 2021). As climate change continues, increasing numbers of studies on how glacial retreat affects coastal ecosystems are being conducted; however, knowledge about the responses of benthic megafauna in nearshore areas to glacial retreat in Antarctica is not enough. To date, many studies only have focused on community structure and/or distribution of benthic communities in limited regions, narrow depths (Sahade et al.,

2015; Lager et al., 2018), or for specific taxa (Rimondino et al., 2015; Kim et al., 2021), as well as quantitative data and/or studies in terms of function are rare.

To understand the response of marine ecosystems to environmental changes, it is necessary to comprehend both the overall structure of the community and its function. Quantitative taxonomic distinctness (TD) is often used to define the average length of taxonomic hierarchy between any two randomly chosen individuals based on the abundance of each species (Clarke and Warwick, 1998). Therefore, this approach provides more comprehensive information on structural characteristics compared to species richness or abundance. When the environment changes, only species with suitable traits survive. Structural indices are limited in determining changes to functional components. Previous studies showed that functional diversity (FD) is useful for assessing functional changes in ecosystems (Vandewalle et al., 2010; Ricotta and Moretti, 2011). Despite the utility of these two indices, few studies have used them to determine the response of Antarctic benthic assemblages to climate change (Moon et al., 2015; Hussin, 2016).

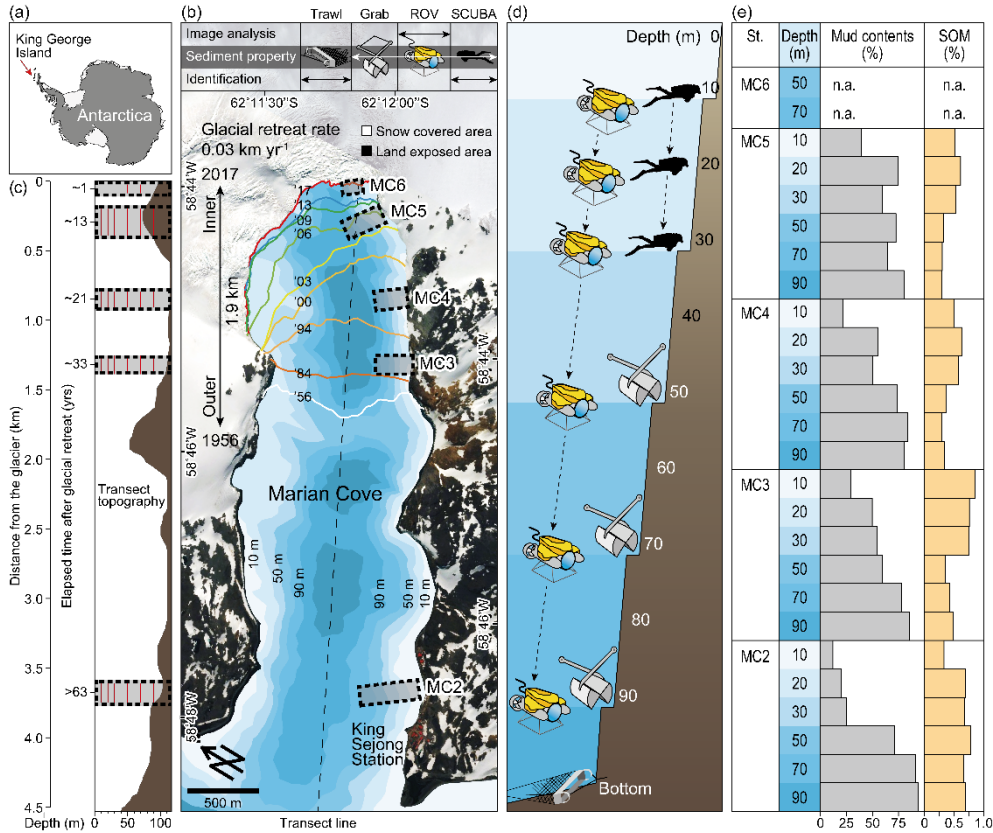
Therefore, to understand how continuous warming is impacting the Antarctic marine ecosystem, we evaluated how deglaciation impacts the structure and function of the benthic megafauna community at Marian Cove. We investigated: 1) distributions of benthic megafauna at sites with different elapsed time after deglaciation; 2) structural and functional diversity of these communities; 3) how structure and function, and related factors, changed with time that elapsed after deglaciation and depth where glaciers have retreated over the last few decades. A ROV was used to collect images on the distribution of benthic megafauna throughout the MC. This approach was used because ROVs can access areas below glaciers and to depths that are difficult to access with SCUBA diving. Data collected during the imaging surveys were used to construct structural and functional indices, which were analyzed to determine the responses of benthic megafauna communities to glacial retreat. This study is expected to provide information on the processes driving shifts to the structure and function of the benthic megafauna community after climate-induced glacial retreat in the nearshore areas of Antarctica.

## **2.2. Materials and methods**

### **2.2.1. Study area**

Marian Cove is a small glacial fjord (length: ~4.5 km, width: ~1.5 km) on King George Island, located at the northern tip of the WAP (Figure. 2.1). The mean annual temperature was -1.8°C from 1988 to 2018 (min. -5.7°C in July, max. 1.9°C in January), and generally exceeds 0°C from December to March (Hong et al., 2019). MC has three basins with a maximum depth of ca. 130 m, and is separated from Maxwell Bay by a sill (~40 m) at its mouth (Yoon et al., 1997). The sill restricts the exchange of water masses with Maxwell Bay (Yoo et al., 2015). Seawater temperature changes seasonally (max. 1.5°C in February, min. -1.8°C in August); however, salinity remains constant year-round (33.8–34.1 psu), and tends to decrease slightly near the surface (Hong et al., 2019). There is no significant spatial variation in water temperature or salinity vary spatially in relation to distance from the glacier (-0.3 to -0.4°C, 33.9 to 34.0 psu) or water depth (-0.3 to -0.6°C, 33.9 to 34.1 psu) (Table 2.1, Table 2.2).





**Figure 2.1.**

(a) Location of Marian Cove (MC). (b) Map showing the bathymetry of MC and survey stations. MC has three basins and is separated from Maxwell Bay by a sill (~40 m) at its mouth. Glacial retreat lines were plotted based on satellite and aerial images (Kim et al., 2021). Image survey and sampling stations (black dashed boxes) were selected based on the period of exposure after glacial retreat, disturbance level, and topography. (c) Topography of MC transect. Black dashed boxes are survey stations and red lines are survey depths. (d) Survey design. Benthic images and samples were collected at six depths (10, 20, 30, 50, 70, and 90 m) at each station, except MC6 (see Table 2.3 for details). At MC6, image surveys were only conducted at 50 m and 70 m. (e) Sediment properties at six depths at each station. SOM is sediment organic matter.

**Table 2.1.**

Overview of the sampling, environmental conditions, and benthic megafauna community. Acronyms for phylum are given in parenthesis: (A) ascidian, (P) polychaeta, (B) bryozoa, (M) mollusca.

	MC2	MC3	MC4	MC5	MC6	Total
<b>Number of sampling depths</b>	6	6	6	6	2	6
<b>Number of samples</b>						
ROV	83	68	75	108	33	367
Grab	9	9	9	9	-	36
SCUBA	9	9	9	9	-	36
Trawl	1	1	1	-	-	3
<b>Environmental conditions</b>						
<b>(Mean±SD)</b>						
Distance from the glaciers (km)	3.5	1.2	0.8	0.2	0	
Period of seabed exposure (yr)	>63	32–34	18–24	8–14	<5	
Water temperature (°C)	-0.32±1.25	-0.33±1.21	-0.34±1.17	-0.40±1.13	-	-0.35±0.04
Salinity (psu)	34.01±0.08	33.96±0.08	33.96±0.08	33.99±0.09	-	33.98±0.02
Grain size (Φ)	4.08±3.00	4.13±2.19	4.90±1.95	5.14±1.03	-	4.56±0.54
Sorting (Φ)	3.00±0.85	3.29±0.58	3.48±0.40	3.37±0.49	-	3.29±0.21
Sediment organic matter (%)	0.64±0.22	0.60±0.22	0.45±0.15	0.43±0.18	-	0.53±0.11
<b>Benthic community</b>						
Number of taxa	55	44	40	26	5	70
Total mean density (ind. m <sup>-2</sup> )	87	54	96	116	29	76
Taxonomic distinctness	72.5	73.7	63.9	64.4	11.1	57.1
Functional diversity	2.9	2.2	1.8	1.3	0.1	1.7
Dominant taxa (>2%), (%)						
(A) <i>Molgula pedunculata</i>	4.2	15.5	22.8	31.0	1.1	19.8
(P) Serpulidae spp.	2.2	8.5	9.8	5.3	81.0	6.3
(A) <i>Cnemidocarpa verrucosa</i>	3.6	4.7	17.2	16.1	0.0	11.6
(A) <i>Ascidia challengeri</i>	12.8	10.6	9.9	3.3	0.0	8.5
(P) Terebellidae spp.	2.4	7.1	10.0	8.9	0.0	7.3
(B) Bryozoa sp. 5	0.9	1.1	4.9	12.3	9.4	5.8
(P) Sabellidae spp.	4.1	0.1	0.7	11.8	0.0	5.1
(M) <i>Margarella antarctica</i>	13.8	2.4	1.1	1.6	0.0	4.6
(M) <i>Laternula elliptica</i>	6.8	5.0	3.8	0.2	0.0	3.5

**Table 2.2.**

Environmental characteristics among ROV survey stations (MC2–MC6) in Marian Cove, Antarctica. \*Data were obtained from long-term monitoring project for King Sejong Station (KOPRI 2018). Water temperature and salinity data represent annual mean values. For sediment properties, mean±standard deviation values are presented.

Station	Period of sea bed exposure (yr)	Distance from glacier front (km)	Water depth (m)	Water column properties*				Sediment properties						
				Temp. (°C)	Salinity (psu)	TOC ( $n = 3$ ) (%)	TN ( $n = 3$ ) (%)	$n$	Composition (%)				Mean grain size ( $\phi$ )	Sorting ( $\phi$ )
									Gravel	Sand	Silt	Clay		
MC6	<5	0.0	50	n.a.	n.a.	n.a.	n.a.		n.a.	n.a.	n.a.	n.a.	n.a.	n.a.
			70	n.a.	n.a.	n.a.	n.a.		n.a.	n.a.	n.a.	n.a.	n.a.	n.a.
MC5	8–14	0.2	10	-0.27	33.99	0.4±0.2	0.08±0.05	13	18±7	43±3	27±2	13±1	3.6±0.5	3.5±0.3
			20	-0.27	34.03	0.5±0.2	0.09±0.04	19	3±0	22±0	50±0	25±0	6.0±0.0	2.6±0.0
			30	-0.28	34.05	0.5±0.1	0.07±0.01	16	19±7	22±2	41±3	19±2	4.4±0.7	3.8±0.3
			50	-0.32	34.07	0.3±0.1	0.03±0.01	14	12±19	16±3	44±10	28±6	5.5±2.0	3.2±0.9
			70	-0.38	34.09	0.3±0.1	0.03±0.01	16	19±7	17±1	39±3	25±2	4.9±0.7	3.9±0.4
			90	-0.58	34.15	0.3±0.0	0.03±0.01	22	8±4	12±1	44±2	36±2	6.3±0.4	3.2±0.4
MC4	18–24	0.8	10	-0.26	33.97	0.4±0.1	0.07±0.03	12	45±15	33±9	13±4	9±2	1.4±1.3	3.7±0.3
			20	-0.28	34.02	0.5±0.1	0.09±0.02	14	14±4	31±1	31±1	24±1	4.7±0.4	3.7±0.2
			30	-0.29	34.04	0.5±0.1	0.07±0.01	11	20±1	30±0	27±0	23±0	4.2±0.1	4.0±0.0
			50	-0.33	34.07	0.3±0.1	0.03±0.00	14	10±5	16±1	40±2	34±2	5.9±0.5	3.5±0.4
			70	-0.40	34.09	0.3±0.0	0.03±0.00	10	6±7	10±1	45±3	39±3	6.6±0.7	2.9±0.8
			90	-0.54	34.11	0.3±0.1	0.03±0.01	13	7±2	13±0	43±1	38±1	6.5±0.2	3.2±0.3
MC3	32–34	1.2	10	-0.22	33.97	0.7±0.1	0.12±0.01	9	58±28	12±9	18±12	11±8	0.8±2.7	3.8±1.5
			20	-0.27	34.02	0.7±0.2	0.11±0.04	11	33±27	17±7	33±13	17±7	3.2±2.5	3.8±1.3
			30	-0.29	34.04	0.7±0.1	0.09±0.02	10	36±44	9±7	35±24	20±14	3.3±4.4	2.3±1.6
			50	-0.32	34.07	0.3±0.1	0.04±0.01	13	16±19	24±6	38±9	22±5	4.6±2.0	3.6±0.6
			70	-0.45	34.09	0.4±0.0	0.05±0.01	11	10±5	12±1	48±3	30±2	6.0±0.6	3.3±0.5
			90	-0.55	34.01	0.4±0.0	0.06±0.00	11	6±6	9±1	42±3	43±3	6.9±0.7	2.9±0.8

**Table 2.2.**  
(continued)

Station	Period of sea bed exposure (yr)	Distance from glacier front (km)	Water depth (m)	Water column properties*				Sediment properties						
				Temp. (°C)	Salinity (psu)	TOC ( <i>n</i> = 3) (%)	TN ( <i>n</i> = 3) (%)	<i>n</i>	Composition (%)				Mean grain size (Φ)	Sorting (Φ)
									Gravel	Sand	Silt	Clay		
MC2	> 63	3.5	10	-0.20	34.01	0.3±0.1	0.03±0.01	11	49±21	39±16	4±2	8±3	0.4±1.6	3.1±0.9
			20	-0.25	34.04	0.6±0.3	0.09±0.05	5	29±1	51±1	12±0	8±0	2.1±0.1	3.4±0.0
			30	-0.28	34.06	0.6±0.3	0.09±0.05	7	39±2	36±1	15±0	9±0	1.9±0.1	3.8±0.0
			50	-0.35	34.09	0.7±0.1	0.09±0.01	14	16±3	13±0	42±1	29±1	5.5±0.3	3.8±0.2
			70	-0.42	34.11	0.6±0.1	0.08±0.01	10	1±1	7±0	56±0	35±0	7.1±0.0	2.1±0.1
			90	-0.47	34.13	0.6±0.1	0.08±0.01	15	1±0	5±0	55±0	39±0	7.4±0.0	1.8±0.1

Sediment properties vary with distance from the glacier and depth (Table 2.1, Table 2.2). Gravel and sand dominate at 10 m, but decline with water depth, whereas silt and clay increased sharply (Figure 2.1). At shallow depths (10–30 m), silt and clay increase with proximity to the glacier. The opposite pattern occurs with increasing depth (50–90 m), and the finest grain size (7.2–7.4  $\Phi$ ) and the most well-sorted sediment (1.8–2.1  $\Phi$ ) occur at the outermost site. There is no significant spatial variation in sediment organic matter (SOM) or sediment C/N ratio at shallow depths (10–30 m) (Figure 2.1). At greater depths (50–70 m), SOM increases and C/N ratio decreases with increasing distance from the glacier. SOM is more abundant in shallow depths than greater depths at all sites, but is similar in the outermost site.

Tidewater glaciers are well developed in the innermost part of MC. From 1956 to 2017, the glaciers collapsed during the austral summer, retreating about 1.9 km (~45% of the ice-free area) (Figure 2.1). Glacier collapse introduces large amounts of meltwater, terrigenous sediment, and icebergs to MC (Yoon et al., 1998; Ahn et al., 2004; Yoo et al., 2015). Glacial retreat proceeded more rapidly in the cove during warming periods (1989–2000: 64 m yr<sup>-1</sup>, -1.61°C) compared to cooling periods (2000–2015: 40 m yr<sup>-1</sup>, annual mean temperature -1.91°C,) in WAP (Turner et al., 2016; Oliva et al., 2017). Glacial retreats that reflect climate change trends in WAP indicate that MC is a suitable region for monitoring the impact of climate change on the marine ecosystem of WAP.

### **2.2.2. ROV data acquisition**

Five stations (MC2, MC3, MC4, MC5 and MC6) were chosen for this study (Figure 2.1, Table 2.3). For MC2 to MC5, we used seabed images of various water depths (10, 20, 30, 50, 70 and 90 m) obtained in the 2017/2018 summer using an ROV (VideoRay Pro4) equipped with a camera (GoPro Hero5, 1080P, 60fps) and a stainless-steel quadrat (50x50 cm). For MC6, seabed images were obtained in the following summer (December 2018-February 2019). The quadrat images allowing the quantitative data collection on distributions of benthic megafauna were randomly taken (at least 5 m apart) at 50 and 70 m respectively. MC6 was closest to the glacier terminus and newly exposed in recent years (<5 yr) to which was inaccessible in the previous surveys. The details of survey methods are described in 3.2.2.

**Table 2.3.**

Sampling information on water depth in each station.

Station	Survey date	Depth (m)	ROV (n)	Grab (n)	SCUBA (n)	Trawl (n)
MC2	2018	10	11	-	3	-
		20	12	-	3	-
		30	12	-	3	-
		50	18	3	-	-
		70	15	3	-	-
		90	15	3	-	1
MC3	2018	10	11	-	3	-
		20	11	-	3	-
		30	12	-	3	-
		50	13	3	-	-
		70	11	3	-	-
		90	10	3	-	1
MC4	2018	10	12	-	3	-
		20	14	-	3	-
		30	11	-	3	-
		50	15	3	-	-
		70	10	3	-	-
		90	13	3	-	1
MC5	2018	10	14	-	3	-
		20	21	-	3	-
		30	19	-	3	-
		50	16	3	-	-
		70	16	3	-	-
		90	22	3	-	1
MC6	2019	50	19	-	-	-
		70	14	-	-	-

### **2.2.3. Megafaunal community analysis**

The taxonomic composition and abundance of benthic megafauna assemblages were determined from the ROV quadrat images. All benthic megafauna that were recognizable in the images (approximately >1 cm) were counted and identified to the lowest possible level based on morphological characteristics described in the literature (Tatián et al., 1998; Hutchins et al., 2003; Tatián et al., 2005; Hibberd, 2009; Monniot et al., 2011; Alurralde et al., 2013; Danis, 2013; Monteiro et al., 2013; Rauschert and Arntz, 2015; Schories and Kohlberg, 2016; Federwisch et al., 2020), and on the database of the World Register of Marine Species (<http://www.marinespecies.org>). Infauna that could be discernable from visible portion of their bodies were also included (e.g. the bivalve *Laternula elliptica*). For colonial taxa, each colony was counted as a single individual.



#### **2.2.4. Taxonomic and functional diversities**

TD and FD of benthic megafauna assemblages at each depth for each station were calculated to assess community structure and function (Table 2.4). The number of taxa was established by simply counting the number of observed taxa in assemblages. In comparison, TD provided information on abundance and taxonomic differences across the Linnean tree (Clarke and Warwick, 1998). Therefore, TD provided a more comprehensive measure of community diversity.

FD is an effective index measuring community function (Vandewalle et al., 2010; Ricotta and Moretti, 2011). FD was calculated based on density data (Table 2.5–2.9) and a species-by-traits matrix produced on 5 biological traits and their subordinate categories which were assigned numerically (Table 2.10). The traits and categories were chosen based on the previous studies (Moon et al., 2015; Ha et al. 2019).

**Table 2.4.**

Summary of statistical analyses with purpose, data, and software.

Method	Purpose	Remark	Software
Taxonomic distinctness	Determine structural difference among benthic megafauna assemblages	Based on abundance and phylogenetic information	PRIMER 6
Functional diversity	Confirm functional diversity of benthic megafauna assemblages	Based on abundance and functional trait	R
Cluster analysis	Grouping of epibenthic megafauna assemblages	Abundance data square root transformed	PRIMER 6
nMDS	Localize assemblages in two-dimensional plot with station and depth	Abundance data square root transformed	PRIMER 6
BIOENV	Confirm the relationship among environmental parameters and megafauna distribution	Abundance data square root transformed Environmental data normalized	PRIMER 6
IndVal	Identify indicator species for each group classified by cluster analysis	$IndVal_{ij} = A_{ij} \times B_{ij} = 100$ $IndVal_i = \max [IndVal_{ij}]$	R

**Table 2.5.**

Density (ind. m<sup>-2</sup>) of epibenthic megafauna recorded from 10–90 m depth at MC2 in Marian Cove, Antarctica. Abundance data were obtained using a quadrat frame (50×50 cm) attached to the ROV and then transformed to values per square meter. Values are mean±standard error. (n): number of replicates.

Taxa	MC2					
	10 m (11)	20 m (12)	30 m (12)	50 m (18)	70 m (15)	90 m (15)
<i>Aplidium</i> cf. <i>radiatum</i>				39.6±22.4		
<i>Ascidia challengeri</i>			1.0±0.5	52.7±10.2	10.9±3.2	1.9±1.6
<i>Cnemidocarpa verrucosa</i>		1.0±1.0	16.3±5.1	1.3±1.3	0.3±0.3	
<i>Corella eumyota</i>						
<i>Distaplia</i> sp.						
<i>Molgula pedunculata</i>		2.0±2.0	18.3±6.9	1.1±0.6	0.5±0.5	
<i>Pyura</i> cf. <i>discoveri</i>					3.2±1.5	8.8±2.0
<i>Pyura setosa</i>				1.3±0.9	2.7±1.0	4.3±1.6
<i>Pyura</i> sp.1					0.8±0.6	0.5±0.4
<i>Pyura</i> sp.2					1.3±0.9	
<i>Sycozoa sigillinoides</i>			0.3±0.3			
<i>Tylobranchion speciosum</i>			6.0±3.0	2.0±0.9		
Ascidian sp.16				30.0±4.7		
Ascidian sp.17					12.5±5.7	22.7±5.0
<i>Cryptasterias</i> sp.				0.4±0.3		
<i>Diplasterias</i> sp.				0.4±0.3	0.5±0.4	0.5±0.4
<i>Odontaster validus</i>	1.1±0.8	0.7±0.4	1.0±0.5	0.2±0.2		
<i>Perknaster</i> sp.						
<i>Psilaster</i> sp.					0.3±0.3	
Asteroidea sp.3				1.3±0.5	1.1±0.5	0.3±0.3
Asteroidea sp.4					0.3±0.3	
Asteroidea sp.5	0.4±0.4			0.2±0.2		0.5±0.4
Crinoidea					0.3±0.3	0.5±0.5
<i>Abatus</i> sp.				0.2±0.2	0.3±0.3	
<i>Ctenocidaris</i> sp.				0.4±0.3	0.3±0.3	0.5±0.4
<i>Sterechinus</i> sp.						
Ophiuroidea sp.1		0.3±0.3	3.7±0.8	1.8±0.6	1.3±0.5	2.4±0.7
Ophiuroidea sp.2						0.5±0.4
<i>Mycale</i> cf. <i>acerata</i>						
Porifera sp.2					0.3±0.3	
Porifera sp.19						
Porifera sp.22						
Porifera sp.23						
Porifera sp.25						0.3±0.3
Porifera sp.26					1.3±1.1	3.2±3.2

**Table 2.5.**  
(continued)

Taxa	MC2					
	10 m (11)	20 m (12)	30 m (12)	50 m (18)	70 m (15)	90 m (15)
Porifera sp.27				2.2±2.0		
<i>Anoxycalyx</i> cf. <i>joubini</i>					0.5±0.4	
<i>Rossella</i> cf. <i>podagrosa</i>				1.8±1.0	40.5±17.8	
<i>Rossella</i> cf. <i>racovitzae</i>					0.5±0.4	0.8±0.4
<i>Rossella</i> cf. <i>villosa</i>						
<i>Reteporella</i> sp.					0.5±0.4	0.5±0.4
Bryozoa sp.5			4.7±2.1			
Bryozoa sp.6				0.4±0.4	0.5±0.4	1.1±0.6
Bryozoa sp.13					1.1±1.1	0.3±0.3
Bryozoa sp.14						
Bryozoa sp.16					0.3±0.3	
Bryozoa sp.17						
Bryozoa sp.18						0.3±0.3
Bryozoa sp.20				0.2±0.2	1.9±1.2	3.7±1.5
<i>Arntzia gracilis</i>			0.7±0.4	1.3±0.6	0.3±0.3	
<i>Tenuisis microspiculata</i>				0.4±0.4		0.3±0.3
<i>Thouarella</i> sp.					0.3±0.3	
Actiniidae sp.2					0.3±0.3	
Actiniidae sp.5						0.3±0.3
<i>Candelabrum penola</i>				0.9±0.5		
Hydrozoa sp.5					2.1±2.1	5.6±3.1
<i>Amythas membranifera</i>					0.53±0.36	5.60±2.06
<i>Flabegraviera</i> sp.			0.3±0.3		0.5±0.4	1.9±0.7
Sabellidae spp.					7.7±3.9	13.3±2.5
Terebellidae spp.		0.3±0.3	7.3±1.4	4.7±1.5	0.3±0.3	
Serpulidae spp.			2.3±2.3	3.8±3.1	5.3±4.3	
<i>Serolis</i> sp.				0.2±0.2	0.3±0.3	0.3±0.3
Pycnogonida sp.4						
<i>Laternula elliptica</i>	4.0±2.5	12.3±3.4	0.7±0.4	0.9±0.6	12.3±4.2	5.1±3
<i>Doris kerguelenensis</i>						
<i>Margarella antarctica</i>	11.3±3.3	22.7±5.9	37.7±13.3			
<i>Neobuccinum eatoni</i>						
<i>Nacella concinna</i>						
<i>Lyrocteis flavopallidus</i>				4.9±1.8	1.9±0.5	0.8±0.4
<i>Parborlasia corrugatus</i>		3.3±1.5	1.0±0.7	0.7±0.5	0.5±0.5	0.5±0.4

**Table 2.6.**

Density (ind. m<sup>-2</sup>) of epibenthic megafauna recorded from 10–90 m depth at MC3 in Marian Cove, Antarctica. Abundance data were obtained using a quadrat frame (50×50 cm) attached to the ROV and then transformed to values per square meter. Values are mean±standard error. (n): number of replicates.

Taxa	MC3					
	10 m (11)	20 m (11)	30 m (12)	50 m (13)	70 m (11)	90 m (10)
<i>Aplidium cf. radiatum</i>						
<i>Ascidia challengeri</i>		1.1±0.8	4.0±2.5	5.2±2.0	17.5±7.4	6.8±1.8
<i>Cnemidocarpa verrucosa</i>		0.7±0.7	2.3±1.2	5.5±1.9	5.5±2.7	1.2±1.1
<i>Corella eumyota</i>					1.5±1.1	
<i>Distaplia</i> sp.			1.0±0.7	0.9±0.6		0.4±0.4
<i>Molgula pedunculata</i>		3.3±2.5	6.3±4.6	27.7±8.4	5.8±2.9	7.6±3.5
<i>Pyura cf. discoveri</i>						
<i>Pyura setosa</i>						
<i>Pyura</i> sp.1						0.4±0.4
<i>Pyura</i> sp.2						
<i>Sycozoa sigillinoides</i>				0.3±0.3		
<i>Tylobranchion speciosum</i>					0.7±0.7	
Ascidian sp.16				0.6±0.4	1.1±0.8	
Ascidian sp.17					0.4±0.4	
<i>Cryptasterias</i> sp.						
<i>Diplasterias</i> sp.			0.3±0.3	0.3±0.3	0.4±0.4	
<i>Odontaster validus</i>	1.5±0.8	1.5±0.8	1.7±1.2	1.8±1.0		
<i>Perknaster</i> sp.						
<i>Psilaster</i> sp.						
Asteroidea sp.3				0.3±0.3		
Asteroidea sp.4						
Asteroidea sp.5						
Crinoidea			0.7±0.4	0.9±0.6	0.7±0.5	2.0±1.2
<i>Abatus</i> sp.						
<i>Ctenocidaris</i> sp.						
<i>Sterechinus</i> sp.	9.5±4.0	4.7±2.1	0.7±0.4	1.2±0.7		
Ophiuroidea sp.1			0.3±0.3	0.3±0.3	0.4±0.4	
Ophiuroidea sp.2						
<i>Mycale cf. acerata</i>			11.0±11.0		7.3±4.3	
Porifera sp.2		4.0±4.0	12.7±12.7			
Porifera sp.19				8.0±4.2		
Porifera sp.22		1.1±0.8	1.0±1.0			4.0±2.5
Porifera sp.23			4.0±4.0	0.3±0.3	4.0±4.0	0.4±0.4
Porifera sp.25						
Porifera sp.26						

**Table 2.6.**  
(continued)

Taxa	MC3					
	10 m (11)	20 m (11)	30 m (12)	50 m (13)	70 m (11)	90 m (10)
Porifera sp.27						
<i>Anoxycalyx</i> cf. <i>joubini</i>						
<i>Rossella</i> cf. <i>podagrosa</i>						
<i>Rossella</i> cf. <i>racovitzae</i>						
<i>Rossella</i> cf. <i>villosa</i>			0.3±0.3			
<i>Reteporella</i> sp.				0.3±0.3	3.6±1.9	2.0±1.0
Bryozoa sp.5			1.0±1.0	2.5±1.3		
Bryozoa sp.6				0.3±0.3	2.2±1.5	0.8±0.5
Bryozoa sp.13					0.4±0.4	0.4±0.4
Bryozoa sp.14				2.2±1.6		
Bryozoa sp.16					2.9±2.2	1.2±1.1
Bryozoa sp.17					0.4±0.4	
Bryozoa sp.18				0.6±0.4		
Bryozoa sp.20						
<i>Arntzia gracilis</i>						
<i>Tenuis microspiculata</i>					0.4±0.4	0.4±0.4
<i>Thouarella</i> sp.						
Actiniidae sp.2		0.4±0.4				
Actiniidae sp.5						
<i>Candelabrum penola</i>						
Hydrozoa sp.5						
<i>Amythas membranifera</i>						
<i>Flabegraviera</i> sp.		0.4±0.4	0.3±0.3	0.6±0.6		
Sabellidae spp.				0.3±0.3		
Terebellidae spp.		5.1±2.8	5.3±1.7	2.2±0.9	6.5±0.8	4.0±1.1
Serpulidae spp.				6.5±3.8	8.4±8.4	12.8±12.2
<i>Serolis</i> sp.		0.7±0.5	0.7±0.7	1.5±0.7		
Pycnogonida sp.4						
<i>Laternula elliptica</i>	13.8±7.0	1.8±1.5	0.3±0.3	0.3±0.3		
<i>Doris kerguelenensis</i>			1.0±1.0			
<i>Margarella antarctica</i>	1.1±1.1		6.7±4			
<i>Neobuccinum eatoni</i>				1.2±0.7		
<i>Nacella concinna</i>	13.5±5.4	0.4±0.4	1.0±1.0			
<i>Lyrocteis flavopallidus</i>			0.3±0.3	1.2±0.5	6.9±3.8	2.4±1.3
<i>Parborlasia corrugatus</i>	0.4±0.4			0.6±0.4	0.4±0.4	0.8±0.5

**Table 2.7.**

Density (ind. m<sup>-2</sup>) of epibenthic megafauna recorded from 10–90 m depth at MC4 in Marian Cove, Antarctica. Abundance data were obtained using a quadrat frame (50×50 cm) attached to the ROV and then transformed to values per square meter. Values are mean±standard error. (n): number of replicates.

Taxa	MC4					
	10 m (12)	20 m (14)	30 m (11)	50 m (15)	70 m (10)	90 m (13)
<i>Aplidium cf. radiatum</i>			7.3±2.7	15.5±4.7	15.6±4.6	18.2±5.8
<i>Ascidia challengeri</i>						
<i>Cnemidocarpa verrucosa</i>		22.6±14.9	35.6±8.5	18.9±4.2	9.6±3.1	12.0±2.9
<i>Corella eumyota</i>			2.9±2.2	2.4±1.5		
<i>Distaplia</i> sp.				0.8±0.8	0.8±0.5	0.3±0.3
<i>Molgula pedunculata</i>		2.0±1.4	32.7±11.7	55.7±11.2	26.0±4.4	14.5±3.8
<i>Pyura cf. discoveri</i>						
<i>Pyura setosa</i>						
<i>Pyura</i> sp.1					0.8±0.8	0.6±0.6
<i>Pyura</i> sp.2						
<i>Sycozoa sigillinoides</i>						
<i>Tylobranchion speciosum</i>			0.4±0.4	0.5±0.5		
Ascidian sp.16				11.5±2.8	0.4±0.4	
Ascidian sp.17						
<i>Cryptasterias</i> sp.						
<i>Diplasterias</i> sp.						
<i>Odontaster validus</i>	0.3±0.3		1.1±0.6	1.1±0.5	0.4±0.4	0.3±0.3
<i>Perknaster</i> sp.				0.3±0.3		
<i>Psilaster</i> sp.				0.3±0.3		
Asteroidea sp.3						0.3±0.3
Asteroidea sp.4						
Asteroidea sp.5						
Crinoidea		0.3±0.3	1.1±0.6	1.1±0.5	4.4±2.1	1.2±0.7
<i>Abatus</i> sp.						
<i>Ctenocidaris</i> sp.						
<i>Sterechinus</i> sp.						
Ophiuroidea sp.1				0.3±0.3		0.3±0.3
Ophiuroidea sp.2						
<i>Mycale cf. acerata</i>					6.0±4.0	0.6±0.6
Porifera sp.2			9.5±9.5	0.3±0.3		
Porifera sp.19				2.9±2.7		
Porifera sp.22				0.3±0.3	6.0±6.0	4.0±3.1
Porifera sp.23			1.5±1.5	0.5±0.5	0.4±0.4	
Porifera sp.25						
Porifera sp.26						

**Table 2.7.**  
(continued)

Taxa	MC4					
	10 m (12)	20 m (14)	30 m (11)	50 m (15)	70 m (10)	90 m (13)
Porifera sp.27						
<i>Anoxycalyx</i> cf. <i>joubini</i>						
<i>Rossella</i> cf. <i>podagrosa</i>						
<i>Rossella</i> cf. <i>racovitzae</i>					0.4±0.4	
<i>Rossella</i> cf. <i>villosa</i>					0.4±0.4	
<i>Reteporella</i> sp.				0.5±0.4	3.6±2.4	1.8±0.9
Bryozoa sp.5		4±2.1	15.3±7.2	7.5±3.3	1.6±1.2	
Bryozoa sp.6				1.3±0.8	8.4±3.4	2.5±1.4
Bryozoa sp.13			1.1±1.1	1.1±0.6	3.2±2.4	0.3±0.3
Bryozoa sp.14			4.0±4.0	2.7±1.9		
Bryozoa sp.16					1.2±0.6	0.6±0.6
Bryozoa sp.17						
Bryozoa sp.18						
Bryozoa sp.20						
<i>Arntzia gracilis</i>						
<i>Tenuisis microspiculata</i>					0.4±0.4	
<i>Thouarella</i> sp.						
Actiniidae sp.2				0.3±0.3		
Actiniidae sp.5						
<i>Candelabrum penola</i>						
Hydrozoa sp.5						
<i>Amythas membranifera</i>						
<i>Flabegraviera</i> sp.			0.4±0.4	0.8±0.4		0.6±0.6
Sabellidae spp.				1.6±1.6	0.8±0.8	1.5±1.1
Terebellidae spp.		2.6±0.9	7.6±1.7	14.9±3.1	12±2.1	20±6.6
Serpulidae spp.		6.9±2.9	24±15.8	15.2±6.6	9.2±7.0	0.9±0.7
<i>Serolis</i> sp.		1.4±0.7	0.7±0.7	0.5±0.5	0.4±0.4	
Pycnogonida sp.4						
<i>Laternula elliptica</i>	13.3±6.3	5.7±2.1	1.8±1	0.8±0.6		
<i>Doris kerguelenensis</i>						
<i>Margarella antarctica</i>	0.7±0.7	1.7±0.9	0.4±0.4	2.4±0.9	0.4±0.4	0.6±0.4
<i>Neobuccinum eatoni</i>						0.3±0.3
<i>Nacella concinna</i>	1.3±1.3					
<i>Lyrocteis flavopallidus</i>				0.5±0.4	2.4±1.4	1.8±1.1
<i>Parborlasia corrugatus</i>	0.3±0.3	0.6±0.4		1.1±0.8	0.4±0.4	0.3±0.3



**Table 2.8.**

Density (ind. m<sup>-2</sup>) of epibenthic megafauna recorded from 10–90 m depth at MC5 in Marian Cove, Antarctica. Abundance data were obtained using a quadrat frame (50×50 cm) attached to the ROV and then transformed to values per square meter. Values are mean±standard error. (n): number of replicates.

Taxa	MC5					
	10 m (14)	20 m (21)	30 m (19)	50 m (16)	70 m (16)	90 m (22)
<i>Aplidium cf. radiatum</i>						
<i>Ascidia challengeri</i>		0.2±0.2	6.5±2.5	7.3±2	7.3±2.9	1.6±0.9
<i>Cnemidocarpa verrucosa</i>	3.7±3.7	30.7±6.9	37.3±7.4	20.0±4.1	9.5±2.3	10.9±3
<i>Corella eumyota</i>						
<i>Distaplia</i> sp.						0.2±0.2
<i>Molgula pedunculata</i>		2.3±1.3	82.7±9.6	81.5±12.1	32.5±6.3	17.5±4.7
<i>Pyura cf. discoveri</i>						
<i>Pyura setosa</i>						
<i>Pyura</i> sp.1					1.3±0.6	
<i>Pyura</i> sp.2						
<i>Sycozoa sigillinoides</i>						
<i>Tylobranchion speciosum</i>			0.2±0.2			
Ascidian sp.16						
Ascidian sp.17						
<i>Cryptasterias</i> sp.						
<i>Diplasterias</i> sp.						
<i>Odontaster validus</i>	0.6±0.4	0.8±0.4	2.1±0.6			
<i>Perknaster</i> sp.			0.2±0.2		0.5±0.3	
<i>Psilaster</i> sp.						
Asteroidea sp.3						
Asteroidea sp.4			0.2±0.2			
Asteroidea sp.5						
Crinoidea		0.6±0.3	1.7±0.6	3.5±1.1	3.8±1.1	0.7±0.3
<i>Abatus</i> sp.						
<i>Ctenocidaris</i> sp.						
<i>Sterechinus</i> sp.						
Ophiuroidea sp.1						
Ophiuroidea sp.2						
<i>Mycale cf. acerata</i>						
Porifera sp.2						0.2±0.2
Porifera sp.19					0.3±0.3	
Porifera sp.22						
Porifera sp.23						
Porifera sp.25						
Porifera sp.26						

**Table 2.8.**  
(continued)

Taxa	MC5					
	10 m (14)	20 m (21)	30 m (19)	50 m (16)	70 m (16)	90 m (22)
Porifera sp.27						
<i>Anoxycalyx</i> cf. <i>joubini</i>						
<i>Rossella</i> cf. <i>podagrosa</i>						
<i>Rossella</i> cf. <i>racovitzae</i>						
<i>Rossella</i> cf. <i>villosa</i>						
<i>Reteporella</i> sp.				1.8±1.1	1.5±0.8	0.5±0.4
Bryozoa sp.5		5.1±3.0	74.5±11.8	6.3±3.3		0.2±0.2
Bryozoa sp.6		0.4±0.3	1.1±0.5	1.5±0.6	5.3±1.9	1.8±0.7
Bryozoa sp.13			1.3±0.6	7.8±2.8	1.8±0.8	1.8±0.7
Bryozoa sp.14			12±5.4	5.5±2.4		0.5±0.4
Bryozoa sp.16				0.3±0.3	0.3±0.3	
Bryozoa sp.17						
Bryozoa sp.18						
Bryozoa sp.20						
<i>Arntzia gracilis</i>						
<i>Tenuis microspiculata</i>						
<i>Thouarella</i> sp.						
Actiniidae sp.2						
Actiniidae sp.5						
<i>Candelabrum penola</i>						
Hydrozoa sp.5						
<i>Amythas membranifera</i>						
<i>Flabegreviera</i> sp.						
Sabellidae spp.			12.0±6.7	40.3±17.6	26.0±11.9	4.0±2.0
Terebellidae spp.	1.1±1.1	11.8±2.6	16.4±3.7	10.0±2.5	7.0±1.5	15.8±1.7
Serpulidae spp.			4.4±3.3	4.0±3.0	18.0±12.3	10.9±4.9
<i>Serolis</i> sp.					0.3±0.3	0.2±0.2
Pycnogonida sp.4						
<i>Laternula elliptica</i>	0.6±0.6	0.6±0.4				
<i>Doris kerguelenensis</i>						
<i>Margarella antarctica</i>	0.3±0.3	0.8±0.6	2.1±1.1	8.0±3.3		
<i>Neobuccinum eatoni</i>						
<i>Nacella concinna</i>						
<i>Lyrocteis flavopallidus</i>			0.2±0.2	0.3±0.3	1.0±0.6	2.0±0.5
<i>Parborlasia corrugatus</i>		0.2±0.2	0.2±0.2			0.4±0.3

**Table 2.9.**

Density (ind. m<sup>-2</sup>) of epibenthic megafauna recorded from 10–90 m depth at MC6 in Marian Cove, Antarctica. Abundance data were obtained using a quadrat frame (50×50 cm) attached to the ROV and then transformed to values per square meter. Values are mean±standard error. (n): number of replicates.

Taxa	MC6	
	50 m (19)	70 m (14)
<i>Aplidium</i> cf. <i>radiatum</i>		
<i>Ascidia challengerii</i>		
<i>Cnemidocarpa verrucosa</i>		
<i>Corella eumyota</i>		
<i>Distaplia</i> sp.		
<i>Molgula pedunculata</i>	0.6±0.6	
<i>Pyura</i> cf. <i>discoveri</i>		
<i>Pyura setosa</i>		
<i>Pyura</i> sp.1		
<i>Pyura</i> sp.2		
<i>Sycozoa sigillinoides</i>		
<i>Tylobranchion speciosum</i>		
Ascidian sp.16		
Ascidian sp.17		
<i>Cryptasterias</i> sp.		
<i>Diplasterias</i> sp.		
<i>Odontaster validus</i>		
<i>Perknaster</i> sp.		
<i>Psilaster</i> sp.		
Asteroidea sp.3		
Asteroidea sp.4		
Asteroidea sp.5		
Crinoidea		
<i>Abatus</i> sp.		
<i>Ctenocidaris</i> sp.		
<i>Sterechinus</i> sp.		
Ophiuroidea sp.1		
Ophiuroidea sp.2		
<i>Mycale</i> cf. <i>acerata</i>		
Porifera sp.2		
Porifera sp.19		
Porifera sp.22		
Porifera sp.23		
Porifera sp.25		
Porifera sp.26		

**Table 2.9.**  
(continued)

Taxa	MC6	
	50 m (19)	70 m (14)
Porifera sp.27		
<i>Anoxycalyx</i> cf. <i>joubini</i>		
<i>Rossella</i> cf. <i>podagrosa</i>		
<i>Rossella</i> cf. <i>racovitzae</i>		
<i>Rossella</i> cf. <i>villosa</i>		
<i>Reteporella</i> sp.		
Bryozoa sp.5	5.5±3.2	
Bryozoa sp.6	1.3±1.1	4.3±2.5
Bryozoa sp.13	1.3±0.9	0.3±0.2
Bryozoa sp.14		
Bryozoa sp.16		
Bryozoa sp.17		
Bryozoa sp.18		
Bryozoa sp.20		
<i>Arntzia gracilis</i>		
<i>Tenuis microspiculata</i>		
<i>Thouarella</i> sp.		
Actiniidae sp.2		
Actiniidae sp.5		
<i>Candelabrum penola</i>		
Hydrozoa sp.5		
<i>Amythas membranifera</i>		
<i>Flabegraviera</i> sp.		
Sabellidae spp.		
Terebellidae spp.		
Serpulidae spp.	45.1±19.8	3.7±2.1
<i>Serolis</i> sp.		
Pycnogonida sp.4		
<i>Laternula elliptica</i>		
<i>Doris kerguelenensis</i>		
<i>Margarella antarctica</i>		
<i>Neobuccinum eatoni</i>		
<i>Nacella concinna</i>		
<i>Lyrocteis flavopallidus</i>		
<i>Parborlasia corrugatus</i>		

**Table 2.10.**

List of biological traits for a number of categories used for assessing the functional diversity of benthic megafauna community.

Traits	Type
Adult size	Small (<5 cm)
	Small-medium (5–10 cm)
	Medium-large (10–30 cm)
	Large (>30 cm)
Mobility	Attached
	Tubed-dweller
	Burrower
	Slow moving
	Fast moving
Feeding type	Suspension/filter feeder
	Scraper/Grazer/Deposit feeder
	Scavenger
	Carnivore
	Omnivore
Association	0
	>0
Solitary/Colony	Solitary
	Colony

### **2.2.5. Statistical analysis**

Cluster and MDS analyses were used to characterize benthic megafauna groups and to localize the groups in two-dimensional space based on depth and station, respectively (Table 2.4). Indicator value (IndVal) was measured to identify indicator megafauna species within each group determined by cluster analysis (Dufrêne and Legendre, 1997). Biota-environment (BIOENV) analysis was performed to determine environmental parameters related to the distribution of benthic megafauna. PRIMER (version 6.1.16; Clarke and Gorley, 2006) was used to analyze TD, cluster, MDS, and BIOENV. FD and IndVal analyses were performed in R (version 3.4)

## 2.3. Results

### 2.3.1. Assemblages of benthic megafauna

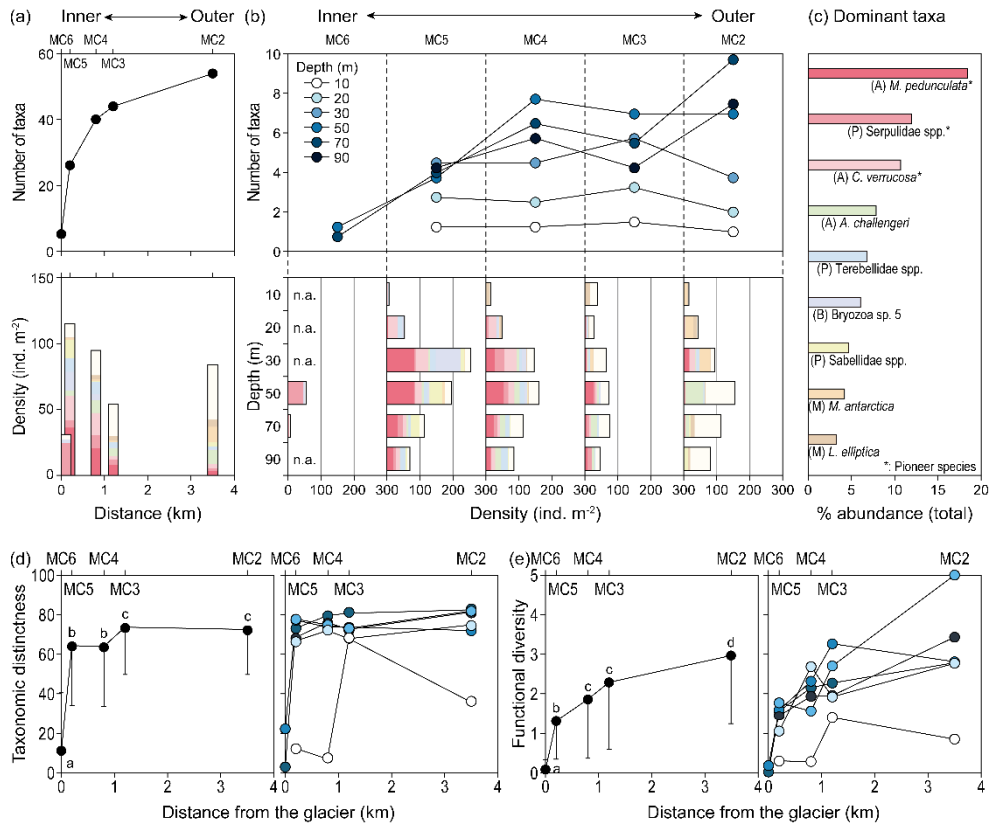
Seventy benthic megafauna taxa were identified from ROV images (Table 2.1, Table 2.5–2.9). The number of taxa at each station increased toward the outside area of the cove (Figure 2.2a). This trend was clear at 70–90 m, where taxa were most diverse (Figure 2.2b). Few taxa were present at 10–20 m, with low spatial variation.

The lowest number of individuals was recorded at the innermost site (MC6, 29.0 ind. m<sup>-2</sup>), and rapidly increased to peak at an inner site (MC5, 116.3 ind. m<sup>-2</sup>) (Figure 2.2a, Table 2.5–2.9). Pioneer species (Figure 2.2c) that appeared at the early successional stage dominated near the glacier (MC6: 82.1%, MC5: 52.4%, MC4: 50.8%), and decreased toward the outer area (MC3: 29.4, MC2: 10.4%). The most ice-proximal zone (MC6) was dominated by Serpulidae spp. (23.49 ind. m<sup>-2</sup>, 81.0%), one of the pioneer species. Sites near the glacier (MC5, MC4) were also dominated by pioneer species, and *Molgula pedunculata* was the most abundant (31.0% and 22.8%, respectively), followed by *Cnemidocarpa verrucosa* (16.1% and 17.2%, respectively). The outermost site (MC2) had the highest abundance of late successional stage species (24.5%) out of all stations, and included taxa that mainly inhabit relatively stable environments, such as *Anoxycalyx cf. joubini*, *Rossella cf. podagrosa*, *Aplidium cf. radiatum*, and *Ascidia challengerii*. Spatial variation in the density and composition of taxa was prominent below 30 m depth (Figure 2.2b). At 50–90 m depth, pioneer species clearly decreased and late successional stage species clearly increased in relation to distance from the glacier. At 20–30 m depth, this pattern was also observed, but the density of late successional stage species was very low (0–0.3 ind. m<sup>-2</sup>). At 10 m depth, which had the lowest number of individuals (0–0.3 ind. m<sup>-2</sup>), spatial variation in the composition and abundance of taxa was not clear.

TD was very low at the site closest to the glacier (Figure 2.2d), but did not differ significantly between the other stations, due to the rapid increase near the glacier. This spatial trend was observed at all surveyed depths, except 10 m. TD was lower at 10 m depth compared to all other depths. At 10 m, TD was higher in the outer sites (MC2 and MC3) compared to inner sites (MC4 and MC5), and peaked at MC3.

FD was also lowest at the innermost site, but increased with distance from the glacier (Figure 2.2e). The increasing trend toward the outside of the cove was observed at all depths, with FD peaking at 30 m depth at the outermost station (MC2). FD was lowest at 10 m depth compared to all other depths.





**Figure 2.2.**

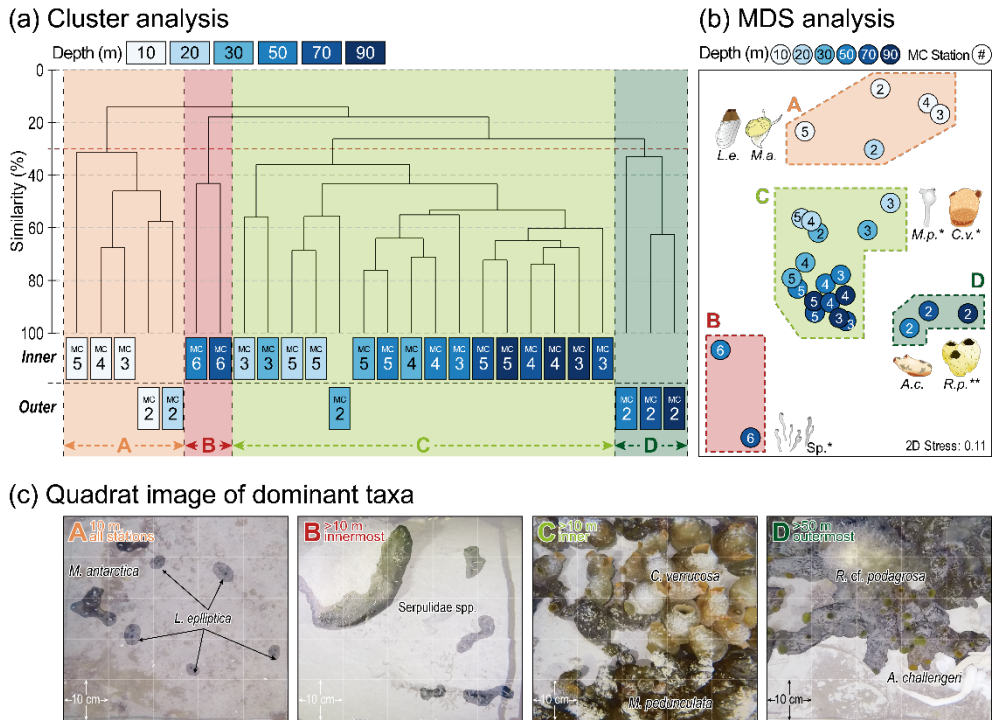
Spatial variation in the benthic megafauna community. (a) Change to the number of taxa and density in relation to distance from the glacier. (b) Variation in the number of taxa and density among stations at each depth. (c) Dominant taxa in MC (>2%). Acronyms for phylum are given in parenthesis: (A) ascidian, (P) polychaeta, (B) bryozoa, (M) mollusca. (d) Taxonomic distinctness changes with distance and depth. (e) Spatial variations in functional diversity. Vertical bars of average data indicate standard deviation. Data denoted by the same letter are not significantly different ( $p > 0.05$ ) based on the Mann-Whitney test.

### 2.3.2. Distribution characteristics of benthic megafauna

Benthic megafauna assemblages of MC were separated into four groups according to depth and distance from the glacier using cluster analysis (Figure 2.3). Sessile fauna was rare in Group A, including assemblages of 10 m and 20 m depth at MC2 (Table 2.5–2.9). Other groups, including assemblages at 20–90 m depth (B, C, and D), were dominated by sessile organisms. The groups at 20–90 m depth were distinguished by distance from the glacier and depth. Within the three groups, the dominance of pioneer species decreased and the size of individuals increased with increasing distance and depth.

The characteristics of shallow depth assemblages belonging to Group A were similar, regardless of distance. Few taxa were present (total 11 taxa), and density was also very low (24.3 ind. m<sup>-2</sup>). Three mollusk species (*Laternulla elliptica*, *Margarella antarctica*, and *Nacella concinna*) dominated group A at most stations (71.6–95.8%), except MC5 (13.6%). At MC5, near the glacier, *C. verrucosa* (pioneer species), a sessile species, was the most abundant (59.1%), but its density was very low (3.71 ind. m<sup>-2</sup>). *Sterechinus* cf. *neumayeri* had the highest density for Group A at MC3 out of all surveyed stations and depths (9.5 ind. m<sup>-2</sup>). *N. concinna* was the indicator species of Group A (Table 2.11). *L. elliptica* and *M. antarctica* contributed the most to Group A (52.7% and 31.6%, respectively).

Group B (the innermost site) had the smallest number of taxa (five taxa) out of the three groups at 20–90 m depth. Most taxa in Group B were mega-benthos from the early successional stage. The density of individuals was low (29.0 ind. m<sup>-2</sup>), and biomass was also low, because most of benthos were a thin tube-shaped Serpulidae spp. a few centimeters in size. The indicator species was Serpulidae spp. (Table 2.11), which contributed the most to Group B (90.0%).



**Figure 2.3.**

Distribution characteristics of benthic megafauna in Marian Cove. (a) Cluster analysis results showing the four groups of benthic megafauna assemblages. (b) MDS plot based on Bray Curtis similarity. Dominant taxa of each group were overlapped on the MDS plot. *L.e.*: *Laternula elliptica*, *M.a.*: *Margarella antarctica*, *M.p.*: *Molgula pedunculata*, *C.v.*: *Cnemidocarpa verrucosa*, *A.c.*: *Ascidia challengerii*, *R.p.*: *Rossella cf. podagrosa*, *Sp.*: *Serpulidae* spp. \* is early successional stage taxa. \*\* is late successional stage taxa. (c) Quadrat images showing the dominant taxa of each group.

**Table 2.11.**

Indicator megafauna species for clustered groups in Marian Cove. Given groups representing depths and distance from the glacier, such as A: ice-scouring depths of every stations (10–20 m); B: rarely scoured depths of innermost area (50–70 m); C: rarely scoured depths of inner to outer area (20–90 m); D: deep depths of outermost area (50–90 m).

Indicator taxa	Group			
	A	B	C	D
<i>Nacella concinna</i>	0.247***			
Serpulidae spp.		0.213**		
<i>Molgula pedunculata</i>			0.533***	
<i>Cnemidocarpa verrucosa</i>			0.467***	
Ascidian sp.17				0.459***
<i>Ascidia challengeri</i>				0.445***
<i>Amythas membranifera</i>				0.313***
<i>Rossella</i> cf. <i>racovitzae</i>				0.274**
<i>Rossella</i> cf. <i>podagrosa</i>				0.267***
<i>Aplidium</i> cf. <i>radiatum</i>				0.210***
<i>Anoxycalyx</i> cf. <i>joubini</i>				0.178*

\* $p < 0.05$ , \*\* $p < 0.01$ , \*\*\* $p < 0.001$

Assemblages at 20–90 m depth near the glacier (where the glacier retreated 13–33 years ago) and at 30 m at the outermost site belonged to Group C. *M. pedunculata* and *C. verrucosa* (both are pioneer species) were the most abundant species in Group C. In particular, the density was extremely high at sites near the glacier (maximum 120.0 ind. m<sup>-2</sup> at 30 m, MC5). The density of *M. pedunculata* and *C. verrucosa* decreased with increasing depth and distance from the glacier. IndVal analysis confirmed that *M. pedunculata* and *C. verrucosa* were indicator species of Group C (Table 2.11). A few *Rossella* spp. were observed at 30–90 m depth in the outer site of Group C.

Assemblages at 50–90 m depth for the outermost station (more than 60 years exposure from the glacier) belonged to Group D. Pioneer species were rare in Group D (3.4%), with late successional stage species dominating. *A. challengerii* was the most abundant species (21.8 ind. m<sup>-2</sup>), followed by *R. cf. podagrosa* (14.1 ind. m<sup>-2</sup>) and *A. cf. radiatum* (13.2 ind. m<sup>-2</sup>). Of note, *A. cf. joubini* individuals that were larger than 50 cm were only observed in Group D. Ascidian sp.17, *A. challengerii*, *R. cf. racovitzae*, *R. cf. podagrosa*, *A. cf. radiatum*, and *A. cf. joubini* were indicator species of Group D (Table 2.11).

### **2.3.3. Relationship between the benthic megafauna community and environmental parameters**

BIOENV analysis was performed to determine the environmental factors that best explained spatial variation in the benthic megafauna community (Table 2.12). MC6 lacked environmental data, and so was excluded from the analysis. BIOENV results showed that different factors affected the structure and function of the benthic community. For the composition and density of taxa, the most influential single variable was silt, followed by grain size, gravel, clay, seabed depth, sand, and distance (Table 2.12). A combination of these variables (except clay) best explained the spatial distribution of the megafauna community ( $R = 0.749$ ). TD was also most affected by silt, gravel, grain size, and sand, but was relatively less affected by depth and distance. The best combination for TD was sand and silt ( $R = 0.372$ ). In contrast, FD was less correlated to sediment composition. Distance and SOM were the most influential single factors for FD. The combination of distance and SOM best explained spatial variation in FD.

**Table 2.12.**

Biota-environment (BIOENV) analysis of the relationships between environmental factors and spatial variations in benthic megafauna in Marian Cove, Antarctica. *R*: Spearman correlation coefficient. \* indicates the best results.  $p < 0.05$ .

Community characteristic	No. of factors	R	Environmental factors						
Structure (Diversity, Abundance)	1	0.634	Silt						
	1	0.633	Grain size						
	1	0.544	Gravel						
	1	0.493	Clay						
	1	0.454	Depth						
	1	0.375	Sand						
	1	0.260	Distance						
	1	0.148	SOM						
	1	0.081	Sorting						
	1	0.030	C/N ratio						
		<b>6*</b>	<b>0.749</b>	<b>Distance</b>	<b>Depth</b>	<b>Grain size</b>	<b>Gravel</b>	<b>Sand</b>	<b>Silt</b>
Taxonomic diversity	1	0.430	Silt						
	1	0.374	Grain size						
	1	0.351	Gravel						
	1	0.316	Sand						
	1	0.286	Clay						
	1	0.257	Depth						
	1	0.020	SOM						
	1	-0.008	C/N ratio						
	1	-0.030	Distance						
	1	-0.128	Sorting						
		<b>2*</b>	<b>0.493</b>	<b>Gravel</b>	<b>Sand</b>				
Functional diversity	1	0.255	Distance						
	1	0.219	SOM						
	1	0.156	Gravel						
	1	0.138	Grain size						
	1	0.104	C/N ratio						
	1	0.081	Silt						
	1	0.060	Sand						
	1	0.054	Clay						
	1	-0.039	Sorting						
	1	-0.062	Depth						
		<b>2*</b>	<b>0.291</b>	<b>Distance</b>	<b>SOM</b>				

## **2.4. Discussion**

### **2.4.1. Spatial variation in the structure of the benthic megafauna community**

The structure of the benthic megafauna community in a deglaciated region changed with increasing depth and distance from the glacier. Benthic megafauna communities at all surveyed sites were similar at shallow depths (10 m). Low numbers of taxa and individuals were present, with sessile organisms being rare. A few *C. verrucosa* individuals (pioneer species) were observed near the glacier, and were the only sessile organisms. The mortality rate of benthic megafauna increases with the frequency of disturbance (Smale et al., 2008; Barnes et al. 2017). Therefore, benthic fauna communities in regions frequently disturbed by ice-scouring only contained pioneer species, or a few species with avoidance capabilities, and only at low abundance (Table 2.13). These characteristics limited the development and succession of communities. Ice-scouring along the Antarctic coast was concentrated at shallow depths. In particular, in MC, the shallow sill (40 m) at the entrance blocked the inflow of large draft ice from an open ocean (Yoon et al., 1997). In addition, draft ice was deposited on the shore by the wind and tide in MC (Yoo et al., 2000; Yoo et al., 2015). The accumulation of draft ice increases the amount of ice-scouring, which inhibits the growth of benthic organisms (Tatián et al., 1998; Smale et al., 2007; Barnes, 2017). As a result, the abundance and diversity of benthic megafauna communities at shallow depths in MC were low, regardless of site. Thus, if disturbance persists, the benthic megafauna community cannot mature, and early successional stages would persist, regardless of the length of exposure after glacier retreat.



**Table 2.13.**

Factors affecting benthic communities and their effects in Antarctica.

Factor	Impact type	Effect	Depth (m)	Reference
Inorganic factor	Ice scour	Physical impact	0–1000	Barnes and Souster, 2011;
				Shokr and Sinha, 2015; Barnes, 2017
				Barnes, 1995a; Gutt et al., 2001;
				Smale et al., 2008
				Brown et al., 2004; Gutt et al., 2001
				Brown et al., 2004
				Lien et al., 1989
Sea ice/Ice foot	Scour	Refer to the 'Ice scour'	0–3	
	Protect from ice scour	Benthic community formation		Rogers et al., 2012
	Light blocking	Benthic fauna density decrease due to food shortage by reduction of primary production		Thrush and Cummings, 2006
Anchor ice	Organism and sediment removal	Decrease of community diversity/density	0–33	Dayton et al., 1969
		Dominated by pioneer species and mobile species		Dayton et al., 1969;
		Restrict of community development		Rogers et al., 2012
Glacial retreat	Instable environment	Decrease of community diversity/density		Dayton et al., 1969
				Richardson and Hedgpeth, 1977;
				Gutt and Starman, 2001
				Richardson and Hedgpeth, 1977
	Sedimentation increase	Dominated by opportunistic species		Sahade et al., 2015
				Hambrey and Alean, 2004;
	Substratum gradient	Community structure change		Beaman and Harris, 2005
				Lagger et al., 2017
Depth	New habitat supply	Benthic organisms colonization		
	Ice scouring frequency change	Diversity, density and biomass of benthic community increase with depth		Barnes, 1999; Faranda et al., 2000;
				Smale et al., 2007
Freshwater	Depth increase	Community structure change		
Wave action	Inundation	Zoobenthos mortality increase		Stockton, 1984
	Turbulence	Abrasion of biota	0–10	Rogers et al., 2012
		Zoobenthos redistribution		Peck et al., 1999

**Table 2.13.**  
(Continued)

Factor	Impact type	Effect	Depth (m)	Reference	
Inorganic factor	Sediment	Slumping		Slattery and Bockus, 1997	
		Sedimentation increase	Zoobenthos motility increase Opportunistic species dominant	Sahade et al., 2015	
	Substratum type	Composition	Major factor determining community structure in areas not subjected to ice-scouring	Beaman and Harris, 2005	
	Temperature	Warming/Cooling	Growth rate increase/decrease Locomotor activity Zoobenthos motility increase	Ashton et al., 2017 Peck et al., 2006 Peck et al., 2009a, 2009b	
Organic factor	Primary Production	Food supply	Zoobenthos density increase/decrease	Thrush and Cummings, 2006	
	Macroalgae	Density	Zoobenthos density increase/decrease	Faranda et al., 2000	
	Megafauna	Settlement substrate supply	Increase of community diversity/density		Moon et al., 2015
		Siliceous mat formation (Hexactinellid)	Substrate quality change Increase of chl-a and species richness		Barthel, 1992 Barthel, 1992; Cattaneo-Vietti et al., 2000; Faranda et al., 2000
		Space and food Competition	Major factor determining community structure in areas not subjected to ice-scouring		Dayton et al., 1974
	Predation pressure	Major factor determining community structure in areas not subjected to ice-scouring		Dayton et al., 1974	

In contrast, the characteristics of deep-water communities differed with site. Most benthic individuals at the innermost site were Serpulidae spp., which were indicator taxa. Serpulidae spp. are dominant at the early stage of habitat development, because of its relatively short lifecycle and rapid recruitment (Bowden et al., 2006). The dominance of Serpulidae spp., and low individual density, indicate that environmental stress of the innermost site is severe as well as the community was colonization stage. *M. pedunculata* and *C. verrucosa* are both pioneer species that dominated the site near the glacier, resulting in their being indicator species of this area (Sahade et al., 1998; Lagger et al., 2018). Both species were abundant at frequently disturbed regions, or early successional stages, due to their growing faster than other ascidians and having a relatively short life span (~3.4 years) (Kowalke et al., 2001). High densities of *M. pedunculata* and *C. verrucosa* have frequently been reported at newly exposed areas in Antarctica (Sahade et al., 1998; Lagger et al., 2018). *M. pedunculata* also recruits rapidly in disturbed areas (Barnes and Conlan 2007; Gutt et al., 2013). The noticeable increase of *M. pedunculata* and *C. verrucosa* near the glacier indicates that the site was exposed to severe environmental stresses, with the benthic community being at an early successional stage.

However, pioneer species were rare at the outer site, where *A. challengeri*, colonial ascidians, and glass sponges dominated. *A. challengeri* occurs at low abundance in unstable environments (Gutt et al., 2013; Lagger et al., 2018). In MC, although *A. challengereri* was observed at all sites below 20 m depth, it was abundant at the outer site, which had a more stable environment. The high density of colonial ascidians (*A. cf. radiatum* and Ascdiaceae sp. 17) indicated that the outermost site had been stable for longer than the area closer to the glacier, which was mostly occupied by solitary ascidians. This is because colonial ascidians reproduce by budding, resulting in their dispersion lagging compared to the external fertilization of solitary ascidians (Svane and Young, 1989; Ayre et al., 1997; Lambert, 2005; Teixidó et al., 2007). Because glass sponges have a very long lifespan (>10000 years) and slow growth, they need to inhabit a stable environment (Dayton, 1979; McClintock et al., 2005; Trush et al., 2006). In addition, glass sponges contribute to community diversity by providing habitats and food to symbionts and spongivorous, respectively, in addition to forming 3D silica mats that become habitats for other organisms

(McClintock et al., 2005; Maldonado et al., 2017). The characteristics of indicator taxa (*A. challengeri*, colonial ascidians, glass sponges) and the community structure with very low density of pioneer species and various taxa showed that the outer site had been stable for a long time, with a mature benthic megafauna community.

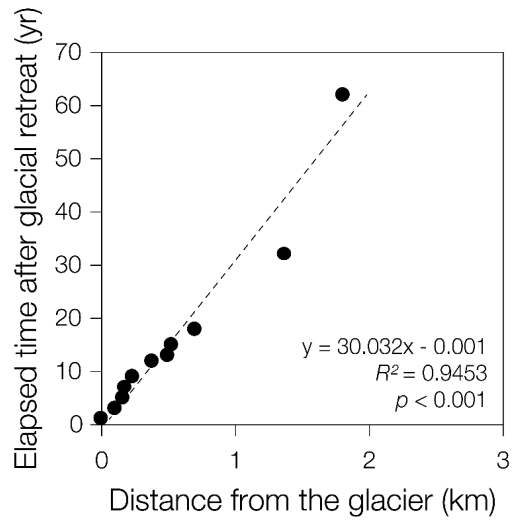
The size of individuals also indicated that the successional stages of benthic megafauna communities differed with distance from the glacier. *M. pedunculata* and *C. verrucosa* were the dominant species near the glacier, and were 10–20 cm in size, with relatively short lifespans (~3.4 years) (Kowalke et al., 2001). In contrast, *A. cf. joubini* (glass sponge) individuals that were larger than 50 cm were observed at the outermost site. The presence of large individuals of slow-growing glass sponges indicated that the outermost site had been stable for longer than the inner sites. Even for same species, the average size of individuals increased toward the outer area of the cove (Kim et al., 2021). This result supports that the average lifespan of benthic megafauna was longer at the outer site compared to the inner sites near the glacier, and that the environment was also more stable.

BIOENV analysis showed that the composition and abundance of species in the benthic megafauna community were significantly related to sediment composition, grain size, water depth, and distance from the glacier (Table 2.12). Shallow areas in MC were exposed to high environmental stresses due to the inflow of suspended particles and fluctuation of water temperature and salinity by meltwater, as well as physical impact by ice-scour (Yoon et al., 1998). The influence of glacial retreat (and consequent processes) decreased with increasing distance from the glacier (Yoon et al., 1998; Yoo et al., 2015). Sediments at the deeper and outer sites were better sorted and contained more silt and clay than those near the glacier (Table 2.2). The environmental characteristics supported that greater depths of the outermost site were more stable than the inner sites (Kim et al., 2021). Notably, in MC, distance to the glacier not only represented just space but also reflected the period of habitat formation because the distance was proportional to the exposure period of the seabed from the glacier (Figure 2.4). Therefore, the BIOENV results indicated that both stability and the formation period of habitat were major factors structuring the benthic megafauna community in this deglaciated fjord.

Spatial variation in TD was only significant at the innermost site. The low TD of the ice-proximal zone was caused by the lower average number of taxa (0.02 taxa m<sup>-2</sup>) and lower density (29.0 ind. m<sup>-2</sup>) compared to other sites (1.3–2.1 taxa m<sup>-2</sup>, 54.4–116.3 ind. m<sup>-2</sup>). Other sites had similar numbers of taxa from high classification levels (Phylum: 2.9–3.5, Class: 3.1–3.9), despite different exposure periods (~13 to >63 years). Although the number of ascidians was 1.5–2 times greater at the outermost site compared to the innermost site, they minimally contributed to the increase in TD, because all taxa belonged to the same class (Asciacea). There were 4–9 times more mollusks at the outermost site compared the innermost site; however, all mollusks were gastropods and bivalves, which are taxonomically similar, and so contributed little to the increase in TD. Most species belonging to the same order or class had similar morphology, structure, or function. Thus, the benthic megafauna community rapidly matured (within about 10 years) after the colonization in high classification levels.

Depths of 10 m had lower TD than other depths (Figure 2.2d). The low number of taxa and density likely arose due to frequent disturbance, causing TD to decrease. The outer sites had higher TD than inner sites at 10 m depth. TD might have increased because more classes were present at the outer site (MC2: 1.4 class, MC3: 2.2 class) compared to the inner site (MC4: 0.8 class, MC5: 0.4 class). The TD of MC3 was particularly high, due to the taxonomic diversity of the communities at high classification levels by *S. cf. neumayeri*, which was only observed at this site.

TD was mainly related to sediment properties, rather than distance from the glacier (Table 2.12). In particular, the combination of sand and silt content best explained spatial variation in TD. Sedimentation rates might have been lower at the outer site compared to the site near the glacier because sediment particles decreased with increasing distance from the source. Therefore, fine and well-sorted sediments at the outermost site indicated that the environment had been stable for a long period. Thus, sand and silt explaining TD meant that sediment composition reflected the physical stability of habitats.



**Figure 2.4.**  
Correlation between distance from the glacier and elapsed time after deglaciation.

#### **2.4.2. Changes to the functional diversity of the benthic megafauna community in the deglaciated fjord**

In this study, we provided that spatial variation of FD based on quantitative data for benthic megafauna communities inhabiting glacial retreated fjord, Antarctica for the first time. FD of the marine benthic ecosystem was low in high stressed environments and increased as community succession progressed (Dykman et al., 2021; Wang et al., 2021). Benthic megafauna communities of inner sites had the highest density (95.6–116.3 ind. m<sup>-2</sup>); however, the functional traits of observed taxa were monotonous (Table 2.5–2.9, Table 2.14). Most benthic megafauna recorded near the glacier were filter feeders (87–89%) of 10–30 cm body size (71–77%). In contrast, although the density of benthic megafauna was lower in the outer sites of the cove (54.4–86.6 ind. m<sup>-2</sup>), the communities at these sites had relatively diverse functional traits, due to lower bias to certain functional traits (Table 2.14). The glacier impacted the outermost site of the cove less, resulting in lower environmental stresses, which allowed a longer period for habitat formation. This shows that FD shifted with the colonization period of the benthic community and the stability of the environment after glacial retreat. This result was supported by the BIOENV results, which showed that distance from the glacier reflecting the period of exposure after deglaciation was a major factor correlated to FD (Table 2.12).

**Table 2.14.**

Relative abundance of functional traits (%) in each station.

Trait	Type	Station			
		MC2	MC3	MC4	MC5
Adult size	Small (<5 cm)	28.72	20.00	21.29	21.99
	Small-medium (5–10 cm)	14.22	11.41	1.75	0.99
	Medium-large (10–30 cm)	47.40	57.34	71.49	76.75
	Large (>30 cm)	9.66	11.25	5.47	0.27
Mobility	Attached	61.99	57.43	70.00	69.43
	Tubed-dweller	9.86	15.65	20.45	26.05
	Burrower	6.78	4.99	3.78	0.16
	Slow moving	0.10	0.11	0.05	4.36
	Fast moving	21.27	21.82	5.72	0.00
Feeding type	Suspension/filter feeder	76.73	75.75	86.55	88.69
	Scraper/Deposit feeder	18.00	14.41	11.58	10.51
	Scraper/Deposit feeder + Scavenger	0.00	4.93	0.00	0.00
	Scavenger	1.30	2.06	0.61	0.49
	Scavenger + Carnivore	0.24	0.38	0.05	0.00
	Carnivore	0.00	0.00	0.00	0.00
	Carnivore + Omnivore	3.38	1.86	1.15	0.17
Association	0	72.23	64.42	48.92	37.68
	>0	27.77	35.58	51.08	62.32
Solitary/Colony	Solitary	63.08	73.96	81.08	81.10
	Colony	36.92	26.04	18.92	18.90
Total number of traits		19	20	19	17

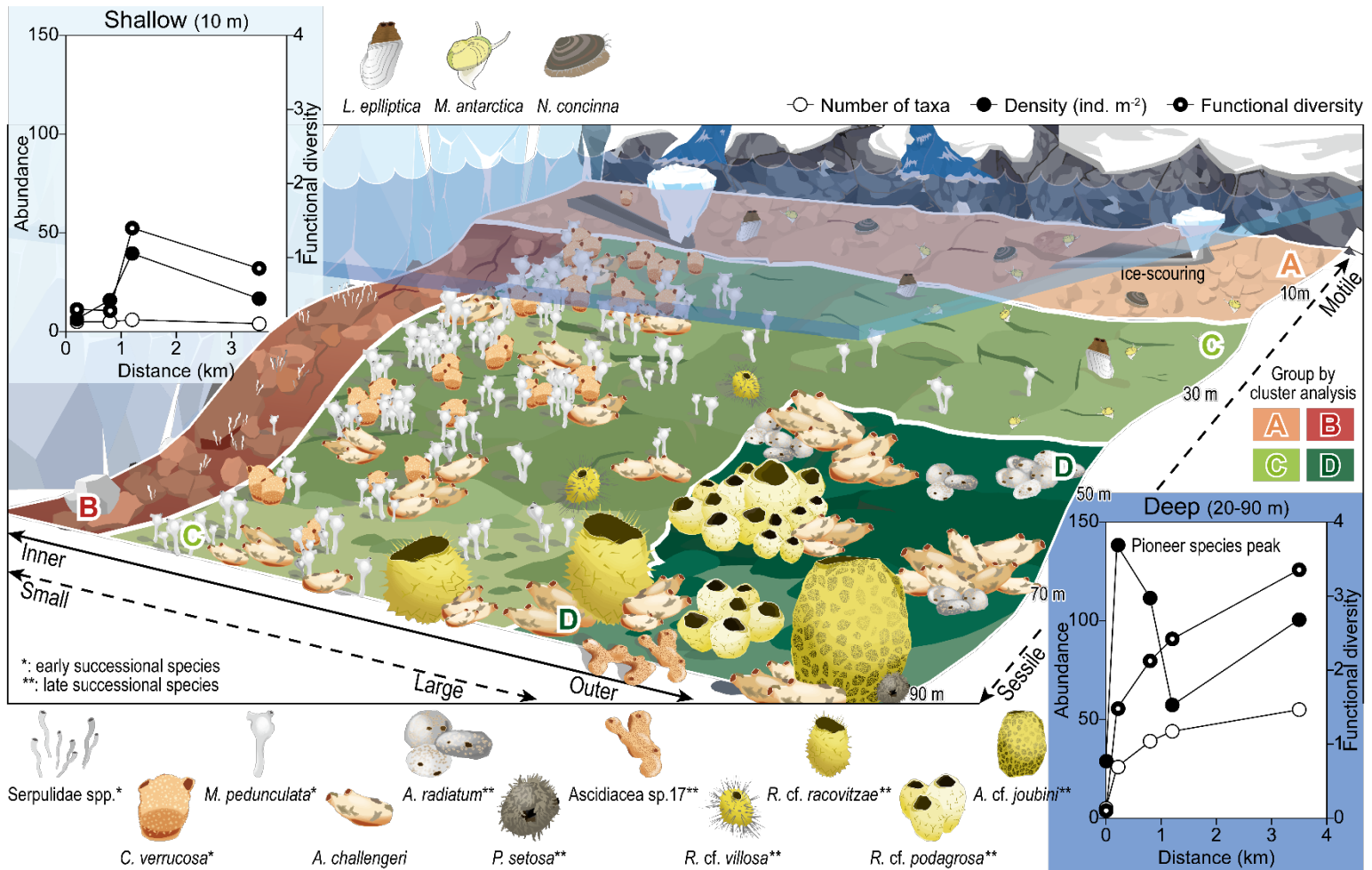


Benthic megafauna communities of 10 m had lower FD compared to other communities occurring at greater depths, and had relatively low spatial variation (Figure 2.2e). The environment at 10 m depth was subject to high stress due to the influx of meltwater and sediments, especially frequent ice-scour accompanied by glacial retreat. It is reported that FD decreases with increasing environmental stress, with the biological/ecological characteristics of organisms becoming similar in highly constrained environments (Statzner et al., 2004; Hewitt et al., 2014). The composition of benthic communities was similar at 10 m depth in MC, being dominated by gastropods and bivalves, except for the inner site (MC5), which had the lowest abundance (Table 2.5–2.9). Because most dominant taxa were small motile mollusks, functional traits were similar. It seems that benthic communities and FD of shallow depths had become monotonous due to the high stress caused by severe disturbance.

Although FD tended to increase when environmental stress declined, it peaked at 30 m depth in the outmost site (Figure 2.2e). Most individuals at 50–90 m depth in the outermost site, with the most stable environment, were filter feeders (91.7%). This phenomenon was attributed to food sources for benthic fauna being limited. The organic contents of suspended matter and sediments was major food sources for the benthic fauna due fewer macroalgae and microphytobenthos occurring with increasing depth, as photosynthesis was inhibited. Compared to 10 m depth, the environment was more stable at 30 m depth, where ice-scour had no effect, and supported a higher abundance of macroalgae and microphytobenthos (Ahn et al., 2016; Ko et al., 2020). The abundance of macroalgae and microphytobenthos in this area enhanced the availability of food for benthic megafauna. The feeding type of benthic megafauna at 30 m depth in the outermost site was relatively diverse, because there were fewer filter feeders (49.8%) and more grazer/deposit feeders (44.9%) present compared to 50–90 m depth. This shows that FD was influenced by both environmental stability and food availability. BIOENV analysis revealed that distance from the glacier reflecting environmental stability and SOM were significantly related to FD variation, supporting the concept that habitat stability and food availability are important factors driving shifts in the FD of benthic megafauna communities after glacial retreat in an Antarctic fjord.

### **2.4.3. Impact of glacial retreat on the benthic community**

Given that, in Marian Cove, the distance from the glacier was proportional to the period of exposure of the seabed after deglaciation (Figure 2.4), the spatial distribution of benthic megafauna communities reflected the long-term successional processes of communities that occurred in the past. Benthic megafauna communities in shallow depths exhibited low variation in structure and function in relation to the period after glacial retreat (Figure 2.5). In Antarctica, shallow depths are frequently disturbed by deglaciation and consequent processes, especially ice-scouring (Smale et al., 2007). Ice-scour is a major factor determining the structure of benthic megafauna communities in Antarctica (Gutt, 2001; McClintock et al., 2005), increasing mortality and reducing biomass (Smale et al., 2007; Barnes and Souster, 2011; Barnes, 2017). Consequently, benthic communities of simple structure and function are likely maintained because density was low and functionally similar species with motility to evade disturbances and/or return quickly after environmental changes dominated, regardless of the habitat formation period (Table 2.13). This shows that the structural and functional diversity of benthic communities declines when continuous glacial retreat induces an increase in disturbance. A decline in benthic fauna reduces secondary production, with immobilized benthic carbon potentially generating positive feedback on global warming.



**Figure 2.5.**

Schematic summarizing the benthic megafauna community in a glacial retreated fjord in Antarctic nearshore. The illustration shows the distribution of benthic megafauna including abundance of key taxa and functional changes to communities. The shifts in number of taxa, density, and functional diversity of the communities according to distance from the glacier at shallow and deep depths were respectively plotted in the two graphs. The words under the dotted lines indicate the characteristics of the benthic megafauna communities.

Benthic megafauna communities occurring at greater depths (rarely ice-scoured depths) in Antarctica had a distinctly different structure and function, depending on the period after glacial retreat, and were separated into three stages. At the colonization stage (beginning), the benthic community had the lowest number of taxa and abundance; however, the number of individuals peaked following a sharp increase in pioneer species (*Serpulidae* spp., *M. pedunculata*, and *C. verrucosa*). At the transition stage, the density decreased because of a decline in pioneer species, and the number of taxa increased, because certain megafauna that inhabit relatively stable environments appeared. The benthic communities of the maturing stage had a small number of pioneer species and had abundant slow-growing and/or slow-recruiting taxa (glass sponges, colonial ascidians). The lifespan and body size of individuals increased at the maturing stage. FD was low at the colonization stage, which was dominated by pioneer species with similar functional traits, whereas it increased and peaked as the community shifted to the maturing stage. This indicates that the succession of benthic megafauna communities in Antarctica progressed in newly exposed areas from the glacier depending on the time that had elapsed after deglaciation. This also shows that both the structure and function of benthic megafauna should be considered to understand how the community responds to environmental changes, because the mechanisms of change in structure and function are different.

This study provides information on the process of structural and functional changes in the benthic megafauna communities of newly exposed areas following glacier retreat in the Antarctic. In particular, our results indicate that, if ongoing global warming exacerbates disturbance through glacial retreat, the diversity and succession of benthic megafauna communities would be interrupted in these disturbed regions, especially at ice-scouring depths. A decline in benthic fauna might contribute to global warming by reducing secondary production and immobilized benthic carbon (Barnes, 2017). However, newly exposed areas were colonized by a new benthic community, with the structure and function of the community shifting in relation to the time that had elapsed after glacial retreat. Newly formed benthic communities absorb carbon corresponding to their biomass (Barnes et al., 2020). As the lifespan and body size of individuals increases with community succession,

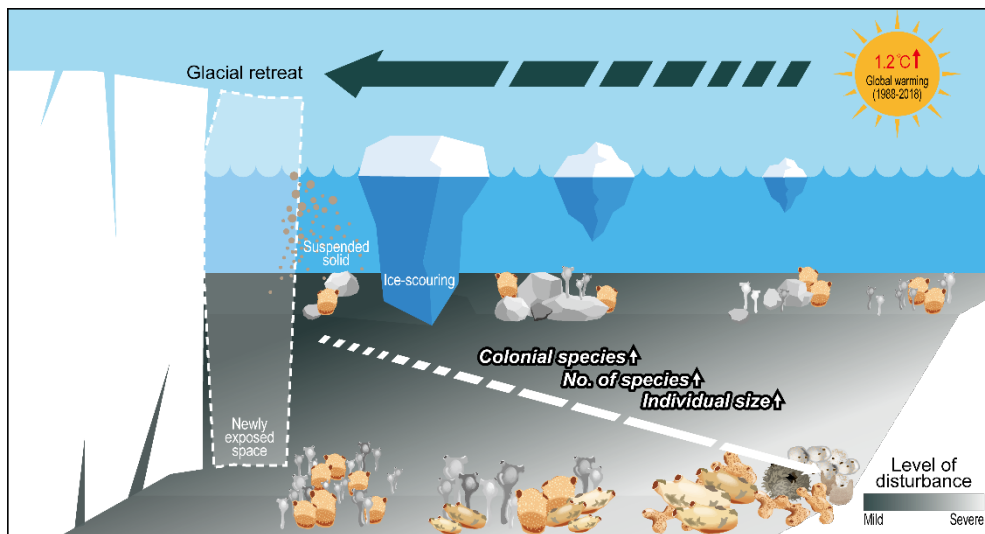
carbon storage capacity might also increase. Of note, glass sponges that live longer than 10,000 years can store carbon for a very long time. Therefore, glacial retreat might generate both negative and positive feedback to global warming. Global warming and glacial retreat are expected to proceed over the next decade, or even longer, particularly in the WAP (Clem et al., 2020; Pörtner et al., 2019). This study on the structural and functional shift of benthic megafauna community in relation to glacial retreat provides new insights on how global warming will impact and alter the Antarctic ecosystem.

## **2.5. Conclusions**

This study showed that shifts in both the structure and function of the benthic megafauna community in an Antarctic deglaciated fjord varied with depth and distance from the glacier. These findings were based on ROV surveys of assemblages in entire region of Marian Cove, where climate change of WAP was reflected in glacial retreat. The development of the communities was limited at shallow depths, due to frequent disturbance. At greater depths, where the influence of the glacier differed according to distance, benthic communities shifted to the maturing stage, via colonization and transition stages. Community structure was mainly affected by physical stability and the habitat formation period, but function was also affected by food availability. Thus, it is important to obtain information on both the structure and function of benthic megafauna communities to determine their responses to environmental changes, because the mechanisms driving shifts in structure and function are different. In particular, this study demonstrated that benthic megafauna with different sensitivities to environmental changes could be used as valuable and suitable indicators of the impact of glacial retreat induced by climate change in Antarctica. Given that the distance from the glacier was proportional to seabed exposure time in Marian Cove, spatial variation in the benthic megafauna community across the area indicates the successional processes that occurred in the past after glacial retreats. In conclusion, this study provides a basis for predicting future scenarios of the response of benthic ecosystems to climate change in the Antarctic.

## CHAPTER 3.

# PATTERNS, DRIVERS AND IMPLICATIONS OF ASCIDIAN DISTRIBUTIONS IN A RAPIDLY DEGLACIATING FJORD, KING GEORGE ISLAND, WEST ANTARCTIC PENINSULA



This chapter has been published in *Ecological Indicators*.

Kim, D. U., Khim, J. S., & Ahn, I. Y. (2021). Patterns, drivers and implications of ascidian distributions in a rapidly deglaciating fjord, King George Island, West Antarctic Peninsula. *Ecological Indicators*, **125**, 107467.



### 3.1. Introduction

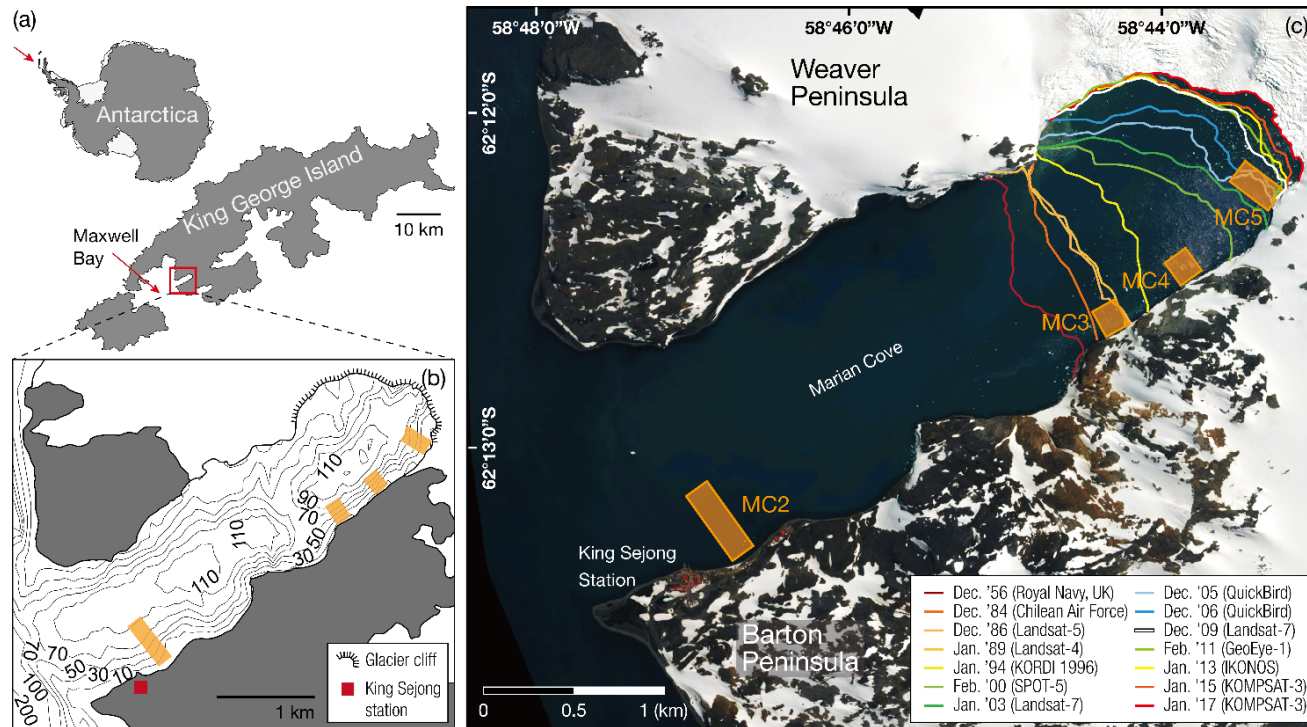
The West Antarctic Peninsula (WAP) has warmed significantly over the last half century and, consequently, both marine-terminating and land glaciers have been rapidly shrinking (Cook et al. 2014; Rignot et al. 2019). In particular, marine-terminating glacial retreat, which is accompanied by a variety of processes, including ice scouring and inflow of sediment-laden meltwater, appears to exert a profound influence on coastal marine ecosystems by altering habitat environments, and eventually impacting inhabitants (Smale and Barnes 2008). Slow-moving or sedentary benthic communities in shallow nearshore areas are most vulnerable to these processes with their species richness and diversity strongly impacted (Siciński et al. 2012; Moon et al. 2015; Sahade et al. 2015). On the other hand, some opportunistic species colonize rapidly newly exposed habitats after glacial retreat (Peck et al. 2010; Quartino et al. 2013; Lagger et al. 2018). Thus, biological response to glacial retreat is highly species specific, which complicates assessment of the overall ecosystem response. Therefore, selection of sentinel organisms that can be used to assess reliably the responses of benthic communities to glacial retreat and to predict future shifts in overall benthic communities is of critical concern.

Ascidians are among the most common benthic fauna in the Antarctic, with a broad distribution from shallow to deep waters (Primo and Vazquez 2014; Segelken-Voigt et al. 2016). In particular, they have been found to occur at high densities around the South Shetland archipelago, including King George Island (KGI) (Sahade et al. 1998; Tatián et al. 1998; Lagger et al. 2018). They colonize rapidly through fast growth and reproduction in areas that are newly exposed after glacial retreat (Teixidó et al. 2004; Sahade et al. 2015; Lagger et al. 2017). Some ascidian species act as foundation species by stabilizing habitat for other species or providing substrates for their own juveniles as well as other species (Lagger et al. 2018). Ascidians are also one of the dominant sessile suspension feeders in Antarctic epibenthic megafaunal communities (Gili et al. 2006), and they appear to act as an important mediator of energy transfer between the pelagic and benthic ecosystems (Gili et al. 2001). Together, these characteristics make ascidians excellent organisms for monitoring changes in Antarctic benthic ecosystems. Nonetheless, their distribution and its determinants have rarely been studied particularly in relation to climate-induced

processes such as glacial retreat.

Marian Cove (MC) is a rapidly warming and deglaciating fjord in the WAP, where tidewater glaciers have retreated approximately 1.9 km over the last six decades (Figure 3.1). Benthic faunal assemblages in MC well represent those in shallow Antarctic waters with dominant occurrence (~60%) of suspension feeders, such as ascidians, bryozoans and demosponges (Moon et al. 2015). Moon et al. also demonstrated that glacial retreats have altered habitat properties and consequently impacted the species number and functional diversity of megabenthic communities in the area adjacent to glacier front, and suggested that MC could serve as a model ecosystem for climate-related studies. Further studies on the megabenthic communities in the cove revealed a unique and highly efficient trophic structure based on benthic diatom blooms in association with a variety of filter feeders, including ascidians, sponges and polychaetes (Ahn et al. 2016; Ha et al. 2019). Thus, the previous studies strongly suggested that ascidian communities in this fjord play a key role in terms of both structural and functional aspect. However, quantitative data on ascidian spatial patterns, particularly those on their abundance are scarce, which warrants further studies into their spatial patterns and the determinants as well as their relevance to glacial retreat. Moreover, those previous studies have been conducted only at shallow waters (<35 m) and little is known for benthic communities at deeper waters (a maximum depth of 130 m).

The objectives of this study are to characterize the spatial patterns of ascidians in MC and to identify key drivers structuring the communities, and furthermore to assess their relevance to glacial retreat, with the aim of facilitating their use and enhancing their value for climate-related studies. We used a remotely operated vehicle (ROV) for the first time in MC at depths that were not reachable by SCUBA diving surveys in previous studies. Using the ROV survey, we obtained quantitative images of benthic communities at several sites at varying distance from the glacier front across almost the entire water depth profile.



**Figure 3.1.**

(a) Map showing the locations of King George Island, Maxwell Bay, and its tributary embayments including Marian Cove (MC). (b) Bathymetry of MC. The bathymetric contours were constructed from data obtained through a seismic survey (KOPRI 2011). The area in white represents glacier or snow cover. (c) ROV survey and sampling stations (MC2, MC3, MC4, and MC5) in orange squares and glacial retreat lines over six decades. Glacial retreat lines were drawn based on information obtained from satellite images and aerial photographs (updated from Moon et al. 2015).

## 3.2. Materials and methods

### 3.2.1. Study area

Marian Cove, where King Sejong Station ( $62^{\circ} 13' \text{ S}$ ,  $58^{\circ} 46' \text{ W}$ ) is located, is a small and confined fjord-like embayment ( $\sim 4.5 \text{ km}$  long and  $\sim 1.5 \text{ km}$  wide,  $\sim 130 \text{ m}$  deep) within Maxwell Bay at KGI. KGI is the largest island of the South Shetland Islands, which are located off the northern tip of the WAP (Figure 3.1). KGI has a relatively mild maritime climate, and meteorological data from King Sejong Station over recent decades (1988–2018) show an average annual air temperature of  $-1.8^{\circ}\text{C}$  (min= $-5.7^{\circ}\text{C}$  in July, max= $1.9^{\circ}\text{C}$  in January), and generally  $>0^{\circ}\text{C}$  from December through March (KOPRI 2018).

Seawater temperature in MC varies seasonally from a maximum of ca.  $1.5^{\circ}\text{C}$  in February to a minimum of ca.  $-1.8^{\circ}\text{C}$  in August (see the section 3.2.5). Salinity remains fairly constant from, 33.8 to 34.1 psu, throughout the year, with the tendency to increase slightly toward the bottom (see the section 3.2.5). Water circulation appears very limited except during the summer months (Chang et al. 1990), and exchange of water masses with Maxwell Bay is restricted by a shallow sill ( $\sim 70 \text{ m}$ ) at the entrance of the cove that bathymetrically separates MC from Maxwell Bay (Yoo et al. 2015). Further information on the hydrographic features of MC during summer has been reported by Yoo et al. (2015).

Tidewater glaciers are well developed in the inner part of MC, and these glaciers have retreated approximately  $1.9 \text{ km}$  from 1956 to 2017, leaving  $\sim 45\%$  of its bottom ice free (Figure 3.1). Glacier break-up occurs throughout the summer months (December through March), introducing large volumes of turbid meltwater and icebergs into the cove (Yoon et al. 1998; Ahn et al. 2004; Yoo et al. 2015). A large amount of meltwater is introduced also from the surrounding snowfield throughout the summer months (personal observation). The glaciers in MC are likely to be susceptible to small oscillations in air temperature, as observed at other sites in the northern WAP (Turner et al. 2016; Oliva et al. 2017), corroborating the utility of MC as a site monitoring climate impacts on marine ecosystem in the northern WAP. Notably, glacial retreat in the cove slowed during the cooling period ( $40 \text{ m yr}^{-1}$ , with mean annual temperature of  $-1.91^{\circ}\text{C}$  in 2000–2015), as compared with the preceding

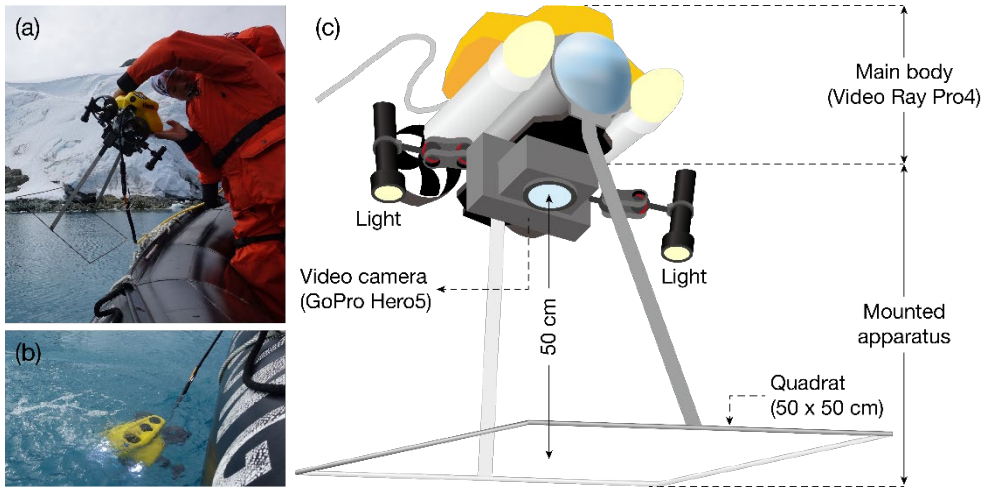
warmer period ( $64 \text{ m yr}^{-1}$  with  $-1.61^\circ\text{C}$  in 1989–2000) (see the section 3.2.5 for the data acquisition).

### 3.2.2. ROV survey and sampling

Epibenthic megafaunal assemblages and seabed sediment characteristics were determined from underwater photographs. In-situ images of epibenthic megafauna and substrate types were obtained to depths of 90 m using an ROV (VideoRay Pro4) operated from a rubber boat from December 2017 to February 2018. The ROV was equipped with a video camera (GoPro Hero5), and a stainless-steel quadrat (50×50 cm) was mounted on the ROV frame to obtain quantitative data on the epifaunal distribution and seabed sediment composition (Figure 3.2).

ROV survey stations (MC2, MC3, MC4, and MC5; Figure 3.1) were selected based on the previous reports of the level of glacial influence, bottom topography, distance from the glacier terminus, and the time period (in years) of seabed exposure after glacial retreat (Ahn et al. 2004; Moon et al. 2015; Yoo et al. 2015). At each station, the ROV was descended from a boat along the bottom slope in a direction roughly perpendicular to the shoreline, and seabed images within the quadrat frame were taken from each of six water depths (10, 20, 30, 50, 70, and 90 m). The area surveyed by the ROV spanned over 90 m depth and 200 m wide at each station. For obtaining unbiased representative images, images were taken from flat bottom and the distance between the images was kept at least 5 m. Due to differences in slope and bottom topography, total number of images taken (10–22; Table 3.1–3.5) at each depth varied among the stations. Intertidal and shallow (<10 m) subtidal bottom areas that were composed mainly of gravels were excluded from this study, as they were nearly devoid of large animals.

Ascidian samples were collected by divers and using a dredge from the R/V Araon to aid with species identification in images taken by the ROV. Sediment samples were also collected by divers using a hand-held corer (6.5 cm in diameter, 6 cm in length) (<30 m depths) and from a boat (>30 m depths) with a Van Veen grab (0.05 m<sup>2</sup> in surface area, maximum depth of 15 cm) to supplement the seabed substrate information obtained from the ROV images. The sediment samples were also used for analysis of organic matter content as described below.



**Figure 3.2.**

(a), (b) ROV (VideoRay Pro4) operated from a rubber boat; (c) ROV equipped with an external video camera (GoPro Hero5), a pair of downward lights and a stainless-steel quadrat (50×50 cm).

**Table 3.1.**

Taxonomic composition and abundance (ind. m<sup>-2</sup>) of epibenthic megafauna recorded from 10-90 m depth at MC2 in Marian Cove. Data were obtained from underwater photographic images collected using a remotely operated vehicle (ROV) during the period of December 31st, 2017, to February 12th, 2018. Abundance data were obtained using a quadrat frame (50×50 cm) attached to the ROV and then transforming the data to values per square meter. Values are mean±standard error. (n): number of replicates.

Taxa	MC2					
	10 m (11)	20 m (12)	30 m (12)	50 m (18)	70 m (15)	90 m (15)
<b>Chordata</b>						
<b>Class Ascidiacea</b>						
<i>Aplidium</i> cf. <i>radiatum</i>				39.6±22		
<i>Ascidia challengerii</i>			1.00±0.5	52.7±10	10.9±3	1.87±1.6
<i>Cnemidocarpa verrucosa</i>		1.00±1.0	16.3±5	1.33±1.3	0.27±0.27	
<i>Corella antarctica</i>						
<i>Distaplia</i> sp.						
<i>Molgula pedunculata</i>		2.00±2.0	18.3±7	1.11±0.6	0.53±0.53	
<i>Pyura</i> cf. <i>discoveri</i>					3.20±1.5	8.80±2.0
<i>Pyura setosa</i>				1.33±0.9	2.67±1.0	4.27±1.5
<i>Pyura</i> cf. <i>bouvetensis</i>					0.80±0.58	0.53±0.36
<i>Pyura</i> sp.1					1.33±0.9	
<i>Sycozoa sigillinoides</i>			0.33±0.33			
<i>Tylobranchion speciosum</i>			6.00±3.0	2.00±0.9		
Ascidacea sp.16				30.0±5		
Ascidacea sp.17					12.5±6	22.7±5
<b>Total</b>		3.0±2.2	42±7.4	128±24.6	32±8.5	38±5.8
<b>Echinodermata</b>						
<b>Class Asteroidea</b>						
<i>Cryptasterias</i> sp.				0.44±0.30		
<i>Diplasterias</i> sp.				0.44±0.30	0.53±0.36	0.53±0.36
<i>Odontaster validus</i>	1.09±0.8	0.67±0.45	1.00±0.5	0.22±0.22		
<i>Perknaster</i> sp.						
<i>Psilaster</i> sp.					0.27±0.27	
Asteroidea sp.3				1.33±0.5	1.07±0.5	0.27±0.27
Asteroidea sp.4					0.27±0.27	
Asteroidea sp.5	0.36±0.36			0.22±0.22		0.53±0.36
<b>Class Crinoidea</b>						
Crinoidea					0.27±0.27	0.53±0.53
<b>Class Echinoidea</b>						
<i>Abatus</i> sp.				0.22±0.22	0.27±0.27	
<i>Ctenocidaris</i> sp.				0.44±0.30	0.27±0.27	0.53±0.36
<i>Sterechinus</i> cf. <i>neumayeri</i>						



**Table 3.1.**  
(continued)

Taxa	MC2					
	10 m (11)	20 m (12)	30 m (12)	50 m (18)	70 m (15)	90 m (15)
<b>Class Ophiuroidea</b>						
Ophiuroidea sp.1		0.33±0.33	3.67±0.8	1.78±0.6	1.33±0.5	2.40±0.7
Ophiuroidea sp.2						0.53±0.36
<b>Total</b>	1.5±0.8	1.0±0.5	4.7±1.0	5.1±0.8	4.3±1.1	5.3±1.1
<b>Porifera</b>						
Porifera sp.2					0.27±0.27	
Porifera sp.11						
Porifera sp.19						
Porifera sp.22						
Porifera sp.23						
Porifera sp.25						0.27±0.27
Porifera sp.26					1.07±0.8	0.53±0.53
Porifera sp.27			4.00±4.0	2.22±2.0		
<b>Cl. Hexactinellida</b>						
<i>Anoxycalyx</i> cf. <i>joubini</i>					0.53±0.36	
Rossellidae sp.1					0.53±0.36	0.53±0.36
Rossellidae sp.2				1.33±0.8	40.5±18	
<b>Total</b>			4.0±4.0	3.6±2.1	43±17	1.3±0.6
<b>Bryozoa</b>						
Bryozoa sp.5						
Bryozoa sp.6				0.44±0.44	0.27±0.27	0.80±0.43
Bryozoa sp.13				0.22±0.22	1.33±1.1	2.93±1.5
Bryozoa sp.14			1.33±1.3			
Bryozoa sp.15					0.53±0.36	0.53±0.36
Bryozoa sp.16					0.27±0.27	
Bryozoa sp.17						
Bryozoa sp.18						
<b>Total</b>			1.3±1.3	0.7±0.5	2.4±1.2	4.3±1.4
<b>Cnidaria</b>						
<b>Class Anthozoa</b>						
Actiniidae sp.2					0.27±0.27	
Actiniidae sp.5						0.27±0.27
<i>Arntzia gracilis</i>			0.67±0.45	1.33±0.7	0.27±0.27	

**Table 3.1.**  
(continued)

Taxa	MC2					
	10 m (11)	20 m (12)	30 m (12)	50 m (18)	70 m (15)	90 m (15)
<i>Tenuisis microspiculata</i>				0.44±0.44		0.27±0.27
<i>Thouarella</i> sp.					0.27±0.27	
<b>Class Hydrozoa</b>						
Hydrozoa sp.4				0.89±0.52		
Hydrozoa sp.5						5.60±3.1
<b>Total</b>			0.7±0.4	2.7±1.3	0.8±0.4	6.1±3.0
<b>Annelida</b>						
<b>Class Polychaeta</b>						
<i>Flabelligera</i> sp.			0.33±0.33		0.53±0.36	1.87±0.7
Sabellidae spp.					7.47±4.0	12.3±3
Terebellidae spp.		0.33±0.33	7.33±1.4	4.67±1.5	0.27±0.27	
<b>Total</b>		0.3±0.3	7.7±1.4	4.7±1.5	8.3±4.2	14±2.5
<b>Arthropoda</b>						
<b>Class Malacostraca</b>						
<i>Serolis</i> sp.						0.27±0.27
<b>Class Pycnogonida</b>						
Pycnogonida sp.4						
<b>Total</b>						0.3±0.3
<b>Mollusca</b>						
<b>Class Gastropoda</b>						
<i>Doris kerguelenensis</i>						
<i>Nacella concinna</i>						
<i>Neobuccinum eatoni</i>						
<b>Total</b>						
<b>Ctenophora</b>						
<b>Class Tentaculata</b>						
<i>Lyrocteis flavopallidus</i>				4.89±1.8	1.87±0.5	0.80±0.43
<b>Nemertea</b>						
<b>Class Pilidiophora</b>						
<i>Parborlasia corrugatus</i>		3.33±1.5	1.00±0.7	0.67±0.49	0.53±0.53	0.53±0.36
<b>Abundance of total fauna</b>	1.5±0.8	7.7±2.3	61±8.5	150±25	93±18	71±8.2
<b>Total number of taxa</b>	2	6	13	25	33	26

**Table 3.2.**

Taxonomic composition and abundance (ind. m<sup>-2</sup>) of epibenthic megafauna recorded from 10-90 m depth at MC3 in Marian Cove. Data were obtained from underwater photographic images collected using a remotely operated vehicle (ROV) during the period of December 31st, 2017, to February 12th, 2018. Abundance data were obtained using a quadrat frame (50×50 cm) attached to the ROV and then transforming the data to values per square meter. Values are mean±standard error. (n): number of replicates.

Taxa	MC3					
	10 m (11)	20 m (11)	30 m (12)	50 m (13)	70 m (11)	90 m (10)
<b>Chordata</b>						
<b>Class Ascidiacea</b>						
<i>Aplidium</i> cf. <i>radiatum</i>						
<i>Ascidia challengerii</i>		1.09±0.8	4.00±2.5	4.86±2.0	17.5±7	7.64±1.9
<i>Cnemidocarpa verrucosa</i>		0.73±0.73	2.33±1.2	5.14±1.9	5.45±2.7	1.09±1.1
<i>Corella antarctica</i>					1.45±1.1	
<i>Distaplia</i> sp.			1.00±0.7	0.86±0.62		0.36±0.36
<i>Molgula pedunculata</i>		3.27±2.5	6.33±4.6	25.7±8	5.82±2.9	6.91±3.4
<i>Pyura</i> cf. <i>discoveri</i>						
<i>Pyura setosa</i>						
<i>Pyura</i> cf. <i>bouvetensis</i>						0.36±0.36
<i>Pyura</i> sp.1						
<i>Sycozoa sigillinoides</i>				0.29±0.29		
<i>Tylobranchion speciosum</i>					0.73±0.73	
Ascidiacea sp.16				0.57±0.39	1.09±0.8	
Ascidiacea sp.17					0.36±0.36	
<b>Total</b>		5.1±3.3	14±6.1	37±8.8	32±11	16±3.6
<b>Echinodermata</b>						
<b>Class Asteroidea</b>						
<i>Cryptasterias</i> sp.						
<i>Diplasterias</i> sp.			0.33±0.33	0.29±0.29		0.36±0.36
<i>Odontaster validus</i>	1.45±0.8	1.45±0.8	1.67±1.2	1.71±1.0		
<i>Perknaster</i> sp.						
<i>Psilaster</i> sp.						
Asteroidea sp.3				0.29±0.29		
Asteroidea sp.4						
Asteroidea sp.5						
<b>Class Crinoidea</b>						
Crinoidea			0.67±0.45	1.43±0.8	0.73±0.49	1.82±1.1
<b>Class Echinoidea</b>						
<i>Abatus</i> sp.						
<i>Ctenocidaris</i> sp.						
<i>Sterechinus</i> cf. <i>neumayeri</i>	9.45±4.0	4.73±2.2	0.67±0.45	1.14±0.7		

**Table 3.2.**  
(continued)

Taxa	MC3					
	10 m (11)	20 m (11)	30 m (12)	50 m (13)	70 m (11)	90 m (10)
<b>Class Ophiuroidea</b>						
Ophiuroidea sp.1			0.33±0.33	0.29±0.29	0.36±0.36	
Ophiuroidea sp.2						
<b>Total</b>	11±3.9	6.2±2.1	3.7±1.6	5.1±1.5	1.5±0.6	1.8±1.1
<b>Porifera</b>						
Porifera sp.2		1.09±1.1	0.67±0.67			
Porifera sp.11			0.33±0.33		1.09±0.6	
Porifera sp.19				1.43±0.9		
Porifera sp.22		0.73±0.49	0.33±0.33			0.73±0.49
Porifera sp.23			0.33±0.33	0.29±0.29	0.36±0.36	
Porifera sp.25						
Porifera sp.26						
Porifera sp.27						
<b>Cl. Hexactinellida</b>						
<i>Anoxycalyx</i> cf. <i>joubini</i>						
Rossellidae sp.1						
Rossellidae sp.2						
<b>Total</b>		1.8±1.5	1.7±0.8	1.7±1.0	1.5±0.8	0.7±0.5
<b>Bryozoa</b>						
Bryozoa sp.5			1.00±1.0	2.00±1.4		
Bryozoa sp.6				0.29±0.29	2.18±1.5	0.36±0.36
Bryozoa sp.13						1.82±1.5
Bryozoa sp.14				0.29±0.29		
Bryozoa sp.15				0.29±0.29	3.64±1.9	1.82±1.0
Bryozoa sp.16					2.91±2.2	1.09±1.1
Bryozoa sp.17					0.36±0.36	
Bryozoa sp.18				0.29±0.29		
<b>Total</b>			1.0±1.0	3.1±1.3	9.1±2.7	5.1±2.0
<b>Cnidaria</b>						
<b>Class Anthozoa</b>						
Actiniidae sp.2		0.36±0.36				
Actiniidae sp.5						
<i>Arntzia gracilis</i>						

**Table 3.2.**  
(continued)

Taxa	MC3					
	10 m (11)	20 m (11)	30 m (12)	50 m (13)	70 m (11)	90 m (10)
<i>Tenuis microspiculata</i>					0.36±0.36	0.36±0.36
<i>Thouarella</i> sp.						
<b>Class Hydrozoa</b>						
Hydrozoa sp.4						
Hydrozoa sp.5						
<b>Total</b>		0.4±0.4			0.4±0.4	0.4±0.4
<b>Annelida</b>						
<b>Class Polychaeta</b>						
<i>Flabelligera</i> sp.		0.36±0.36	0.33±0.33	0.57±0.57		
Sabellidae spp.						
Terebellidae spp.		5.09±2.8	5.33±1.7	2.29±0.9	6.55±0.8	4.00±1.1
<b>Total</b>		5.5±2.8	5.7±1.8	2.9±1.0	6.5±0.8	4.0±1.1
<b>Arthropoda</b>						
<b>Class Malacostraca</b>						
<i>Serolis</i> sp.		0.73±0.49	0.67±0.67	1.43±0.7		
<b>Class Pycnogonida</b>						
Pycnogonida sp.4						0.36±0.36
<b>Total</b>		0.7±0.5	0.7±0.7	1.4±0.7		0.4±0.4
<b>Mollusca</b>						
<b>Class Gastropoda</b>						
<i>Doris kerguelenensis</i>			1.00±1.0			
<i>Nacella concinna</i>	13.5±5	0.36±0.36	1.00±1.0			
<i>Neobuccinum eatoni</i>				1.14±0.7		
<b>Total</b>	13±5.4	0.4±0.4	2.0±1.3	1.1±0.7		
<b>Ctenophora</b>						
<b>Class Tentaculata</b>						
<i>Lyrocteis flavopallidus</i>			0.33±0.33	1.14±0.5	6.91±3.8	2.18±1.3
<b>Nemertea</b>						
<b>Class Pilidiophora</b>						
<i>Parborlasia corrugatus</i>	0.36±0.36			0.57±0.39	0.36±0.36	0.73±0.49
<b>Abundance of total fauna</b>	11±3.8	20±7.2	28±6.8	55±9.7	59±14	32±5.0
<b>Total number of taxa</b>	3	11	19	25	20	16

**Table 3.3.**

Taxonomic composition and abundance (ind. m<sup>-2</sup>) of epibenthic megafauna recorded from 10-90 m depth at MC4 in Marian Cove. Data were obtained from underwater photographic images collected using a remotely operated vehicle (ROV) during the period of December 31st, 2017, to February 12th, 2018. Abundance data were obtained using a quadrat frame (50×50 cm) attached to the ROV and then transforming the data to values per square meter. Values are mean±standard error. (n): number of replicates.

Taxa	MC4					
	10 m (12)	20 m (14)	30 m (11)	50 m (15)	70 m (10)	90 m (13)
<b>Chordata</b>						
<b>Class Ascidiacea</b>						
<i>Aplidium</i> cf. <i>radiatum</i>			7.27±2.7	15.5±5	15.6±5	18.2±6
<i>Ascidia challengerii</i>			35.6±9	18.9±4	9.60±3.1	12.0±3
<i>Cnemidocarpa verrucosa</i>		22.6±15	2.91±2.2	2.40±1.5		
<i>Corella antarctica</i>				0.80±0.80	0.80±0.53	0.31±0.31
<i>Distaplia</i> sp.						
<i>Molgula pedunculata</i>		2.00±1.4	32.7±12	55.7±11	26.0±4	14.5±4
<i>Pyura</i> cf. <i>discoveri</i>						
<i>Pyura setosa</i>						
<i>Pyura</i> cf. <i>bouvetensis</i>					0.80±0.80	0.62±0.62
<i>Pyura</i> sp.1						
<i>Sycozoa sigillinoides</i>						
<i>Tylobranchion speciosum</i>			0.36±0.36	0.53±0.53		
Ascidacea sp.16				11.5±3	0.40±0.40	
Ascidacea sp.17						
<b>Total</b>		25±15	79±14	105±15	53±7.8	46±8.4
<b>Echinodermata</b>						
<b>Class Asteroidea</b>						
<i>Cryptasterias</i> sp.						
<i>Diplasterias</i> sp.						
<i>Odontaster validus</i>	0.33±0.33		1.09±0.6	1.07±0.5	0.40±0.40	0.31±0.31
<i>Perknaster</i> sp.				0.27±0.27		
<i>Psilaster</i> sp.				0.27±0.27		
Asteroidea sp.3						0.31±0.31
Asteroidea sp.4						
Asteroidea sp.5						
<b>Class Crinoidea</b>						
Crinoidea		0.29±0.29	1.09±0.6	1.07±0.5	4.40±2.1	1.23±0.7
<b>Class Echinoidea</b>						
<i>Abatus</i> sp.						
<i>Ctenocidarid</i> sp.						
<i>Sterechinus</i> cf. <i>neumayeri</i>						

**Table 3.3.**  
(continued)

Taxa	MC4					
	10 m (12)	20 m (14)	30 m (11)	50 m (15)	70 m (10)	90 m (13)
<b>Class Ophiuroidea</b>						
Ophiuroidea sp.1				0.27±0.27		0.31±0.31
Ophiuroidea sp.2						
<b>Total</b>	0.3±0.3	0.3±0.3	2.2±0.8	2.9±0.8	4.8±2.2	2.2±0.7
<b>Porifera</b>						
Porifera sp.2			0.36±0.36	0.27±0.27		
Porifera sp.11					1.60±1.2	0.31±0.31
Porifera sp.19				0.53±0.36		
Porifera sp.22				0.27±0.27	0.40±0.40	1.23±0.7
Porifera sp.23			0.36±0.36	0.27±0.27	0.40±0.40	
Porifera sp.25						
Porifera sp.26						
Porifera sp.27						
<b>Cl. Hexactinellida</b>						
<i>Anoxycalyx</i> cf. <i>joubini</i>						
Rossellidae sp.1						
Rossellidae sp.2					0.40±0.40	
<b>Total</b>			0.7±0.5	1.3±0.5	2.8±1.2	1.5±0.7
<b>Bryozoa</b>						
Bryozoa sp.5		2.29±1.8	13.09±6.4	1.07±1.1		
Bryozoa sp.6				1.07±0.8	2.40±0.9	1.23±0.8
Bryozoa sp.13			1.09±1.1		3.60±2.4	1.54±1.2
Bryozoa sp.14			0.73±0.73	1.33±1.3	1.60±1.2	
Bryozoa sp.15				0.53±0.36	3.60±2.4	2.15±0.9
Bryozoa sp.16					1.20±0.6	0.62±0.62
Bryozoa sp.17						
Bryozoa sp.18						
<b>Total</b>		2.3±1.8	15±7.5	4.0±2.3	12±3.0	5.5±2.0
<b>Cnidaria</b>						
<b>Class Anthozoa</b>						
Actiniidae sp.2				0.27±0.27		
Actiniidae sp.5						
<i>Arntzia gracilis</i>						

**Table 3.3.**  
(continued)

Taxa	MC4					
	10 m (12)	20 m (14)	30 m (11)	50 m (15)	70 m (10)	90 m (13)
<i>Tenuis microspiculata</i>					0.40±0.40	
<i>Thouarella</i> sp.						
<b>Class Hydrozoa</b>						
Hydrozoa sp.4						
Hydrozoa sp.5						
<b>Total</b>				0.3±0.3	0.4±0.4	
<b>Annelida</b>						
<b>Class Polychaeta</b>						
<i>Flabelligera</i> sp.			0.36±0.36	0.80±0.43		0.62±0.62
Sabellidae spp.				1.60±1.6		
Terebellidae spp.		2.57±0.9	7.64±1.7	14.9±3	12.0±2	20.0±7
<b>Total</b>		2.6±0.9	8.0±1.9	17±3.1	12±2.1	21±6.5
<b>Arthropoda</b>						
<b>Class Malacostraca</b>						
<i>Serolis</i> sp.		1.43±0.7	0.73±0.73	0.53±0.53	0.40±0.40	
<b>Class Pycnogonida</b>						
Pycnogonida sp.4						
<b>Total</b>		1.4±0.7	0.7±0.7	0.5±0.5	0.4±0.4	
<b>Mollusca</b>						
<b>Class Gastropoda</b>						
<i>Doris kerguelensis</i>						
<i>Nacella concinna</i>	1.33±1.3					
<i>Neobuccinum eatoni</i>						0.31±0.31
<b>Total</b>	1.3±1.3					0.3±0.3
<b>Ctenophora</b>						
<b>Class Tentaculata</b>						
<i>Lyrocteis flavopallidus</i>				0.53±0.36	2.40±1.4	1.85±1.1
<b>Nemertea</b>						
<b>Class Pilidiophora</b>						
<i>Parborlasia corrugatus</i>	0.33±0.33	0.57±0.39		1.07±0.8	0.40±0.40	0.31±0.31
<b>Abundance of total fauna</b>	0.7±0.4	32±15	105±20	133±17	89±8.6	78±12
<b>Total number of taxa</b>	2	7	15	27	22	20



**Table 3.4.**

Taxonomic composition and abundance (ind. m<sup>-2</sup>) of epibenthic megafauna recorded from 10-90 m depth at MC5 in Marian Cove. Data were obtained from underwater photographic images collected using a remotely operated vehicle (ROV) during the period of December 31st, 2017, to February 12th, 2018. Abundance data were obtained using a quadrat frame (50×50 cm) attached to the ROV and then transforming the data to values per square meter. Values are mean±standard error. (n): number of replicates.

Taxa	MC5					
	10 m (14)	20 m (21)	30 m (19)	50 m (16)	70 m (16)	90 m (22)
<b>Chordata</b>						
<b>Class Ascidiacea</b>						
<i>Aplidium</i> cf. <i>radiatum</i>						
<i>Ascidia challengerii</i>		0.19±0.19	6.53±2.5	7.25±2.0	7.25±2.9	1.64±0.9
<i>Cnemidocarpa verrucosa</i>	3.71±3.7	30.7±7	37.3±7	20.0±4	9.50±2.3	10.9±3
<i>Corella antarctica</i>						
<i>Distaplia</i> sp.						0.18±0.18
<i>Molgula pedunculata</i>		2.29±1.3	82.7±10	81.5±12	32.5±6	17.5±5
<i>Pyura</i> cf. <i>discoveri</i>						
<i>Pyura setosa</i>						
<i>Pyura</i> cf. <i>bouvetensis</i>					1.25±0.6	
<i>Pyura</i> sp.1						
<i>Sycozoa sigillinoides</i>						
<i>Tylobranchion speciosum</i>			0.21±0.21			
Ascidacea sp.16						
Ascidacea sp.17						
<b>Total</b>	3.7±3.7	33±7.0	127±14	109±15	51±7.5	30±7.4
<b>Echinodermata</b>						
<b>Class Asteroidea</b>						
<i>Cryptasterias</i> sp.						
<i>Diplasterias</i> sp.						
<i>Odontaster validus</i>	0.57±0.39	0.76±0.45	2.11±0.6			
<i>Perknaster</i> sp.			0.21±0.21		0.50±0.34	
<i>Psilaster</i> sp.						
Asteroidea sp.3						
Asteroidea sp.4			0.21±0.21			
Asteroidea sp.5						
<b>Class Crinoidea</b>						
Crinoidea		0.57±0.31	1.68±0.6	3.50±1.1	3.75±1.1	0.73±0.34
<b>Class Echinoidea</b>						
<i>Abatus</i> sp.						
<i>Ctenocidarid</i> sp.						
<i>Sterechinus</i> cf. <i>neumayeri</i>						

**Table 3.4.**  
(continued)

Taxa	MC5					
	10 m (14)	20 m (21)	30 m (19)	50 m (16)	70 m (16)	90 m (22)
<b>Class Ophiuroidea</b>						
Ophiuroidea sp.1						
Ophiuroidea sp.2						
<b>Total</b>	0.6±0.4	1.3±0.5	4.2±0.8	3.5±1.1	4.3±1.1	0.7±0.3
<b>Porifera</b>						
Porifera sp.2						0.18±0.18
Porifera sp.11						
Porifera sp.19					0.25±0.25	
Porifera sp.22						
Porifera sp.23						
Porifera sp.25						
Porifera sp.26						
Porifera sp.27						
<b>Cl. Hexactinellida</b>						
<i>Anoxycalyx</i> cf. <i>joubini</i>						
Rossellidae sp.1						
Rossellidae sp.2						
<b>Total</b>					0.3±0.3	0.2±0.2
<b>Bryozoa</b>						
Bryozoa sp.5		3.24±2.0	37.89±10	3.75±1.8		
Bryozoa sp.6		0.57±0.31	1.26±0.5	1.25±0.6	4.75±1.7	1.82±0.7
Bryozoa sp.13			0.84±0.49	4.75±2.1	1.25±0.8	1.64±0.7
Bryozoa sp.14			0.21±0.21	1.50±1.1	1.00±0.8	0.36±0.25
Bryozoa sp.15				1.75±1.1	1.50±0.8	0.36±0.25
Bryozoa sp.16				0.25±0.25	0.25±0.25	
Bryozoa sp.17						
Bryozoa sp.18						
<b>Total</b>		3.8±1.9	40±10	13±3.0	8.8±2.4	4.2±1.0
<b>Cnidaria</b>						
<b>Class Anthozoa</b>						
Actiniidae sp.2						
Actiniidae sp.5						
<i>Arntzia gracilis</i>						

**Table 3.4.**  
(continued)

Taxa	MC5					
	10 m (14)	20 m (21)	30 m (19)	50 m (16)	70 m (16)	90 m (22)
<i>Tenuisis microspiculata</i>						
<i>Thouarella</i> sp.						
<b>Class Hydrozoa</b>						
Hydrozoa sp.4						
Hydrozoa sp.5						
<b>Total</b>						
<b>Annelida</b>						
<b>Class Polychaeta</b>						
<i>Flabegroviera</i> sp.			6.95±4.0	37.8±18	24.8±12	3.45±1.7
Sabellidae spp.						
Terebellidae spp.	1.14±1.1	11.8±3	16.4±4	10.0±3	7.00±1.5	15.8±2
<b>Total</b>	1.1±1.1	12±2.6	23±4.6	48±17	32±12	19±2.1
<b>Arthropoda</b>						
<b>Class Malacostraca</b>						
<i>Serolis</i> sp.						0.18±0.18
<b>Class Pycnogonida</b>						
Pycnogonida sp.4						
<b>Total</b>						0.2±0.2
<b>Mollusca</b>						
<b>Class Gastropoda</b>						
<i>Doris kerguelenensis</i>						
<i>Nacella concinna</i>						
<i>Neobuccinum eatoni</i>						
<b>Total</b>						
<b>Ctenophora</b>						
<b>Class Tentaculata</b>						
<i>Lyrocteis flavopallidus</i>			0.21±0.21	0.25±0.25	1.00±0.6	2.00±0.5
<b>Nemertea</b>						
<b>Class Pilidiophora</b>						
<i>Parborlasia corrugatus</i>		0.19±0.19	0.21±0.21			0.36±0.25
<b>Abundance of total fauna</b>	5.4±4.8	50±7.9	195±23	174±30	97±20	57±8.7
<b>Total number of taxa</b>	3	9	16	13	15	15

**Table 3.5.**

Taxonomic composition and average abundance of epibenthic megafauna recorded from 10-90 m depth in Marian Cove. Data were obtained from underwater photographic images collected using a remotely operated vehicle (ROV) during the period of December 31st, 2017, to February 12th, 2018. Abundance data were obtained using a quadrat frame (50×50 cm) attached to the ROV and then transforming the data to values per square meter. Values are mean±standard error. (n): number of replicates.

Taxa	Total		
	Absolute abundance (ind. m <sup>-2</sup> )	Relative abundance (%)	Relative abundance within phylum (%)
<b>Chordata</b>			
<b>Class Ascidiacea</b>			
<i>Aplidium</i> cf. <i>radiatum</i>	1.65	2.44	3.92
<i>Ascidia challengerii</i>	7.54	11.16	17.9
<i>Cnemidocarpa verrucosa</i>	10.2	15.09	24.2
<i>Corella antarctica</i>	0.28	0.42	0.67
<i>Distaplia</i> sp.	0.18	0.27	0.43
<i>Molgula pedunculata</i>	17.4	25.77	41.4
<i>Pyura</i> cf. <i>discoveri</i>	0.50	0.74	1.19
<i>Pyura setosa</i>	0.34	0.51	0.82
<i>Pyura</i> cf. <i>bouvetensis</i>	0.18	0.27	0.43
<i>Pyura</i> sp.1	0.06	0.08	0.13
<i>Sycozoa sigillinoides</i>	0.03	0.04	0.06
<i>Tylobranchion speciosum</i>	0.41	0.61	0.97
Ascidiacea sp.16	1.81	2.69	4.31
Ascidiacea sp.17	1.48	2.20	3.53
<b>Total</b>	<b>42.04</b>	<b>62.28</b>	<b>100.00</b>
<b>Echinodermata</b>			
<b>Class Asteroidea</b>			
<i>Cryptasterias</i> sp.	0.02	0.03	0.57
<i>Diplasterias</i> sp.	0.10	0.15	3.19
<i>Odontaster validus</i>	0.66	0.98	20.32
<i>Perknaster</i> sp.	0.04	0.06	1.25
<i>Psilaster</i> sp.	0.02	0.03	0.68
Asteroidea sp.3	0.14	0.20	4.16
Asteroidea sp.4	0.02	0.03	0.61
Asteroidea sp.5	0.05	0.07	1.43
<b>Class Crinoidea</b>			
Crinoidea	0.99	1.47	30.33
<b>Class Echinoidea</b>			
<i>Abatus</i> sp.	0.02	0.03	0.62
<i>Ctenocidaris</i> sp.	0.05	0.08	1.59
<i>Sterechinus</i> cf. <i>neumayeri</i>	0.67	0.99	20.43

**Table 3.5.**  
(continued)

Taxa	Total		
	Absolute abundance (ind. m <sup>-2</sup> )	Relative abundance (%)	Relative abundance within ascidians (%)
<b>Class Ophiuroidea</b>			
Ophiuroidea sp.1	0.46	0.68	14.14
Ophiuroidea sp.2	0.02	0.03	0.68
<b>Total</b>	<b>3.26</b>	<b>4.83</b>	100.00
<b>Porifera</b>			
Porifera sp.2	0.12	0.18	4.30
Porifera sp.11	0.14	0.21	5.05
Porifera sp.19	0.09	0.14	3.35
Porifera sp.22	0.15	0.23	5.58
Porifera sp.23	0.08	0.12	3.05
Porifera sp.25	0.01	0.02	0.40
Porifera sp.26	0.07	0.10	2.42
Porifera sp.27	0.26	0.38	9.42
<b>Cl. Hexactinellida</b>			
<i>Anoxycalyx</i> cf. <i>joubini</i>	0.02	0.03	0.81
Rossellidae sp.1	1.76	2.61	64.01
Rossellidae sp.2	0.04	0.07	1.62
<b>Total</b>	<b>2.75</b>	<b>4.08</b>	100.00
<b>Bryozoa</b>			
Bryozoa sp.5	2.68	3.97	47.19
Bryozoa sp.6	0.78	1.15	13.71
Bryozoa sp.13	0.88	1.30	15.42
Bryozoa sp.14	0.35	0.52	6.13
Bryozoa sp.15	0.70	1.03	12.26
Bryozoa sp.16	0.27	0.41	4.83
Bryozoa sp.17	0.02	0.02	0.27
Bryozoa sp.18	0.01	0.02	0.21
<b>Total</b>	<b>5.68</b>	<b>8.42</b>	100.00
<b>Cnidaria</b>			
<b>Class Anthozoa</b>			
Actiniidae sp.2	0.04	0.06	7.46
Actiniidae sp.5	0.01	0.02	2.22
<i>Arntzia gracilis</i>	0.09	0.14	18.85

**Table 3.5.**  
(continued)

Taxa	Total		
	Absolute abundance (ind. m <sup>-2</sup> )	Relative abundance (%)	Relative abundance within ascidians (%)
<i>Tenuis microspiculata</i>	0.08	0.11	15.29
<i>Thouarella</i> sp.	0.04	0.05	7.39
<b>Class Hydrozoa</b>			0.00
Hydrozoa sp.4	0.01	0.02	2.22
Hydrozoa sp.5	0.23	0.35	46.57
<b>Total</b>	<b>0.50</b>	<b>0.74</b>	100.00
<b>Annelida</b>			
<b>Class Polychaeta</b>			
<i>Flabegraviera</i> sp.	0.24	0.36	2.27
Sabellidae spp.	3.93	5.82	36.93
Terebellidae spp.	6.47	9.58	60.81
<b>Total</b>	<b>10.6</b>	<b>15.8</b>	100.00
<b>Arthropoda</b>			
<b>Class Malacostraca</b>			
<i>Serolis</i> sp.	0.27	0.39	94.59
<b>Class Pycnogonida</b>			
Pycnogonida sp.4	0.02	0.02	5.41
<b>Total</b>	<b>0.28</b>	<b>0.42</b>	100.00
<b>Mollusca</b>			
<b>Class Gastropoda</b>			
<i>Doris kerguelenensis</i>	0.04	0.06	5.38
<i>Nacella concinna</i>	0.67	1.00	86.83
<i>Neobuccinum eatoni</i>	0.06	0.09	7.80
<b>Total</b>	<b>0.78</b>	<b>1.15</b>	100.00
<b>Ctenophora</b>			
<b>Class Tentaculata</b>			
<i>Lyrocteis flavopallidus</i>	1.10	1.63	100.00
<b>Nemertea</b>			
<b>Class Pilidiophora</b>			
<i>Parborlasia corrugatus</i>	0.48	0.71	
<b>Abundance of total fauna</b>	<b>67</b>	<b>100</b>	100.00
<b>Total number of taxa</b>	<b>63</b>		

### 3.2.3. ROV images and sample analysis

The taxonomic composition and abundance of epibenthic megafauna were determined from images collected by the ROV. All epifaunal animals that were discernable in the images (approximately >1 cm in the longest dimension) were recorded and identified to the lowest taxonomic level possible, using identification descriptions in the literature (Hibberd and Moore 2009; Rauschert and Arntz et al. 2015; Danis 2013; Schories and Kohlberg 2016) and through the database of the World Register of Marine Species (<http://www.marinespecies.org>) (accessed on May 25, 2020). Small bivalves, gastropods, amphipods and other organisms that occurred mostly as epibionts were not easily discernable in the images and were therefore excluded from analysis. For each image, the percentage of area covered by animals was also determined.

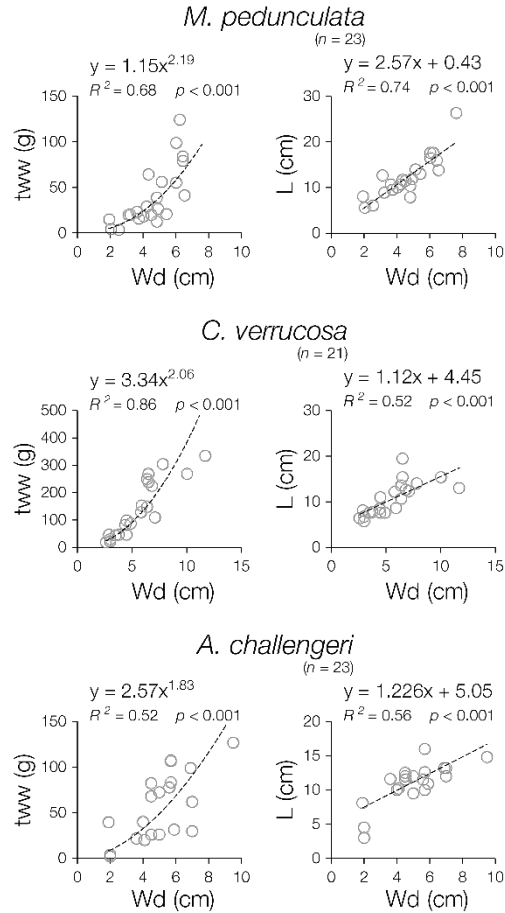
Ascidian taxa were identified to the lowest possible level based on specific morphological characteristics described in the literature (Tatiàn et al. 1998, 2005; Monniot et al. 2011; Alurralde et al. 2013; Schories and Kohlberg 2016) and also with the aid of ascidian taxonomists (Boon-Jo Rho and Su-Yuan Seo from Natural History Museum, Ewha Womans University, Republic of Korea). Abundance data for each ascidian taxon were then obtained by counting the number within a quadrat frame (50×50 cm) and transforming the counted numbers to values per square meter (Table 3.1–3.5). For colonial taxa, each colony was counted as a single individual (Segelken-Voigt et al. 2016).

Linear dimension of each individual was also determined from the ROV-acquired images using ImageJ software (National Institutes of Health, USA). ROV images were taken from above in the water, and body length (L, the longest dimension) of many individuals, particularly those in an upright or standing position could not be determined directly from the images. Therefore, the width (Wd) of each individual was determined, and the measured Wd values were converted to body weight (total wet weight, tww) and L values, using allometric relationships of the three most abundant species (*M. pedunculata*, *C. verrucosa* and *A. challengerii*) (Figure 3.3). For the other species, one of the three allometric equations were used based on the similarity of body form. Biomass for each taxon in each quadrat was calculated by summing up the estimated tww of individuals.

Seabed sediment composition was determined from the ROV images as well as the collected sediment samples. Only images with at least 25% bare sediment area (without animals or plants) were used for composition analysis. From these images, the percentages of boulder (>25.5 cm), cobble (6.5–25.5 cm), pebble (6.5–1.0 cm), and smaller sediments (<1 cm) coverage were determined using ImageJ software (Anderson et al. 2007; Smale et al. 2007; Dorschel et al. 2014). Sediment particles smaller than 1 cm in diameter were not distinguishable in the images and were further analyzed using the sediment samples collected by divers and grab sampling. Sediment particles larger than 63  $\mu\text{m}$  were measured with a Ro-Tap<sup>®</sup> sieve shaker after removal of organic matter using  $\text{H}_2\text{O}_2$ , followed by elimination of calcium carbonate with 35% HCl. The finer fractions (<63  $\mu\text{m}$ ) were analyzed using a sediment particle size analyzer (Sedigraph<sup>®</sup> 5120, Micrometrics Inc.).

Total organic carbon (TOC) and total nitrogen (TN) were determined from the surface flocculent layer, which was collected by divers at <30 m and Van Veen grab at >30 m. Sediment samples were freeze-dried and ground, and then total carbon (TC) and TN were analyzed using a Flash 2000 elemental analyzer (Thermo Fisher scientific). TOC was calculated by subtracting total inorganic carbon (TIC) from TC. TIC was measured using a CM5017  $\text{CO}_2$  coulometer attached to a CM5240 auto-acidification module (UIC Inc.).





**Figure 3.3.**

Allometric relationships of the three most abundant ascidian species (*C. verrucosa*, *M. pedunculata* and *A. challengeri*). The ascidian samples used for analysis were collected randomly by divers from about 30 m depth. ROV images were taken from above in the water, and body length (L, the longest dimension) of many individuals, particularly those in an upright or standing position could not be determined directly from the images. Therefore, the width (Wd) of each individual was determined from the images and the measured Wd values were converted to body weight (total wet weight, tww) and L, using the allometric relationships. For other species, the relationship obtained from one of the three dominant species was used based on similarity of body form and position. For stalked species (*Distalpia* sp., *Pyura* sp.1, *Pyura* cf. *bouvetensis*, *S. sigillinoides* and *T. speciosum*), the equations for *M. pedunculata* were used, while those of *C. verrucosa* for non-stalked and elongated species (*Pyura* cf. *discoveri*, and Ascidian sp. 17) and those of *A. challengeri* for ovoid or flattened species (e.g. *Aplidium* cf. *radiatum*, *Corella antarctica*, *P. setosa* and Ascidian sp. 16).

### **3.2.4. Statistical analyses**

Multivariate statistical techniques were applied to biotic and abiotic data, and the results of each analysis were used collectively to identify the key environmental variables structuring ascidian communities in this glacial cove. Similarity of assemblages (total epibenthic fauna and ascidian communities, respectively) among stations and depths was assessed using non-parametric multidimensional scaling (MDS) analysis. A two-dimensional ordination plot was produced based on the Bray-Curtis similarity matrix constructed from square-root transformation of the abundance data (Table 3.1–3.5). Statistical differences among assemblages at different stations or depths were tested using one-way analysis of similarities (ANOSIM) and the similarity percentage procedure (SIMPER). SIMPER was also used to determine the species contributing most to those differences. Principle component analysis (PCA) was performed to identify the groups of samples (stations and depths) with similar environmental characteristics. Finally, biota-environment (BIOENV) analysis was used to determine which environmental parameters best explain the distribution of ascidians. All abiotic variables were normalized prior to analysis. Univariate non-parametric analyses (Kruskal-Wallis test and Mann-Whitney U test) were performed using PASW Statistics (version 18.0). All other statistical analyses were performed using PRIMER software (version 6.1.16) (Clarke and Gorley 2006).

### **3.2.5. Supporting datasets**

Air temperature (1988–2018), suspended particulate matter (SPM, 1996–2018), and seawater temperature and salinity (2011–2019) data, were obtained from the long-term environmental monitoring dataset for King Sejong Station.

### 3.3. Results

#### 3.3.1. Environmental characteristics of the study area

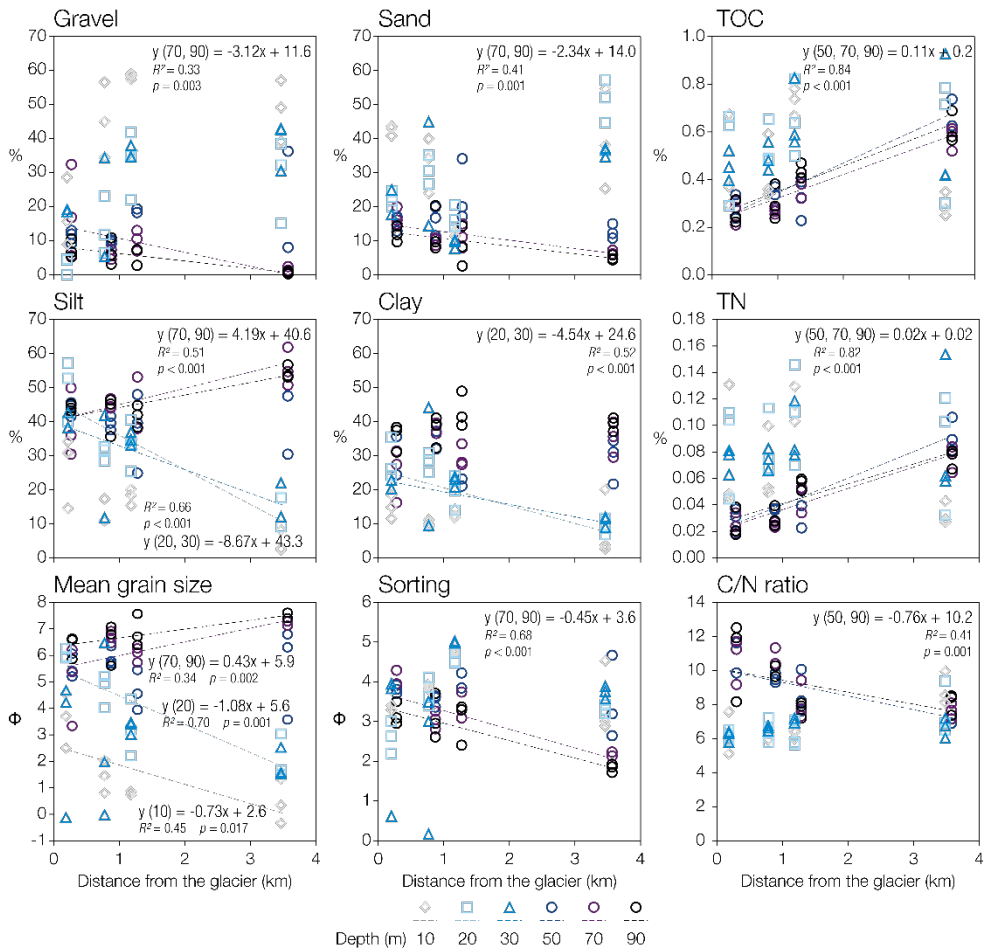
The environmental characteristics of each station at various depths are summarized in Table 3.6. Analysis showed that over the last six decades the period (in years) of seabed exposure after deglaciation were highly correlated with the longitudinal distance to the present glacier front ( $Y=26.415X+0.782$ ,  $r^2=0.89$ ,  $p<0.001$ , where  $X$  is the distance to the glacier and  $Y$  is the estimated years after retreat). The period of seabed exposure after glacial retreat at the stations in the inner cove was estimated into a narrow range of years based on the satellite images (Figure 3.1). No information, however, was available on glacier position before 1956, and MC2 was assumed as exposed for at least 62 years.

The monitoring data obtained from the station (2011–2019) (see the section 3.2.5) showed that distinct spatial and temporal gradients of seawater temperature and salinity developed in the surface layer (<20 m) during the summer months (December through February) due to inflow of glacial meltwater. However, the annual mean values showed only slight differences among stations (-0.3 to -0.4°C, 33.9 to 34.0 psu) and among depths (-0.3 to -0.6°C, 33.9 to 34.1 psu). On the other hand, sediment properties exhibited distinct spatial variations (Figure 3.4, Table 3.6). For example, gravelly sediments mixed with sand dominated (>60–88%) to a 10 m depth at all stations, while silt and clay comprised the largest portion of sediment at greater depths. Silt and clay contents increased most dramatically toward the bottom ( $p<0.01$ , regression analysis) at the remote site (MC2) (means=12% at 10 m, 25 at 30 m, 71 at 50 m, and 94 at 90 m), while these contents varied less (40–80%) with depth at the site closest to the glacier (MC5).

**Table 3.6.**

Comparison of environmental characteristics among ROV survey stations (MC2, MC3, MC4, and MC5) in Marian Cove. Distances of the stations from the glacier front were determined using the glacier front in the year of 2017 as a baseline (Figure 3.1). \*The periods of seabed exposure at the stations were estimated based on glacial retreat lines in Figure 3.1. \*\*Data were obtained from the long-term monitoring dataset collected at the station (see section 3.2.5). \*\*\*Sediment composition was determined from quadrat images obtained using an ROV in combination with the results from analysis of sediments collected by divers and grab sampling (refer to section 3.2.3 for more details). Mean±standard deviation values are presented.

Station	Period of seabed exposure (yr)*	Distance from glacier front (km)	Water depth (m)	Water column properties**		Sediment properties								
				Annual mean temp. (°C)	Annual mean salinity (psu)	TOC (n=3) (%)	TN (n=3) (%)	Sediment composition (%)***				Mean grain size (φ)	Sorting (φ)	
								n	Gravel	Sand	Silt			Clay
MC2	> 62	3.5	10	-0.20	34.01	0.29±0.03	0.033±0.008	11	48.5±21	39.5±16	4.4±1.8	7.6±3.1	0.43±1.6	7.80±1.4
			20	-0.25	34.04	0.60±0.27	0.085±0.047	5	28.8±1.1	51.5±0.8	12.1±0.2	7.7±0.1	2.06±0.1	6.36±0.1
			30	-0.28	34.06	0.59±0.30	0.09±0.054	7	38.9±1.9	36.4±1.1	15.4±0.5	9.4±0.3	1.87±0.1	6.74±0.1
			50	-0.35	34.09	0.69±0.07	0.09±0.013	14	15.7±2.8	13.0±0.4	42.0±1.4	29.3±1.0	5.53±0.3	4.30±0.3
			70	-0.42	34.11	0.58±0.05	0.08±0.010	10	1.5±0.5	7.1±0.0	56.1±0.3	35.3±0.2	7.15±0.1	2.12±0.1
			90	-0.47	34.13	0.61±0.07	0.08±0.007	15	0.7±0.5	5.2±0.0	54.6±0.3	39.4±0.2	7.44±0.1	1.82±0.1
MC3	31-33	1.2	10	-0.22	33.97	0.73±0.03	0.116±0.01	9	58.5±28	12.4±8.5	18.0±12	11.0±7.5	0.77±2.7	8.01±1.9
			20	-0.27	34.02	0.66±0.25	0.109±0.04	11	33.1±27	17.1±6.8	33.1±13	16.7±6.6	3.23±2.5	6.00±2.0
			30	-0.29	34.04	0.66±0.13	0.093±0.02	10	35.9±44	9.4±6.6	35.1±24	19.5±14	3.29±4.4	5.66±3.4
			50	-0.32	34.07	0.32±0.11	0.038±0.01	13	16.2±19	24.0±5.6	37.7±8.7	22.1±5.1	4.63±2.0	4.70±1.8
			70	-0.45	34.09	0.37±0.04	0.046±0.01	11	10.3±5.0	11.6±0.6	48.2±2.7	29.9±1.7	5.99±0.6	3.66±0.7
			90	-0.55	34.01	0.44±0.02	0.056±0.004	11	5.9±6.2	8.7±0.6	42.0±2.8	43.3±2.9	6.85±0.7	3.00±1.0
MC4	17-23	0.8	10	-0.26	33.97	0.43±0.18	0.068±0.03	12	45.5±15	32.8±9.0	13.0±3.6	8.7±2.4	1.43±1.3	7.12±1.0
			20	-0.28	34.02	0.54±0.09	0.085±0.03	14	13.8±4.1	31.0±1.5	31.0±1.5	24.2±1.2	4.72±0.4	4.63±0.4
			30	-0.29	34.04	0.49±0.07	0.074±0.008	11	20.1±0.7	29.9±0.3	27.0±0.2	23.1±0.2	4.22±0.1	5.12±0.1
			50	-0.33	34.07	0.33±0.05	0.034±0.005	14	9.9±4.9	16.3±0.9	39.9±2.2	33.9±1.8	5.91±0.5	3.83±0.6
			70	-0.40	34.09	0.27±0.02	0.025±0.002	10	5.9±7.2	10.1±0.8	45.2±3.5	38.8±3.0	6.65±0.7	3.01±1.0
			90	-0.54	34.11	0.30±0.10	0.031±0.008	13	6.7±2.0	12.9±0.3	42.7±0.9	37.7±0.8	6.47±0.2	3.31±0.3
MC5	7-13	0.2	10	-0.27	33.99	0.45±0.20	0.075±0.05	13	17.8±6.7	42.7±3.5	26.6±2.2	12.8±1.1	3.58±0.6	5.25±0.6
			20	-0.27	34.03	0.53±0.22	0.086±0.04	19	3.0±0.4	22.3±0.1	50.2±0.2	24.5±0.1	6.0±0.03	2.99±0.1
			30	-0.28	34.05	0.46±0.07	0.074±0.01	16	19.0±6.7	21.6±1.8	40.7±3.4	18.7±1.5	4.44±0.7	4.88±0.7
			50	-0.32	34.07	0.30±0.04	0.029±0.008	14	11.6±19	15.9±3.4	44.2±9.5	28.3±6.1	5.53±2.0	3.83±2.0
			70	-0.38	34.09	0.27±0.10	0.026±0.008	16	18.5±7.0	17.2±1.5	39.0±3.4	25.2±2.2	4.94±0.7	4.67±0.7
			90	-0.58	34.15	0.26±0.05	0.026±0.01	22	7.6±4.3	12.2±0.6	44.3±2.1	35.9±1.7	6.32±0.4	3.36±0.5



**Figure 3.4.**

Spatial variations in sediment properties across stations (MC5, MC4, MC3, and MC2) and water depths (10, 20, 30, 50, 70 and 90 m). All replicate data from each station were plotted in terms of distance from the glacier, showing stations MC5, MC4, MC3, and MC2 from left to right. Regression lines that are statistically significant are plotted. Data from lines representing statistically insignificant differences (analysis of covariance, ANCOVA,  $p > 0.05$ ) were pooled for construction of a single regression equation.

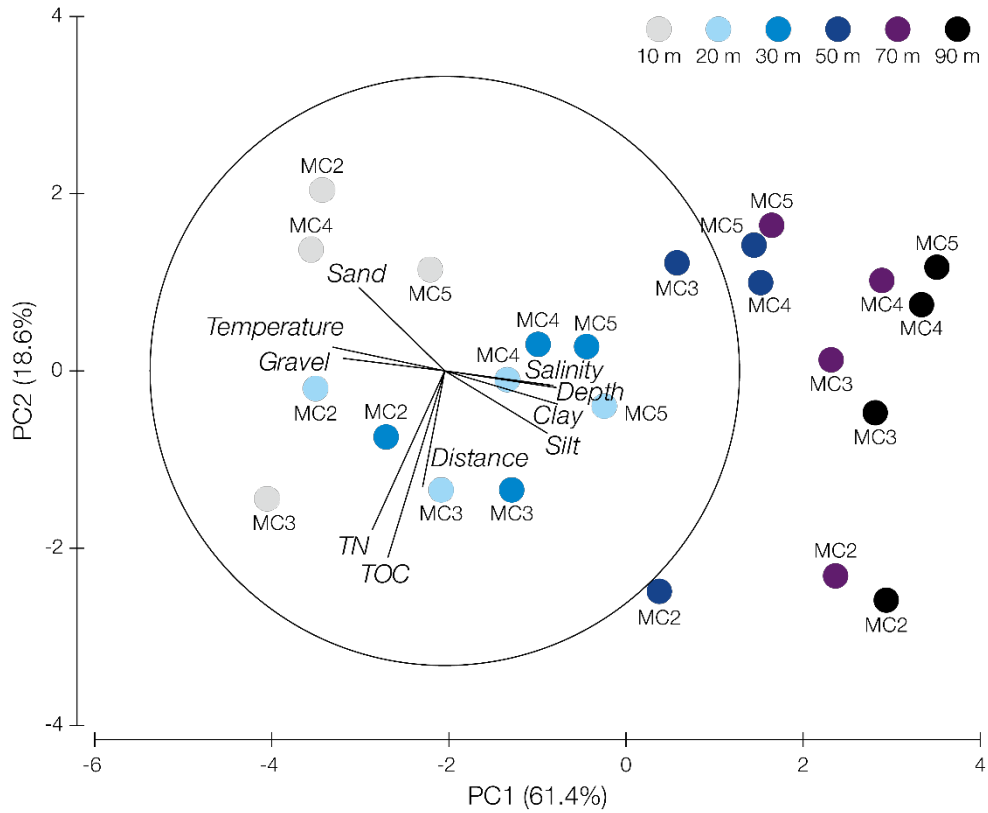
Notably, silt and clay contents increased toward the glacier front at <30 m depths, but these contents showed an opposite trend in deeper waters. In particular, silt contents increased distinctly toward the outer cove, reaching the highest values at 70–90 m at MC2. At 70–90 m depth at station MC2, silt and clay dominated (>90%) the bottom sediment, comprising clayey silty sediment, while at the same depth range of station MC5, silt and clay comprised <80% of sediment and substantial portions (>20–36%) of gravel and sand were present. As a result, the sediments at 70–90 m at MC2 were the finest (means=7.2 phi at 70 m, 7.4 at 90 m) and best sorted (means=2.1 phi at 70 m, 1.8 at 90 m) across the entire cove. Overall, the sediment composition, mean grain size, and level of sorting among the stations differed more distinctly in the deeper waters, while these variations with water depth were most distinct at MC2, the most distant site from the glacier front.

As with sediment grain size, sediment TOC and TN contents and C/N ratios varied significantly among stations and water depths (Figure 3.4). In shallow waters (20–30 m), no significant differences were observed in organic matter content or C/N ratio among stations. However, in deep waters (70–90 m), distinct differences were found among stations; the organic contents tended to decrease toward the inner cove and reached their lowest values at MC4 and MC5; C/N ratios varied from 6.2 to 10.9 in the opposite manner to organic content, with the highest values (9.6–10.9) at MC4 and MC5. Organic matter contents were significantly higher in shallow waters (<30 m) (TOC: 0.43–0.73%, TN: 0.068–0.12%) compared to those at 50–90 m (0.26–0.44%, 0.025–0.056%) (Mann-Whitney U-test,  $p < 0.001$ ) at all stations except MC2. At MC2, organic contents in deep waters (TOC: 0.58–0.69%, TN: 0.076–0.093%) were as high as those at 20–30 m depth (TOC: 0.59–0.60%, TN: 0.085–0.091%). Likewise, the C/N ratios at MC2 were similar across all water depths investigated. Overall, the quantity and quality of organic matter decreased clearly toward the glacier front in deep waters (50–90 m), but the differences in shallow waters were less distinct.

These distinct environmental variations observed among stations and water depths are well reflected in the PCA plot (Figure 3.5). The first principal component axis (PC1) was explained primarily by depth, water column properties and sediment grain size (coefficient >0.3), and could classify the habitat largely into three depth



ranges (10, 20–30 m and 50–90 m). In addition, PC2 explained the differences among the stations mainly through distance from the glacier, TOC and TN (coefficient >0.4). Notably, the differences among stations were more prominent in deep waters (50–90 m) than in shallow waters. The environmental characteristics observed at depths of 50–90 m at MC2 differed markedly from those at the same depths at other stations (MC3, MC4, and MC5) in the inner cove, while the differences among stations in shallow waters were much smaller. Thus, multivariate and univariate analyses on habitat properties demonstrated a major shift in habitat properties between the depths of 30 and 50 m (Figure 3.4 and 3.5) and showed that properties were far more differentiated among stations in deeper waters (>50 m).



**Figure 3.5.**

Principal component analysis (PCA) plot showing spatial variations in environmental parameters among stations (MC2, MC3, MC4, and MC5) and depths (10–90 m). Constructed based on the data presented in Table 3.6.

### **3.3.2. Ascidian contribution to the spatial variations of total epibenthic megafauna**

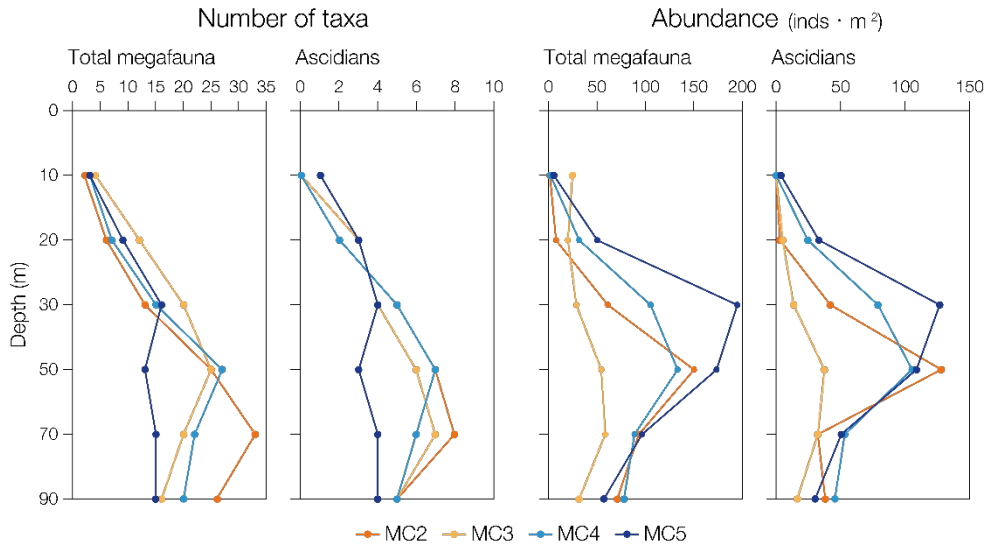
A total of 64 epibenthic megafaunal taxa (16 phyla, 11 classes, 6 families, 16 genera, and 15 species) were identified from the ROV images (Table 3.1–3.5). Ascidians and echinoderms were the most diverse (14 taxa, respectively) followed by sponges (11 taxa), bryozoans (8 taxa) and cnidarians (7 taxa). Among 14 ascidian taxa observed (nine solitary and five colonial), seven were identified to the level of species, five to genus, and two to class (Table 3.7). These 14 ascidian taxa exhibited wide variations in size (from tens of centimeters to less than one), color, body form (stalked, non-stalked, and irregular), and life mode (solitary and colonial). In addition, ascidians were the most abundant group (mean=42 ind. m<sup>-2</sup>) accounting for 63% of total megafauna throughout the cove, followed by annelids (16%), and echinoderms comprised only 5% of the total. Overall, ascidians were the most diverse and most abundant taxonomic group.

The species number and abundance of megabenthic fauna varied distinctly among the stations and with water depths. The highest species number (33 taxa) was observed at 70 m of MC2, while the highest abundance occurred at 30 m (mean=195 ind. m<sup>-2</sup>) of MC5. Ascidians also showed similar patterns with those of total benthos with the highest species number (8 taxa) at 70 m of MC2 and the highest abundances at 30 m of MC5 (mean=127 ind. m<sup>-2</sup>) and 50 m of MC2 (mean=128 ind. m<sup>-2</sup>) (Figure 3.6).

**Table 3.7.**

List of ascidian taxa occurring at depths of 10–90 m in Marian Cove constructed from the images taken by ROV survey in December 2017 to February 2018.

Ascidian species	Description in Moon et al. 2015	Life mode	Morphological description
<i>Molgula pedunculata</i>		Solitary	Fairly translucent, with long stalk or peduncle
<i>Cnemidocarpa verrucosa</i>		Solitary	Brown or yellow to white and translucent, cylindrical and covered with protuberances
<i>Ascidia challengerii</i>	Asciadiacea sp.14 Asciadiacea sp.15	Solitary	Translucent and smooth tunic, body lying flat on the bottom without stalk, oral siphon at the end of body, atrial siphon at 1/4 to 1/3 of body length
<i>Tylobranchion speciosum</i>	Asciadiacea sp.12	Colonial	Translucent, short peduncle, club-shaped head, occurs as epibiont on other ascidians and algae
<i>Pyura setosa</i>	Asciadiacea sp.2	Solitary	Grayish to brownish, ovoid shape with surface completely covered in flexible bristles
<i>Corella antarctica</i>	Asciadiacea sp.4	Solitary	Translucent, flat and smooth tunic
<i>Distaplia</i> sp.	Asciadiacea sp.10	Colonial	Translucent and yellow, cotton ball-shaped with slender stem, occurs in Magellan region, sub-Antarctic islands, South Shetland Islands, and Antarctic Peninsula
<i>Sycozoa sigillinoides</i>		Colonial	Thick peduncle, cylindrical head
Asciadiacea sp.16		Solitary	Translucent and soft tunic, elliptical body, attached to surface of other organisms
Asciadiacea sp.17		Colonial	Yellow or orange, irregular shape, usually settled on other organisms
<i>Aplidium</i> cf. <i>radiatum</i>		Colonial	Round shape, settled on muddy or sandy bottom
<i>Pyura</i> cf. <i>discoveri</i>		Solitary	Brown, hard, corrugated tunic, triangular body shape with protruding siphons away from each other
<i>Pyura</i> cf. <i>bouvetensis</i>		Solitary	Spherical body with long stiff peduncle, distinct oral and atrial siphons
<i>Pyura</i> sp.1		Solitary	Elliptical body with long stiff peduncle, distinct siphons

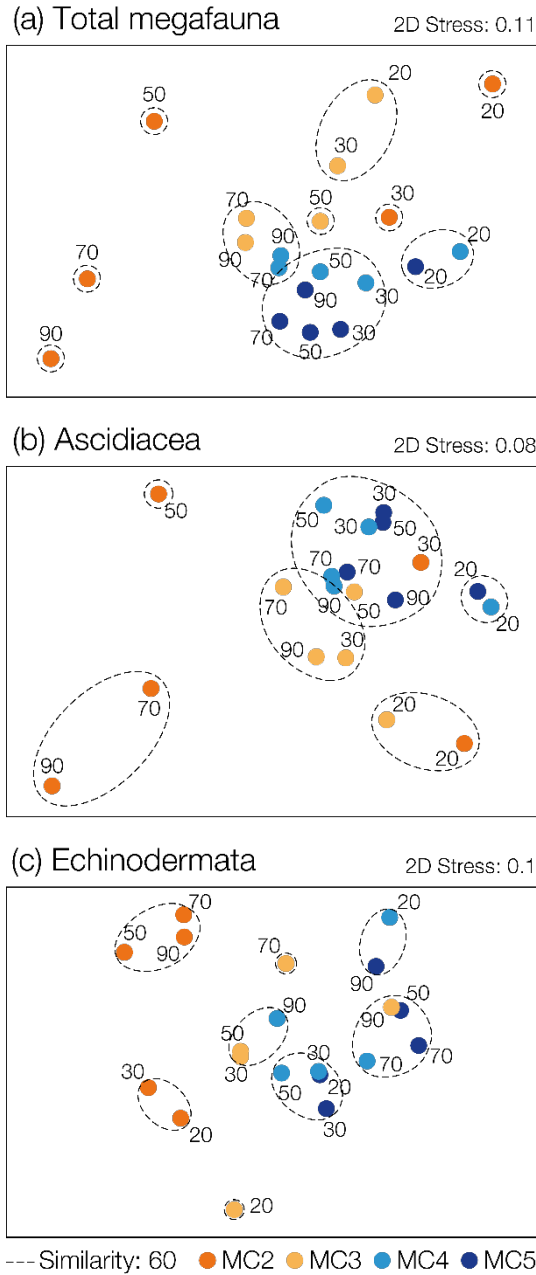


**Figure 3.6.**

Ascidian abundance and number of taxa present across various depths (10, 20, 30, 50, 70, and 90 m) at four stations (MC2, MC3, MC4, and MC5) in comparison with those of the total megafauna. Total number of taxa represents total sum of taxa occurred at a specific depth of each station. Only mean values represent for abundance (refer to Table 3.1–3.5 for the details of data).

Similarity between the total epibenthic and ascidian assemblages was further assessed using MDS plots. Total benthic assemblages were clearly distinguished by longitudinal distance from the glacier and water depth (Figure 3.7a) (ANOSIM test: global  $R=0.509$ ,  $p=0.001$ ). The assemblages at MC4 and MC5 in the inner cove were more closely clustered than those at either MC3 or MC2, and MC2 assemblages were most distinctly discriminated from those of other stations. Among depths, the assemblages at 20 m were distinct from those in deeper waters at all stations, while those in deeper waters (30 to 90 m) were closely grouped at all stations except MC2. Notably, the assemblages at MC2 were clearly distinguished, with depth to 70 m (global  $R=0.631$ ,  $p=0.001$ ).

Ascidians showed assemblage patterns (ANOSIM test: global  $R=0.394$ ,  $p=0.001$ ) very similar to those of total epibenthic megafauna (Figure 3.7b). SIMPER analysis revealed that ascidians contributed most (36 to 69%) to the dissimilarity of the total megafaunal communities among stations and water depths, except at 20 m depth in MC3, where the tube-building polychaete *Terebellidae* sp. (25% to the total) and the sea urchin *Sterechinus* sp. (24%) were as abundant as ascidians (25%) (Table 3.1–3.5). Although echinoderms were as taxonomically diverse as ascidians, they showed less similarity in assemblage patterns (global  $R=0.125$ ,  $p=0.001$ ) (Figure 3.7c) and contributed only 5–30% to the dissimilarities of the total benthos. Notably, the ascidian assemblage at 30 m of MC2 clustered closely with those observed at 30 to 90 m of MC4 and MC5 (Figure 3.7b).



**Figure 3.7.**

Non-metric multidimensional scaling (MDS) plots for total epibenthic megafauna and the two dominant taxa based on Bray-Curtis similarity matrix data (Table 3.1–3.5). Numbers near the symbols represent water depth (m) of each habitat. Data from 10 m depth were excluded for MDS analysis, as only a few taxa were present at this depth (in the case of ascidians present only at MC5).

### 3.3.3. Spatial patterns of ascidian distribution

#### 3.3.3.1 Abundance, species composition and diversity

Ascidian abundance, species composition and diversity varied greatly among stations and water depths (Figure 3.8, Table 3.1–3.5 and Table 3.8). Few ascidians occurred at <10 m depth, with only one species (*Cnemidocarpa verrucosa*) recorded at MC5. A moderate increase in density, mostly related to *C. verrucosa* (>90% to the total) was observed at 20 m in the innermost cove station, near the glacier (means=25 ind. m<sup>-2</sup> at MC4, 31 ind. m<sup>-2</sup> at MC5), while ascidians remained at low levels at more distant sites (means=5 ind. m<sup>-2</sup> at MC3, 3 ind. m<sup>-2</sup> at MC2). With increasing water depth, the ascidian density and biomass increased sharply, reaching a peak at 30–50 m depth at all stations.

Overall, *Molgula pedunculata* (41% to the number) was the most abundant ascidian in the cove, followed by *C. verrucosa* (24%) and *Ascidia challengeri* (18%). In terms of biomass, however, *C. verrucosa* (61%) outweighed *M. pedunculata* (19%) and *A. challengeri* (14%) at almost all stations and depths. Moreover, *M. pedunculata* and *C. verrucosa* predominated at the sites near the glacier and at shallow water (<30 m), while *A. challengeri* was most abundant at the distant site (MC2) and at deeper water (>50 m).

Ascidians were most abundant at the innermost station (MC5) near the glacier in terms of both density (~264 ind. m<sup>-2</sup>) and biomass (~15.7 kg m<sup>-2</sup>). The peak abundance (means=127 ind. m<sup>-2</sup> and 6.3 kg m<sup>-2</sup>) was observed at 30 m depth of this station, where *M. pedunculata* (mean=83 ind. m<sup>-2</sup>, max=144) and *C. verrucosa* (37 ind. m<sup>-2</sup>, max=108) together comprised 95% of total ascidians. *M. pedunculata* and *C. verrucosa* flourished across all depths at MC5 for the majority of ascidians present (83–100% to the total number, 87–100% to the total biomass). *M. pedunculata* and *C. verrucosa* also predominated down to a depth of 30 m at all stations, but their abundance tended to decrease toward the outer cove. The peak densities of *M. pedunculata* (mean=18 ind. m<sup>-2</sup>, max=72 at 30 m) and *C. verrucosa* (mean=16 ind. m<sup>-2</sup>, max=52 at 30 m) at the most distant site (MC2) were several times lower than those in the inner cove.



**Table 3.8.**

Ascidian biomass (g wet wt m<sup>-2</sup>) at various water depths across all stations (MC2, MC3, MC4 and MC5). Biomass was estimated using the density data obtained from ROV-acquired images (Table 3.1–3.5) and the allometric relationships shown in Figure 3.3. Values are mean±standard error. n: number of replicates

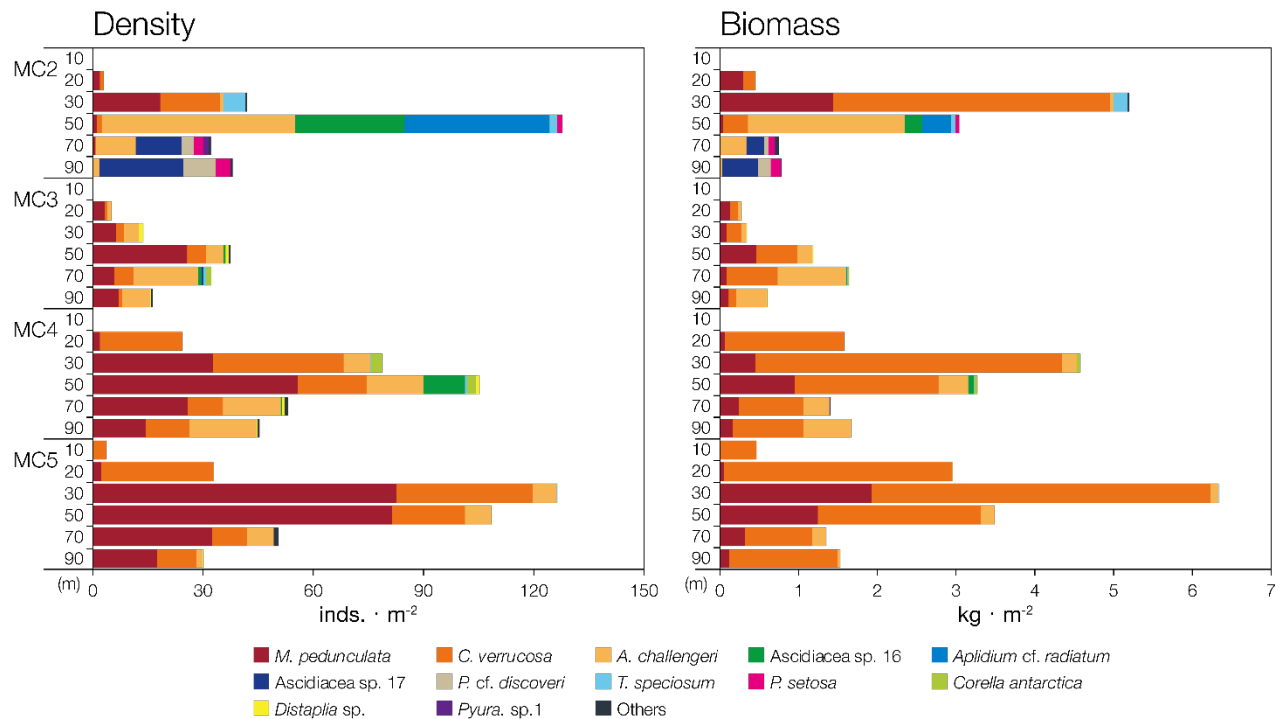
Station	Species	Depth					
		10 m	20 m	30 m	50 m	70 m	90 m
MC2	<i>A. cf. radiatum</i>				369±164		
	<i>A. challengeri</i>			47±27	1996±351	327±120	28±23
	<i>C. verrucosa</i>		153±153	3514±1093	314±314	5.2±5.2	
	<i>C. antarctica</i>						
	<i>Distaplia</i> sp.						
	<i>M. pedunculata</i>		297±297	1439±620	43±34	3.2±3.2	
	<i>P. cf. discoveri</i>					55±29	162±37
	<i>P. setosa</i>				54±45	81±29	131±51
	<i>P. cf. bouvetensis</i>					7.6±5.6	6.7±4.6
	<i>Pyura</i> sp.1					43±30	
	<i>S. sigillinoides</i>			19±19			
	<i>T. speciosum</i>			179±89	48±23		
	Ascidiacea sp.16				216±34		
	Ascidiacea sp.17					225±140	456±101
<b>Total</b>		450±321	5197±1061	3040±438	748±205	784±116	
MC3	<i>A. cf. radiatum</i>						
	<i>A. challengeri</i>		44±32	68±42	187±71	874±289	393±105
	<i>C. verrucosa</i>		95±95	190±102	521±224	654±333	96±96
	<i>C. antarctica</i>					15±11	
	<i>Distaplia</i> sp.			1.2±0.9	4.4±4.0		2.8±2.8
	<i>M. pedunculata</i>		133±119	85±41	462±179	80±43	112±72
	<i>P. cf. discoveri</i>						
	<i>P. setosa</i>						
	<i>P. cf. bouvetensis</i>						3.5±3.5
	<i>Pyura</i> sp.1						
	<i>S. sigillinoides</i>				2.8±2.8		
	<i>T. speciosum</i>					9.2±9.2	
	Ascidiacea sp.16				5.3±3.8	6.8±4.6	
	Ascidiacea sp.17					3.1±3.1	
<b>Total</b>		272±174	344±139	1183±309	1643±443	607±145	

**Table 3.8.**  
(continued)

Station	Species	Depth					
		10 m	20 m	30 m	50 m	70 m	90 m
MC4	<i>A. cf. radiatum</i>						
	<i>A. challengeri</i>			185±65	377±105	325±128	608±213
	<i>C. verrucosa</i>		1521±760	3897±1026	1828±484	826±285	896±191
	<i>C. antarctica</i>			41±30	38±24		
	<i>Distaplia</i> sp.				1.2±1.2	0.8±0.5	0.3±0.3
	<i>M. pedunculata</i>		62±43	449±171	949±231	239±31	166±60
	<i>P. cf. discoveri</i>						
	<i>P. setosa</i>						
	<i>P. cf. bouvetensis</i>					13.4±13.4	3.3±3.3
	<i>Pyura</i> sp.1						
	<i>S. sigillinoides</i>						
	<i>T. speciosum</i>			5.6±5.6	5.1±5.1		
	Asciadiacea sp.16				72±19	2.1±2.1	
	Asciadiacea sp.17						
		<b>Total</b>		1583±756	4577±1079	3271±711	1406±377
MC5	<i>A. cf. radiatum</i>						
	<i>A. challengeri</i>		5.6±5.6	102±36	180±63	173±66	30±14
	<i>C. verrucosa</i>	466±466	2900±659	4302±824	2071±409	859±206	1378±321
	<i>C. antarctica</i>						
	<i>Distaplia</i> sp.						0.3±0.3
	<i>M. pedunculata</i>		48±31	1927±259	1244±206	314±92	118±32
	<i>P. cf. discoveri</i>						
	<i>P. setosa</i>						
	<i>P. cf. bouvetensis</i>					5.8±3.4	
	<i>Pyura</i> sp.1						
	<i>S. sigillinoides</i>						
	<i>T. speciosum</i>			4.0±4.0			
	Asciadiacea sp.16						
	Asciadiacea sp.17						
		<b>Total</b>	466±466	2954±653	6336±926	3494±577	1353±235

**Table 3.8.**  
(continued)

Station	Species	Total	
		Absolute abundance (g wwt m <sup>-2</sup> )	Relative abundance (%)
Total	<i>A. cf. radiatum</i>	15.4	0.9
	<i>A. challengeri</i>	247.9	13.9
	<i>C. verrucosa</i>	1103.6	61.7
	<i>C. antarctica</i>	4.0	0.2
	<i>Distaplia</i> sp.	0.5	0.0
	<i>M. pedunculata</i>	340.5	19.0
	<i>P. cf. discoveri</i>	9.1	0.5
	<i>P. setosa</i>	11.1	0.6
	<i>P. cf. bouvetensis</i>	1.7	0.1
	<i>Pyura</i> sp.1	1.8	0.1
	<i>S. sigillinoides</i>	0.9	0.1
	<i>T. speciosum</i>	10.4	0.6
	Ascidiacea sp.16	12.6	0.7
	Ascidiacea sp.17	28.5	1.6
	<b>Total</b>	1787.9	100.0

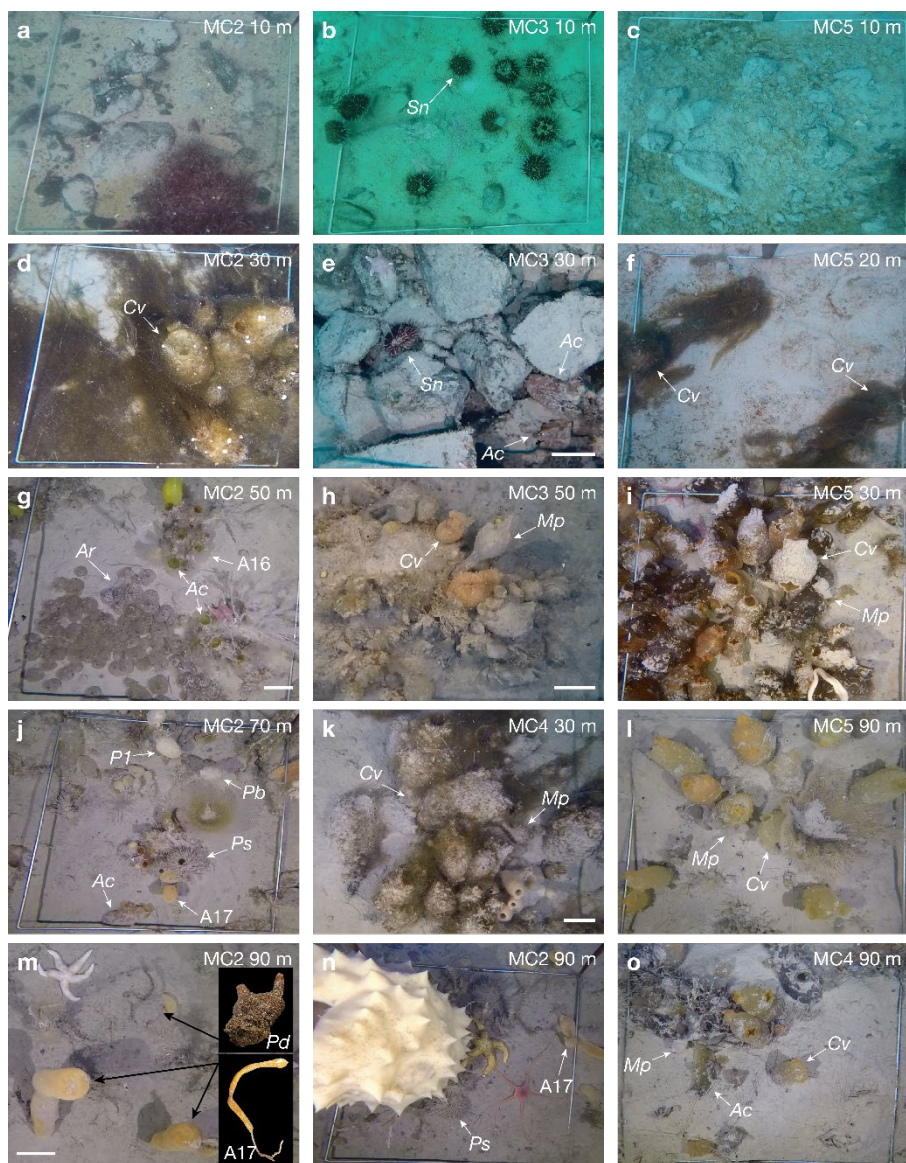


**Figure 3.8.**

Ascidian abundance and composition among various depths (10, 20, 30, 50, 70, and 90 m) at four stations (MC2, MC3, MC4, and MC5) in Marian Cove (MC). Most density peaks occurred at 30 or 50 m, while biomass peaks at 30 m were observed at all stations except MC3. Others include ascidian taxa that account for <3% of the total number of ascidian individuals at all stations. The horizontal bars indicate mean values. Refer to Tables 3.1–3.5 and 3.8 for the data and standard errors.

Unlike the ascidian communities at the ice-proximal zone and the shallow water, those in the deeper waters (>50 m) differed markedly with longitudinal distance from the glacier front. More diverse taxa were observed toward the outer cove, with the highest species richness (8 taxa) at 70 m of MC2. Moreover, at MC2, the species richness and composition differed distinctly with water depth (Figure 3.8 and 3.9). *M. pedunculata* and *C. verrucosa* dominated to the depth of 30 m, but decreased sharply (<2 ind. m<sup>-2</sup> each) to 70 m, and none were observed at 90 m. At 50 m, *A. challengerii* (mean=53 ind. m<sup>-2</sup>, 41% to the total) was most abundant, followed by *Aplidium* cf. *radiatum* (40 ind. m<sup>-2</sup>, 31%) and Ascidiacea sp.16 (30 ind. m<sup>-2</sup>, 23.4%). On the other hand, at 70 m, Ascidiacea sp.17 was most abundant (12.5 ind. m<sup>-2</sup>, 38.8%), followed by *A. challengerii* (11 ind. m<sup>-2</sup>, 32%), while at 90 m, Ascidiacea sp.17 was most abundant (23 ind. m<sup>-2</sup>, 59%), then *Pyura* cf. *discoverii* (9 ind. m<sup>-2</sup>) and *Pyura setosa* (4 ind. m<sup>-2</sup>).

At MC2, many individuals of the diverse taxa observed in the deep water were small in size, as compared to *M. pedunculata* and *C. verrucosa* occurring at shallow water (Figure 3.9). As a result, overall ascidian biomass (mean=3.2 kg m<sup>-2</sup>) at MC2 was not proportional to the density. Ascidian density peaked at 50 m (mean=128 ind. m<sup>-2</sup>, max=244) due to the presence of diverse taxa, while the biomass peaked at 30 m (mean=5.2 kg m<sup>-2</sup>, max=11.6) where the ascidian communities were predominated by large *M. pedunculata* and *C. verrucosa*.



**Figure 3.9.**

Images of ascidians within a quadrat (50x50 cm) taken by a ROV, showing distinct shifts in key taxa and the diversity of ascidian communities among stations and water depths in Marian Cove. (a, b) bottom substrates dominated by gravel at 10 m; sea urchins occurring at the highest numbers at this depth at MC3; (c) seabed covered by sand and silty sediment indicating heavy sedimentation near glacier (d) Ascidian communities, mostly comprised of *Molgula pedunculata* and *Cnemidocarpa verrucosa*, covered by dense blooms of the benthic diatom *Paralia* sp. (refer to Ha et al. 2019); (e) Relatively low ascidian abundance on boulder-sized substrate in shallow waters at MC3; (f) *C. verrucosa* population entangled with massive growth of benthic diatom and the surrounding bare seabed covered with a thick layer of

muddy sediment at 20 m depth, indicating heavy sedimentation at this site; (g) *A. challengeri*, *Aplidium* cf. *radiatum* and Ascidiacea sp.16 population dominating at 50 m at the distant site; (k, i) *M. pedunculata* and *C. verrucosa* predominating at 30 m depth in the inner cove (MC4, MC5); (h, l, o) *M. pedunculata* and *C. verrucosa*, less abundant but still dominating at 50–90 m in the inner cove; (j, m, n) Diverse taxa occurring at 70–90 m at MC2. Large hexactinellid sponges commonly occurred together. *Mp*: *M. pedunculata*; *Cv*: *C. verrucosa*; *Ac*: *A. challengeri*; *Pd*: *P. cf. discoveri*; *Ps*: *P. setosa*; *Pb*: *P. cf. bouvetensis*; *Ar*: *Aplidium* cf. *radiatum*; A16: Ascidiacea sp.16; A17: Ascidiacea sp.17; *Sn*: *Sterechinus* cf. *neumayeri*. Scale bars: 5 cm

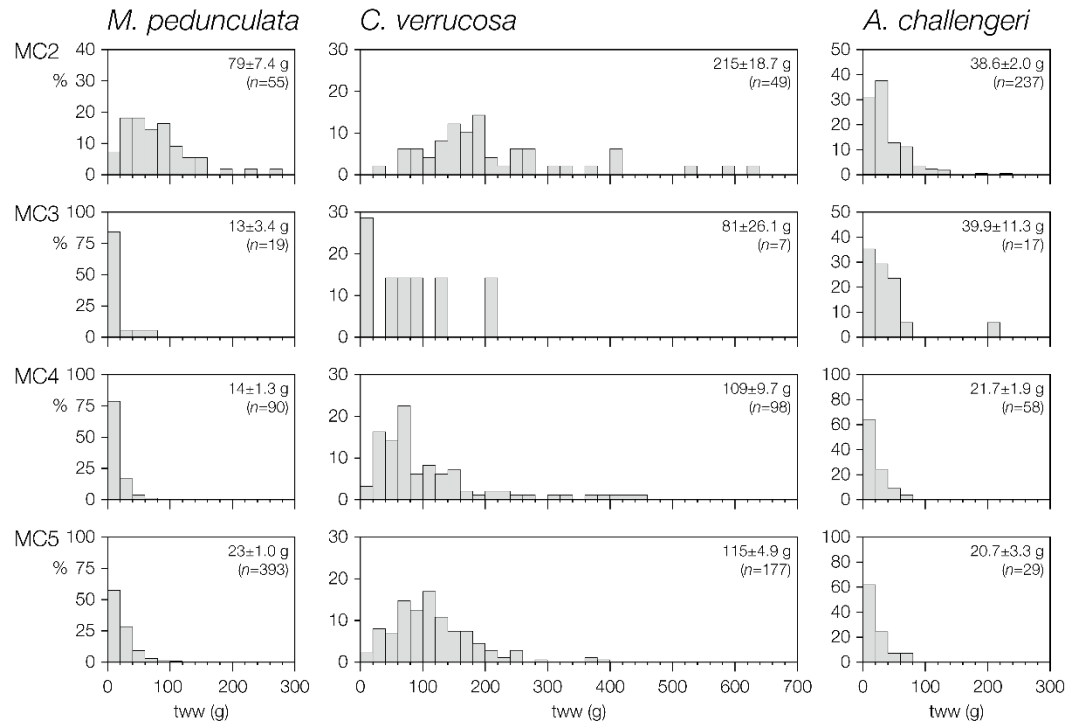
### 3.3.3.2 Differences in body size among stations

As shown in Figure 3.10, size frequency distributions of three dominant ascidian species were strongly skewed to the left (skewness values  $>1$ ), representing a large proportion of small size classes and a long tail with a small number of large individuals, and this trend was most prominent for *M. pedunculata* in the inner cove (MC3, MC4, and MC5). The average body size of *M. pedunculata* was several times larger (Mann-Whitney test  $p<0.001$ ) at the outer cove station (MC2) (mean=79 g tww, equivalent to 20.1 cm L) compared to those in the inner cove (13–23 g tww, 6.8–9.9 cm L). In addition, ascidians in the outer cove showed a wider range of size classes ( $<20$ –280 g tww,  $<9.0$ –38.9 cm L) compared to the size range ( $<20$ –160 g tww,  $<9.0$ –29.3 cm L) observed in the inner cove. Moreover, the majority of inner cove populations ( $>95\%$ ) belonged to classes of  $<60$  g tww ( $<17.4$  cm L), while only 44% belonged to the same classes at MC2, leading to extreme kurtosis values at MC3 (5.1), MC4 (4.0) and MC5 (7.6).

*C. verrucosa* showed a similar trend to *M. pedunculata*; average body sizes were several times larger (Mann-Whitney test  $p<0.01$ ) at MC2 (mean=215 g tww, 14.8 cm L) than in the inner cove (MC3, MC4, and MC5) (81–115 g tww, 8.7–10.6 cm L). *C. verrucosa* also showed a broader size range ( $>20$ –640 g tww,  $>3.8$ –26 cm L) in the outer cove compared to the range ( $<20$ –460 g tww,  $<3.8$ –21.9 cm L) in the inner cove. Likewise, *A. challengeri* showed smaller body size at MC4 and MC5 than those at MC2 ( $p<0.001$ ) and MC3 ( $p<0.05$ ), but this trend was not as prominent as those of *M. pedunculata* and *C. verrucosa*.

Despite having much lower mean density values (18 and 16 ind.  $m^{-2}$ , respectively), the peak biomass values (at 30 m) of *C. verrucosa* and *M. pedunculata* at MC2 (3.5  $kg\ m^{-2}$  and 1.4  $kg\ m^{-2}$ ) were disproportionately high compared to values at MC5 (4.3  $kg\ m^{-2}$  and 1.9  $kg\ m^{-2}$ ), where the densities of the two species were several times higher (82 and 37 ind.  $m^{-2}$ , respectively) (Figure 3.8). This discrepancy can be attributed to differing frequency distributions of ascidian size classes among stations (Figure 3.10).





**Figure 3.10.**

Comparison of size frequency distributions of three ascidian species among stations (MC2, MC3, MC4, and MC5) at their depth of peak abundance (*M. pedunculata* and *C. verrucosa* at 30 m, *A. challengeri* at 50 m). Size classes were determined based on total wet weight (tww), which was determined from body width or body length measurements obtained from ROV-acquired images using allometric relationships (refer to the Fig. 3.3 for the details). Figures inside the plots are mean±standard error. *n*: number of replicates

### **3.3.4. Relationship between ascidian assemblages and environmental parameters**

BIOENV analysis was performed to determine environmental variables which best explain the ascidian distribution. Environmental variables for the analysis were chosen based on the analysis results on the habitat properties (Figure 3.4, 3.5 and 3.7; Table 3.6). Distance from the glacier front was also added as a variable for the analysis. The high correlation between the distance to glacier and the period of deglaciation over the last six decades supported the notion that the distance may be used as a proxy of how long the seabed has been exposed after glacial retreat. Given a major shift in the habitat properties between the depths of 30 and 50 m (Figure 3.4 and 2.5), the analysis was conducted for two subdivided depth ranges (20–30 m and 50–90 m) in addition to the entire depth range (20–90 m). The depth of 10 m was excluded from analysis, as ascidians occurred at that depth only at MC5.

The single and combined parameters that best explain the ascidian distributions in the three depth categories are listed in Table 3.9. Over all depths except 10 m, the most influential single variable was distance ( $R=0.446$ ), followed by %silt, %sand, %TOC, and the combination of these variables best explained the spatial variations of ascidian assemblages ( $R=0.584$ ). For shallow depths (20–30 m), in contrast, distance had little effect on the assemblages, which were mostly affected by organic contents and sediment composition. Meantime, at 50–90 m depth, %TOC ( $R=0.802$ ) was the most influential single factor, along with %TN ( $R=0.756$ ), distance ( $R=0.700$ ), and %silt ( $R=0.493$ ) in order. Of note, the combination of these variables was most influential in structuring ascidian assemblages ( $R=0.820$ ). Seawater temperature and salinity had weak correlations in all depth categories.

**Table 3.9.**

Summary of biota-environment (BIOENV) analysis of the relationships between environmental factors and ascidian assemblages in Marian Cove. *R*: Spearman correlation coefficient. \* indicates the best results.  $p < 0.01$

Depth	Number of factors	R	Environmental factors			
20–90 m	1	0.446	Distance			
	1	0.345	Silt			
	1	0.268	Sand			
	1	0.247	TOC			
	1	0.222	Salinity			
	1	0.204	Gravel			
	1	0.189	Depth			
	1	0.188	Temperature			
	1	0.137	Clay			
	1	0.104	TN			
	3*	0.584	Distance	Sand	TOC	
	4*	0.584	Distance	Sand	Silt	TOC
	3*	0.582	Distance	Sand	Silt	
2*	0.580	Distance	Silt			
3*	0.578	Distance	Silt	TOC		
20–30 m	1	0.573	TOC			
	1	0.286	Sand			
	1	0.252	TN			
	1	0.155	Temperature			
	1	0.117	Salinity			
	1	0.103	Gravel			
	1	0.045	Clay			
	1	-0.027	Distance			
	1	-0.251	Silt			
50–90 m	1	0.802	TOC			
	1	0.756	TN			
	1	0.700	Distance			
	1	0.493	Silt			
	1	0.322	Gravel			
	1	0.248	Sand			
	1	0.056	Salinity			
	1	-0.031	Temperature			
	1	-0.100	Clay			
	4*	0.820	Distance	Silt	TN	TOC
	3*	0.819	Distance	Silt	TN	
	3*	0.818	Distance	Silt	TOC	
	3*	0.812	Silt	TN	TOC	
	2*	0.802	Silt	TN		

### 3.4. Discussion

#### 3.4.1. Ascidians as a key megabenthic community in an Antarctic fjord

A total of 64 taxa were described from the ROV images in this study, which was much less than the number of taxa described by direct sampling at <35 m depths in the previous study (117 taxa in Moon et al. 2015). That is because the ROV captured only two-dimensional images, and fauna covered by or underneath other organisms could not be detected in the images. In addition, small bivalves, bryozoans and amphipods were not discernable in the images. Nonetheless, most common epibenthic megafauna (e.g. *M. pedunculata*, *C. verrucosa*, *Odontaster validus*, *Sterechinus* sp., *Flabegraviera* sp., *Nacella concinna*, *Neobuccinum eatoni*, *Pabolarsia corrugatus*, and *Serolis* sp.) that occur in shallow Antarctic waters (Sahade et al. 1998, Barnes et al. 2006, Siciński et al. 2011) were identified from the images (Table 3.1–3.5). As for the ascidians, the total number of species (14) described from the images are comparable to those identified by direct samplings in adjacent nearshore bays in KGI, such as PC (17 in Tatiàn et al. 1998), and Admiralty Bay (16 in Siciński et al. 2011). Thus, despite some disadvantages (e.g., size limitation for taxonomic identification, underestimation of abundance and species richness), the ROV survey proved to be an efficient and reliable tool in this glacial cove for investigating large epibenthic megafauna such as ascidians, providing sufficient quantitative data to determine their distributional patterns.

Overall, the ROV survey revealed that ascidians were the most diverse (14 out of 64 taxa captured in the ROV images) and most abundant (mean=42 ind. m<sup>-2</sup>, 63% to the total) taxa among the epibenthic megafaunal communities in this glacial cove. The ascidian community was most responsible for the spatial variations of the total megafaunal communities across the cove (Figure 3.7). Furthermore, the spatial distribution patterns of ascidians and benthic megafauna were roughly matched (Figure 2.5 and figure 3.11). These results suggest that ascidians could be utilized as a key

community representing the benthic megafaunal community in this fjord and other similar Antarctic nearshore environments.

### **3.4.2. Ascidian assemblages in the ice-proximal zone**

The ice-proximal zone (the area in the innermost cove near the glacier front) represents apparently most unstable habitat for benthic organisms. Retreating glaciers are accompanied by generation of hundreds of floating ice pieces and massive inflow of turbid melt-water, consequently impacting benthic inhabitants, especially in shallow seabed. Ice-related disturbance and sedimentation have been considered as two principal disturbances associated with the retreat of marine-terminating glaciers in the coastal areas of WAP, acting detrimentally on benthic communities, particularly in shallow waters (Smale and Barnes 2008; Moon et al. 2015; Sahade et al. 2015). These two types of disturbance are also likely acting on the benthic communities in MC. Based on the observations on sea surface coverage by floating and/or grounded ices, Moon et al. (2015) reported that floating ice occurred at a much higher density in the inner cove, and suggested that scouring by ices generated from glacier carving is most intense close to retreating glaciers and is attenuated toward the outer cove.

Sedimentation also appears to be most intense at the area close to the glacier front. The high silt and clay contents throughout almost the entire water column at MC5, strongly indicated that heavy sedimentation of terrigenous particles nearly reached the bottom in the area near the glacier. Silt and clay contents decreased significantly toward the outer cove in shallow waters (<30 m) apparently as a result of decrease of turbid meltwater influence. The photographic images (Figure 3.9), where the seabeds and organisms were covered by fine sediment, support the idea that sedimentation is most intense close to the retreating glaciers. Previous studies in the cove also reported that sedimentation of terrigenous particles (mostly clastic silt-sized) carried by melt water occurred heavily in the ice-proximal zone (Yoon et al. 1997, 1998, Yoo et al. 2015).

Notably, ascidians were most abundant at this area, where physical disturbance associated with glacial retreat was extremely severe. In particular,

the two species, *M. pedunculata* and *C. verrucosa*, predominated across all depths at sites near the glacier with the peak abundances at 30 m (Figure 3.8). Furthermore, at the depth of peak abundance, most individuals of the two species were very small compared to those observed at the same depth from the distant site in the outer cove (MC2) (Figure 3.10), corroborating the idea that communities near the glacier front were at an early colonization stage. The predominance of small *M. pedunculata* and *C. verrucosa* individuals also suggested that they are short-lived in the ice-proximal zone. However, the high densities and biomass of small *M. pedunculata* and *C. verrucosa* individuals indicated that their populations could be maintained through rapid colonization and growth outweighing mortality. *M. pedunculata* and *C. verrucosa* are known to grow at least several times faster than other ascidian species, while they have relatively short life spans (~3.4 yrs) compared to other species (e.g., *A. challengerii* at ~11 yrs) (Kowalke et al. 2001).

Rapid colonization by *M. pedunculata* and *C. verrucosa* at high densities has frequently been reported in Antarctic nearshore embayments undergoing marine-terminating glacial retreat (Sahade et al. 1998; Lager et al. 2018). In the adjacent PC, very high numbers of ascidians (~310 ind. m<sup>-2</sup>) colonized a newly exposed area (<30 m) after glacial retreat, with *M. pedunculata* and *C. verrucosa* together constituting the majority of colonizing ascidians (~220 ind. m<sup>-2</sup>, >70% to the total) (Lager et al. 2018). In this study, we observed similar ascidian densities (264 ind. m<sup>-2</sup>) and the predominance of the same two species (252 ind. m<sup>-2</sup>) at similar environments in MC. Thus, the findings from this study strongly suggested that the highest ascidian abundance at sites near the glacier front is due to rapid colonization of the two opportunistic species that have competitive advantages over other species for newly exposed and highly disturbed habitats following glacial retreat.

### 3.4.3. Physical disturbance structuring ascidian communities in shallow habitats

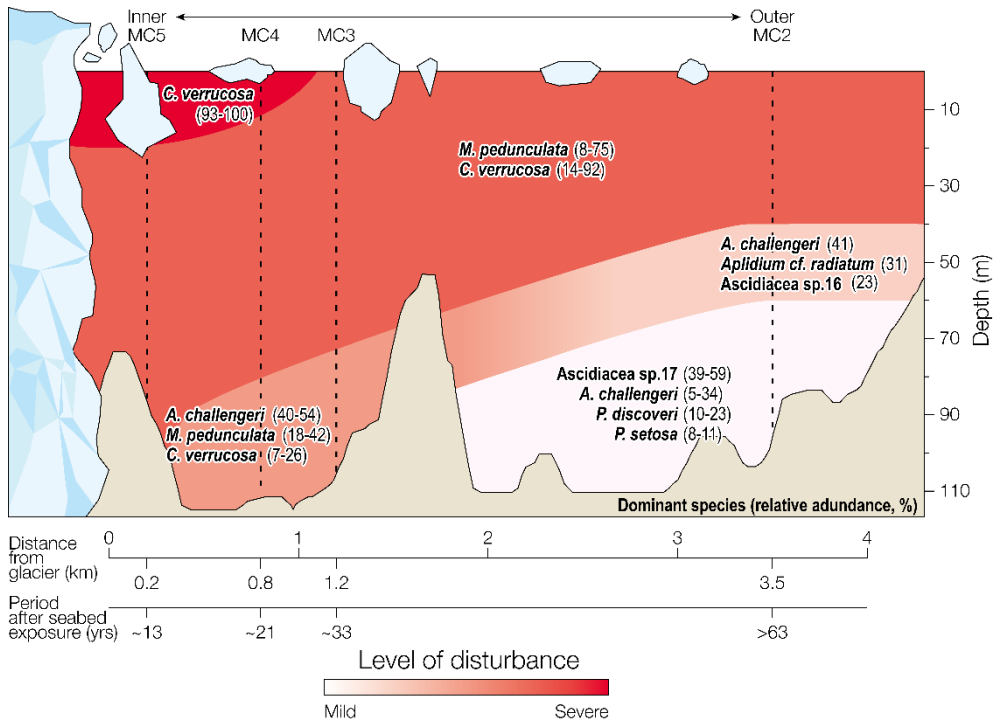
In addition to their dominance at the innermost sites, the two opportunistic ascidian species (*M. pedunculata* and *C. verrucosa*) predominated (79–100% to the total) down to a depth of 30 m at all stations across the cove, indicating that shallow habitats in the cove were highly disturbed. Notably, the ascidian assemblages at 30 m at station MC2 in the outer cove clustered closely with those at 30 to 90 m at MC4 and MC5 in the innermost cove (Figure 3.7b), apparently due to the predominance of *M. pedunculata* and *C. verrucosa*, which had comparable abundance values.

The shallow habitats showed much less distinct variations in the environmental properties across the stations, as compared to the deep habitats (Figure 3.4 and 2.5, Table 3.6), indicating that major determinants or forces structuring ascidian communities are different from those in the deep habitats. The most-likely cause is ice scouring, which is prevalent throughout the year in the Antarctic nearshore areas irrespective of glacial retreat. Ice scouring is known to be most intense at <15–20 m in Antarctic nearshore areas, resulting in low abundance and diversity of benthic communities at those depths (Smale et al. 2008; Barnes and Souster 2011; Barnes 2017). Likewise, in this study, abundances of ascidian as well as other taxa were very low at <20 m at all stations (Table 3.1–3.5), supporting the idea that physical disturbance due to ice scouring is one major force structuring benthic communities in this cove.

Overall physical disturbance in shallow waters, however, was apparently much more severe at the site nearest the glacier front due to additional perturbation associated with glacial retreat (Figure 3.11). Interestingly, *C. verrucosa* occurred in relatively high numbers at 20 m at the sites near the glacier front (mean=23 ind. m<sup>-2</sup>, max=212 at MC4; mean=31 ind. m<sup>-2</sup>, max=108 at MC5), where they outnumbered *M. pedunculata* (~2 ind. m<sup>-2</sup>). Similar patterns were observed in the adjacent PC, where *C. verrucosa* showed much higher densities (~160 ind. m<sup>-2</sup>) at 10–15 m depth than *M.*



*pedunculata* (<60 ind. m<sup>-2</sup>) along a newly exposed island, whereas *M. pedunculata* occurred with higher densities at 20–30 m, with its peak (>160 ind. m<sup>-2</sup>) at 25 m (Lagger et al. 2018). *C. verrucosa* is known to tolerate heavy sedimentation better than *M. pedunculata* and other species (Torre et al. 2012). Thus, *C. verrucosa* appears to be most tolerant among the ascidian taxa in the cove to the physical disturbance associated with glacial retreat, which allow them colonize the extremely disturbed seabed.



**Figure 3.11.**

Conceptual drawing of successional shifts in dominant ascidian taxa in Marian Cove, a fjord in the northern WAP that has been rapidly warming and deglaciating over the last six decades. This drawing illustrates how the intensity of physical disturbance, due to ice scouring and sedimentation associated with glacial retreat, acts as a key driver structuring ascidian communities.

With increasing water depth, ascidian abundance increased sharply, reaching its peak at 30 m (Figure 3.8, Table 3.1–3.5 and 3.8), which can be attributed primarily to reduced ice scouring and, at least in part, to enhanced food availability at this depth. BIOENV analysis revealed that the ascidian assemblages were significantly related to sediment organic carbon content, supporting the idea that food availability is an important factor structuring the shallow-water ascidian communities. Although no significant differences in sediment organic matter content (indicative of food amount) or C/N ratio (indicative of food quality) were found at <30 m, availability of other food sources appeared to be greater at 30 m than <20 m. Recent studies have reported that benthic diatom blooms overgrowing a variety of benthic filter feeders, including ascidians, occur sporadically at depths of >20–50 m, with a peak occurrence around 30 m depth at most distances from retreating glaciers within the cove (Ahn et al. 2016; Ha et al. 2019). Ha et al. (2019) reported that these diatom blooms were intense and persistent, at least during the austral summer. Using isotopic tracers, Ha et al. (2019) further demonstrated that massive benthic diatom blooms were consumed as the primary food source by ascidians and other filter feeding benthic fauna, including sponges, bivalves, and terebellid polychaetes. In this study, we also observed widespread benthic diatom blooms at shallow seabeds particularly at ~30 m depth (Figure 3.9). Benthic diatom blooms were observed even at the sites adjacent to glacier front, despite the apparent heavy sedimentation (Figure 3.9f, 3.9i, 3.9k). This strongly suggested that food is not limiting for ascidian growth even at the sites close to glacier, which could explain rapid colonization of the two ascidian species at these sites.

At MC3, ascidian abundance was low relative to those in the other stations. Interestingly, *Sterechinus* sp. were observed at this site in relatively high numbers at <20 m (mean=9.5 ind. m<sup>-2</sup>, max=44 at 10 m; mean=4.7 ind. m<sup>-2</sup>, max=20 at 20 m). This can be attributed to substrate type. The bottom substrates of shallow waters (<30 m) at MC3 were comprised of relatively

high proportions (19-46%) of cobble- (>64–256 mm) and boulder-sized (>256 mm) clastic rock fragments compared to the same depths at other stations (~20% at MC2, ~11% at MC4 and ~3% at MC5), which was likely to favor the sea urchin *Sterechinus* sp.

Overall, physical disturbance by ice scouring is apparently a most influential driver shaping ascidian assemblages in shallow habitats of this cove. In addition, food availability, bottom substrate type and species-specific tolerance to disturbance likely act differentially along the distance from the glacier and also with water depth, affecting, in part, ascidian assemblages. Nonetheless, the predominance of the two species, *M. pedunculata* and *C. verrucosa*, showed that the shallow-water communities remain at an early colonization stage regardless of the distance of the glacier front.

#### **3.4.4. Successional shifts of ascidian communities in deep habitats**

Unlike the ascidian communities at the ice-proximal zone and the shallow water, the deep ascidian community structure differed markedly with longitudinal distance from the glacier front, ranging from communities at the early colonization stage near the glacier front to more mature communities with diverse taxa at the remote site. The high correlation between the distance from the glacier front and the time after deglaciation suggests that we can infer the successional shift in the past from the spatial pattern in the present.

As demonstrated in the BIOENV analysis (Table 3.9), the ascidian assemblages in the deep-waters (50-90 m) were distinctly related to the distance from the glacier (Table 3.9), indicating a successional shift over a long-term period (for at least six decades) (Figure 3.11). The analysis also revealed that ascidian assemblages were strongly related to sediment properties (composition, mean grain size, level of sorting, organic contents etc.) that varied significantly with the distance from the glacier in association with glacial retreat processes. The overall results of sediment analyses clearly showed that habitat stability increased toward the outer cove in the deep water.

Notably, the silt and clay contents in deeper water (>50 m) increased toward the outer cove, reaching their highest levels at 70 m (mean=91%) and 90 m (94%) at MC2, despite the long distance between this station and the source of turbid meltwater. Moreover, these sediments were much better sorted (mean sorting values=2.1 phi at 70 m, 1.8 at 90 m) and finer (mean grain sizes=7.2 phi at 70 m, 7.4 at 90 m) at this distant site than those at the same depth of the nearest site (mean sorting values=4.7 phi at 70 m, 3.4 at 90 m; mean grain sizes=4.9 phi at 70 m, 6.3 at 90 m), suggesting that transport processes affect differentially various sizes of sediment particles in suspension. A meltwater plume carrying sediment particles (mostly angular silt-sized) was reported to extend far beyond the cove into Maxwell Bay (Yoon et al. 1998). While relatively large particles (e.g. sand) settle to the bottom near the meltwater source, fine particles travel longer distances,

eventually dominated by fine silt and clay at greater distances (Yoon et al. 1997), which could explain the extremely high percentages of silt and clay (most sorted) observed at 70–90 m depth of MC2.

Sedimentation rates at MC2, the most distant site from the glacier front, are likely to be much lower than those at sites near the glacier, as influence of meltwater carrying sediment particles decreases with increased distance from the source. The annual average concentrations of SPM recorded at MC ranged from  $<3$  to  $30 \text{ mg l}^{-1}$  over the last two decades (1997–2017) with higher values in the inner cove near the meltwater sources during the summer months ( $>28 \text{ mg l}^{-1}$ , compared to  $4 \text{ mg l}^{-1}$  at the distant site in Yoon et al. 1998;  $>10 \text{ mg l}^{-1}$  compared to  $1 \text{ mg l}^{-1}$  in Ahn et al. 2004). Thus, fine and most sorted sediment in the deep waters of the outer cove may have accumulated without frequent disturbance over a long period of time, resulting in a most stabilized habitat for benthic communities in the cove.

Shifts in ascidian taxa associated with habitat stability were reported across several stages of recolonization on a deep shelf floor ( $>100$ – $270 \text{ m}$ ) of the Weddell Sea that was impacted by ice scouring (Teixidó et al. 2004). *M. pedunculata* occurred at all successional stages, but was most dominant in the early stage of colonization. On the other hand, *P. setosa* occurred only at the late colonization stage (in the undisturbed assemblage), while *A. cf. radiatum* and *Sycozoa sigillinoides* were present in both the relatively stable and undisturbed stages.

In this study, we observed similar patterns in ascidian community shift with the previous studies, although the depth ranges surveyed in the cove were shallower ( $10$ – $90 \text{ m}$ ). For example, *M. pedunculata* and *C. verrucosa* were dominant across the entire water depths at sites near the glacier, the most disturbed habitats. On the other hand, *P. setosa* was recorded from  $50$ – $90 \text{ m}$  at MC2, and had its highest density values at  $90 \text{ m}$  (mean= $4.3 \text{ ind. m}^{-2}$ ), which was apparently the most stable habitat among surveyed areas in this glacial cove. Furthermore, *A. cf. radiatum* (at  $50 \text{ m}$ ) and *P. cf. discoveri* ( $70$ – $90 \text{ m}$ )

were observed only at MC2, and *S. sigillinoides* was found at both MC2 (30 m) and MC3 (50 m), indicating a shift in habitat stability with distance as well as with water depth. Moreover, at MC2, the species composition differed distinctly with water depth and shifts occurred in the dominant species (Figure 3.11): *M. pedunculata* and *C. verrucosa* at <30 m; *A. challengerii* at 50–70 m; *A. cf. radiatum* and Ascidiacea sp.16 at 50 m; and Ascidiacea sp.17, *P. cf. discoverii* and *P. setosa* at 70–90 m. Thus, at the distant site, habitat stability appeared to increase rapidly with depth. The occurrence of abundant large (>20 cm L) hexactinellid sponges (*Anoxycalyx cf. joubini* and Rossellidae spp.) at 50–90 m depth in MC2 (Table 3.1–3.5, Figure 3.9n) also supported the idea that the habitat at 50–90 m of MC2 was relatively stable and may have been undisturbed for at least several decades (Gutt and Starmans 2001, Teixidó et al. 2004).

*A. challengerii*, the third most abundant species after *M. pedunculata* and *C. verrucosa* in this cove, occurred across all stations, mostly at >50 m, with the highest abundance (means=53 ind. m<sup>-2</sup> and 2 kg m<sup>-2</sup>) at 50 m in MC2. This finding suggested that *A. challengerii* is more sensitive to disturbance than *M. pedunculata* or *C. verrucosa*. Unlike *M. pedunculata* and *C. verrucosa* with inflated and erect bodies, *A. challengerii*, is laterally flattened and lie in most cases on the seabed with their siphonal openings near the sediment-water interface, where turbidity is very high due to frequent resuspension of sediment, as compared to the water column above. This difference could explain why *A. challengerii* occurred more abundantly in deeper waters, as turbidity likely decreases with increasing water depth. Its occurrence at all stations, on the one hand, indicates that *A. challengerii* is more tolerant to disturbance than taxa occurring only in deep waters at MC2.

Altogether, sediment properties showed that the deep seabed is physically stabilized toward the outer cove, which contributed strongly to the marked shifts in ascidian assemblages observed across the cove. BIOENV

analysis also revealed that ascidian assemblages were strongly related to sediment organic contents, which increased significantly toward the outer cove, suggesting that food availability also contribute, in part, to the observed shifts of ascidian communities in the deep seabed.



### 3.5. Conclusions

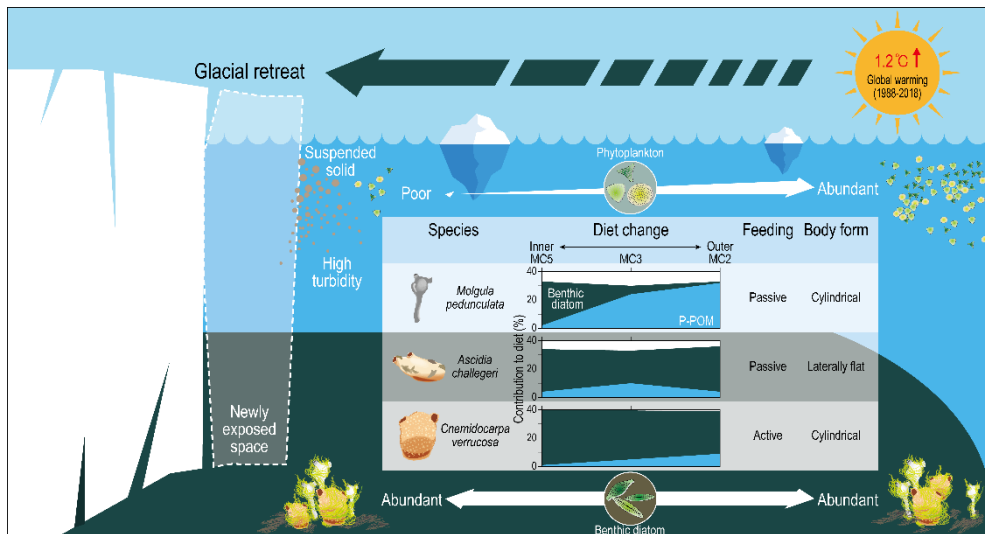
The first ROV survey in Marian Cove, a rapidly warming fjord in WAP, revealed that ascidian community represents epibenthic communities in aspects of abundance, taxonomic diversity and spatial distribution pattern. A set of analyses indicated that ascidian communities shifted drastically in abundance, species composition, and diversity with the longitudinal distance (~3.5 km) across the cove. In particular, such benthic community shift in deep seafloor areas (50–90 m) clearly indicated early colonizing communities near glaciers to more diverse communities at a distant site. The ascidian community shift was related mostly to sediment properties that develop in association with glacial retreat and consequent processes. The sediment properties showed that the deep seabeds are physically stabilized toward the outer cove, which contributed strongly to the marked changes in ascidian assemblages being evidenced across the cove environment.

The results of this study strongly indicated that physical disturbances (sedimentation and ice scouring) accompanying glacial retreat and consequent processes are an important force shaping ascidian assemblages in this cove, and these forces are altered by the distance from the glacier and water depth. In addition to numerical abundance and taxonomic diversity, the differential sensitivity, as reflected by their distributions, of ascidian taxa to habitat perturbation make ascidian communities valuable and sensitive indicators of the impacts of the climate-induced glacial retreat.

Ongoing warming and consequent glacier melting are expected to proceed over the next decade or even longer, particularly in the Antarctic Peninsula Region. Given that distance from the glacier front was roughly proportional to the time of seabed exposure after glacial retreat over the last six decades, the observed ascidian community shift in deep seabed across the cove reflects long-term successional processes that occurred in the past, which in turn provide us an insight into future scenarios for climate-induced changes.

## CHAPTER 4.

# CHANGES IN ASCIDIAN DIETS UNDER THE INFLUENCE OF GLACIAL RETREAT IN A FJORD, ANTARCTIC NEARSHORE



This chapter has prepared to submit.

Kim, D. U., Ahn, I. Y., Gal, J. K., Ha, S. Y., & Khim, J. S. Changes in ascidian diets under the influence of glacial retreat in a fjord, Antarctic nearshore.

## 4.1. Introduction

The MC in the WAP, one of the most rapidly warming regions on earth, is an area where glaciers have retreated about 1.9 km over the past 60 years, and it is one of the regions where ecological changes after glacial retreat have been well studied. In the cove, the distribution of benthic megafauna communities had changed depending on the influence of glaciers (Moon et al., 2015; D. Kim et al., 2021). In addition, the distribution of microphytobenthos, plankton, and suspended particles known as one of the major food sources for Antarctic filter feeders (Tatián et al., 2004; Pasotti et al., 2015; Ha et al., 2019), has also changed (Yoon et al., 1998; Bae et al., 2021; B. Kim et al., 2021). MC, where the habitat environments and communities are significantly different subject to glacial impact provide a good place to study the effects of glacial retreat by warming on the marine ecosystem.

Filter feeders are one of the key taxa of the Antarctic marine ecosystem because they are distributed throughout Antarctic and serve as a major energy path between the pelagic and benthic ecosystems (Gili et al., 2001; Gili et al., 2006; Tatián et al., 2008; Primo and Vázquez, 2014; Segelken-Voigt et al., 2016). Climate change-induced glacial retreat alters the distributions of macroalgae, microphytobenthos, phytoplankton, and suspended particles, the food sources of filter feeders (Yoon et al., 1998; Quartino et al., 2013; Bae et al., 2021; Ingels et al., 2020). Distribution changes in the food sources lead to changes in community structure of the filter feeders (Pineda-Metz et al., 2020). Filter feeders in the Antarctic coasts, mostly sponges, ascidians, and bivalves, are easily exposed to disturbances by environmental change because they do not have mobility or have very low. Therefore, the feeding characteristics of Antarctic filter feeders may vary according to glacial retreat. Changes in the diets of filter feeders according to habitat environmental changes were reported in other regions besides the Antarctic (Jung et al., 2019). However, it is not yet known how the environmental changes in habitats accompanying glacial retreats alter feeding strategies of the filter feeders.

Ascidian is a representative filter feeder in Antarctica (Gili et al., 2006). Ascidians are suitable as indicator taxa for environmental changes because their responses to environmental changes varies depending on the species. The pioneer species, *Cnemidocarpa verrucosa* and *Molgula pedunculata*, increased rapidly in

densities in areas where ice-scoured or newly exposed from the glaciers (Teixido et al., 2004; Sahade et al., 2015; Lagger et al., 2018; D. Kim et al., 2021). On the other hand, *Ascidia challengerii* had high densities in relatively stable habitats (D. Kim et al., 2021). The distribution of ascidians was affected by SPM because of their different sensitivities to the SPM concentration (Torre et al., 2012; Torre et al., 2021). Although the relationship between the environment and ascidian distribution relatively well studied, little was known about the diet change of ascidians with different distribution patterns. Studies on the effects of changes in food sources on ascidians are also insufficient. Therefore, it is difficult to understand the relationship between the changes in food sources and ascidian communities, such as what kind of food the dramatic increase in ascidian density is based on after glacial retreat and how the ascidian diet changes as the community succession.

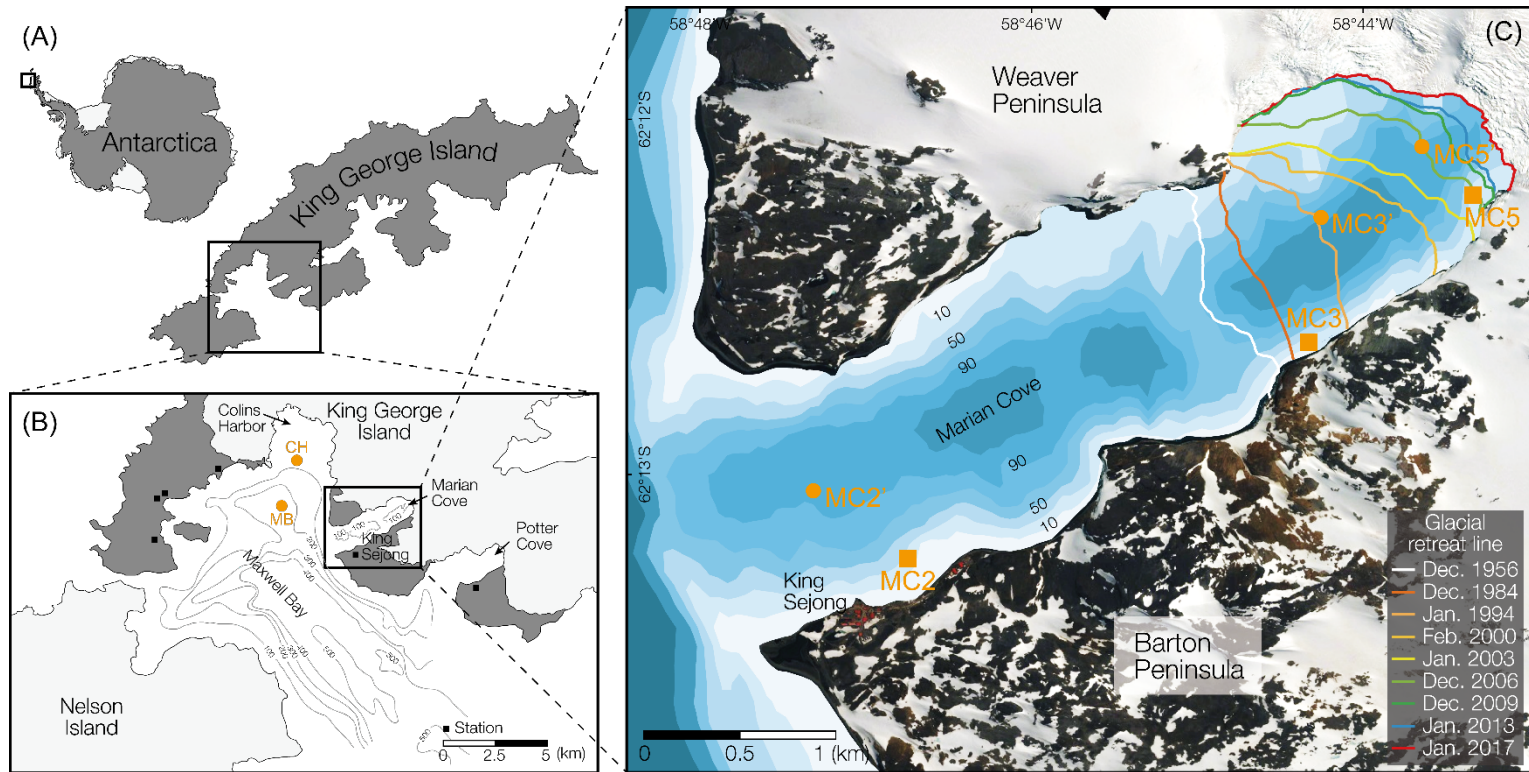
The objectives of this study are to confirm the changes in food source composition and ascidian diets in deglaciating fjord in order to understand shifts of ascidian communities in Antarctic nearshore. We investigated: 1) spatial variation of C and N stable isotopes of three dominant ascidians with their potential food sources at three sites where the influence of the glacier was different; 2) dietary changes among species according to glacial effects. In addition, one ascidian species dominated in deep depths was analyzed to confirm the effects of water depth. The findings from this study will enhance our understanding of the differences in feeding responses of ascidians depending on species to glacial influences.

## 4.2. Materials and methods

### 4.2.1. Study area

Tidewater glaciers are well developed on the inner site of the MC. The glaciers have retreated 1.9 km of glaciers from 1956 to 2017, causing the ice-free area to expand by 45% (Figure 4.1). Glacial carving and melting that occur throughout the summer introduce large amounts of fresh water, ices, and terrestrial sediment into the cove (Yoon et al., 1998; Ahn et al., 2004; Yoo et al., 2015). Glacial retreats of the MC were slower in cooling period (2000-2015: 40 m yr<sup>-1</sup>, annual mean temperature -1.91°C) than warming period (1989-2000: 64 m yr<sup>-1</sup>, -1.61°C) of the WAP (Turner et al., 2016; Oliva et al., 2017). Glacial retreats that reflect the climate change trends of WAP shows that the MC is a natural laboratory to monitor the impact of climate change on the marine ecosystem of WAP.

MC is a small and confined fjord-like embayment (~4.5 km long and ~1.5 km wide) located at the northern tip of the WAP. Meteorological data (1988-2018) in the MC showed an average air temperature of -1.8°C (min=-5.7°C in July, max=1.9°C in January), and generally >0°C from December through March (Hong et al., 2019). The MC consists of three basins with a maximum depth of about 130 m, and is separated from the Maxwell Bay by a shallow sill (~40 m) at the entrance (Yoon et al., 1997). Water circulation with Maxwell Bay is restricted by the sill (Yoo et al., 2015). The water temperature changed with the seasons (max=1.5°C in February, min=-1.8 in August), but salinity remains fairly constant throughout the year (33.8 to 34.1 psu) except for the surface layer in the summer where melt water flows in. Salinity showed a tendency to slightly decreased toward surface (D. Kim et al., 2021). The water temperature and salinity showed only slight differences according to the distance from the glacier (-0.3 to -0.4°C, 33.9 to 34.0 psu) and water depth (-0.3 to -0.6°C, 33.9 to 34.1 psu) (D. Kim et al., 2021).



**Figure 4.1.**

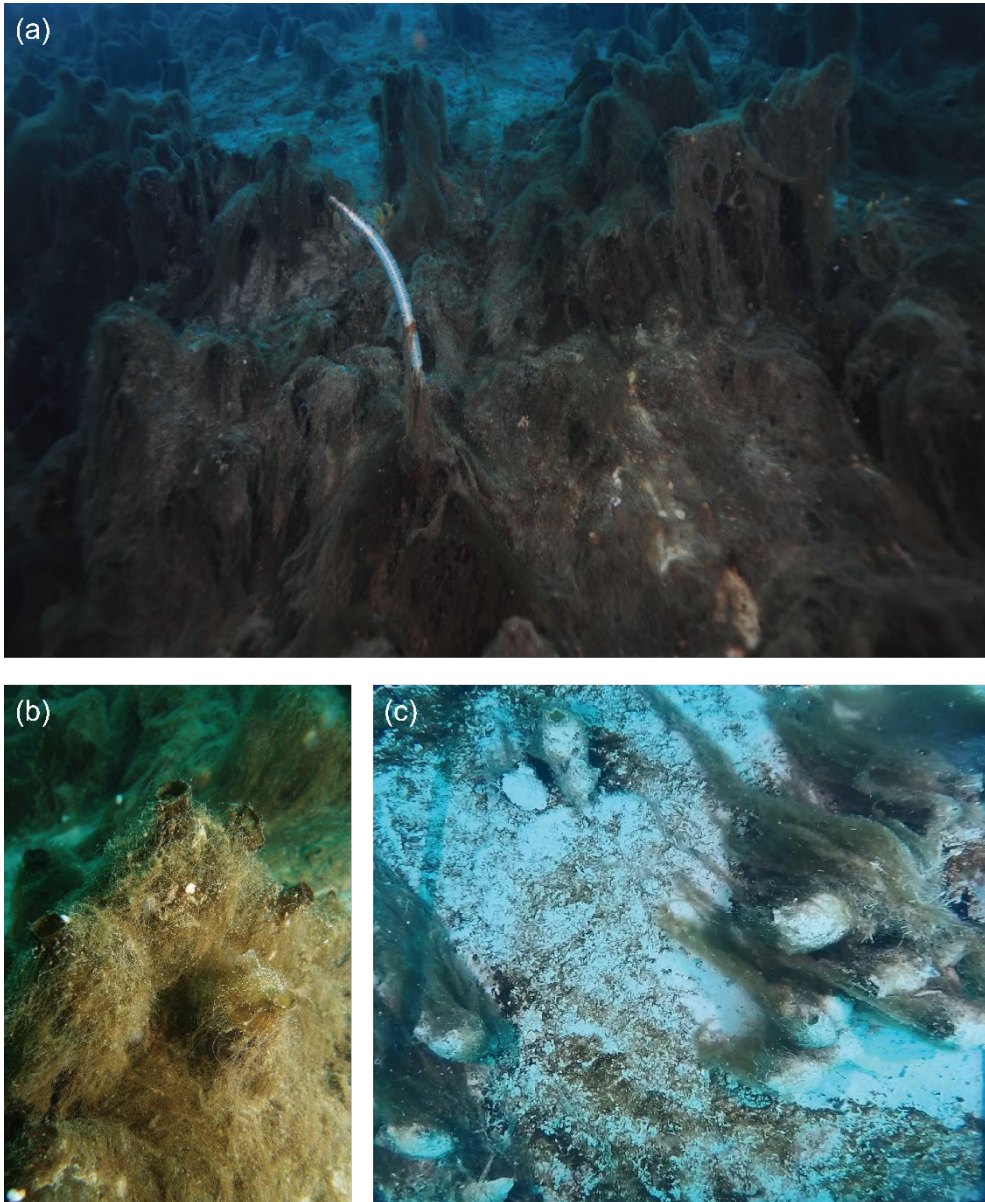
(a) Map showing the locations of King George Island, Maxwell Bay, and its tributary embayments including Marian Cove (MC). (b) Bathymetry and sampling stations of Maxwell Bay. Bathymetric contours are drawn based on information from the Atlas Hidrografico Chileno Antarctica from the Instituto Hidrografico de la Armada, Chile (1982). The area in white represents glacier or snow cover. (c) Sampling stations and glacial retreat

lines over six decades. Glacial retreat lines were drawn based on information obtained from satellite images and aerial photographs (updated from D. Kim et al., 2021). Orange squares are stations for sediment and ascidian samples at 30 m. Seawater properties and ascidians at deep depths were collected at orange circles.

#### **4.2.2. Potential food sources selection**

Previous study reported that filter feeders mainly consume benthic diatoms in MC (Ha et al., 2019). Although benthic diatoms primarily inhabit surfaces of sediments or megabenthos, they are easily resuspended (Brandini and Rebello, 1994; Ahn et al., 1997a; Kang et al., 1997). The wide distribution of benthic diatoms (Figure 4.2) provides opportunities for consumers to easily eat the diatoms everywhere in the cove (Ha et al., 2019). In particular, benthic diatom bush (BDB, diatoms that grow in the form of bushes on the surface of megabenthos or sediments; Ha et al., 2019) that is physically close to filter feeders is apparently consumed more easily. To confirm the contribution of benthic diatoms to diet of ascidians, BDB and benthic diatom mat (BDM, brownish flocculent matter at the surface of sediments) was collected respectively. Ascidians are filter feeder known as rely on particulate organic matter (POM) such as phytoplankton, detritus (Klumpp, 1984; Tatian et al., 2002; Pasotti et al., 2015; Tatian et al., 2004). In general, pelagic particulate organic matter (P-POM), indicating pelagic primary production, settles to the bottom and becomes part of sedimentary organic matters or food for filter feeders. Benthic particulate organic matter (B-POM) reflects the resuspended organic particles. Sediment resuspension is a common phenomenon in Antarctic nearshore, and particularly in MC, resuspension is an important source of suspended particulate matter (Kang et al., 1997; Yoon et al., 1998; Gili et al., 2001). Therefore, in this study, POM was collected from the surface and bottom respectively. SOM containing not only POM and benthic diatoms but fragments of flora and fauna was also sampled as potential food sources of ascidians.





**Figure 4.2.**

(a) *Molgula pedunculata* assemblages densely covered by benthic diatom bush at the outermost site (MC2, the photo from Ahn et al. 2016). in the Marian Cove. (b) A close-up picture showing the thread-like diatom bush attached to the *M. pedunculata*. (c) Diatom bushes covered ascidians and diatom mats on the surface sediments in the innermost site (MC5).

### 4.2.3. Sample collection

Three dominant ascidians (*Molgula pedunculata*, *Ascidia challengerii*, and *Cnemidocarpa verrucosa*) and five potential food sources (BDB, BDM, P-POM, B-POM and SOM) were collected for stable isotope analysis. Three ascidians and potential food sources except P-POM were collected by SCUBA divers at 30 m depths of three stations (MC2, MC3, and MC5) with different distance from the glacier from December 2017 to February 2018 (Figure 4.1). The BDB was retrieved from benthic fauna, mostly from ascidians and demosponges, while the BDM was scraped from the sediment surface. Surface sediments collected using a hand core (diameter: 6.5 cm, height: 6 cm), and top 2 cm was subsampled for SOM analyses. B-POM was analyzed from water samples obtained by SCUBA divers using water sample bottles at organism collected sites. P-POM were collected by a Niskin bottle from seawater surfaces in stations (MC2', MC3', and MC5') where distance from glaciers were similar to other samples collected stations (MC2, MC3, and MC5), respectively. To confirm the effect of water depth on ascidian diet, *Pyura bouvetensis* was collected at 95 m (MC2 and CH) and 260 m (MB) by Agassiz trawl on April 2018. Collected samples were frozen (-20°C) before isotopic analysis.

#### 4.2.4. Stable isotope analysis

For isotopic analysis, the gut-free soft tissues were excised from half-frozen ascidian specimens. The soft tissues and food sources were freeze-dried and finely ground. Inorganic C was removed via treatment with 1M HCl, and lipid compounds were extracted using a mixture of methanol and chloroform (1:2, v/v) before measuring the stable organic  $\delta^{13}\text{C}$  ratio. The lipid-extraction was skipped for food source samples. Samples for the  $\delta^{15}\text{N}$  analysis were used without pretreatment (Carabel et al., 2006).

The  $\delta^{13}\text{C}$  and  $\delta^{15}\text{N}$  ratios were determined using an isotope ratio mass spectrometer (Isoprime 100; Elementar, Manchester, UK) connected to an elemental analyzer (Euro EA3028; EuroVector, Milan, Italy). Running standards was CH-6 and N-1 (IAEA,  $\delta^{13}\text{C}$  and  $\delta^{15}\text{N}$  values were -24.7‰, relative to V-PDB, and 0.4‰, relative to air, respectively). These standards were analyzed after every 10 samples, and the standard deviation was <0.2‰. Stable isotopic ratio was expressed in delta ( $\delta$ ) notation relative to the conventional standard (C, Vienna Pee Dee Belemnite; N, atmospheric  $\text{N}_2$ ), with the following formula:

$$\delta X (\text{‰}) = (R_{\text{sample}}/R_{\text{standard}} - 1) \times 1000$$

where X is  $^{13}\text{C}$  or  $^{15}\text{N}$  and R is the ratios,  $^{13}\text{C}/^{12}\text{C}$  or  $^{15}\text{N}/^{14}\text{N}$ .

#### **4.2.5. Data analysis and statistics**

The relative contributions of the potential food sources to the diets of ascidians were estimated using a Bayesian isotopic mixing model in the R package (Stable Isotope Analysis software in R: versions SIAR 4.2 and R 4.1.1). Expected fractionation values ( $\delta^{13}\text{C}$ :  $0.5 \pm 0.13\%$ ,  $\delta^{15}\text{N}$ :  $2.2 \pm 0.3\%$ ) were applied for the SIAR modeling (McCutchan et al., 2003). The proportion of each source in the diet of ascidians was plotted with Bayesian model. The probability and distribution of prey contributions to each ascidian was expressed as 50, 75, and 95% confidence intervals and mean values, considering the within-individual variability and the uncertainties of the parameters. Univariate non-parametric analyses (Kruskal-Wallis test and Mann-Whitney U test) and Levene's test were performed using PASW Statistics (version 18.0).

## 4.3. Results

### 4.3.1. Stable isotope signatures of ascidians and potential food sources

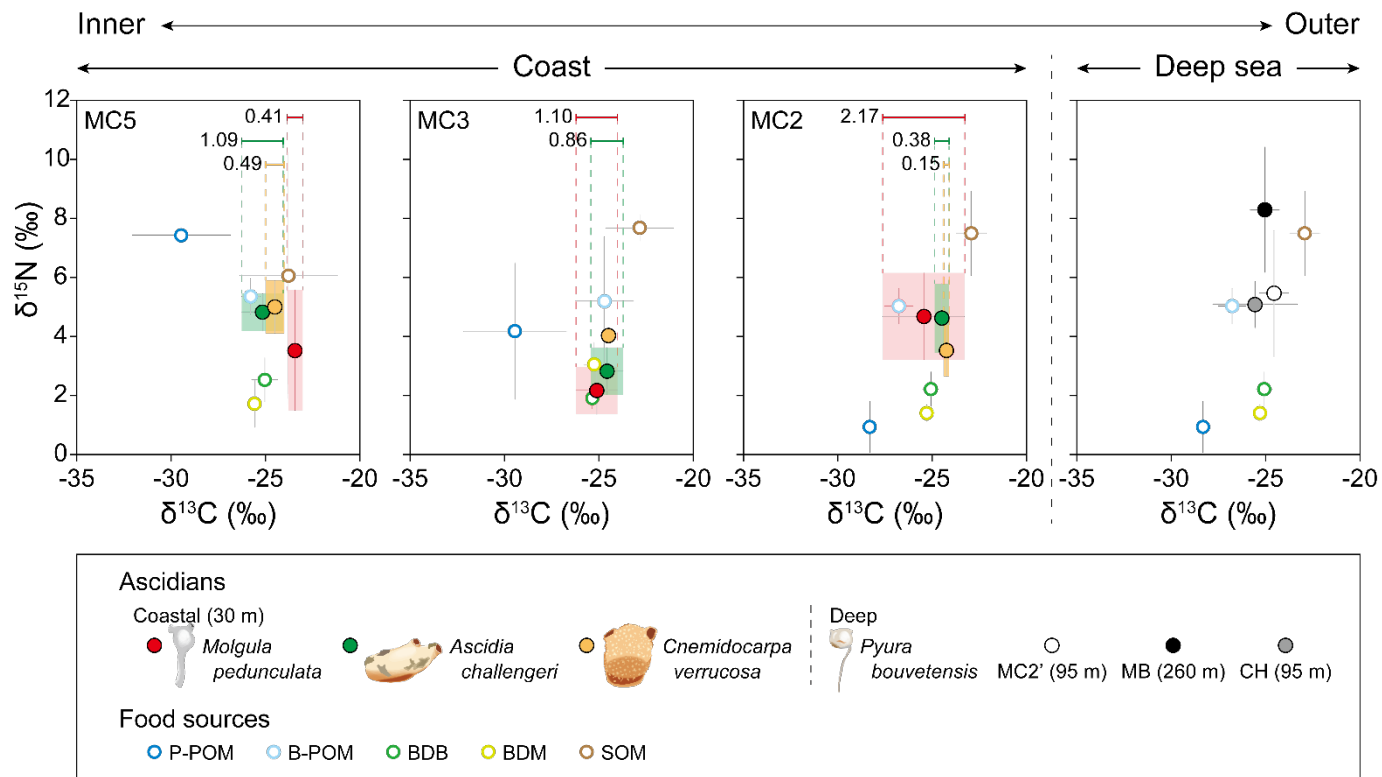
The  $\delta^{13}\text{C}$  and  $\delta^{15}\text{N}$  values of three ascidians were similar at all stations (Table 4.1, Kruskal-Wallis test,  $p>0.05$ ). However, the  $\delta^{13}\text{C}$  deviation was different depending on the species and station (Figure 4.3). *M. pedunculata* had a large deviation in  $\delta^{13}\text{C}$  values among individuals (Levene's test,  $p<0.001$ ), compared to the other two species. The deviation increased with distance from the glacier. The  $\delta^{13}\text{C}$  values of *A. challegeri* and *C. verrucosa* were relatively constant (-24.2‰ to -25.4‰) regardless of the distance from the glacier (Kruskal-Wallis test,  $p>0.05$ ). In particular, *C. verrucosa* showed very constant  $\delta^{13}\text{C}$  values within 0.5‰ deviation at all stations.  $\delta^{15}\text{N}$  values was not show significant trend with species or stations. *P. bouvetensis* had similar  $\delta^{13}\text{C}$  ratio at the two depths (Mann-Whitney test,  $p>0.05$ ), but was enriched in  $\delta^{15}\text{N}$  at deep depths (Mann-Whitney test,  $p<0.05$ ; Figure 4.3).

The  $\delta^{13}\text{C}$  and  $\delta^{15}\text{N}$  values of ascidian diets ranged from -22.8 to -29.5‰ and 0.9 to 7.7‰, respectively (Table 4.1).  $\delta^{13}\text{C}$  values of the potential food sources were similar except P-POM which more depleted (Figure 4.3). On the other hand,  $\delta^{15}\text{N}$  varied distinctly among the sources, and the stations (Figure 4.3). BDB ( $\delta^{13}\text{C}$ : -25.3 to -25.0‰,  $\delta^{15}\text{N}$ : 1.9 to 2.5‰) and BDM ( $\delta^{13}\text{C}$ : -25.6 to -25.3‰,  $\delta^{15}\text{N}$ : 1.4 to 3.0‰) had similar  $\delta^{13}\text{C}$  and  $\delta^{15}\text{N}$  values (Mann-Whitney test,  $p>0.05$ ). The  $\delta^{13}\text{C}$  and  $\delta^{15}\text{N}$  values of B-POM and P-POM were significantly different. The  $\delta^{13}\text{C}$  was more enriched in the bottom than surface (Mann-Whitney test,  $p<0.005$ ). The difference in  $\delta^{13}\text{C}$  value between B-POM and P-POM decreased at MC2 the outermost site. The  $\delta^{15}\text{N}$  did not show a clear trend with distance from the glacier in B-POM (linear regression,  $R^2=0.011$ ,  $p>0.05$ ), but were more depleted toward outer of the cove in P-POM (linear regression,  $R^2=0.831$ ,  $p<0.05$ ).

**Table 4.1.**

The  $\delta^{13}\text{C}$  and  $\delta^{15}\text{N}$  values of three ascidians and potential food sources in Marian Cove. Food sources and consumers were collected at 30 m depths from December 2017 to February 2018 except P-POM and *P. bouvetensis*. P-POM was collected at surface water from January to February 2019. *P. bouvetensis* was collected at 95 m at MC2' and Collins Harbor (CH) and 260 m of Maxwell Bay (MB) to use as a reference to compare the three shallow-water species on late April 2018. BDB; benthic diatom bush. BDM; benthic diatom mat. P-POM; pelagic particulate organic matter. B-POM; benthic particulate organic matter. SOM; sedimentary organic matter.

Group	Sample	Station	Replicate (n)	$\delta^{13}\text{C}$ (‰)	$\delta^{15}\text{N}$ (‰)	
Consumers	<i>Molgula pedunculata</i>	MC2	4	-25.4±2.2	4.7±1.5	
		MC3	3	-25.1±1.1	2.2±0.8	
		MC5	3	-23.5±0.4	3.5±2.0	
	<i>Ascidia challengeri</i>	MC2	4	-24.5±0.4	4.6±1.2	
		MC3	4	-24.6±0.9	2.8±0.8	
		MC5	3	-25.2±1.1	4.8±0.6	
	<i>Cnemidocarpa verrucosa</i>	MC2	6	-24.2±0.1	3.5±0.9	
		MC3	1	-24.5±0.0	4.1±0.0	
		MC5	4	-24.5±0.5	5.0±0.9	
	<i>Pyura bouvetensis</i>	MB	5	-25.0±0.8	8.3±2.1	
		CH	3	-25.6±2.2	5.1±0.8	
		MC2'	3	-24.5±1.6	5.5±0.7	
	Food sources	BDB	MC2	6	-25.1±0.4	2.2±0.6
			MC3	3	-25.3±0.3	1.9±0.4
			MC5	3	-25.0±0.7	2.5±0.7
BDM		MC2	2	-25.3±0.1	1.4±0.3	
		MC3	4	-25.3±0.5	3.0±0.8	
		MC5	2	-25.6±0.3	1.7±0.8	
P-POM		MC2'	2	-28.3±0.3	0.9±0.9	
		MC3'	2	-29.4±2.7	4.2±2.3	
		MC5'	2	-29.5±2.6	7.4±0.0	
B-POM		MC2	3	-26.8±0.8	5.0±0.6	
		MC3	4	-24.7±1.5	5.2±2.2	
		MC5	3	-25.8±0.5	5.4±0.6	
SOM		MC2	6	-22.9±0.8	7.5±1.4	
		MC3	5	-22.8±1.8	7.7±0.5	
		MC5	5	-23.8±2.6	6.1±4.2	



**Figure 4.3.**

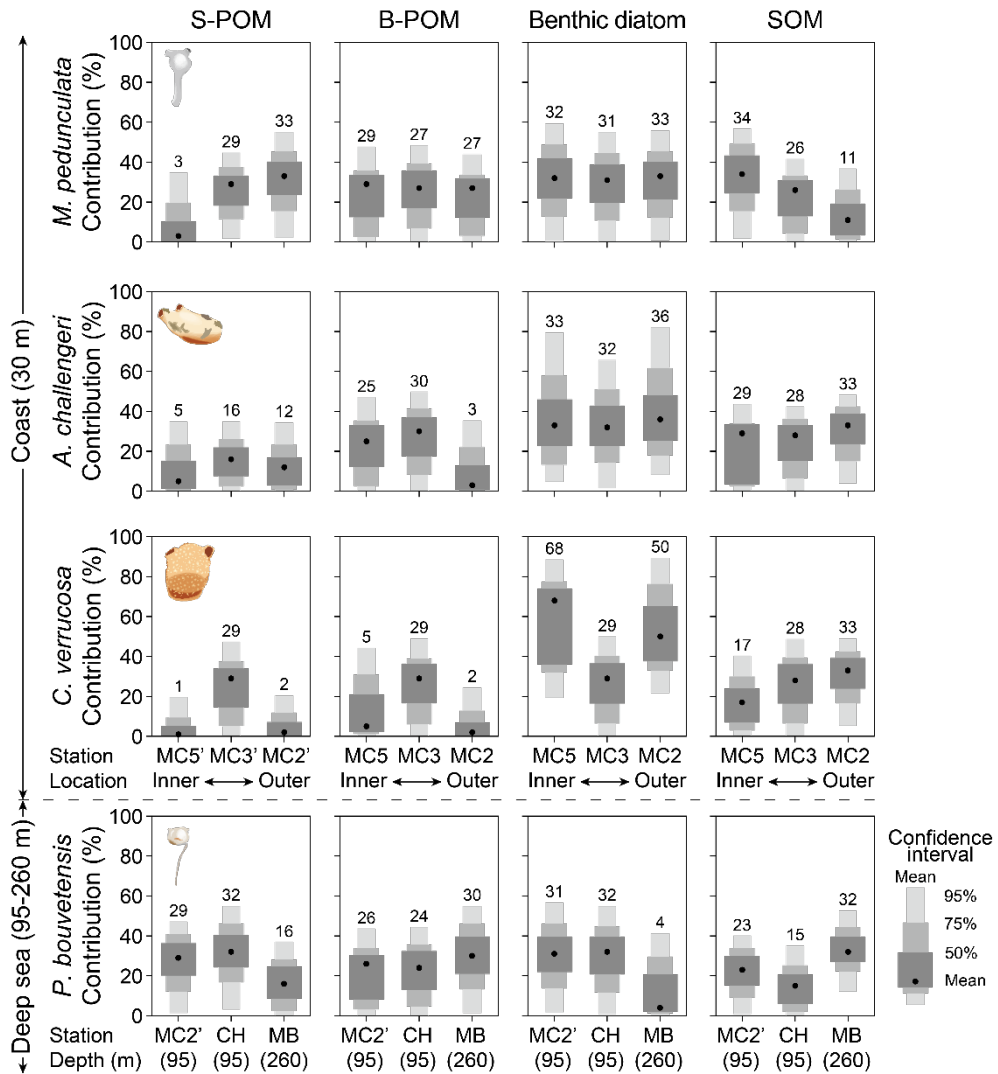
Dual plots of  $\delta^{13}\text{C}$  and  $\delta^{15}\text{N}$  for three dominant ascidians of shallow depths (~30 m) and one ascidian of deep depths (95 m and 260 m) with potential food sources. P-POM; pelagic particulate organic matter. B-POM; benthic particulate organic matter. BDB; benthic diatom bush. BDM; benthic diatom mat. SOM; sediment organic matter.

### **4.3.2. Variations of relative contributions of the potential food sources to the diets of the ascidians among the stations and the species**

Benthic diatoms most contributed to diets of three dominant ascidians at most stations in MC (Figure 4.4). Benthic diatoms had dominant contribution (30–33%) to diets of *M. pedunculata* followed by SOM (28–32%) and B-POM (26–27%) except outermost site (MC2). At the outermost site, P-POM (32%) as well as benthic diatoms (33%) were the major food sources of *M. pedunculata*. Diets of *A. challengeri* had most contributions from benthic diatoms (33–36%) at all stations followed by SOM (30–33%). Unlike *M. pedunculata*, the contributions of P-POM to *A. challengeri* were relatively low at all sites (4–10%). B-POM had a higher contribution at inner sites (MC3 and MC5: 4–31%) than outermost site (MC2: 4%). For *C. verrucosa* diets, benthic diatoms most contributed, both on the innermost and outermost sites (39–40%), and SOM second contributed (37–39%), except MC3 which had no replicate. Both P-POM (1–9%) and B-POM (2–4%) had low contributions regardless of stations. *C. verrucosa* had the lowest contribution of POM among the three ascidians.

Food sources had different contributions to *P. bouvetensis* according to water depths (Figure 4.4). The benthic diatoms and P-POM most contributed in both MC and Collins Harbor, followed by the B-POM and SOM at 95 m depth. At 260 m depth, contributions of the benthic diatoms and P-POM decreased while contributions of B-POM and SOM increased.





**Figure 4.4.**

SIAR model showing the relative contributions of potential food sources to the diet of three ascidians dominated at shallow depths (~30 m) and one ascidian of deep depths (95 and 260 m) at each station. The gray bars of different widths indicate the 95, 75, and 50% confidence intervals (from lightest to darkest) and the black dots are mean values. Figures on the bars are mean values. P-POM; pelagic particulate organic matter. B-POM; benthic particulate organic matter. SOM; sediment organic matter. Benthic diatom bush and mat was pooled to benthic diatom based on their C and N stable isotope values.

## 4.4. Discussion

### 4.4.1. Diet change of ascidians

$\delta^{13}\text{C}$  and  $\delta^{15}\text{N}$  values and SIAR model show that benthic diatoms were the major food for ascidians in MC, regardless of the distance from the glacier (Figure 4.3 and 4.4). Because Antarctic benthic diatoms bloom in summer and grow thick, a large amount of them can be provided to filter feeders (Ahn et al., 2016). In addition, benthic diatoms such as *Paralia sulcata* inhabit the surface of benthic megafaunas in the form of bushes (Ahn et al., 2016; Bae et al., 2021). As a result, the physical distance becomes closer, making it easier for the filter feeders to consume the benthic diatoms. Several pioneer species of *Fragilaria* also grow in a bush form, and were abundant in areas where glacial retreats had been relatively recent (Barnes and Colan, 2007; Bae et al., 2021). This indicates that filter feeders can use diatoms for food in newly exposed areas from glaciers. B-POM and SOM also greatly contributed as food sources of ascidians in the MC (Figure 4.4).  $\delta^{13}\text{C}$  and  $\delta^{15}\text{N}$  were a little enriched in B-POM and SOM than benthic diatoms, except B-POM of MC2 (Figure 4.3). This shows that the proportions of benthic diatoms were large among the components of the two food sources.  $\delta^{13}\text{C}$  of B-POM was more depleted in MC2 than two other stations. This seems to be a result of the increase in the biomass and primary production of phytoplankton on the outer sites compared to the inner sites of the MC in summer (B. Kim et al., 2021). Even on the outermost site (MC2) which had the largest biomass of phytoplankton, the contributions of benthic diatoms and food sources originated from the benthic diatoms (SOM and B-POM) to diets of ascidians were significant (Figure 4.4). These results indicate that benthic diatoms were the major food for the filter feeders on the MC, and changes in the distribution of benthic diatoms can have more effects on filter feeders than phytoplankton in the MC.

P-POM had larger contributions to *P. bouvetensis* at 95 m depths than ascidians at 30 m depths, but benthic diatoms were still one of the major food sources (Figure 4.4). Benthic primary producers such as seaweeds are transported to the deep sea by currents and gravity (Kokubu et al., 2019). This mechanism seems to make benthic diatoms to become one of the major food sources for filter feeders in Antarctic nearshore, despite the limited light in deep depths, which makes primary production difficult (Bodungen et al., 1986; Longhi et al., 2003). The contribution of benthic

diatoms to the ascidian diets decreased at a deep depth (Figure 4.4). This means that the contribution of benthic diatoms to the feeding of Antarctic filter feeders was significant up to about 100 m.

The diet of ascidians in Antarctica differed according to species as well as spatial factors such as distance from the glaciers and depth (Figure 4.4). The contribution of each food source to *M. pedunculata* varied with distance from the glaciers. Near the glaciers, benthic diatoms and food sources containing benthic diatoms (B-POM and SOM) significantly contributed to diet of *M. pedunculata*. The ice-proximal zone is the area most affected by glacial retreats, and it is an unstable environment with frequent disturbances due to the iceberg and meltwater input and a high concentration of SPM (Yoon et al., 1998; Yoo et al., 2015; D. Kim et al., 2021). High concentrations of SPM near the glaciers restrict light penetration, inhibiting primary production and reducing biomass of phytoplankton (Schloss and Ferreyra, 2002; B. Kim et al., 2021). In spite of unstable environment of near the glaciers, benthic diatoms formed bushes and mats that could be identified with the naked eye although the biomasses were smaller than that of outer sites of the cove (Figure 4.2). The large contributions of benthic diatom-related food sources to *M. pedunculata* near the glaciers seems to be a result of a lack of phytoplankton. Compared to the inner sites, the SOM contribution decreased and the P-POM contribution rapidly increased (Figure 4.4). The large contribution of P-POM may be due to the increased opportunity for *M. pedunculata* to feed them because of the increase in phytoplankton at the outer sites (B. Kim et al., 2021). It seems that the major food source was determined by the amount of each food sources because *M. pedunculata* does not have the ability to selectively consume SPM according to the quality, and because of its elongated shape with columns, it is less affected by sediment than the flat form species (Torre et al., 2014). The feeding patten that changed depending on the environment indicated that *M. pedunculata* is valuable as an environmental indicator.

Although *A. challengeri*, like *M. pedunculata*, do not have the ability to selectively consume SPM (Torre et al., 2014), a relatively consistent feeding pattern with large contributions of benthic diatoms and SOM was confirmed in all stations (Figure 4.4). Because of laterally flattened shape of *A. challengeri*, the buccal siphon

is closer to the sediments than the other two ascidians. Due to the morphological characteristic that are physically close to the sediments, *A. challengerii* was relatively more affected by benthic diatoms, SOM, and B-POM located near the bottom than P-POM sinking from the water column. Therefore, it seems that benthic diatoms have more influence on the diet of *A. challengerii* than phytoplankton, regardless of the composition of food sources.

*C. verrucosa* preferred benthic diatoms and SOM for food in all stations with different glacial influences (Figure 4.4). *C. verrucosa* can selectively consume food compared to the other two ascidians through a squirting mechanism of excreting unwanted matters (Torre et al., 2012; Torre et al., 2014). It seems that food sorting ability of *C. verrucosa* had given them narrow  $\delta^{13}\text{C}$  values in all stations, regardless of the change in food sources distribution, despite cylindrical shape of *C. verrucosa* similar with *M. pedunculata* rather than *A. challengerii* laterally flattened (Figure 4.3). Benthic diatoms were major food sources for *C. verrucosa* in the cove (Figure 4.4). At the outermost site of the cove where phytoplankton biomass increased, the contribution of P-POM increased by up to 40% in *M. pedunculata*, and also up to 14% in *A. challengerii*, laterally flattened ascidian (Figure 4.4). Although *C. verrucosa* was cylindrical, the contribution of P-POM was only 12%, and the contribution of benthic diatoms was still the largest (51%). Even in the phytoplankton abundant site, the contribution of P-POM was small and benthic diatoms were the major food sources, suggesting that *C. verrucosa* prefer benthic diatoms as food.

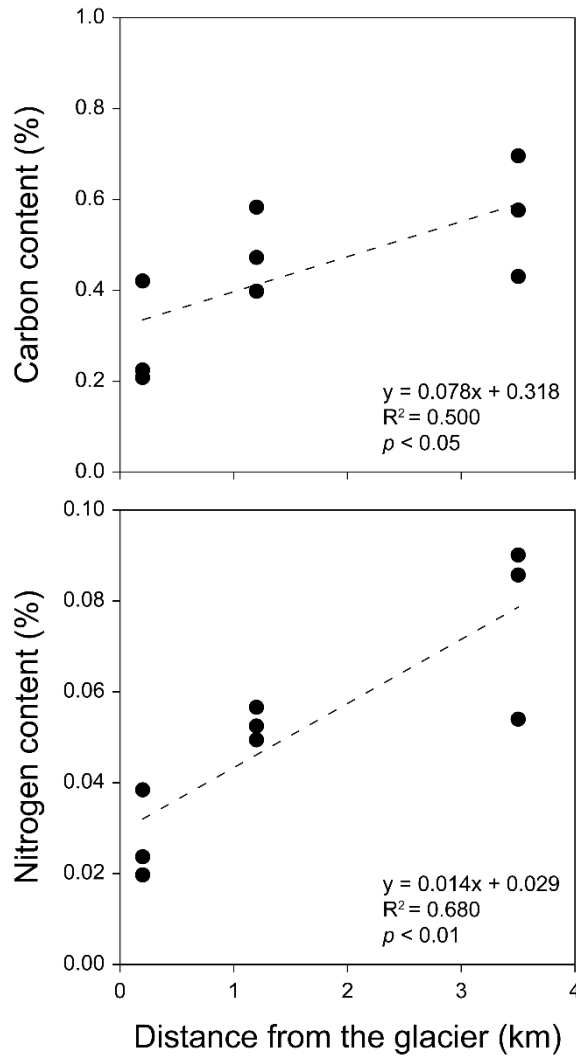
#### 4.4.2. Effects of glacial retreat on food sources and distribution of ascidians

Glacial retreat accompanied by various phenomena such as ice-scouring and input of iceberg, melt water, and sediment (Gutt and Starmans, 2001; Smale and Barnes, 2008) affect the distributions of ascidians and their food sources (Bae et al., 2021; B. Kim et al., 2021; D. Kim et al., 2021). Due to the high turbidity near the glaciers, phytoplankton, generally known as food sources for filter feeders, is not abundant at the ice-proximal zone (Schloss and Ferreyra, 2002; B. Kim et al., 2021). Field images showed that, unlike phytoplankton, benthic diatoms were abundant in areas near glacier which had severe disturbances (Figure 4.2). And the isotope analysis results confirmed that benthic diatoms were the major food sources for ascidians at the ice-proximal zone (Figure 4.4). The results show that the ascidians rapidly colonizing at newly ice-free area as pioneer species were supplied the energy needed for growth and reproduction from benthic diatoms.

In areas far from the glaciers, the influences of glacial retreat are reduced, and the habitat is relatively stable and turbidity decreased compared to the areas near the glacier, thereby increasing the productivity of phytoplankton (Schloss and Ferreyra, 2002; Moon et al., 2015; Yoo et al., 2015; B. Kim et al., 2021). The increase in phytoplankton leads to an increase in pelagic food sources for ascidians, which are filter feeders. Due to the abundance of phytoplankton, the contribution of pelagic food sources was larger in area far from the glaciers than in near the glaciers (Figure 4.4). However, the contributions of food sources differed according to the food sorting ability or body shape of ascidian species, and the contribution of benthic diatoms was still large at the outermost site (MC2) even in *M. pedunculata* that had nonselective feeding and stalk suitable to feeding on P-POM. A stable environment in water mass increased the biomass of benthic diatoms as well as phytoplankton (Figure 4.2; Ahn et al., 2016). Since benthic diatoms are more densely clustered around the benthic megafauna than phytoplankton distributed in the water layers, they are still the major food sources for filter feeders even in relatively stable habitats far from the glaciers (Ahn et al., 2016; Ha et al., 2019).

Glacial retreats also affect the amount of organic matters in food sources of filter feeders. Carbon and nitrogen contents in sediments decreased toward the glacier in MC (Figure 4.5). Terrestrial sediments introduced by the retreat of

Antarctic glaciers had low organic contents (Kang et al., 1993). This means that although the amount of food sources for filter feeders near the glacier was large, but the energy supply was poor due to the low organic matter content. Ascidians in newly exposed areas with high concentrations of SPM had gut contents with low percentage of organic matter (Torre et al., 2021). Therefore, even if the filter feeders consumed the same amount of food, the energy absorption in the ice-proximal zone was relatively lower than in the areas far from the glaciers. The low organic matter contents in food sources seem to reduce the size of ascidians near the glaciers, along with shortened lifespan by disturbances (D. Kim et al., 2021).



**Figure 4.5.** Changes in carbon and nitrogen content in sediments with distance from the glacier.

## 4.5. Conclusions

This study showed that the major food sources for filter feeders, one of the key components in benthic ecosystems, were benthic diatoms, and that the contribution of pelagic sources depends on the glacier influence and kinds of species in Antarctic nearshore. Benthic diatoms were primary food sources for all three ascidians dominant in Marian Cove, regardless of distance from the glacier (31–68%). Contributions of benthic diatoms to diets of Antarctic nearshore ascidians were significant up to about 100 m. P-POM contributions to ascidian diets were varied by the effects of glaciers and kinds of ascidian species. The contributions of P-POM were low in the diets of *C. verrucosa* that feed more selectively through squirting behavior and *A. challengeri*, laterally flattened species, relatively more affected by benthic sources. However, the P-POM contribution to the diet of *M. pedunculata* with non-selective feeding and cylindrical shape increased toward the outside, where phytoplankton was plentiful. These results showed that diets of Antarctic nearshore ascidians varied with the characteristics of the species, such as body form and/or feeding behavior. In addition, this study suggested that diet of *M. pedunculata* reflects the composition of food sources. Given the relationship between individual growth and prey, this study provides the information necessary to understand the impact of glacial retreats caused by climate change on food sources and the resulting changes in benthic communities.



## **CHAPTER 5.**

### **CONCLUSIONS**

## 5.1. Summary

The present study provides comprehensive insights into the responses of benthic megafauna communities to glacial retreat including structural and functional changes (Figure 5.1). To understand the structural changes in the benthic communities according to glacial retreat, shifts in the benthic megafauna communities after deglaciation were estimated at the Antarctic nearshore. Additionally, sentinel taxa reflecting changes in the benthic megafauna community were identified, and environmental factors structuring the community were determined in a deglaciated fjord. To examine and understand the deglaciation influences on the function of the benthic community, the diets of three dominant ascidians and their potential food sources were investigated. The major findings of the present study are summarized below:

**Chapter 2** reports that the structural and functional diversities of benthic megafauna communities significantly changed in space (distance from the glacier and depths) in MC based on the ROV data. The number of taxa increased toward the outside of the cove, but the density peaked near the glacier by a rapid increase of the pioneer species *M. pedunculata* and *C. verrucosa*. The pioneer species were replaced by late-successional species (giant glass sponges and colonial ascidians) at the outermost site. The dramatic increase in taxonomic diversity near the glacier (MC5; ~10 years after seabed exposure) indicated that the benthic communities matured rapidly in terms of structure at higher taxonomic levels. The increase in functional diversity with distance from the glacier and peaked diversity observed at a 30 m depth of the outermost site could reflect different mechanisms of change between functional and structural diversities. Meanwhile, shifts in the benthic communities after glacial retreat likely weakened at 10 m, reflecting the environment where ice-scouring was frequently observed. Except very shallow depths (<10 m), the benthic community shifts in both functional and structural diversities were clear, which reflected the typical characteristics of successional processes of the benthic community in the Antarctic nearshore.

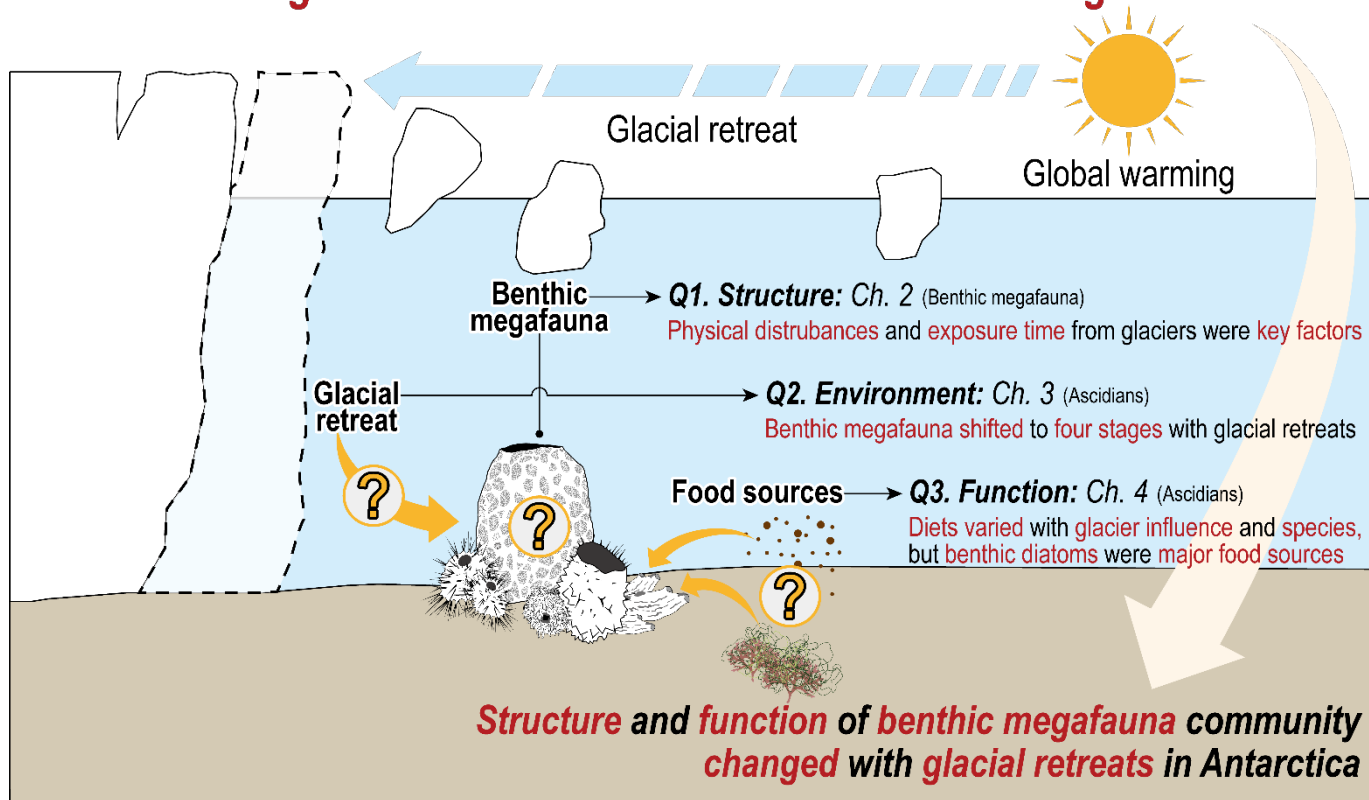
**Chapter 3** provides strong evidence for the utility of ascidian communities as sentinel taxa for monitoring the nearshore Antarctic marine ecosystem response to glacial retreat induced by climate change. Key drivers structuring the communities

and relevance to glacial retreat and the following processes also are reported. The first applied ROV survey in MC discovered that ascidians were the most diverse taxa (14 out of 64 taxa) with the greatest abundance (264 ind. m<sup>-2</sup>). Ascidian abundance and diversity greatly varied in space (distance from glacier and depth), explaining ~64% of the total megafaunal variations. Notably, in the deep seabed (50–90 m), ascidian communities shifted distinctly from colonization near the glacier (0.2 km to glacier) to mature at the most remote site (3.5 km). Communities near the glacier had the highest density (63 ind. m<sup>-2</sup>) and low diversity (5 taxa) because they were dominated by two pioneer species (*M. pedunculata* and *C. verrucosa*). The outermost site was more diverse (11 taxa) and abundant in ascidian species that mainly inhabited a stable environment (e.g., *A. challengerii* and *A. cf. radiatum*). The spatial pattern was not distinct at shallow depths (10–30 m) which had relatively severe disturbances. Sediment properties and distance to the glacier that indicate the physical disturbance level by deglaciation were key factors related to the ascidian distributions.

**Chapter 4** confirmed the primary food sources of the three dominant ascidians and examined their diet changes according to the influences of the glacial retreats using the stable isotopes of C and N. Benthic diatoms were the major food for the ascidians in MC, regardless of the distance from the glacier (30–70%). Benthic diatom contributions to ascidian diets were significant up to about 100 m. The diet of ascidians in Antarctica differed according to species. Contributions of pelagic production to *M. pedunculata*, which had a non-selective feeding activity and cylindrical body form, dramatically increased with the distance from the glacier. The large contribution of pelagic production may be due to the increased opportunity to feed them because of the increase in phytoplankton at the outer sites. On the other hand, *C. verrucosa* with a squirting behavior and *A. challengerii* with a laterally flat body consumed mainly benthic diatoms and SOM in all regions regardless of the influences of the glacier. Although *C. verrucosa* is cylindrical, the contribution of pelagic sources was low even in areas with abundant phytoplankton, and benthic diatoms were the primary food, indicating that *C. verrucosa* preferred benthic diatoms as food.

This study showed three successional processes of the benthic megafaunal communities in the deglaciated Antarctic nearshore: colonization, transition, and maturing stages. The shifts were weakened at the shallow depths where the disturbances were frequent but were clear in the deep depths. Physical disturbance associated with the glacial retreat was a major factor for the community structure while functional diversity was affected additionally by food availability. The ascidian spatial distributions explained 64% of the benthic megafaunal variations. This result indicates that ascidians are suitable as sentinel taxa for monitoring the response of Antarctic marine ecosystems to glacial retreat induced by climate change. Moreover, the diets of the ascidians with large contributions of benthic diatoms show that the benthic diatoms were the major food sources for Antarctic coastal ecosystems and were the basis for the rapid increase in density following the glacial retreat. Overall, this study provides quantitative background data for the megabenthic community structure and function in Marian Cove, Antarctica, warranting further in-depth monitoring of polar benthos under accelerating global warming.

## How do glacial retreats affect Antarctic benthic megafauna?



**Figure 5.1.**

Research questions and key findings in the present study.

## **5.2. Environmental implications and limitations**

This dissertation provides information on the response of the benthic megafauna communities to glacial retreat induced by climate change in the Antarctic nearshore (Figure 5.1). The benthic megafauna communities were divided into three stages (colonizing, transitional, and maturing stages) according to the physical stability in the glacial retreated region. Community changes caused by the glacial retreat of benthic megafauna, one of the major ecotypes in Antarctica, are essential to understanding the response of Antarctic ecosystems to climate change. Because climate change is accelerating, it is very important to understand the ecosystems in Antarctica, one of the regions that is most rapidly and significantly affected by global warming, to predict the future. The information on changes in the benthic megafauna communities of the Antarctic nearshore due to glacial retreat revealed in this study will provide background knowledge to respond to climate change.

This study also provides information on the food sources of benthic megafauna in the Antarctic nearshore. Benthic diatoms were the major food for filter feeders in the Antarctic nearshore, and their contribution was particularly high in areas with low pelagic production due to high turbidity. This result shows that benthic diatoms were the major energy source for the benthic megafauna communities dominated by filter feeders in Antarctica (Gili et al., 2001; Gili et al., 2006). This provides information on what Antarctic benthic megafauna feed on, especially in newly exposed areas from glaciers with low biomass of macroalgae and phytoplankton. Insights on the major food sources of the benthic megafauna will provide an important basis for identifying the energy flow in the change processes of Antarctic marine ecosystems due to climate change.

Nevertheless, this study has two limitations. The first one is a temporal limitation. Benthic megafauna community successional processes after glacial retreat revealed in this study were inferred from the spatial distribution based on the exposure period from ice proportional to the distance from the glaciers. Therefore, it is necessary to compare the results with the successional processes observed for a long time in the field. The second one is a spatial limitation. The survey was conducted only on MC; thus, additional investigation is needed to confirm that the results of this study are a general phenomenon in Antarctica. Future research

directions for benthic megafauna community are suggested based on current knowledge and limitations in the following section.

### **5.3. Future research directions**

This study provided essential information for understanding the Antarctic ecosystem change due to climate change by revealing the structural and functional changes in benthic megafauna communities according to glacial retreat. Further studies based on the results of this study will help us better understand the responses of Antarctic ecosystems to climate change.

First, it is necessary to confirm the change process over time in the benthic megafauna community of glacial retreated regions based on long-term monitoring. Most previous studies on ecosystems in Antarctica provide only short-term information due to methodological limitations. Although this study reported the process of long-term change from the spatial distribution, verification based on direct observation is necessary to understand the Antarctic ecosystem change more accurately. Therefore, long-term monitoring of the benthic megafauna community in the glacial retreated regions of Antarctic is required.

Second, it is necessary to compare the benthic community shifts in MC and other glacial retreated regions. To better understand the responses of benthic ecosystems to glacial retreat in the Antarctic nearshore, it is important to comprehend the benthic succession processes across Antarctica through regional comparisons. Characteristics of the benthic community may be predicted according to the properties of each glacial retreated region (distance and exposure period from the glaciers) based on the information of benthic community succession. The distance and exposure period from the glaciers can be determined by satellite data. Based on the benthic succession and satellite data, it will be possible to estimate the benthic megafauna distribution of the Antarctic nearshore and predict changes in benthic communities according to glacial retreat induced by climate change. Therefore, it is important to expand the results of this study on the changes in benthic megafauna communities with glacial retreat to the entire Antarctic nearshore.

Finally, to comprehend the relationship between climate change and Antarctic ecosystems, it is necessary to estimate the change in the carbon storage capacity of the benthic megafauna community according to succession in Antarctica based on the above results. This study reported that new benthic communities colonized in the areas newly exposed from the glaciers, and the species composition and density and



the size of the individual changed with the community succession. In particular, as the environment became more stable, the size and lifespan of the individual increased. Newly colonized benthic communities store carbon in proportion to their biomass. As the biomass of the communities increases, the amount of carbon storage also increases, and as the lifespans of the organisms increase, the carbon storage period also increases. Carbon dynamics are essential to understanding the fate of carbon dioxide, one of the major greenhouse gases. Therefore, information on the carbon storage capacity of benthic megafauna communities distributed throughout the Antarctic Ocean should be reported to better understand how the Antarctic ecosystem interacts with climate change.

## BIBLIOGRAPHY

- Ahn, I. Y. (1993). Enhanced particle flux through the biodeposition by the Antarctic suspension-feeding bivalve *Laternula elliptica* in Marian Cove, King George Island. *Journal of Experimental Marine Biology and Ecology*, 171(1), 75-90.
- Ahn, I.-Y., Chung, H., Kang, J.-S., & Kang, S.-H. (1997a). Diatom composition and biomass variability in nearshore waters of Maxwell Bay, Antarctica, during the 1992/1993 austral summer. *Polar Biology*, 17, 8.
- Ahn, I. Y. (1997b). Feeding ecology of the Antarctic lamellibranch *Laternula elliptica* (Laternulidae) in Marian Cove and vicinity, King George Island, during one austral summer. *Antarctic Communities. Species, Structure and Survival*. Cambridge University Press, UK, 1-464.
- Ahn, I. Y., & Shim, J. H. (1998). Summer metabolism of the Antarctic clam, *Laternula elliptica* (King and Broderip) in Maxwell Bay, King George Island and its implications. *Journal of Experimental Marine Biology and Ecology*, 224(2), 253-264.
- Ahn, I. Y., Woong Cho, K., Choi, K. S., Seo, Y., & Shin, J. (2000). Lipid content and composition of the Antarctic lamellibranch, *Laternula elliptica* (King & Broderip)(Anomalodesmata: Laternulidae), in King George Island during an austral summer. *Polar Biology*, 23(1), 24-33.
- Ahn, I. Y., Surh, J., Park, Y. G., Kwon, H., Choi, K. S., Kang, S. H., ... & Chung, H. (2003). Growth and seasonal energetics of the Antarctic bivalve *Laternula elliptica* from King George Island, Antarctica. *Marine Ecology Progress Series*, 257, 99-110.
- Ahn, I.-Y., Chung, K. H., & Choi, H. J. (2004). Influence of glacial runoff on baseline metal accumulation in the Antarctic limpet *Nacella concinna* from King George Island. *Marine Pollution Bulletin*, 49(1-2), 119-127. <https://doi.org/10.1016/j.marpolbul.2004.03.008>
- Ahn, I.-Y., Moon, H.-W., Jeon, M., & Kang, S.-H. (2016). First record of massive blooming of benthic diatoms and their association with megabenthic filter feeders on the shallow seafloor of an Antarctic Fjord: Does glacier melting fuel the bloom? *Ocean Science Journal*, 51(2), 273-279. <https://doi.org/10.1007/s12601-016-0023-y>
- Alurralde, G., Torre, L., Schwindt, E., Castilla, J. C., & Tatián, M. (2013). A re-evaluation of morphological characters of the invasive ascidian *Corella eumyota* reveals two different species at the tip of South America and in the

- South Shetland Islands, Antarctica. *Polar Biology*, 36(7), 957-968.  
<https://doi.org/10.1007/s00300-013-1319-3>
- Anderson, T. J., Cochrane, G. R., Roberts, D. A., Chezar, H., & Hatcher, G. (2007). A rapid method to characterize seabed habitats and associated macro-organisms. *Special Paper - Geological Association of Canada*, (47), 71-79.  
<http://pubs.er.usgs.gov/publication/70009844>
- Ayre, D. J., Davis, A. R., Billingham, M., Llorens, T., & Styan, C. (1997). Genetic evidence for contrasting patterns of dispersal in solitary and colonial ascidians. *Marine Biology*, 130(1), 51-61. <https://doi.org/10.1007/s002270050224>
- Bacastow R. B., K. C. D., Whorf T. P. (1985). Seasonal Amplitude Increase in Atmospheric CO<sub>2</sub> Concentration at Mauna Loa, Hawaii, 1959-1982. *Journal of geophysical research*, 90, 12.
- Bae, H., Ahn, I. Y., Park, J., Song, S. J., Noh, J., Kim, H., & Khim, J. S. (2021). Shift in polar benthic community structure in a fast retreating glacial area of Marian Cove, West Antarctica. *Scientific Reports*, 11(1), 241.  
<https://doi.org/10.1038/s41598-020-80636-z>
- Barnes, D. K. A. (2017). Iceberg killing fields limit huge potential for benthic blue carbon in Antarctic shallows. *Global Change Biology*, 23(7), 2649-2659.  
<https://doi.org/10.1111/gcb.13523>
- Barnes, D. K. A., & others (2006). Shallow benthic fauna communities of South Georgia Island. *Polar Biology*, 29: 223-228.
- Barnes, D. K. A., & Souster, T. (2011). Reduced survival of Antarctic benthos linked to climate-induced iceberg scouring. *Nature Climate Change*, 1(7), 365-368.  
<https://doi.org/10.1038/nclimate1232>
- Barnes, D. K. A., Sands, C. J., Cook, A., Howard, F., Roman Gonzalez, A., Munoz-Ramirez, C., Retallick, K., Scourse, J., Van Landeghem, K., & Zwierschke, N. (2020). Blue carbon gains from glacial retreat along Antarctic fjords: What should we expect? *Global Change Biology*, 26(5), 2750-2755.  
<https://doi.org/10.1111/gcb.15055>
- Barnes, D. K., & Conlan, K. E. (2007). Disturbance, colonization and development of Antarctic benthic communities. *Philosophical Transactions of the Royal Society B Biological Sciences*, 362(1477), 11-38.  
<https://doi.org/10.1098/rstb.2006.1951>
- Bodungen Bodo V., S. V. S., Tilzer Max M., Zeitzschel B.. (1986). Primary production and sedimentation during spring in the Antarctic Peninsula region.

Deep sea research, 33, 18.

- Boetius, A., Anesio, A. M., Deming, J. W., Mikucki, J. A., & Rapp, J. Z. (2015). Microbial ecology of the cryosphere: sea ice and glacial habitats. *Nature Reviews Microbiology*, 13(11), 677-690. <https://doi.org/10.1038/nrmicro3522>
- Bowden, D. A., Clarke, A., Peck, L. S., & Barnes, D. K. (2006). Antarctic sessile marine benthos: colonisation and growth on artificial substrata over three years. *Marine Ecology Progress Series*, 316, 1-16.
- Braeckman, U., Pasotti, F., Hoffmann, R., Vazquez, S., Wulff, A., Schloss, I. R., Falk, U., Deregibus, D., Lefaible, N., Torstensson, A., Al-Handal, A., Wenzhofer, F., & Vanreusel, A. (2021). Glacial melt disturbance shifts community metabolism of an Antarctic seafloor ecosystem from net autotrophy to heterotrophy. *Communications Biology*, 4(1), 148. <https://doi.org/10.1038/s42003-021-01673-6>
- Brandini, F. P., & Rebello, J. (1994). Wind field effect on hydrography and chlorophyll dynamics in the coastal pelagial of Admiralty Bay, King George Island, Antarctica. *Antarctic Science*, 6(4), 433-442.
- Carabel, S., Godínez-Domínguez, E., Verísimo, P., Fernández, L., & Freire, J. (2006). An assessment of sample processing methods for stable isotope analyses of marine food webs. *Journal of Experimental Marine Biology and Ecology*, 336(2), 254-261. <https://doi.org/10.1016/j.jembe.2006.06.001>
- Chang, K. I., Jun, H. K., Park, G. T., & Eo., Y. S. (1990). Oceanographic conditions of Maxwell Bay, King George Island, Antarctica (austral summer 1989). *Korean Journal of Polar Research*, 1: 27-46
- Choy, E. J., Park, H., Kim, J. H., Ahn, I. Y., & Kang, C. K. (2011). Isotopic shift for defining habitat exploitation by the Antarctic limpet *Nacella concinna* from rocky coastal habitats (Marian Cove, King George Island). *Estuarine Coastal and Shelf Science*, 92(3), 339-346.
- Clarke, K. R., & Warwick, R. M. (1998). A taxonomic distinctness index and its statistical properties. *Journal of applied ecology*, 35(4), 523-531. <https://doi.org/https://doi.org/10.1046/j.1365-2664.1998.3540523.x>
- Clem, K. R., Fogt, R. L., Turner, J., Lintner, B. R., Marshall, G. J., Miller, J. R., & Renwick, J. A. (2020). Record warming at the South Pole during the past three decades. *Nature Climate Change*, 10(8), 762-770. <https://doi.org/10.1038/s41558-020-0815-z>
- Cook, A. J., Vaughan, D. G., Luckman, A. J., & Murray., T. (2014). A new Antarctic

- Peninsula glacier basin inventory and observed area changes since the 1940s. *Antarctic Science*. 26: 614-624.
- Danis, B. (2013). A field guide to Antarctic sponges. Project implemented by SCAR-MarBIN and ANTABIF, Available online at <http://afg.scarmarbin.be/guides/144164-a-field-guide-to-antarctic-sponges> (accessed 27.10.14).
- Dayton, P. (1979). Observations of growth, dispersal and population dynamics of some sponges in McMurdo Sound, Antarctica. *Colloques internationaux du CNRS*, 291, 271-282
- Dorschel, B., Gutt, J., Piepenburg, D., Schröder, M., & Arndt, J. E. (2014). The influence of the geomorphological and sedimentological settings on the distribution of epibenthic assemblages on a flat topped hill on the over-deepened shelf of the western Weddell Sea (Southern Ocean). *Biogeosciences*, 11(14), 3797-3817. <https://doi.org/10.5194/bg-11-3797-2014>
- Dufrêne, M., & Legendre, P. (1997). Species assemblages and indicator species: the need for a flexible asymmetrical approach. *Ecological monographs*, 67(3), 345-366.
- Dykman, L. N., Beaulieu, S. E., Mills, S. W., Solow, A. R., & Mullineaux, L. S. (2021). Functional traits provide new insight into recovery and succession at deep-sea hydrothermal vents. *Ecology*, e03418.
- Federwisch, L., Janussen, D., & Richter, C. (2020). Macroscopic characteristics facilitate identification of common Antarctic glass sponges (Porifera, Hexactinellida, Rossellidae). *Polar Biology*, 43(2), 91-110. <https://doi.org/10.1007/s00300-019-02612-2>
- Gerdes, D., Isla, E., Knust, R., Mintenbeck, K., & Rossi, S. (2008). Response of Antarctic benthic communities to disturbance: first results from the artificial Benthic Disturbance Experiment on the eastern Weddell Sea Shelf, Antarctica. *Polar Biology*, 31(12), 1469-1480. <https://doi.org/10.1007/s00300-008-0488-y>
- Gili, J.-M., Arntz, W. E., Palanques, A., Orejas, C., Clarke, A., Dayton, P. K., Isla, E., Teixidó, N., Rossi, S., & López-González, P. J. (2006). A unique assemblage of epibenthic sessile suspension feeders with archaic features in the high-Antarctic. *Deep Sea Research Part II: Topical Studies in Oceanography*, 53(8-10), 1029-1052. <https://doi.org/10.1016/j.dsr2.2005.10.021>
- Gili, J.-M., Coma, R., Orejas, C., López-González, P., & Zabala, M. (2001). Are Antarctic suspension-feeding communities different from those elsewhere in

- the world? *Polar Biology*, 24(7), 473-485.  
<https://doi.org/10.1007/s003000100257>
- Grange, L. J., & Smith, C. R. (2013). Megafaunal communities in rapidly warming fjords along the West Antarctic Peninsula: hotspots of abundance and beta diversity. *PLoS One*, 8(12), e77917.  
<https://doi.org/10.1371/journal.pone.0077917>
- Gutt Julian, P. D. (2003). Scale-dependent impact on diversity of Antarctic benthos caused by grounding of icebergs. *Marine Ecology Progress Series*, 253, 7.
- Gutt, J., & Starms, A. (2001). Quantification of iceberg impact and benthic recolonisation patterns in the Weddell Sea (Antarctica). *Polar Biology*, 24(8), 615-619. <https://doi.org/10.1007/s003000100263>
- Gutt, J., Cape, M., Dimmler, W., Fillinger, L., Isla, E., Lieb, V., Lundälv, T., & Pulcher, C. (2013). Shifts in Antarctic megabenthic structure after ice-shelf disintegration in the Larsen area east of the Antarctic Peninsula. *Polar Biology*, 36(6), 895-906. <https://doi.org/10.1007/s00300-013-1315-7>
- Gyeong, H., Hyun, C. U., Kim, S. C., Tripathi, B. M., Yun, J., Kim, J., Kang, H., Kim, J. H., Kim, S., & Kim, M. (2021). Contrasting early successional dynamics of bacterial and fungal communities in recently deglaciated soils of the maritime Antarctic. *Molecular Ecology*, 30(17), 4231-4244.  
<https://doi.org/10.1111/mec.16054>
- Ha, S.-Y., Ahn, I.-Y., Moon, H.-W., Choi, B., & Shin, K.-H. (2019). Tight trophic association between benthic diatom blooms and shallow-water megabenthic communities in a rapidly deglaciated Antarctic fjord. *Estuarine, Coastal and Shelf Science*, 218, 258-267. <https://doi.org/10.1016/j.ecss.2018.12.020>
- Hewitt, J., De Juan, S., Lohrer, D., Townsend, M., & Archino, R. (2014). Functional traits as indicators of ecological integrity. NIWA client report No: HAM2014-001.
- Hibberd, T. (2009). Field identification guide to Heard Island and McDonald Islands benthic invertebrates. *Deep-Sea Research Part II-Topical Studies in Oceanography*, 53(8-10), 985-1008.
- Hong, S. G., Park, H., Park, S., Lee, S., Lee, K., Park, J., Lee, S., Choi, B., Cho, G., Cho, H., Lee, S., Gong, M., Yoon, Y., Park, W., Lee, S., Jin, H., & Son, Y. (2019). Overwintering report of the antarctic King Sejong Station 31st Overwintering Party.
- Hussin, W. M. R. W. (2016). Comparing the structure and function of the Antarctic

- and Tropic benthic communities following environmental changes. *Aquaculture, Aquarium, Conservation & Legislation*, 9(6), 1244-1250.
- Hutchins, M., Thoney, D. A., & Schlager, N. (2003). *Grzimek's Animal Life Encyclopedia*. Library Media Connection.
- Ingels, J., & others (2020). Antarctic ecosystem responses following ice-shelf collapse and iceberg calving: Science review and future research. *WIREs Climate Change*, 12(1). <https://doi.org/10.1002/wcc.682>
- James H. McCutchan Jr, W. M. L. J., Carol Kendall and Claire C. McGrath. (2003). Variation in trophic shift for stable isotope ratios of carbon, nitrogen, and sulfur. *OIKOS*, 102, 13.
- Jung, A. S., van der Veer, H. W., van der Meer, M. T. J., & Philippart, C. J. M. (2019). Seasonal variation in the diet of estuarine bivalves. *PLoS One*, 14(6), e0217003. <https://doi.org/10.1371/journal.pone.0217003>
- Kang, J. S., Kang, S. H., Lee, J. H., Chung, K. H., & Lee, M. Y. (1997). Antarctic Micro-and Nano-Sized Phytoplankton Assemblages in the Surface Water of Maxwell Bay During the 1997 Austral Summer. *Korean Journal of Polar Research*, 8, 11.
- Kang, Y.-C. (1993). Vertical Distribution of Suspended Particulate Matter in Bransfield Strait and Adjacent Embayments, February 1993: Modified Niskin Bottles for Near-bottom Water Samples. *Korean Journal of Polar Research*, 4, 6.
- Kim, B. K., Jeon, M., Joo, H. M., Kim, T.-W., Park, S.-J., Park, J., & Ha, S.-Y. (2021). Impact of Freshwater Discharge on the Carbon Uptake Rate of Phytoplankton During Summer (January–February 2019) in Marian Cove, King George Island, Antarctica. *Frontiers in Marine Science*, 8. <https://doi.org/10.3389/fmars.2021.725173>
- Kim, D.-U., Khim, J. S., & Ahn, I.-Y. (2021). Patterns, drivers and implications of ascidian distributions in a rapidly deglaciating fjord, King George Island, West Antarctic Peninsula. *Ecological Indicators*, 125. <https://doi.org/10.1016/j.ecolind.2021.107467>
- Klumpp, D. W. (1984). Nutritional ecology of the ascidian *Pyura stolonifera*: influence of body size, food quantity and quality on filter-feeding, respiration, assimilation efficiency and energy balance. *Marine Ecology Progress Series*, 19, 16.
- Ko, Y. W., Choi, H. G., Lee, D. S., & Kim, J. H. (2020). 30 years revisit survey for

- long-term changes in the Antarctic subtidal algal assemblage. *Scientific Reports*, 10(1), 8481. <https://doi.org/10.1038/s41598-020-65039-4>
- Kokubu, Y., Rothausler, E., Filippi, J. B., Durieux, E. D. H., & Komatsu, T. (2019). Revealing the deposition of macrophytes transported offshore: Evidence of their long-distance dispersal and seasonal aggregation to the deep sea. *Scientific Reports*, 9(1), 4331. <https://doi.org/10.1038/s41598-019-39982-w>
- Kowalke, J., Tatián, M., Sahade, R., & Arntz, W. (2001). Production and respiration of Antarctic ascidians. *Polar Biology*, 24(9), 663-669. <https://doi.org/10.1007/s003000100266>
- Lagger, C., Nime, M., Torre, L., Servetto, N., Tatián, M., & Sahade, R. (2018). Climate change, glacier retreat and a new ice-free island offer new insights on Antarctic benthic responses. *Ecography*, 41(4), 579-591. <https://doi.org/10.1111/ecog.03018>
- Lagger, C., Servetto, N., Torre, L., & Sahade, R. (2017). Benthic colonization in newly ice-free soft-bottom areas in an Antarctic fjord. *PLoS One*, 12: e0186756.
- Lambert, C. C. (2005). Historical introduction, overview, and reproductive biology of the protochordates. *Canadian Journal of Zoology*, 83(1), 1-7. <https://doi.org/10.1139/z04-160>
- Longhi M. L., S. I. R., Wiencke C. (2003). Effect of Irradiance and Temperature on Photosynthesis and Growth of Two Antarctic Benthic Diatoms, *Gyrosigma subsalinum* and *Odontella litigiosa*. *Botanica Marina*, 46, 9.
- Maldonado, M., & Others (2017). Sponge Grounds as Key Marine Habitats: A Synthetic Review of Types, Structure, Functional Roles, and Conservation Concerns. In *Marine Animal Forests* (pp. 145-183). [https://doi.org/10.1007/978-3-319-21012-4\\_24](https://doi.org/10.1007/978-3-319-21012-4_24)
- McClintock, J. B., Amsler, C. D., Baker, B. J., & Van Soest, R. W. (2005). Ecology of Antarctic marine sponges: an overview. *Integrative and Comparative Biology*, 45(2), 359-368.
- Monniot, F., Dettai, A., Eleaume, M., Cruaud, C., & Ameziane, N. (2011). Antarctic Ascidians (Tunicata) of the French-Australian survey CEAMARC in Terre Adélie. *Zootaxa*, 2817(1), 1-54.
- Monteiro, G. S., Nonato, E. F., & Petti, M. A. (2013). Scientific Note A retrospective of *Helicosiphon biscoeensis* Gravier, 1907 (Polychaeta: Serpulidae): morphological and ecological characteristics. *Pan-American Journal of*



Aquatic Sciences, 8(3), 204-208.

- Moon, H.-W., Wan Hussin, W. M. R., Kim, H.-C., & Ahn, I.-Y. (2015). The impacts of climate change on Antarctic nearshore mega-epifaunal benthic assemblages in a glacial fjord on King George Island: Responses and implications. *Ecological Indicators*, 57, 280-292. <https://doi.org/10.1016/j.ecolind.2015.04.031>
- Murray, J. W., & Pudsey, C. J. (2004). Living (stained) and dead foraminifera from the newly ice-free Larsen Ice Shelf, Weddell Sea, Antarctica: ecology and taphonomy. *Marine Micropaleontology*, 53(1-2), 67-81. <https://doi.org/10.1016/j.marmicro.2004.04.001>
- Oliva, M., Navarro, F., Hrbacek, F., Hernandez, A., Nyvlt, D., Pereira, P., Ruiz-Fernandez, J., & Trigo, R. (2017). Recent regional climate cooling on the Antarctic Peninsula and associated impacts on the cryosphere. *Science of the Total Environment*, 580, 210-223. <https://doi.org/10.1016/j.scitotenv.2016.12.030>
- Pasotti, F., Saravia, L. A., De Troch, M., Tarantelli, M. S., Sahade, R., & Vanreusel, A. (2015). Benthic Trophic Interactions in an Antarctic Shallow Water Ecosystem Affected by Recent Glacier Retreat. *PLoS One*, 10(11), e0141742. <https://doi.org/10.1371/journal.pone.0141742>
- Peck, L. S., Barnes, D. K. A., Cook, A. J., Fleming, A. H., & Clarke, A. (2010). Negative feedback in the cold: ice retreat produces new carbon sinks in Antarctica. *Global Change Biology*, 16: 2614-2623.
- Pineda-Metz, S. E. A., Gerdes, D., & Richter, C. (2020). Benthic fauna declined on a whitening Antarctic continental shelf. *Nature Communications*, 11(1), 2226. <https://doi.org/10.1038/s41467-020-16093-z>
- Pörtner, H.-O., Roberts, D. C., Masson-Delmotte, V., & Zhai, P. (2019). The Ocean and Cryosphere in a Changing Climate: A Special Report by the Intergovernmental Panel on Climate Change. Intergovernmental Panel on Climate Change.
- Primo, C., & Vazquez, E. (2014). Ascidian fauna south of the Sub-Tropical Front. *SCAR*. 221-228.
- Primo, C., & Vázquez, E. (2014). Ascidian fauna south of the sub-tropical front. Biogeographic atlas of the southern ocean. Scientific Committee on Antarctic Research, Cambridge, 221-228.
- Quartino, M. L., Deregibus, D., Campana, G. L., Latorre, G. E., & Momo, F. R.

- (2013). Evidence of macroalgal colonization on newly ice-free areas following glacial retreat in Potter Cove (South Shetland Islands), Antarctica. *PLoS One*, 8(3), e58223. <https://doi.org/10.1371/journal.pone.0058223>
- Raes, M., Rose, A., & Vanreusel, A. (2010). Response of nematode communities after large-scale ice-shelf collapse events in the Antarctic Larsen area. *Global Change Biology*, 16(5), 1618-1631. <https://doi.org/10.1111/j.1365-2486.2009.02137.x>
- Rauschert, M., & Arntz, W. (2015). *Antarctic Macroenthos: A Field Guide of the Invertebrates Living at the Antarctic Seafloor*. Arntz & Rauschert Selbstverlag. <https://books.google.co.kr/books?id=of70jgEACAAJ>
- Ricotta, C., & Moretti, M. (2011). CWM and Rao's quadratic diversity: a unified framework for functional ecology. *Oecologia*, 167(1), 181-188. <https://doi.org/10.1007/s00442-011-1965-5>
- Rignot, E., Mouginot, J., Scheuchl, B., van den Broeke, M., van Wessem, M. J., & Morlighem, M. (2019). Four decades of Antarctic Ice Sheet mass balance from 1979-2017. *Proceedings of the National Academy of Sciences*, 116(4), 1095-1103.
- Rimondino, C., Torre, L., Sahade, R., & Tatián, M. (2015). Sessile macro-epibiotic community of solitary ascidians, ecosystem engineers in soft substrates of Potter Cove, Antarctica. *Polar Research*, 34(1). <https://doi.org/10.3402/polar.v34.24338>
- Robinson, B. J. O., Barnes, D. K. A., Grange, L. J., & Morley, S. A. (2021). Intermediate ice scour disturbance is key to maintaining a peak in biodiversity within the shallows of the Western Antarctic Peninsula. *Scientific Reports*, 11(1), 16712. <https://doi.org/10.1038/s41598-021-96269-9>
- Sahade, R., Lagger, C., Torre, L., Momo, F., Monien, P., Schloss, I., Barnes, D. K., Servetto, N., Tarantelli, S., & Tatián, M. (2015). Climate change and glacier retreat drive shifts in an Antarctic benthic ecosystem. *Science Advances*, 1(10), e1500050.
- Sahade, R., Tatián, M., Kowalke, J., Kühne, S., & Esnal, G. (1998). Benthic faunal associations on soft substrates at Potter Cove, King George Island, Antarctica. *Polar Biology*, 19(2), 85-91.
- Schloss, I., & Ferreyra, G. (2002). Primary production, light and vertical mixing in Potter Cove, a shallow bay in the maritime Antarctic. *Polar Biology*, 25(1), 41-48. <https://doi.org/10.1007/s003000100309>

- Schories, D., & Kohlberg, G. (2016). *Marine Wildlife, King George Island, Antarctica*. Dirk Schories Publications.
- Segelken-Voigt, A., Bracher, A., Dorschel, B., Gutt, J., Huneke, W., Link, H., & Piepenburg, D. (2016). Spatial distribution patterns of ascidians (Ascidiacea: Tunicata) on the continental shelves off the northern Antarctic Peninsula. *Polar Biology*, 39(5), 863-879. <https://doi.org/10.1007/s00300-016-1909-y>
- Shin, H. C., & others (2012). Overwintering Report of the 24rd Korea Antarctic Research Program at the King Sejong Station (December 2010-December 2011). Korea Polar Research Institute Report 2011.
- Siciński, J., & others (2011). Admiralty Bay Benthos Diversity—A census of a complex polar ecosystem. *Deep Sea Res. Part II: Topical Studies in Oceanography*, 58(1-2), 30-48.
- Siciński, J., Pabis, K., Jażdżewski, K., Konopacka, A., & Błażewicz-Paszkowycz, M. (2012). Macrozoobenthos of two Antarctic glacial coves: a comparison with non-disturbed bottom areas. *Polar Biology*, 35(3), 355-367. <https://doi.org/10.1007/s00300-011-1081-3>
- Smale, D. A. (2008). Continuous benthic community change along a depth gradient in Antarctic shallows: evidence of patchiness but not zonation. *Polar Biology*, 31(2), 189-198. <https://doi.org/10.1007/s00300-007-0346-3>
- Smale, D. A., & Barnes, D. K. A. (2008). Likely responses of the Antarctic benthos to climate-related changes in physical disturbance during the 21st century, based primarily on evidence from the West Antarctic Peninsula region. *Ecography*, 31, 17. <https://doi.org/10.1111/j.2008.0906-7590.05456.x>
- Smale, D. A., Barnes, D. K. A., & Fraser, K. P. P. (2007a). The influence of depth, site exposure and season on the intensity of iceberg scouring in nearshore Antarctic waters. *Polar Biology*, 30(6), 769-779. <https://doi.org/10.1007/s00300-006-0236-0>
- Smale, D. A., Barnes, D. K. A., & Fraser, K. P. P. (2007b). The influence of ice scour on benthic communities at three contrasting sites at Adelaide Island, Antarctica. *Austral Ecology*, 32(8), 878-888. <https://doi.org/10.1111/j.1442-9993.2007.01776.x>
- Smale, D. A., Brown, K. M., Barnes, D. K., Fraser, K. P., & Clarke, A. (2008). Ice scour disturbance in Antarctic waters. *Science*, 321: 371.
- Smith, K. L., Jr., Sherman, A. D., Shaw, T. J., & Sprintall, J. (2013). Icebergs as unique Lagrangian ecosystems in polar seas. *Annual Review of Marine*

- Science, 5(1), 269-287. <https://doi.org/10.1146/annurev-marine-121211-172317>
- Statzner, B., Dolédec, S., & Hugueny, B. (2004). Biological trait composition of European stream invertebrate communities: assessing the effects of various trait filter types. *Ecography*, 27(4), 470-488.
- Svane, I., & Young, C. M. (1989). The ecology and behaviour of ascidian larvae. *Oceanography and Marine Biology*, 27, 45-90.
- Tatiàn, M., Antacli, J. C., & Sahade, R. (2005). Ascidiaceae (Tunicata, Ascidiacea): species distribution along the Scotia Arc. *Scientia Marina*, 69(S2), 205-214.
- Tatiàn, M., Sahade, R. J., Doucet, M. E., & Esnal, G. B. (1998). Ascidiaceae (Tunicata, Ascidiacea) of Potter Cove, South Shetland Islands, Antarctica. *Antarctic Science*, 10(2), 147-152. <https://doi.org/10.1017/s0954102098000194>
- Tatiàn, M., Sahade, R., & Esnal, G. B. (2004). Diet components in the food of Antarctic ascidians living at low levels of primary production. *Antarctic Science*, 16(2), 123-128. <https://doi.org/10.1017/s0954102004001890>
- Tatiàn, M., Sahade, R., Kowalke, J., Kivatnits, S., & Esnal, G. (2002). Food availability and gut contents in the ascidian *Cnemidocarpa verrucosa* at Potter Cove, Antarctica. *Polar Biology*, 25(1), 58-64. <https://doi.org/10.1007/s003000100311>
- Tatiàn, M., Sahade, R., Mercuri, G., Fuentes, V. L., Antacli, J. C., Stellfeldt, A., & Esnal, G. B. (2008). Feeding ecology of benthic filter-feeders at Potter Cove, an Antarctic coastal ecosystem. *Polar Biology*, 31(4), 509-517. <https://doi.org/10.1007/s00300-007-0379-7>
- Team, I. (2018). Mass balance of the Antarctic Ice Sheet from 1992 to 2017. *Nature*, 558(7709), 219-222. <https://doi.org/10.1038/s41586-018-0179-y>
- Teixidó, N., Garrabou, J., Gutt, J., & Arntz, W. E. (2004). Recovery in Antarctic benthos after iceberg disturbance: trends in benthic composition, abundance and growth forms. *Marine Ecology Progress Series*, 278, 1-16.
- Teixidó, N., Garrabou, J., Gutt, J., & Arntz, W. E. (2004). Recovery in Antarctic benthos after iceberg disturbance: trends in benthic composition, abundance and growth forms. *Marine Ecology Progress Series*, 278: 1-16.
- Teixidó, N., Garrabou, J., Gutt, J., & Arntz, W. E. (2007). Iceberg Disturbance and Successional Spatial Patterns: The Case of the Shelf Antarctic Benthic Communities. *Ecosystems*, 10(1), 143-158. <https://doi.org/10.1007/s10021-006-9012-9>

- Thrush, S., Dayton, P., Cattaneo-Vietti, R., Chiantore, M., Cummings, V., Andrew, N., Hawes, I., Kim, S., Kvitek, R., & Schwarz, A.-M. (2006). Broad-scale factors influencing the biodiversity of coastal benthic communities of the Ross Sea. *Deep Sea Research Part II: Topical Studies in Oceanography*, 53(8-10), 959-971. <https://doi.org/10.1016/j.dsr2.2006.02.006>
- Torre, L., Abele, D., Lagger, C., Momo, F., & Sahade, R. (2014). When shape matters: strategies of different Antarctic ascidians morphotypes to deal with sedimentation. *Marine Environmental Research*, 99, 179-187. <https://doi.org/10.1016/j.marenvres.2014.05.014>
- Torre, L., Alurralde, G., Lagger, C., Abele, D., Schloss, I. R., & Sahade, R. (2021). Antarctic ascidians under increasing sedimentation: Physiological thresholds and ecosystem hysteresis. *Marine Environmental Research*, 167, 105284. <https://doi.org/10.1016/j.marenvres.2021.105284>
- Torre, L., Servetto, N., Eöry, M. L., Momo, F., Tatián, M., Abele, D., & Sahade, R. (2012). Respiratory responses of three Antarctic ascidians and a sea pen to increased sediment concentrations. *Polar Biology*, 35(11), 1743-1748. <https://doi.org/10.1007/s00300-012-1208-1>
- Turner, J., Lu, H., White, I., King, J. C., Phillips, T., Hosking, J. S., Bracegirdle, T. J., Marshall, G. J., Mulvaney, R., & Deb, P. (2016). Absence of 21st century warming on Antarctic Peninsula consistent with natural variability. *Nature*, 535(7612), 411-415. <https://doi.org/10.1038/nature18645>
- Vandewalle, M., de Bello, F., Berg, M. P., Bolger, T., Dolédec, S., Dubs, F., Feld, C. K., Harrington, R., Harrison, P. A., Lavorel, S., da Silva, P. M., Moretti, M., Niemelä, J., Santos, P., Sattler, T., Sousa, J. P., Sykes, M. T., Vanbergen, A. J., & Woodcock, B. A. (2010). Functional traits as indicators of biodiversity response to land use changes across ecosystems and organisms. *Biodiversity and Conservation*, 19(10), 2921-2947. <https://doi.org/10.1007/s10531-010-9798-9>
- Wadham, J. L., De'ath, R., Monteiro, F. M., Tranter, M., Ridgwell, A., Raiswell, R., & Tulaczyk, S. (2013). The potential role of the Antarctic Ice Sheet in global biogeochemical cycles. *Earth and Environmental Science Transactions of the Royal Society of Edinburgh*, 104(1), 55-67. <https://doi.org/10.1017/s1755691013000108>
- Wang, Z., Leung, K. M. Y., Sung, Y. H., Dudgeon, D., & Qiu, J. W. (2021). Recovery of tropical marine benthos after a trawl ban demonstrates linkage between abiotic and biotic changes. *Communications Biology*, 4(1), 212. <https://doi.org/10.1038/s42003-021-01732-y>

- Yoo, K.-C., Kyung Lee, M., Il Yoon, H., Il Lee, Y., & Yoon Kang, C. (2015). Hydrography of Marian Cove, King George Island, West Antarctica: implications for ice-proximal sedimentation during summer. *Antarctic Science*, 27(2), 185-196. <https://doi.org/10.1017/s095410201400056x>
- Yoo, K.-C., Yoon, H.-I., Kang, C.-Y., Kim, B.-K., & Oh, J.-K. (2000). Water column structure and dispersal pattern of suspended particulate matter (SPM) in a floating ice-dominated fjord, Marian Cove, Antarctica during austral summer. *The Sea*, 5(4), 295-304.
- Yoon, H. I., Han, M. W., Park, B.-K., Oh, J.-K., & Chang, S.-K. (1997). Glaciomarine sedimentation and palaeo-glacial setting of Maxwell Bay and its tributary embayment, Marian Cove, South Shetland Islands, West Antarctica. *Marine Geology*, 140(3-4), 265-282.
- Yoon, H., Park, B.-K., Domack, E., & Kim, Y. (1998). Distribution and dispersal pattern of suspended particulate matter in Maxwell Bay and its tributary, Marian Cove, in the South Shetland Islands, West Antarctica. *Marine Geology*, 152(4), 261-275.

## ABSTRACT (IN KOREAN)

빙하후퇴는 퇴적작용이나 입도, 물리적 교란과 같은 환경의 변화를 유발하여 극지 연안의 저서 무척추동물들에게 강한 영향을 미친다. 남극의 천해에서 심해에 이르기까지 널리 분포하고 있는 저서동물들은 육상의 대부분이 빙하로 뒤덮인 극지에서 저서 생태계의 중요성을 보여준다. 하지만 온난화로 인한 빙하후퇴에 대한 저서 생태계의 반응과 변화에 대해서는 많은 것이 알려지지 않았다. 이를 밝히기 위해 다음의 세 가지 질문에 답하고자 빙하가 후퇴한 남극 연안 피요르드만에서 거대저서동물 군집의 구조와 기능을 조사하였다. 1) 거대저서동물 군집은 빙하후퇴 이후에 어떻게 변하는가? 2) 남극 빙하후퇴 지역의 거대저서동물 분포를 지표하는 분류군 및 관련 환경 요인은 무엇인가? 3) 남극의 우점 분류군 중 하나인 멍게의 섭식 양상은 빙하의 영향에 따라 달라지는가? 빙하가 후퇴한 남극 피요르드만의 거대저서동물 군집 분포와 섭식 양상을 확인하기 위해 마리안소만에서 처음으로 수중 ROV 영상조사를 수행하였다. 멍게 섭식 양상은 탄소 및 질소 동위원소 분석을 통해 확인하였다.

빙하후퇴 지역에서 거대저서동물 군집의 구조적, 기능적 다양성은 공간에 따라 뚜렷하게 달랐다. 종 다양성은 빙하의 영향이 감소하는 만의 외측으로 갈수록 증가했으나 서식밀도는 개척종들(*Molgula pedunculata* 및 *Cnemidocarpa verrucosa*)의 급격한 증가로 빙벽 인근에서 가장 높았다. 저서 군집은 빙하후퇴 이후에 상위분류단계 수준에서는 빠르게 성숙되었다(약 10년 이내). 반면, 기능적 다양성은 외측으로 갈수록 증가했으며, 비교적 물리적 교란이 적고 먹이 공급은 풍부한 30 m에서 가장 높았다. 이 연구는 남극 연안에서 빙하후퇴 이후의 3단계 거대저서동물 군집 변화 과정(가입, 전환, 성숙)을 보여주었다.

멍게 분포는 거대저서동물 변화의 64%를 반영하여 남극 빙하후퇴에 대한 저서 생태계 반응을 모니터링하기 위한 지표군으로 적합했다. 멍게의 공간분포는 빙하로부터의 거리와 수심에 따라 뚜렷하게 달랐다. 서식밀도는 개척종들(*M. pedunculata* 및 *C. verrucosa*)의 급격한 증가로 빙벽 인근에서 최대였으나 종다양성은 빙하의 영향이 감소하는 외측으로 갈수록 증가하였다. 이런 공간분포 양상은 비교적 교란이 심한 얕은 수심(10-30 m)에서는 두드러지지 않았다. 물리적 교란 정도를 나타내는 퇴적물 특성과 빙벽으로부터의 거리가 멍게 분포를 결정하는 주요인이었다.

$\delta^{13}\text{C}$ 와  $\delta^{15}\text{N}$  분석은 남극 연안에서 빙하의 영향에 따른 멧게 우점종 3개의 섭식 양상 변화를 보여주었다. 마리안소만에서 멧게의 주요 먹이는 저서규조류였으며(30–70%), 멧게 먹이에 대한 저서규조류의 기여도는 수심 100 m까지 유효했다. 멧게의 섭식은 종에 따라 달랐다. 비선택적 섭식을 하는 기동형 멧게인 *M. pedunculata*의 먹이 대한 수층 생산의 기여는 식물플랑크톤이 풍부한 외층으로 갈수록 증가했다. 하지만 여전히 저서규조류가 주된 먹이원 중 하나였다. 반면, 분출 기작을 가진 *C. verrucosa*와 납작한 형태인 *Ascidia challengerii*는 빙하의 영향과 무관하게 저서규조류를 주로 섭식했다. 이 결과들은 남극 연안에서 저서규조류가 여과섭식자들의 주된 먹이원이며, 특히 빙하후퇴로 인한 높은 탁도로 수층 생산력이 낮은 지역에서 핵심 먹이원임을 보여주었다.

본 연구는 빙하후퇴에 대한 남극 저서생태계의 반응에 대한 정보를 제공한다. 마리안소만 빙하로부터의 거리는 해저가 노출된 시간과 비례하여, 거대저서동물 군집의 공간 분포로부터 빙하 후퇴 이후에 발생한 군집의 천이 과정을 유추할 수 있다. 그러므로 이 연구의 결과는 기후변화에 따른 남극 해양 생태계의 변화를 예측하고 대비하기 위한 토대를 제공한다.

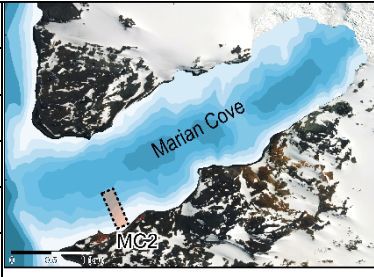
**주제어:** 남극 거대저서동물,  
빙하후퇴,  
멧게,  
구조적 및 기능적 다양성,  
천이,  
먹이원


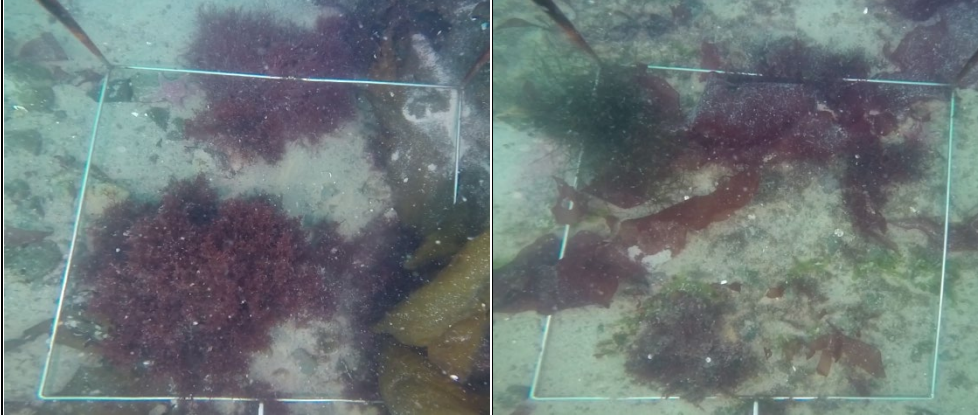
**학 번:** 2015-22652

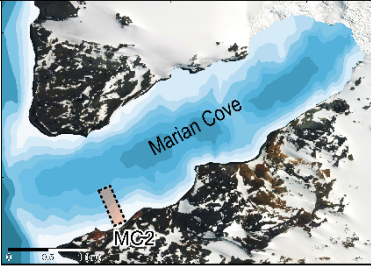


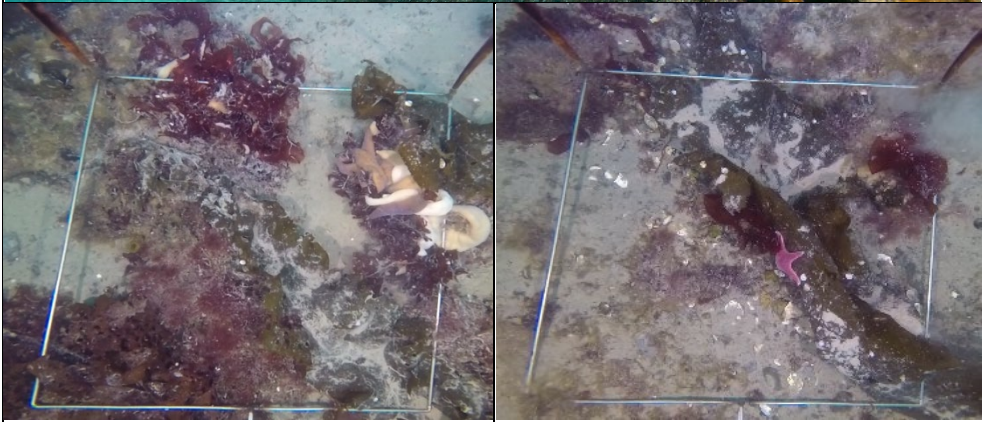
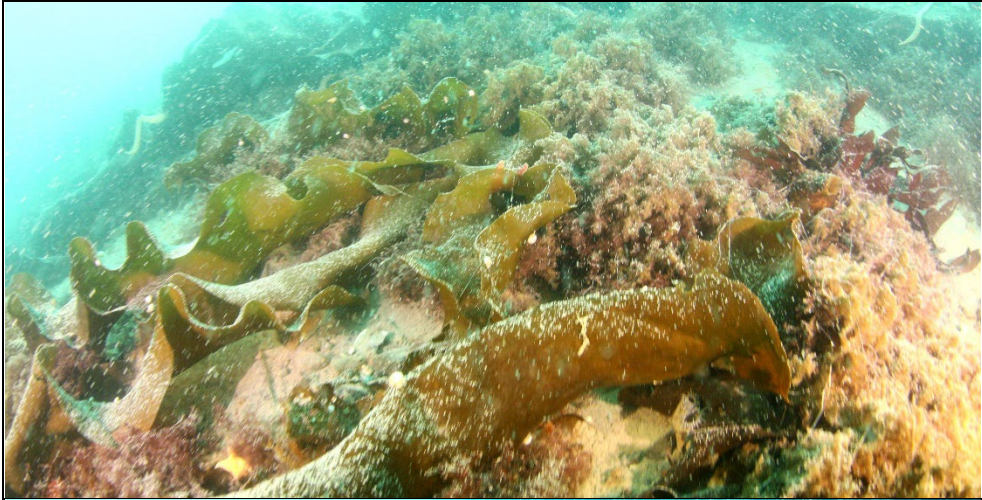
# APPENDIX

## Information and photos for study region: Marian Cove

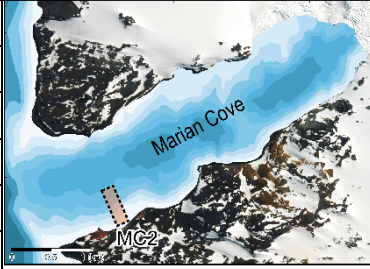
<b>Station ID</b>		MC2	
<b>Location</b>	<b>Latitude</b>	62°13'11.40"S	
	<b>Longitude</b>	58°46'51.06"W	
<b>Depth</b>		10 m	
<b>Distance from the glacier</b>		3.5 km	
<b>Seabed exposure time</b>		>63 yr	

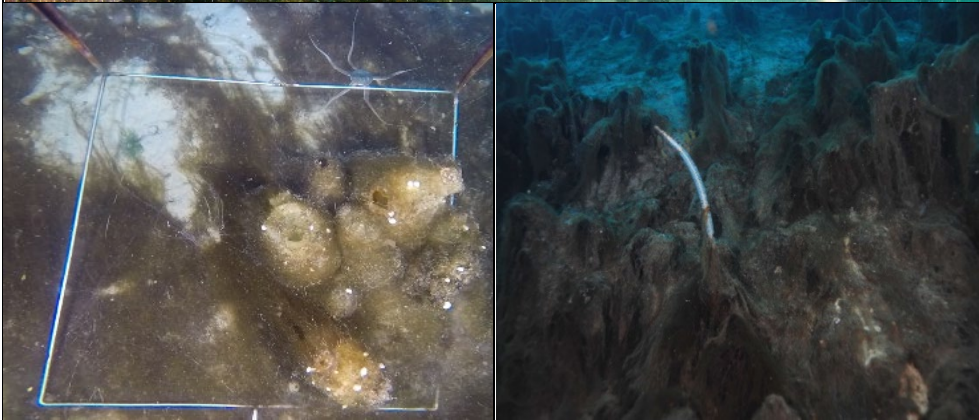
  
  


<b>Station ID</b>		<b>MC2</b>	
<b>Location</b>	<b>Latitude</b>	<b>62°13'11.40"S</b>	
	<b>Longitude</b>	<b>58°46'51.06"W</b>	
<b>Depth</b>		<b>20 m</b>	
<b>Distance from the glacier</b>		<b>3.5 km</b>	
<b>Seabed exposure time</b>		<b>&gt;63 yr</b>	

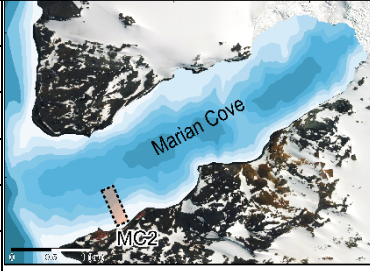


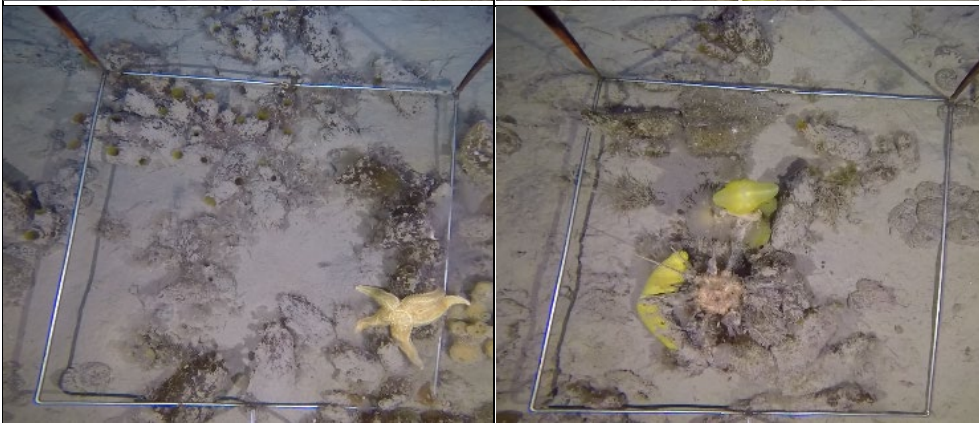
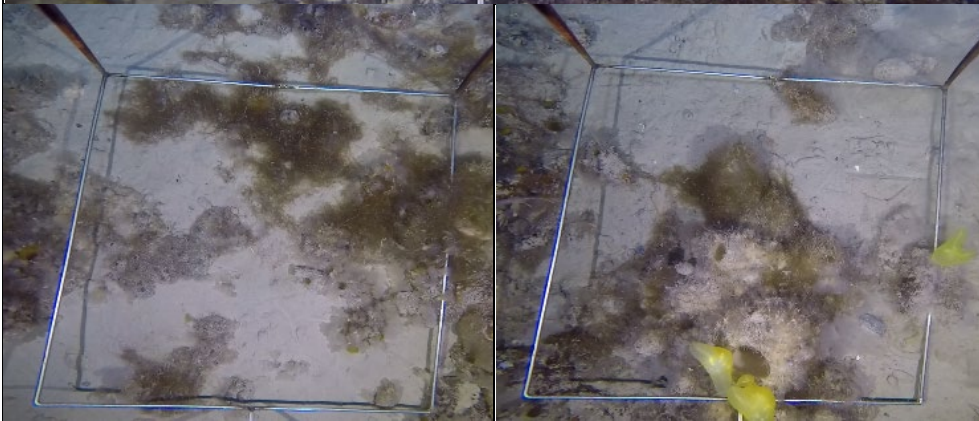


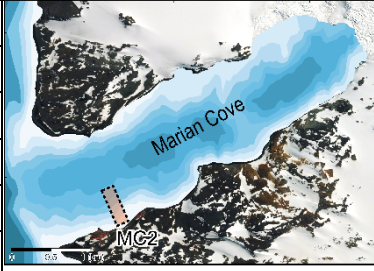
<b>Station ID</b>		MC2	
<b>Location</b>	<b>Latitude</b>	62°13'11.40"S	
	<b>Longitude</b>	58°46'51.06"W	
<b>Depth</b>		30 m	
<b>Distance from the glacier</b>		3.5 km	
<b>Seabed exposure time</b>		>63 yr	

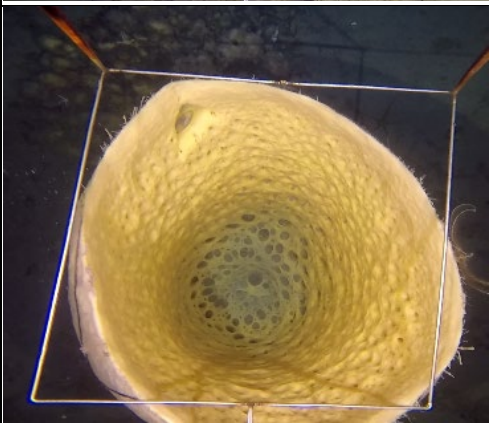
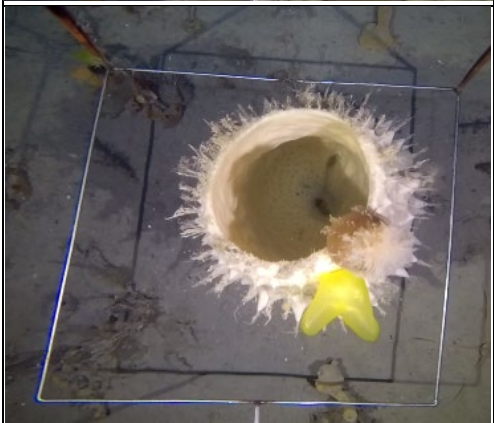
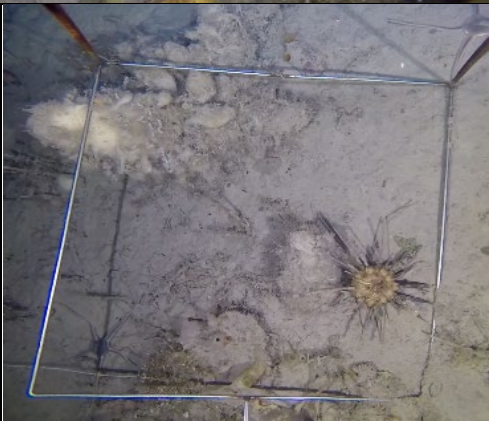
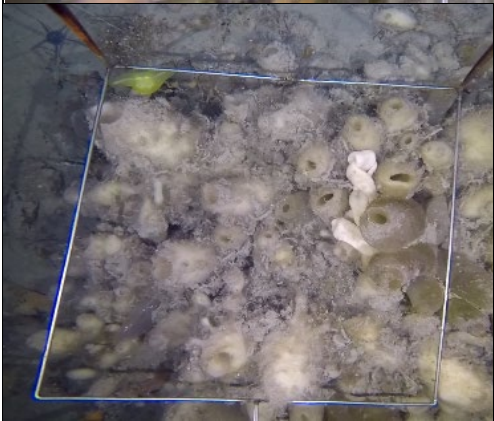




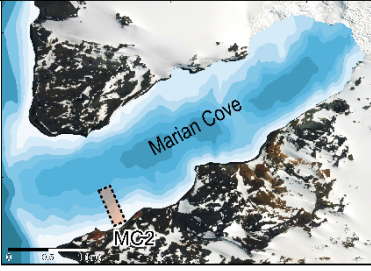
<b>Station ID</b>		<b>MC2</b>	
<b>Location</b>	<b>Latitude</b>	<b>62°13'11.40"S</b>	
	<b>Longitude</b>	<b>58°46'51.06"W</b>	
<b>Depth</b>		<b>50 m</b>	
<b>Distance from the glacier</b>		<b>3.5 km</b>	
<b>Seabed exposure time</b>		<b>&gt;63 yr</b>	

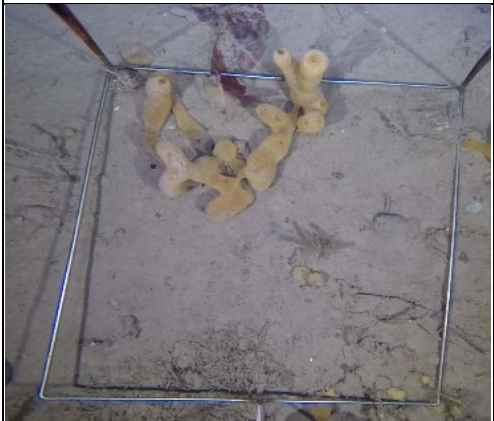
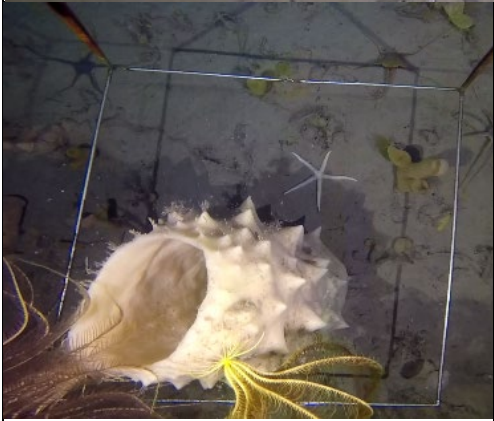


<b>Station ID</b>		MC2	
<b>Location</b>	<b>Latitude</b>	62°13'11.40"S	
	<b>Longitude</b>	58°46'51.06"W	
<b>Depth</b>		70 m	
<b>Distance from the glacier</b>		3.5 km	
<b>Seabed exposure time</b>		>63 yr	

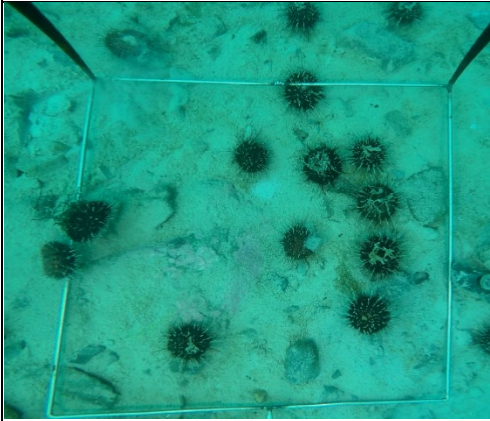
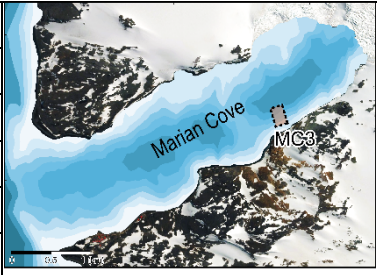




<b>Station ID</b>		<b>MC2</b>	
<b>Location</b>	<b>Latitude</b>	<b>62°13'11.40"S</b>	
	<b>Longitude</b>	<b>58°46'51.06"W</b>	
<b>Depth</b>		<b>90 m</b>	
<b>Distance from the glacier</b>		<b>3.5 km</b>	
<b>Seabed exposure time</b>		<b>&gt;63 yr</b>	

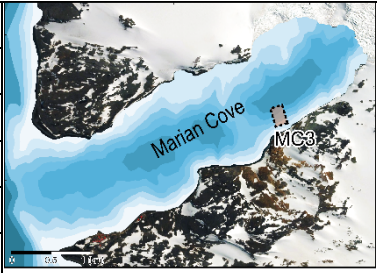


<b>Station ID</b>		MC3
<b>Location</b>	<b>Latitude</b>	62°12'38.88"S
	<b>Longitude</b>	58°44'18.84"W
<b>Depth</b>		10 m
<b>Distance from the glacier</b>		1.2 km
<b>Seabed exposure time</b>		~33 yr



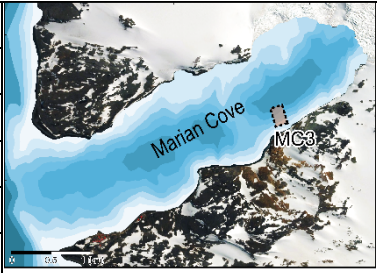


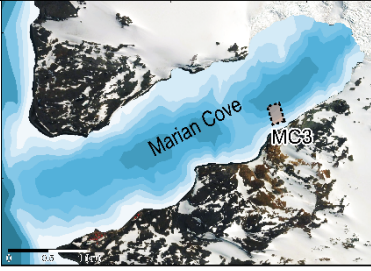
<b>Station ID</b>		<b>MC3</b>
<b>Location</b>	<b>Latitude</b>	<b>62°12'38.88"S</b>
	<b>Longitude</b>	<b>58°44'18.84"W</b>
<b>Depth</b>		<b>20 m</b>
<b>Distance from the glacier</b>		<b>1.2 km</b>
<b>Seabed exposure time</b>		<b>~33 yr</b>





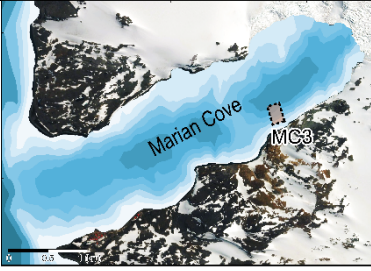
<b>Station ID</b>		<b>MC3</b>
<b>Location</b>	<b>Latitude</b>	<b>62°12'38.88"S</b>
	<b>Longitude</b>	<b>58°44'18.84"W</b>
<b>Depth</b>		<b>30 m</b>
<b>Distance from the glacier</b>		<b>1.2 km</b>
<b>Seabed exposure time</b>		<b>~33 yr</b>

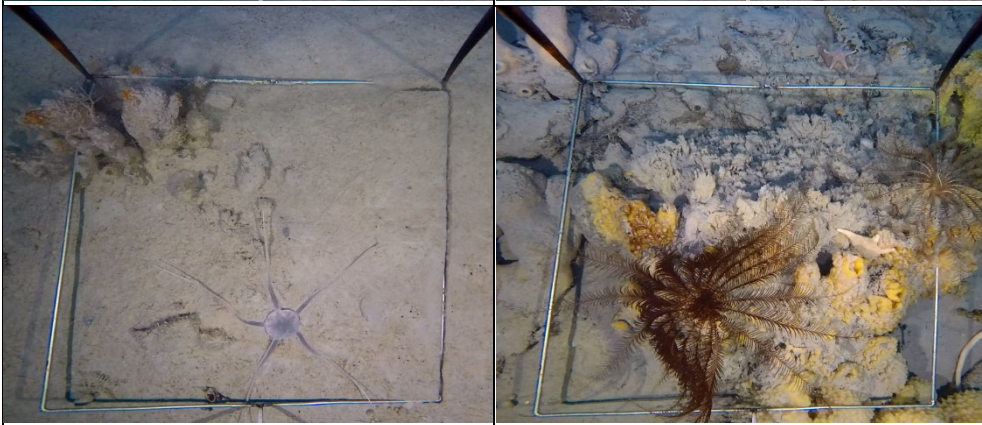
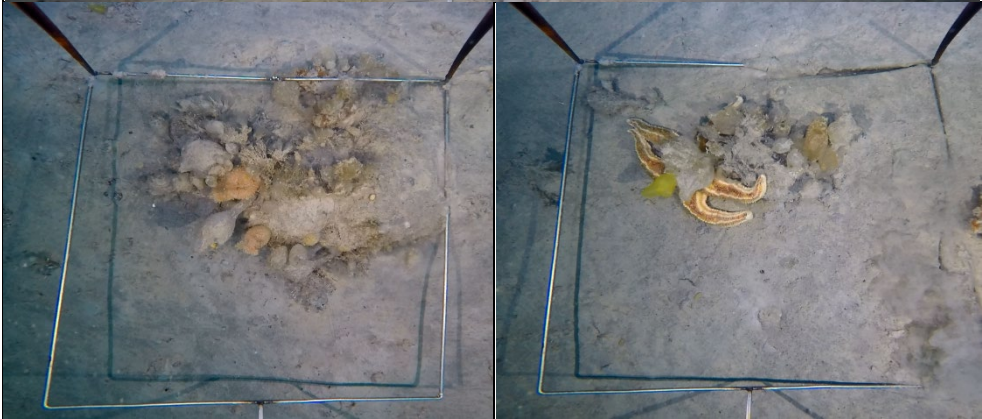


<b>Station ID</b>		<b>MC3</b>	
<b>Location</b>	<b>Latitude</b>	<b>62°12'38.88"S</b>	
	<b>Longitude</b>	<b>58°44'18.84"W</b>	
<b>Depth</b>		<b>30 m</b>	
<b>Distance from the glacier</b>		<b>1.2 km</b>	
<b>Seabed exposure time</b>		<b>~33 yr</b>	

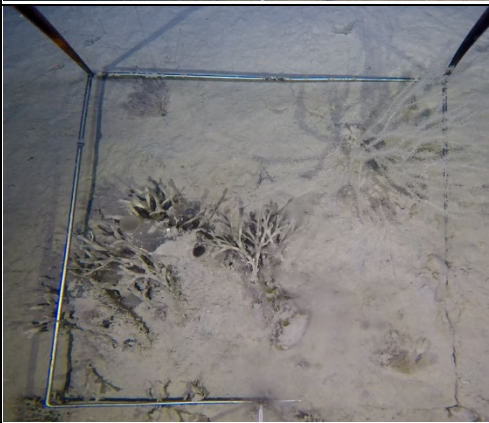
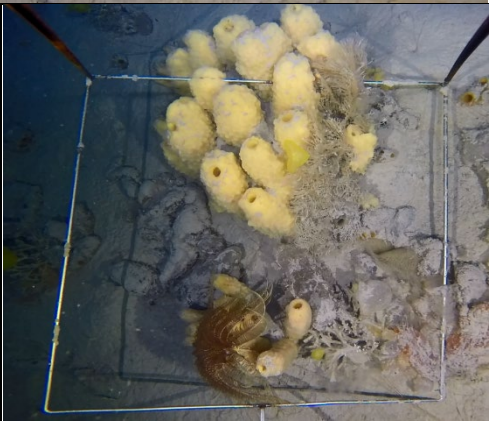
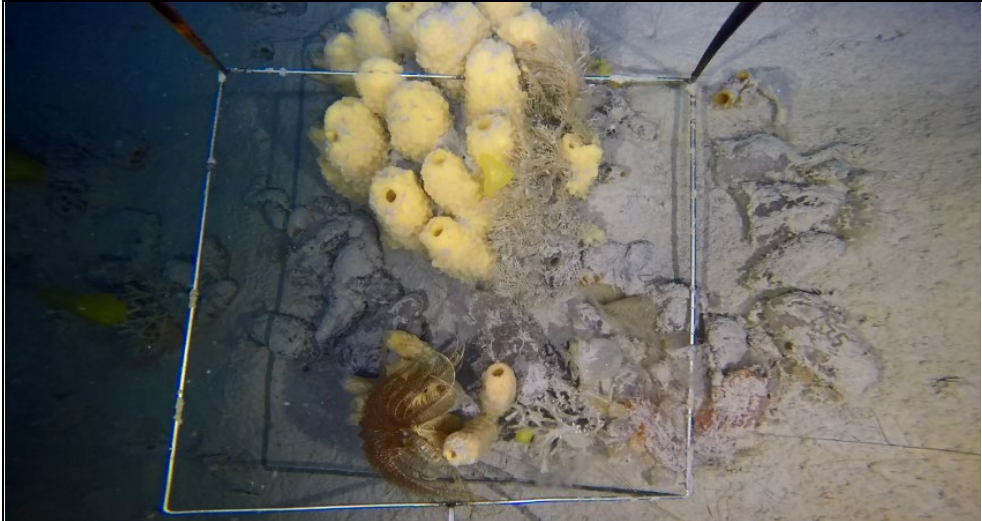
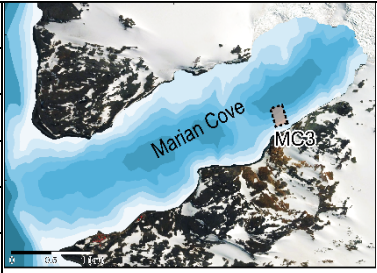




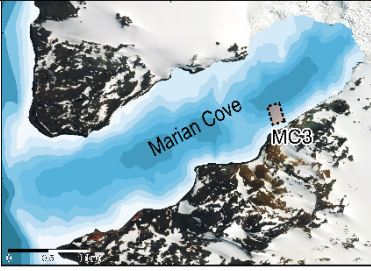
<b>Station ID</b>		<b>MC3</b>	
<b>Location</b>	<b>Latitude</b>	<b>62°12'38.88"S</b>	
	<b>Longitude</b>	<b>58°44'18.84"W</b>	
<b>Depth</b>		<b>50 m</b>	
<b>Distance from the glacier</b>		<b>1.2 km</b>	
<b>Seabed exposure time</b>		<b>~33 yr</b>	

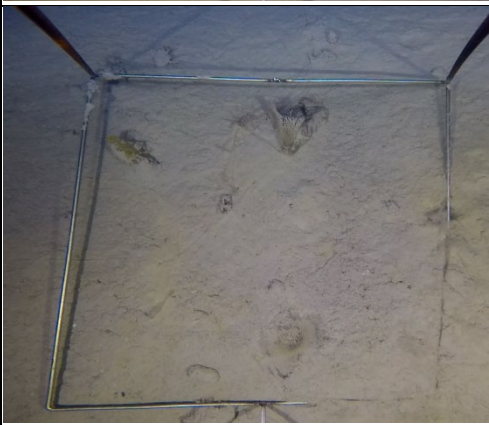
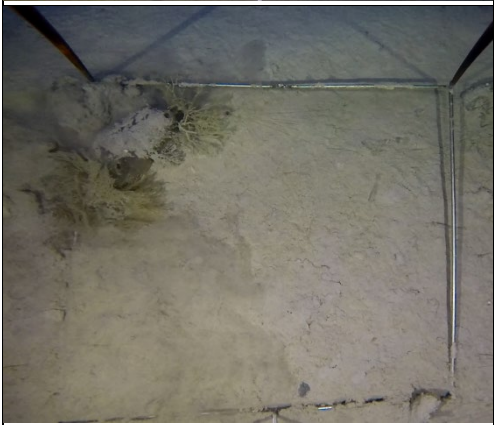
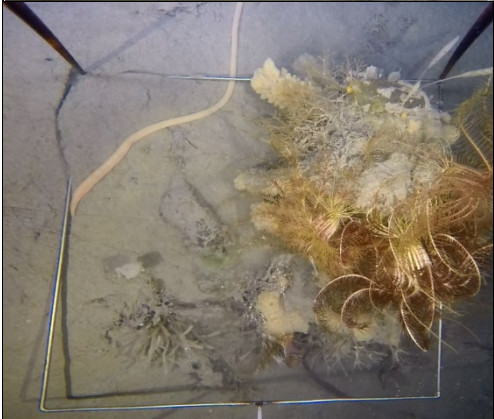


<b>Station ID</b>		<b>MC3</b>
<b>Location</b>	<b>Latitude</b>	<b>62°12'38.88"S</b>
	<b>Longitude</b>	<b>58°44'18.84"W</b>
<b>Depth</b>		<b>70 m</b>
<b>Distance from the glacier</b>		<b>1.2 km</b>
<b>Seabed exposure time</b>		<b>~33 yr</b>

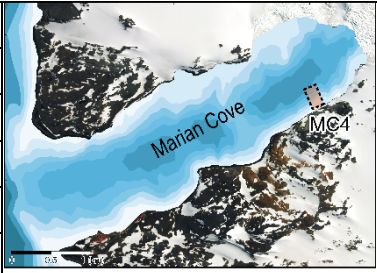




<b>Station ID</b>		<b>MC3</b>	
<b>Location</b>	<b>Latitude</b>	<b>62°12'38.88"S</b>	
	<b>Longitude</b>	<b>58°44'18.84"W</b>	
<b>Depth</b>		<b>90 m</b>	
<b>Distance from the glacier</b>		<b>1.2 km</b>	
<b>Seabed exposure time</b>		<b>~33 yr</b>	

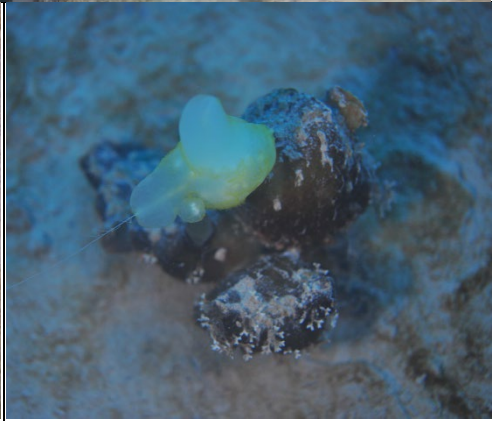
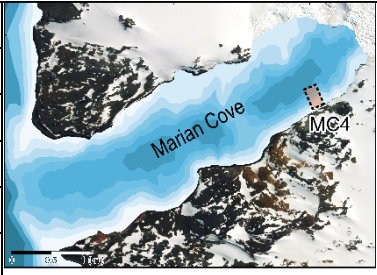


<b>Station ID</b>		<b>MC4</b>
<b>Location</b>	<b>Latitude</b>	<b>62°12'32.11"S</b>
	<b>Longitude</b>	<b>58°43'56.26"W</b>
<b>Depth</b>		<b>10 m</b>
<b>Distance from the glacier</b>		<b>0.8 km</b>
<b>Seabed exposure time</b>		<b>~21 yr</b>



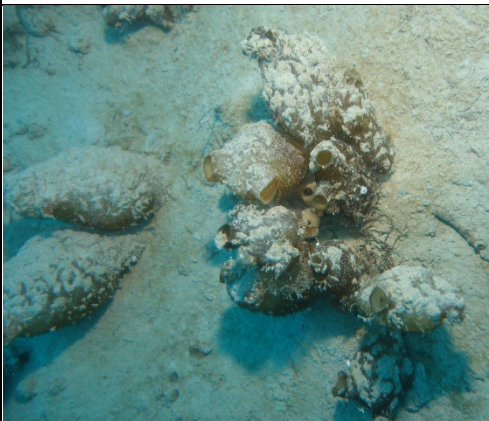
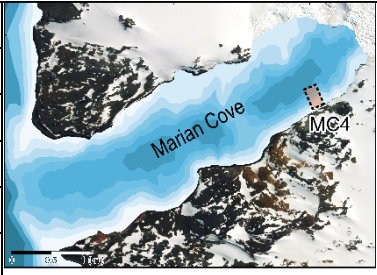


<b>Station ID</b>		MC4
<b>Location</b>	<b>Latitude</b>	62°12'32.11"S
	<b>Longitude</b>	58°43'56.26"W
<b>Depth</b>		20 m
<b>Distance from the glacier</b>		0.8 km
<b>Seabed exposure time</b>		~21 yr

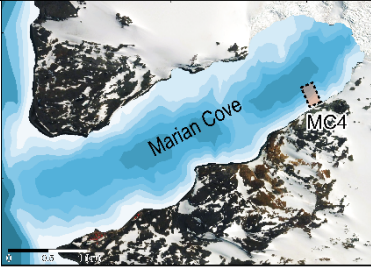


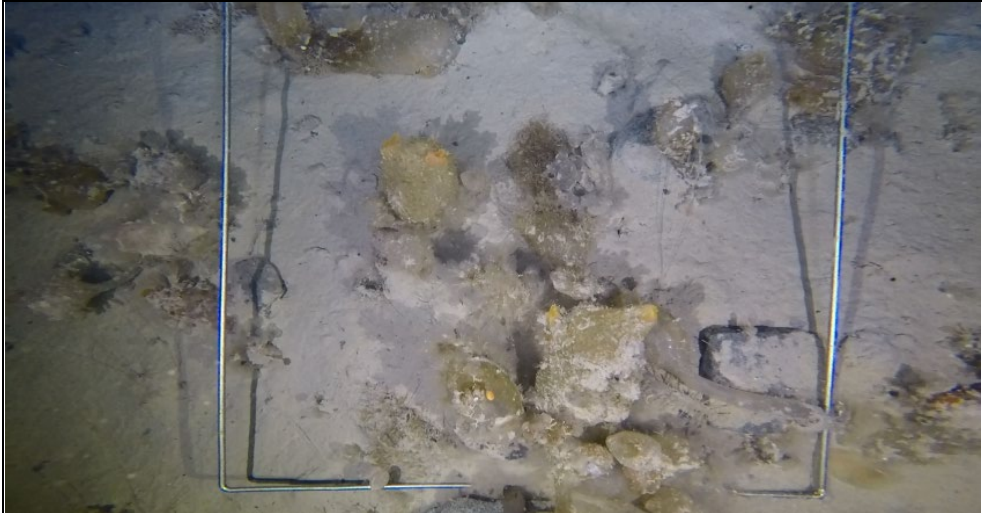


<b>Station ID</b>		MC4
<b>Location</b>	<b>Latitude</b>	62°12'32.11"S
	<b>Longitude</b>	58°43'56.26"W
<b>Depth</b>		30 m
<b>Distance from the glacier</b>		0.8 km
<b>Seabed exposure time</b>		~21 yr

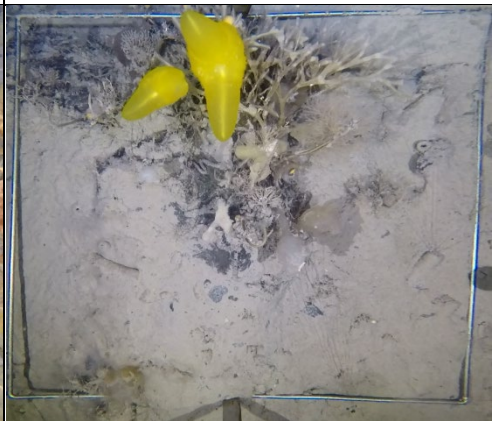
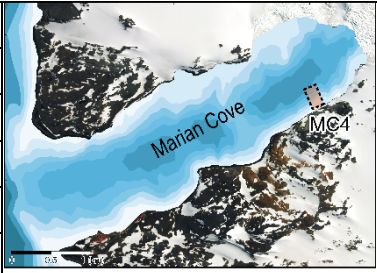




<b>Station ID</b>		<b>MC4</b>	
<b>Location</b>	<b>Latitude</b>	<b>62°12'32.11"S</b>	
	<b>Longitude</b>	<b>58°43'56.26"W</b>	
<b>Depth</b>		<b>50 m</b>	
<b>Distance from the glacier</b>		<b>0.8 km</b>	
<b>Seabed exposure time</b>		<b>~21 yr</b>	



<b>Station ID</b>		<b>MC4</b>
<b>Location</b>	<b>Latitude</b>	<b>62°12'32.11"S</b>
	<b>Longitude</b>	<b>58°43'56.26"W</b>
<b>Depth</b>		<b>70 m</b>
<b>Distance from the glacier</b>		<b>0.8 km</b>
<b>Seabed exposure time</b>		<b>~21 yr</b>



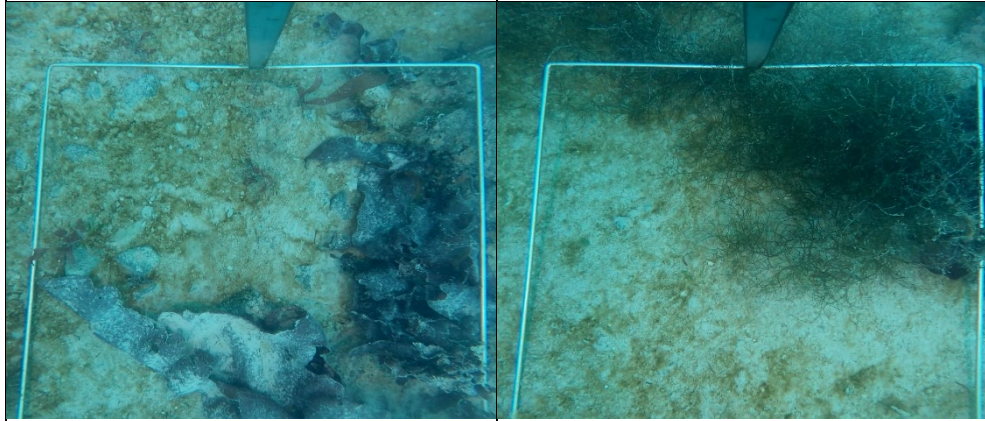
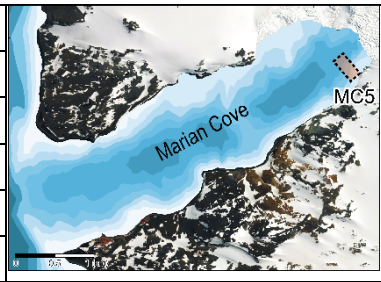


<b>Station ID</b>		<b>MC4</b>	
<b>Location</b>	<b>Latitude</b>	<b>62°12'32.11"S</b>	
	<b>Longitude</b>	<b>58°43'56.26"W</b>	
<b>Depth</b>		<b>90 m</b>	
<b>Distance from the glacier</b>		<b>0.8 km</b>	
<b>Seabed exposure time</b>		<b>~21 yr</b>	



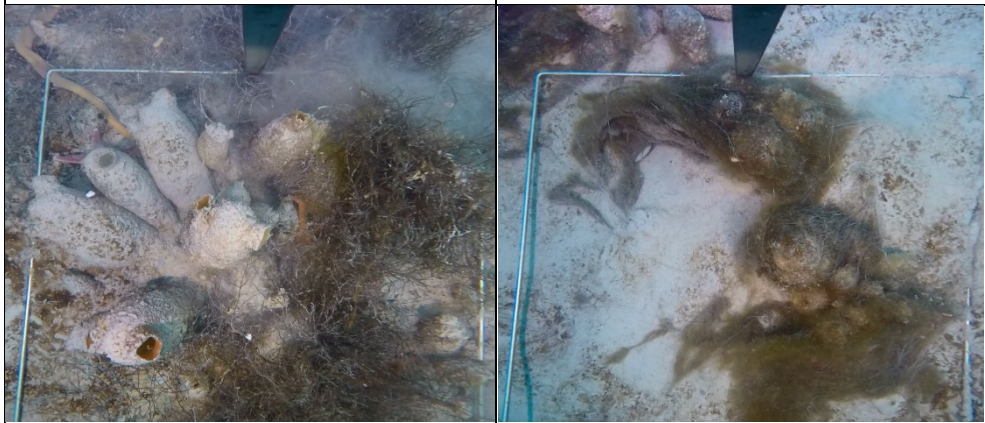
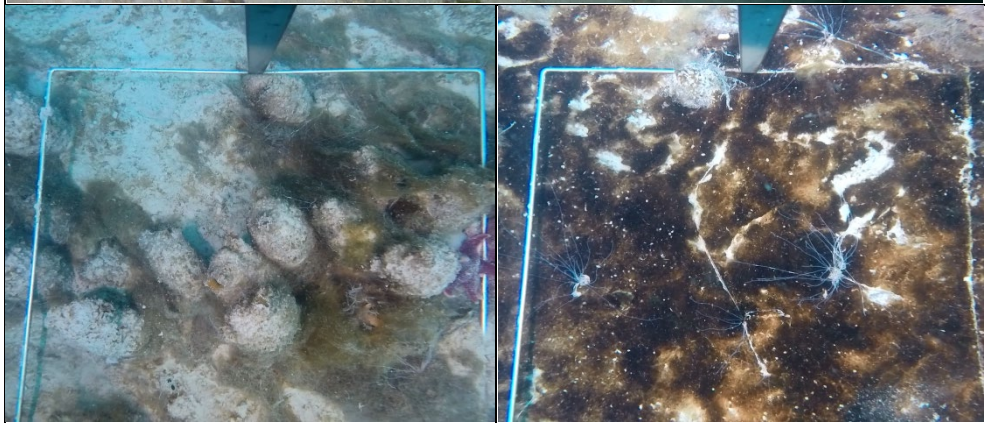
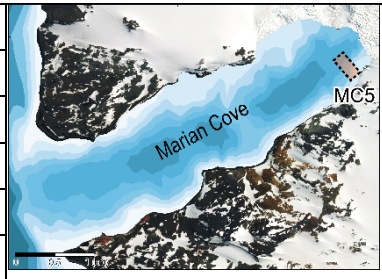


<b>Station ID</b>		<b>MC5</b>
<b>Location</b>	<b>Latitude</b>	<b>62°12'10.56"S</b>
	<b>Longitude</b>	<b>58°43'28.56"W</b>
<b>Depth</b>		<b>10 m</b>
<b>Distance from the glacier</b>		<b>0.2 km</b>
<b>Seabed exposure time</b>		<b>~11 yr</b>



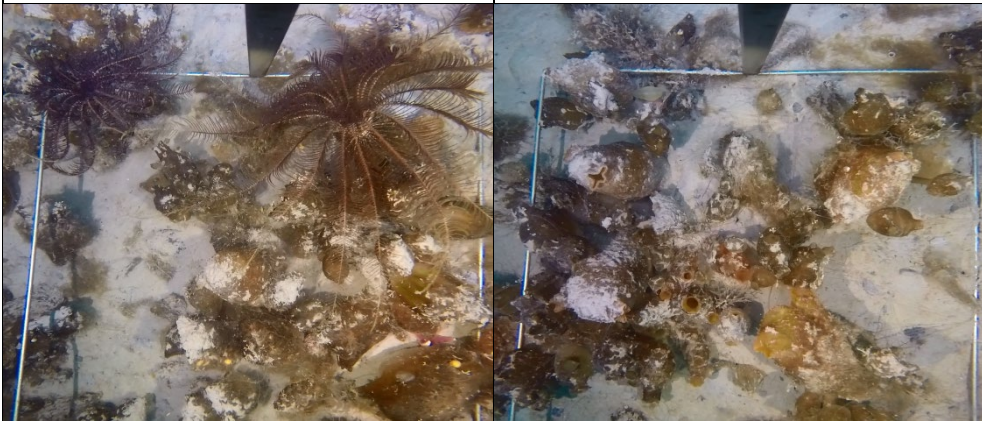
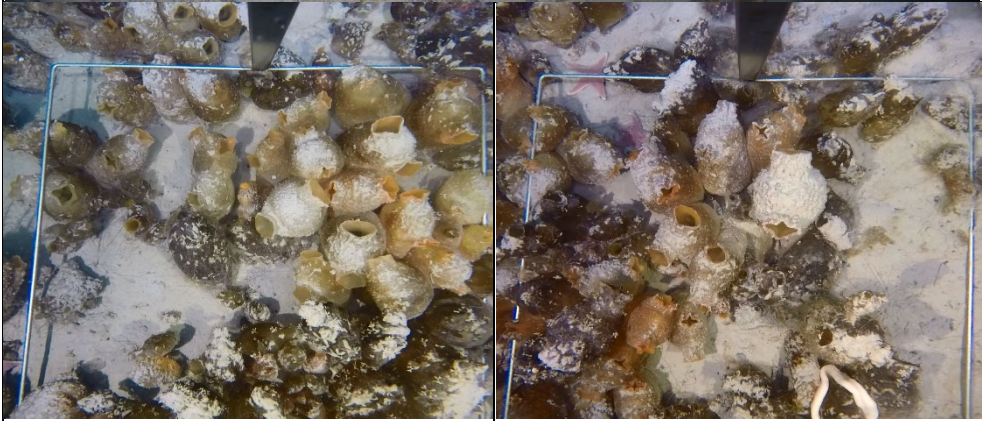
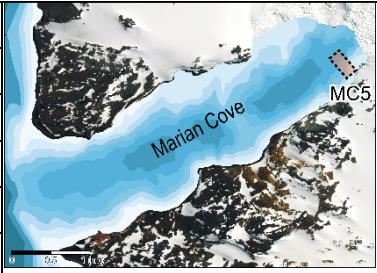


<b>Station ID</b>		<b>MC5</b>
<b>Location</b>	<b>Latitude</b>	<b>62°12'10.56"S</b>
	<b>Longitude</b>	<b>58°43'28.56"W</b>
<b>Depth</b>		<b>20 m</b>
<b>Distance from the glacier</b>		<b>0.2 km</b>
<b>Seabed exposure time</b>		<b>~11 yr</b>



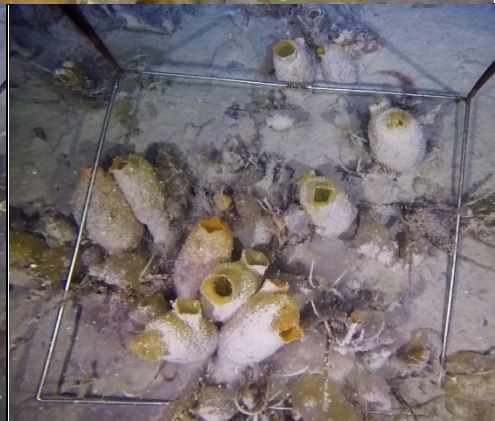
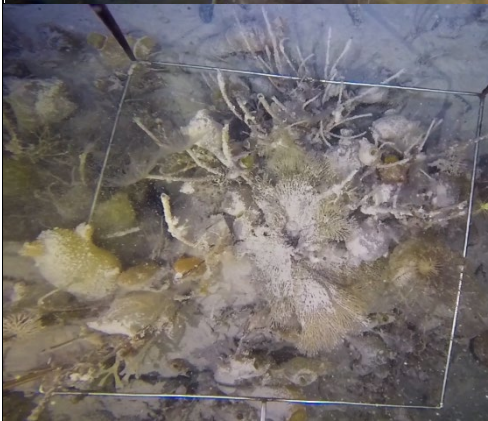
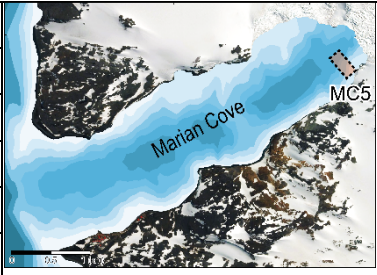


<b>Station ID</b>		<b>MC5</b>
<b>Location</b>	<b>Latitude</b>	<b>62°12'10.56"S</b>
	<b>Longitude</b>	<b>58°43'28.56"W</b>
<b>Depth</b>		<b>30 m</b>
<b>Distance from the glacier</b>		<b>0.2 km</b>
<b>Seabed exposure time</b>		<b>~11 yr</b>

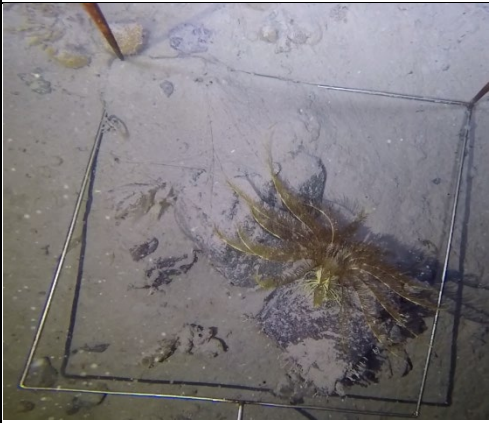
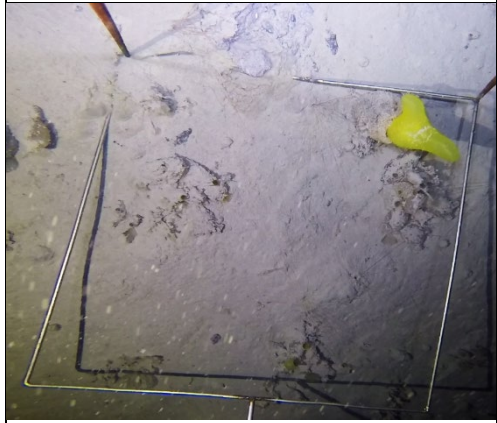
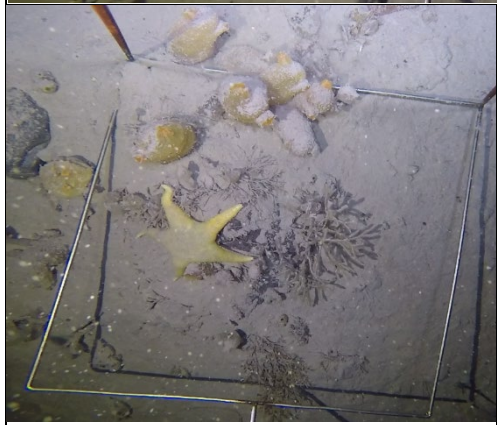
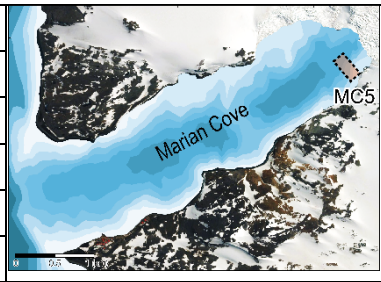




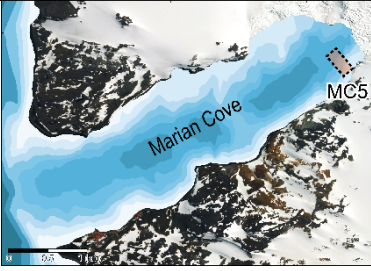
<b>Station ID</b>		<b>MC5</b>
<b>Location</b>	<b>Latitude</b>	<b>62°12'10.56"S</b>
	<b>Longitude</b>	<b>58°43'28.56"W</b>
<b>Depth</b>		<b>50 m</b>
<b>Distance from the glacier</b>		<b>0.2 km</b>
<b>Seabed exposure time</b>		<b>~11 yr</b>

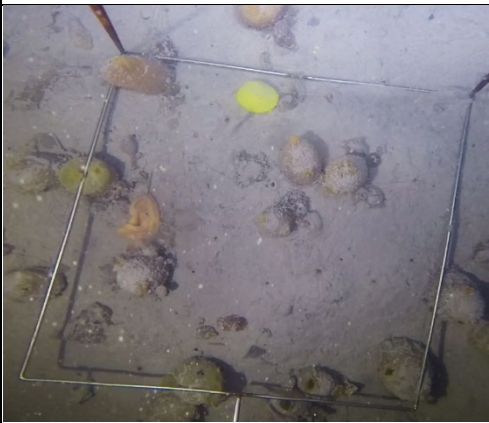
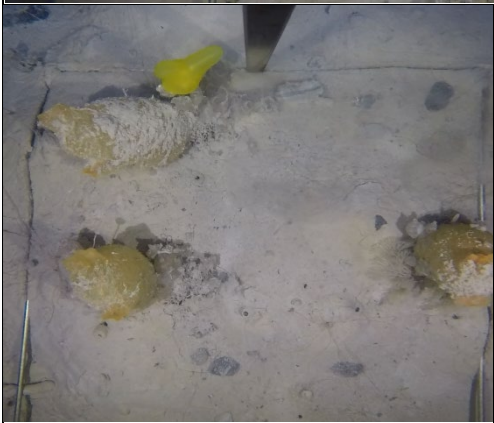


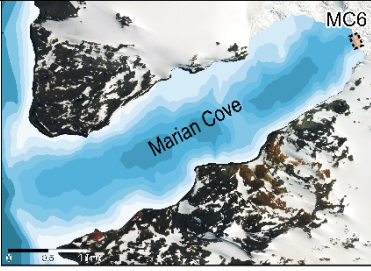
<b>Station ID</b>		<b>MC5</b>
<b>Location</b>	<b>Latitude</b>	<b>62°12'10.56"S</b>
	<b>Longitude</b>	<b>58°43'28.56"W</b>
<b>Depth</b>		<b>70 m</b>
<b>Distance from the glacier</b>		<b>0.2 km</b>
<b>Seabed exposure time</b>		<b>~11 yr</b>





<b>Station ID</b>		<b>MC5</b>	
<b>Location</b>	<b>Latitude</b>	<b>62°12'10.56"S</b>	
	<b>Longitude</b>	<b>58°43'28.56"W</b>	
<b>Depth</b>		<b>90 m</b>	
<b>Distance from the glacier</b>		<b>0.2 km</b>	
<b>Seabed exposure time</b>		<b>~11 yr</b>	



<b>Station ID</b>		MC6	
<b>Location</b>	<b>Latitude</b>	62°12'06.16"S	
	<b>Longitude</b>	58°43'21.48"W	
<b>Depth</b>		50 m	
<b>Distance from the glacier</b>		0 km	
<b>Seabed exposure time</b>		<5 yr	





<b>Station ID</b>		MC6
<b>Location</b>	<b>Latitude</b>	62°12'06.16"S
	<b>Longitude</b>	58°43'21.48"W
<b>Depth</b>		70 m
<b>Distance from the glacier</b>		0 km
<b>Seabed exposure time</b>		<5 yr

